ESCOLA DE DOUTORAMENTO
INTERNACIONAL DA USC

María do Carme
Pacín Salvador

Tese de doutoramento

As macroalgas como ferramentas de control ambiental: da escala rexional ao cambio global

Santiago de Compostela, 2025

Programa de Doutoramento en Medio Ambiente e Recursos Naturais

TESE DE DOUTORAMENTO

AS MACROALGAS COMO FERRAMENTAS DE CONTROL AMBIENTAL: DA ESCALA REXIONAL AO CAMBIO GLOBAL

Autora

María do Carme Pacín Salvador

Director: Jesús R. Aboal Viñas

Massimo Lazzari

Titor/a: Jesús R. Aboal Viñas

PROGRAMA DE DOUTORAMENTO EN MEDIO AMBIENTE E RECURSOS NATURAIS

SANTIAGO DE COMPOSTELA

ÍNDICE

DECLARACIÓN DE CONFLITOS DE INTERESE

Eu, María do Carme Pacín Salvador, presento a miña tese titulada "As macroalgas como ferramentas de control ambiental: da escala rexional ao cambio global" e, seguindo o procedemento adecuado ó regulamento, declaro que:

1) A tese abarca os resultados da elaboración do meu traballo.

2) Non teño ningún conflito de interese respecto á tese.

3) Teño o permiso tanto dos coautores e coautoras como das revistas para empregar os traballos publicados incluídos na tese.

4) Todas as figuras son de elaboración propia, a excepción do Panel B da Figura 2 que foi obtido no portal GBIF (Global Biodiversity Information Facility, https://www.gbif.org/).

En Santiago de Compostela a 11 de xullo de 2025.

Asinado: María do Carme Pacín Salvador

AGRADECEMENTOS

Rematar unha tese é unha excusa perfecta para recoñecernos como o que somos: seres interdependentes. Porque dende logo que non podería ter feito isto sola, pero é que ademais tampouco quero. Gracias a todas por acompañarme nunha etapa na que, honestamente, fun moi feliz :)

Ao meu director e titor de tese Jesús Aboal, porque sen el non estaría hoxe aquí. Tamén por ser o artífice dunha idea moi bonita que se materializou nesta tese, e por ensinarme todo o que sei e darme sempre as ferramentas, o apoio e a confianza para seguir. Por acompañarme e responsabilizarse, non só como titor, senón tamén como amigo. Por tratarme como unha igual e terme sempre en conta, e por ter uns valores de integridade e xustiza nos que quero verme sempre reflexada.

A Ángel Fernández, que non aparece no papel pero que tamén tivo un papel moi importante durante todos estes anos. Gracias pola axuda e pola tranquilidade que proporcionas ás persoas que te rodeamos e por non deixarnos afogar nun vaso de auga.

A Massimo Lazzari, pola súa predisposición, a súa amabilidade e polos comentarios sempre positivos do meu traballo, que me animaron en máis dunha ocasión e me deron a confianza que precisaba.

Aos meus regalitos de Minerva, por ser o mellor que me deron tantas horas metida no cuartucho, e por toda a compañía e axuda que me deron sempre. A Antón, por unha amizade desas que se contan cos dedos das mans, polas conversacións infinitas e os debates. Por nunca estar dacordo pero sempre (ou case) chegar a un punto en común. A Pablo, pola complicidade e os plans en tempos de COVID. Por tantas horas escoitando C Tangana. Grazas por axudar sen pedir nunca nada a cambio, e por ser a persoa que me acolleu dende o primeiro día cos brazos abertos.

A Tere, polos seus consellos valiosísimos e por ser unha referente. A Zule, pola súa forza para loitar contra as inxustizas e a súa solidaridade. Ao resto de compañeiras cas que convivín na área de Ecoloxía e noutros espazos da Universidade, pola súa amabilidade e por crear un ambiente de traballo cómodo e distendido. Tamén a todas as persoas que axudaron a recoller as mostras que se utilizaron nesta tese, porque sen elas este traballo non sería posible.

Ás persoas que me atopei nas estadías que fixen en Praga e Perth, por acollerme tan ben e facer destas experiencias o mellor da tese. Aquí teño que mencionar a varias amigas que me levo para sempre: Jessi, Kris, Marc, Adri, Alba, Rachel e Amine. Tamén a Mary e Julia por ser a miña familia en Australia.

Ás compañeiras da Asemblea de Investigadoras de Compostela por facer da USC un lugar máis amable. Grazas por ser un espazo seguro no que sempre me sentín validada e respectada, e por todos os logros que conseguimos xuntas, que aínda que modestos abondo daban para outra tese. Como dixo Mujica: "Quería cambiar el mundo y no cambié una mierda, pero estuve entretenido".

Ás miñas compañeiras de piso por facer de catro paredes un fogar no que sempre me sentín tranquila e a salvo. Por cociñarme, coidarme cando estaba enferma, traerme comida da horta, e por compartir tempo e espazos comigo. Por ser algo moi parecido a unha familia (bastante estruturada teño que dicir).

Ás miñas amigas, que son o meu maior logro na vida. Por seguirme en cada plan, e non deixarme nunca bailando sola a pera. Polos momentos tan divertidos que pasamos, pero tamén polo apoio incondicional e o acompañamento tan constante que tiven sempre. Por facerme sentir tan querida e coidada. Mención especial ás miñas comadres Sally, Luso, Sabi, Maritza, Gracia, Fedu, Iago, Luis e moitas máis. A Laila, por compartir tantísimos momentos xuntas durante estes anos.

Á miña familia, por darme unha infancia feliz chea de afectos. Á miña nai, por ser o meu referente absoluto na vida e a columna vertebral da familia. Por animarme sempre a vivir a miña vida e facer o que me apetece sen atender ás expectativas do resto. Ao meu pai, pola súa bondade, o seu optimismo desmesurado e a súa creatividade. Porque sempre será quen conta os mellores contos. E ao meu irmán, por ser todo o que a min me falta, e por coidar tanto de mamá e papá.

A Javi, por ser o meu maior apoio e acompañarme nos últimos dez anos dende o amor xenuíno, o respecto e a admiración mutua. Por aguantarme traballando a horas indecentes e darme sempre a tranquilidade que necesito, sobre todo nestes últimos meses. Por facerme rir a cada segundo e por seguir elixíndonos cada día.

Os meus agradecementos á Secretaría Xeral de Universidades da Consellería de Cultura, Educación, Formación Profesional e Universidades da Xunta de Galicia pola súa financiación a través das Axudas de apoio á formación predoutoral (ED481A 2022/374), así como ao CRETUS pola financiación da estadía realizada na Czech University of Life Sciences Prague (CZU), que fixo posible o desenvolvemento do Capítulo 3 desta tese.

ABSTRACT

Brown macroalgae, particularly species of the genus *Fucus*, play key ecological roles in temperate coastal ecosystems, such as primary production and the formation of structural habitats. However, their ability to concentrate potentially toxic elements (PTEs) can alter their physiology and facilitate the transfer of contaminants through the food web. This property has led to their widespread use as biomonitors in marine environmental assessments, though not without limitations.

Despite reductions in certain industrial emissions due to stricter regulations, the current scenario of coastal contamination remains marked by intense human pressures, the emergence of new contaminants—such as metallic nanoparticles—and the effects of global change on key environmental parameters that influence metal mobility and bioavailability.

In this context, this thesis investigates the evolution of contamination by PTEs and silver nanoparticles (AgNPs) in brown algae over the past century, identifying the sources involved and assessing the factors that modulate their accumulation. The work is structured into five complementary chapters, combining different spatial and temporal scales and integrating both absolute concentration and compositional analyses.

Chapter 1 presents a global meta-analysis of PTE concentrations (Cd, Co, Cr, Cu, Fe, Hg, Mn, Pb, Zn) in brown algae from 1930 to 2020, examining their temporal evolution and relationships with environmental variables. **Chapter 2** analyzes regional samples of *Fucus* spp. collected in Galicia (1990–2021), enabling high-resolution assessment of nine PTEs (Al, As, Cd, Cr, Cu, Fe, Hg, Ni, Zn). **Chapter 3** focuses on Pb concentrations and isotopic ratios ($^{206}Pb/^{207}Pb$ and $^{208}Pb/^{206}Pb$) from the same samples to characterize historical and recent sources. **Chapter 4** examines Ag concentrations at the regional scale and includes a global review of published data up to 2024, while also reporting, for the first time under natural conditions, the presence of AgNPs in these organisms. Finally, **Chapter 5** compiles the full dataset for a compositional analysis, evaluating the influence of taxonomy and the temporal evolution of relative elemental proportions.

Results revealed significant global declines in PTE concentrations (–84% for Pb, –60% for Co), with patterns varying by element and region. At the regional level, sharp decreases were observed for Cr (–84.6%), Cu (–84.7%), Hg (–49.6%), Cd (–36.7%), as well as Ni, Zn, and Ag,

while Al, Fe, and As increased. Regional Pb showed a moderate, non-significant decline (–21.9%). Ag also exhibited a global downward trend since the 1980s, which was more clearly evident in Galicia (–58.1%). A decrease in the number of AgNPs was also detected over time, along with a positive correlation between total Ag concentrations and AgNP abundance, suggesting potential *in vivo* formation by the algae.

The compositional analysis revealed substantial changes in elemental proportions, especially in 2021, with Al, Fe, and As becoming more prominent, although the internal structure of the composition remained relatively stable.

Source analysis indicates a clear shift over recent decades, with a progressive reduction in anthropogenic sources and a relative increase in natural ones, identified through PMF models and Pb isotopes. This transition is linked to the implementation of environmental policies, such as the ban on leaded gasoline and improved wastewater treatment. However, global change-related factors—such as acidification, rising temperatures, and salinity fluctuations—may alter metal bioavailability and partially offset the effects of these measures. Additionally, the higher sediment load detected in 2021 may explain the relative stability of certain metals such as Pb or the increase in As.

Overall, this thesis provides an integrated perspective on the evolution of marine contamination by PTEs and AgNPs in brown algae. It contributes to a better understanding of the combined impacts of human activities and global change on coastal ecosystems and on these organisms, offering valuable insights for improving biomonitoring strategies and supporting environmental assessment and sustainable marine management.

RESUMO

As algas pardas, en particular as do xénero *Fucus*, desempeñan funcións ecolóxicas clave nos ecosistemas costeiros temperados, como a produción primaria ou a creación de hábitats estruturais. Porén, a súa capacidade para cargar elementos potencialmente tóxicos (PTEs) pode alterar a súa fisioloxía e facilitar a transferencia de contaminantes a través da cadea trófica. Esta propiedade motivou o seu uso como biomonitores, aínda que con limitacións, na avaliación ambiental mariña.

A pesar da redución dalgunhas emisións industriais grazas a políticas máis estritas, o actual escenario de contaminación costeira segue marcado por presións derivadas da elevada pegada ecolóxica humana, a aparición de contaminantes emerxentes —como as nanopartículas metálicas— e os efectos do cambio global sobre parámetros ambientais que afectan á mobilidade e biodispoñibilidade dos PTEs.

Neste contexto, esta tese analiza a evolución da contaminación por PTEs e nanopartículas de prata (AgNPs) en algas pardas durante o último século, identificando as fontes implicadas e avaliando os factores que modulan a súa concentración. O traballo estrutúrase en cinco capítulos complementarios que combinan diferentes escalas espaciais e temporais, así como enfoques baseados en concentracións absolutas e análises composicionais.

O **Capítulo 1** presenta unha metanálise global das concentracións de nove PTEs (Cd, Co, Cr, Cu, Fe, Hg, Mn, Pb e Zn) en algas pardas entre 1930 e 2020, avaliando a súa evolución e relación con variables ambientais. O **Capítulo 2** analiza mostras rexionais de *Fucus* spp. recollidas en Galicia (1990–2021), permitindo avaliar con alta resolución a evolución de nove PTEs (Al, As, Cd, Cr, Cu, Fe, Hg, Ni, Zn). No **Capítulo 3** estúdanse as concentracións de Pb e as razóns isotópicas ($^{206}Pb/^{207}Pb$ e $^{208}Pb/^{206}Pb$) nas mesmas mostras, para caracterizar as fontes históricas e recentes deste metal. O **Capítulo 4** aborda as concentracións de Ag a escala rexional e realiza unha revisión global de estudos dispoñibles ata 2024, examinando tamén por primeira vez a presenza de AgNPs nestes organismos en condicións naturais. O **Capítulo 5** recompila o conxunto de datos para realizar unha análise composicional, avaliando a influencia da taxonomía e a evolución temporal das proporcións relativas dos elementos.

Os resultados mostran descensos significativos nas concentracións de PTEs a escala global (–84 % para Pb, –60 % para Co), con patróns variables segundo o elemento e a rexión. A nivel

rexional, detectáronse fortes descensos en Cr (–84,6 %), Cu (–84,7 %), Hg (–49,6 %), Cd (–36,7 %), Ni, Zn e Ag, mentres que Al, Fe e As aumentaron. O Pb rexional amosou unha redución moderada (–21,9 %), non significativa. Para a Ag observouse unha tendencia descendente global desde os anos 1980, que foi moi evidente a nivel rexional (–58,1 %). Tamén se rexistrou unha redución no número de AgNPs ao longo do tempo e unha correlación positiva entre a concentración total de Ag e o número de nanopartículas, o que suxire unha posible formación *in vivo* por parte das algas.

A análise composicional revelou cambios substanciais nas proporcións relativas entre elementos, especialmente en 2021, con maior peso de Al, Fe e As, aínda que a estrutura interna da composición se mantivo relativamente estable.

A análise das fontes de contaminación indica unha transición clara nas últimas décadas, cun descenso progresivo das fontes antrópicas e un aumento relativo das naturais, identificado mediante modelos PMF e isótopos de Pb. Esta evolución está asociada á aplicación de políticas ambientais como a prohibición da gasolina con chumbo e a mellora do tratamento de augas residuais. Porén, factores asociados ao cambio global (acidificación, aumento de temperatura, variacións de salinidade) poden alterar a biodispoñibilidade dos PTEs e contrarrestar parcialmente os efectos destas medidas. Ademais, a maior carga de sedimento detectada en 2021 podería explicar a estabilidade dalgúns PTEs como o Pb ou o incremento do As.

En conxunto, esta tese proporciona unha visión integrada da evolución da contaminación mariña por PTEs e AgNPs en algas pardas, contribuíndo á comprensión dos efectos combinados das actividades humanas e o cambio global nos ecosistemas costeiros e nestes organismos. Os resultados achegan coñecemento útil para mellorar as estratexias de biomonitorización e apoiar a avaliación ambiental e a xestión sostible do medio mariño.

PUBLICACIÓNS INCLUÍDAS NA TESE

1. **Estudo 1:** Aboal, J. R.*; Pacín, C.*; García-Seoane, R.; Varela, Z.; González, A. G.; Fernández, J. A. Global Decrease in Heavy Metal Concentrations in Brown Algae in the Last 90 Years. J Hazard Mater 2023, 445, 130511. https://doi.org/10.1016/J.JHAZMAT.2022.130511. **equal contribution*

2. **Estudo 2:** Pacín, C.; Fernández, J. A.; Conde-Amboage, M.; Lazzari, M.; García-Seoane, R.; Viana, I. G.; Varela, Z.; Real, C.; Villares, R.; Aboal, J. R. Three Decades of Change in Potentially Toxic Elements in Brown Algae in the Northeast Atlantic Ocean. Environ Sci Technol 2025, 59(21), 10476-10487. https://doi.org/10.1021/acs.est.4c14013.

3. **Estudo 3:** Pacín, C.; Aboal, J. R.1; Fernández, J.A.1; Vázquez-Arias, A.1; Šípková, A.; Komárek, M.; Chrastný, V. The Return of Natural Lead to the Northeast Atlantic Ocean Captured by Brown Algae. J Hazard Mater 2025, 496, 139289. https://doi.org/10.1016/j.jhazmat.2025.139289

4. **Estudo 4:** Pacín, C.; Lazzari, M; Fernández, J. A.; Aboal, J. R. Long-Term Silver Contamination in the Ocean: Insights from Brown Algae on Dissolved Ag and Nanoparticles. *Under review.*

5. **Estudo 5:** Pacín, C.; Fernández, J.A.; Aboal, J.R. Tracing Pollution in Brown Algae: A Compositional Analysis of Potentially Toxic Element Profiles. *Under review.*

ABREVIATURAS

PTEs:	Elementos potencialmente tóxicos
Al:	Aluminio
Cr:	Cromo
Fe:	Ferro
Ni:	Níquel
Cu:	Cobre
Zn:	Zinc
As:	Arsénico
Ag:	Prata
Cd:	Cadmio
Hg:	Mercurio
Pb:	Chumbo
Co:	Cobalto
Mn:	Manganeso
AgNPs:	Nanopartículas de prata
IQR:	Rango intercuartículo
LOQ:	Límite de cuantificación
ICP-MS:	Espectrometría de masas con plasma acoplado
DMA80:	Analizador Directo de Mercurio 80
nMDS:	Escalamento Multidimensional Non Métrico
ANOSIM:	Análise de Semellanzas
CMEMS:	Copernicus Marine Environment Monitoring Service
NOAA:	National Oceanic and Atmospheric Administration
MixSIAR:	Análise de Isótopos Estables de Mestura en R
PMF:	Factorización Positiva de Matrices
GAMs:	Modelos Aditivos Xeneralizados
LMMs:	Modelos Mixtos Lineais
PCA:	Análise de Compoñentes Principais
CoDA:	Análise de Datos Composicional
CLR:	Transformación centrada en log-ratios
RDA:	Análise de Redundancia
PERMANOVA:	Análise Multivariada de Varianza por Permutacións

1. INTRODUCIÓN

1.1. O Antropoceno

Dende o seu xurdimento como especie hai uns 300.000 anos[1], o *Homo sapiens* transformou significativamente o medio natural, comezando por unha modificación localizada ata a alteración global dos ecosistemas observada a día de hoxe[2–4].

Os primeiros indicios de alteración ambiental xurdiron na Prehistoria, coa minería selectiva para a elaboración de ferramentas líticas no Paleolítico, que deu paso á explotación posterior de PTEs como o cobre e o bronce[5,6]. A **Revolución Neolítica**, hai uns 10.000 anos, marcou un punto de inflexión: transicionouse dunha economía de caza e recolección a unha baseada na agricultura e a gandaría, co conseguinte cambio no uso do solo, deforestación, domesticación de especies e fundación de asentamentos humanos permanentes[7,8]. Estes procesos sentaron as bases para a expansión das sociedades humanas e a transformación dos ecosistemas a escala rexional e continental.

Non obstante, foi coa **Revolución Industrial**, a partir da segunda metade do século XVIII, cando se produciu unha aceleración sen precedentes do impacto humano. A queima masiva de combustibles fósiles como o carbón e o petróleo, e a industrialización provocaron a emisión a grande escala de gases de efecto invernadoiro e contaminantes[9–11]. Estes impactos intensificáronse nos séculos XIX e XX coa **revolución verde**, o uso extensivo de fertilizantes e pesticidas, e o crecemento demográfico[12,13]. Xa no século XXI, estes impactos ambientais non só se mantiveron, senón que se agravaron, provocando unha maior fragmentación e degradación dos ecosistemas terrestres e acuáticos.

Como consecuencia, na actualidade a maior parte dos ecosistemas presentan alteracións significativas, e só uns poucos hábitats se conservan en condicións relativamente prístinas[14,15]. Este conxunto de transformacións a escala global é coñecido como **Cambio Global**, e a súa magnitude levou a propoñer a definición dunha nova época xeolóxica: o **Antropoceno**, recoñecendo a profunda e irreversible pegada que as actividades humanas teñen no sistema Terra[16–18].

1.2. O Cambio Global no medio mariño

Os océanos cobren o 71 % da superficie terrestre e conteñen o 97 % da auga do planeta. De acordo con esta dominancia, desempeñan un papel esencial na regulación do clima, na captura de carbono e no sustento dunha ampla diversidade biolóxica[19].

Non obstante, o medio mariño constitúe un dos sistemas máis afectados polos impactos do Cambio Global. A súa función como principal sumidoiro de carbono do planeta, absorbendo máis do 90% do exceso do calor xerado polo incremento das emisións de gases de efecto invernadoiro[20,21], implica unha serie de desequilibrios no contexto actual do **cambio climático**, como o aumento da **temperatura da superficie do mar (SST)**[22]**.** Este incremento altera as correntes mariñas e os patróns de distribución das especies, ao tempo que reduce os niveis de osíxeno nas augas superficiais. Ademais, a combinación entre a maior absorción de calor, o derretemento das capas de xeo polares e a expansión térmica da auga do mar está provocando **o aumento do nivel do mar**, o que dá lugar a **erosión costeira**, **inundacións** máis frecuentes e a **perda de hábitats** para as especies litorais[23].

Así mesmo, os cambios nas taxas de evaporación, os patróns alterados de precipitación e o derretemento do xeo están tamén contribuíndo ás variacións rexionais na **salinidade** oceánica[23,24]. As emisións crecentes de CO_2 desde a Revolución Industrial tamén están provocando un incremento na absorción deste gas polos océanos, o que dá lugar á formación de ácido carbónico e á diminución do pH da auga mariña. Este proceso, coñecido como **acidificación oceánica**, perturba o equilibrio químico dos océanos e constitúe unha ameaza para a vida mariña[25,26].

Outra compoñente significativa do Cambio Global observado nos océanos é a **perda de biodiversidade**, que se materializa na desaparición ou a degradación intensa de aproximadamente o 50 % dos arrecifes de coral[27], e nun intenso declive de máis dun 30% dos elasmobranquios e dos mamíferos mariños[28], entre outros impactos.

Ademais de todas estas ameazas, a **contaminación** dos océanos, mediante a introdución de diferentes substancias nocivas no medio mariño, constitúe un dos impactos máis preocupantes e complexos[29,30].

1.3. Contaminación mariña

A **contaminación**, definida como a introdución de substancias ou enerxía que provocan desequilibrios ecolóxicos[31], constitúe unha das principais ameazas para os ecosistemas mariños, tanto pola diversidade de compostos implicados como pola complexidade das súas interaccións. Estes compostos poden clasificarse, segundo a súa estrutura química, en contaminantes orgánicos e inorgánicos.

Os **contaminantes orgánicos** caracterízanse por unha estrutura baseada en cadeas de carbono e inclúen compostos como hidrocarburos derivados do petróleo, pesticidas organoclorados (e.g. DDT, dicloro-difenil-tricloroetano), bifenilos policlorados (PCBs, do inglés polychlorinated biphenyls), PFAS, ftalatos, bisfenilos, poliestireno, dioxinas e furanos, etc.[32]

Por outra banda, os **contaminantes inorgánicos** inclúen nutrientes como nitratos e fosfatos, radionúclidos, e de maneira destacada, os **elementos potencialmente tóxicos** (PTEs, do inglés *Potentially Toxic Elements*)[33–35]. Este término utilízase para substituír outras categorías tradicionais e ambiguas como "metais pesados" (e.g. Cr, Fe, Cd, Hg, Pb, Cu, Zn, Ni, Ag), así como outros metais como o Al e metaloides como o As, que comparten características de persistencia e bioacumulación[36,37], sendo o termo recomendado pola Unión Internacional de Química Pura e Aplicada (IUPAC). Os contaminantes orgánicos e inorgánicos tamén poden constituír **complexos organometálicos** como o tributilestaño (TBT) ou o metilmercurio, que combinan características de ambos tipos de contaminantes e presentan elevada toxicidade e persistencia[38,39].

Os PTEs están presentes de forma natural na codia terrestre e poden liberarse mediante procesos xeolóxicos como a erosión de rochas, as emisións volcánicas, ou a actividade termal submarina. Porén, as actividades humanas son as principais responsables da súa presenza no medio mariño a día de hoxe, destacando a **minería** e a **industria metalúrxica**, a **industria química**, a **agricultura** e **acuicultura intensivas**, e a **queima de combustibles fósiles**[40,41].

Estas actividades realízanse esencialmente no medio terrestre, liberando PTEs que chegan ao medio mariño a través de varias vías fundamentais[42–44]:

- Transporte fluvial, mediante a escorrentía superficial.

- Fluxo subterráneo costeiro, resultado da chegada ao medio mariño de augas subterráneas contaminadas
- Deposición atmosférica, resultado da caída de partículas ou gases contaminantes transportados polo aire.
- Vertidos directos de augas residuais urbanas e industriais.

Ademais, tamén existen fontes mariñas directas como o transporte marítimo, incluíndo vertidos e o uso de pinturas antifouling nos cascos dos barcos, que poden liberar PTEs como o Cu ou o Zn directamente na auga[45,46].

Unha das formas máis recentes de contaminación por PTEs é a presenza de **nanopartículas metálicas**, tanto de orixe natural como inxenierizada[47]. Entre elas, destacan as **nanopartículas de prata (AgNPs)**, cuxo uso se incrementou exponencialmente na última década para a fabricación de produtos antimicrobianos[48,49]. Unha vez no ambiente acuático, estas nanopartículas poden comportarse de forma diferente ás formas iónicas, xa que teñen alta mobilidade, capacidade de agregación e unha maior biodispoñibilidade[50,51].

Nos ecosistemas costeiros, a contaminación tende a ser máis intensa pola proximidade ás fontes terrestres e a elevada concentración de actividades humanas nesas zonas[52]. Nestes ambientes, os PTEs distribúense entre diferentes compartimentos ambientais. Parte deles permanece disolta na **columna de auga**, onde poden interactuar con partículas en suspensión, ou complexarse con materia orgánica[53]. Porén, unha proporción significativa é rapidamente secuestrada nos **sedimentos**, que actúan como o principal sumidoiro de PTEs a medio e longo prazo. Non obstante, os sedimentos tamén poden actuar como fontes secundarias, liberando os PTEs acumulados baixo condicións ambientais cambiantes, como variacións no pH, redox ou actividade biolóxica[54]. Por último, os PTEs tamén poden atoparse nos tecidos dos **organismos costeiros** e **biomagnificarse** ao longo da cadea trófica[55,56] (Figura 1).

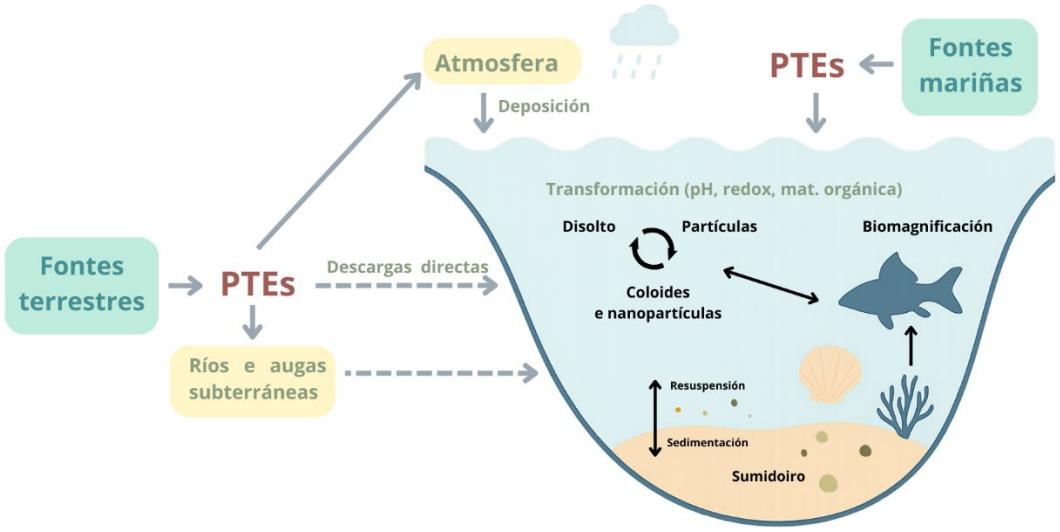

Figura 1. Esquema conceptual das principais vías de entrada, distribución e destino dos Elementos Potencialmente Tóxicos (PTEs) nos ecosistemas costeiros (Elaboración propia).

1.4. Efectos da contaminación por PTEs nos organismos costeiros

A concentración de PTEs nos organismos costeiros pode desencadear unha serie de efectos en cascada, que dependerán tanto da natureza tóxica de cada elemento como da súa concentración e dos órganos diana afectados. Mentres que algúns PTEs teñen funcións esenciais a niveis traza e só resultan tóxicos cando superan certos limiares (e.g. Zn), outros como o Pb, o Cd e o Hg carecen de función biolóxica coñecida e poden provocar efectos adversos mesmo a baixas concentracións. Entre os impactos máis comúns destacan a redución nas taxas de reprodución, o aumento da mortalidade e a diminución da mobilidade dos organismos[57–60]. Así mesmo, as nanopartículas metálicas tamén demostraron presentar unha toxicidade elevada, e incluso superior á das súas formas iónicas[51,61,62].

As algas pardas tamén presentan respostas tóxicas á exposición a PTEs[63–65], o que compromete as súas funcións ecolóxicas, entre as que se inclúen proporcionar estrutura, alimento e refuxio ás comunidades bentónicas[66,67]. Ademais, ao situarse na base das cadeas tróficas costeiras e ser consumidas por organismos como isópodos, moluscos e peixes, á súa vez consumidos por outros organismos, poden iniciar procesos de bioacumulación e biomagnificación[68–70].

A magnitude dos efectos dos PTEs depende non só da súa concentración en compartimentos ambientais como a columna de auga ou o sedimento, senón tamén da súa biodispoñibilidade e especiación química. Parámetros fisicoquímicos como o pH, a salinidade, a temperatura ou a presenza de materia orgánica inflúen directamente na mobilidade e biodispoñibilidade destes contaminantes[71–74]. Neste contexto, os cambios ambientais asociados ao cambio climático e á acidificación oceánica suscitan preocupación, xa que poderían estar incrementando a dispoñibilidade biolóxica dos PTEs, intensificando os seus efectos tóxicos sobre os ecosistemas mariños. Ademais, estes cambios poderían dificultar a avaliación real dos progresos na redución das emisións, ao potenciar efectos adversos incluso en escenarios de mellora aparente da calidade ambiental.

1.5. **Monitorización da contaminación**

Para avaliar o grao de contaminación dun ecosistema é habitual analizar a concentración dos contaminantes en distintos compartimentos ambientais. No medio mariño, isto inclúe a auga e os sedimentos, pero tamén os propios organismos, a través do que se coñece como **biomonitorización**[75,76]. Esta metodoloxía pretende inferir o nivel de contaminación do medio a través da análise das concentracións de contaminantes nos tecidos dos organismos. A biomonitorización lévase empregando durante décadas e susténtase en numerosos programas a nivel nacional e internacional[77,78]. Así, é unha ferramenta recoñecida polas administracións e recollida en lexislacións como a Directiva Marco da Auga[79].

Moitos organismos utilizados como biomonitores responden de maneira cualitativa á contaminación: amosan concentracións elevadas en ambientes con moita contaminación e niveis baixos en zonas non afectadas[80,81]. Porén, as concentracións rexistradas nestes organismos non sempre mostran relacións significativas cos niveis ambientais doutros compartimentos[82–84]. Estas discrepancias poden deberse a múltiples factores, como a integración a longo prazo dos contaminantes nos organismos (en contraste con medidas puntuais en auga ou aire)[85,86], diferenzas na capacidade de absorción e saturación dos organismos, ou a habilidade para regular ou metabolizar estes compostos[87–90].

As algas pardas, e especialmente as do xénero *Fucus* (Figura 2), amplamente distribuídas nas costas atlánticas do hemisferio norte, foron extensamente utilizadas para este fin[91], en parte pola súa capacidade de captar PTEs, facilitada pola presenza de polisacáridos como os alxinatos e os fucoidanos nas paredes celulares[92,93]. Ademais, certos PTEs, como o Cu, o Ni e o Zn, foron

identificados principalmente no interior das súas células, o que suxire a existencia de mecanismos activos de internacionalización que contribúen á súa retención intracelular[94]. De novo, a relación entre a auga e estes organismos parece non ser lineal nin directa[95–97]. Porén, lonxe de invalidar o seu uso, esta complexidade reforza o valor da biomonitorización como ferramenta chave para avaliar os efectos reais da contaminación, pois só a través deste enfoque se poden detectar os impactos acumulativos e as interaccións entre os contaminantes, os organismos e outros impulsores do cambio global, que inflúen na dispoñibilidade e toxicidade dos PTEs no medio mariño.

Figura 2. Exemplares da alga parda *Fucus vesiculosus* durante o intermareal na ría de Noia (Galicia, noroeste da península Ibérica) (Panel A) e distribución global das especies do xénero *Fucus* (Panel B). A área de distribución do panel B foi obtida no portal GBIF (Global Biodiversity Information Facility, https://www.gbif.org/).

1.6. Evolución da contaminación e medidas ambientais asociadas

A monitorización ambiental ao longo do tempo é fundamental para identificar tendencias temporais, avaliar a evolución da contaminación e anticipar posibles riscos futuros. Sen unha perspectiva temporal, a avaliación do estado dun ecosistema resulta incompleta e pouco representativa, xa que non permite distinguir entre variacións naturais e impactos antropoxénicos. Neste contexto, os **bancos de mostras ambientais** representan unha ferramenta de enorme valor, ao permitir análises retrospectivas que axudan a reconstruír a dinámica da contaminación ao longo das décadas[98,99].

Non obstante, os estudos que abordan as **tendencias temporais** de contaminantes como os PTEs en organismos costeiros seguen a ser moi escasos[100–102], especialmente no caso das algas pardas. Así, a maioría destes traballos dispoñen dun número limitado de puntos de mostraxe, abranguen escalas temporais curtas ou empregan metodoloxías non estandarizadas, o que dificulta a comparación e compromete a avaliación rigorosa da evolución da contaminación a longo prazo e da súa repercusión nos ecosistemas mariños[103–105].

Ademais, a análise das tendencias non debe limitarse á mera descrición das concentracións de contaminantes, senón que debe avanzar cara a unha **caracterización integral das fontes de emisión**. Identificar a orixe dos PTEs é esencial para o deseño de medidas correctoras eficaces, avaliar a efectividade de medidas xa implementadas e desenvolver modelos preditivos máis precisos. Non obstante, esta dimensión permanece pouco explorada, especialmente en ambientes costeiros. A falta de estudos específicos sobre a atribución de fontes limita a capacidade de establecer relacións causais entre as actividades humanas e os niveis de contaminación observados nos organismos mariños.

Desde a década dos 90, produciuse un avance significativo no desenvolvemento de normativas ambientais a múltiples escalas que transformaron profundamente a xestión da contaminación. Estas políticas incluíron melloras no tratamento de augas residuais, o control das emisións industriais e restricións crecentes sobre o uso de combustibles fósiles. Exemplos destacados inclúen a Directiva sobre o tratamento das augas residuais urbanas[106], a Directiva Marco da Auga[107] e a Directiva marco sobre a estratexia mariña da Unión Europea[108]. A nivel global, a **prohibición do uso de gasolina con Pb** supuxo un descenso significativo das concentracións ambientais deste metal en moitas rexións[77,109–111].

1.7. **Unidades da tese**

Ao longo desta tese estudamos a evolución temporal da contaminación por PTEs e AgNPs nos ecosistemas costeiros empregando algas pardas. Ademais de avaliar os cambios nas concentracións ao longo do tempo, identificamos as fontes emisoras e a evolución temporal das mesmas.

Para abordar esta cuestión, desenvolvéronse dous enfoques complementarios. Por unha banda, realizouse unha análise a escala global baseada na recompilación de datos de múltiples estudos publicados. Este enfoque abrangue unha ampla escala espazo-temporal, pero está

marcado pola heteroxeneidade metodolóxica e unha resolución limitada, derivada do uso de metodoloxías non estandarizadas. Por outra banda, esta perspectiva contrastouse cun enfoque rexional baseado en series temporais de alta resolución, obtidas mediante metodoloxías estandarizadas e comparables entre anos, grazas ao uso do Banco de Mostras Ambientais de Galicia[112]. Esta aproximación dual permite integrar diferentes niveis de información e avaliar a consistencia dos patróns observados a distintas escalas.

Ademais da análise das concentracións totais, incorporouse unha perspectiva composicional que permite estudar as proporcións relativas entre os distintos PTEs, examinando os perfís elementais como conxuntos interdependentes, o que permite unha interpretación máis robusta dos patróns de relación entre elementos. Esta análise facilitou a identificación de cambios estruturais nos perfís ao longo do tempo, diferenzas entre especies ou taxas e a inferencia de procesos ambientais ou fisiolóxicos subxacentes, como a existencia de fontes comúns, mecanismos de absorción diferencial ou interaccións entre elementos.

En conxunto, esta tese non só documenta a evolución da contaminación en ecosistemas costeiros ao longo de máis de tres décadas, senón que tamén achega ferramentas metodolóxicas e interpretativas para comprender mellor as súas causas, fontes e consecuencias a distintas escalas espaciais e temporais.

2. OBXECTIVOS E HIPÓTESES

O obxectivo principal desta tese é analizar as tendencias temporais da contaminación por PTEs e AgNPs nas algas pardas durante o último século, identificando as fontes implicadas e os factores ambientais e espaciais que modulan a súa captación. A través da integración de diferentes abordaxes metodolóxicas, esta investigación busca avanzar na comprensión da evolución da contaminación mariña e contribuír á avaliación da eficacia das políticas ambientais.

- O **Estudo 1** analiza a evolución temporal das concentracións de PTEs (Cr, Mn, Fe, Co, Cu, Zn, Cd, Pb e Hg) nas algas pardas a nivel global durante os últimos 90 anos a partir da recompilación de datos recollidos entre 1930 e 2020 e publicados en artigos científicos, así como a súa relación con factores ambientais asociados ao cambio global. Neste estudo abordáronse as seguintes hipóteses:
  - **H1.1.** As concentracións de PTEs non experimentan cambios significativos nas últimas décadas, independentemente da implantación de normativas ambientais.
  - **H1.2.** Os factores asociados ao cambio global, como a acidificación oceánica, ou o aumento da temperatura, non se relacionan cas concentracións de PTEs nas algas pardas.
  - **H1.3.** Non existen diferenzas significativas nas concentracións de PTEs segundo a localización xeográfica nin entre familias taxonómicas de algas pardas.

- O **Estudo 2** explora as tendencias temporais e patróns espaciais das concentracións de Al, Cr, Fe, Ni, Cu, Zn, As, Cd e Hg en mostras de *Fucus* spp. recollidas de forma sistemática en 173 estacións de mostraxe do noroeste da Península Ibérica (Galicia) de 1990 a 2021, para analizar os efectos das políticas ambientais, a influencia do sedimento sobre a bioconcentración destes elementos, a evolución das súas fontes e os patróns espaciais.
  - **H2.1.** As concentracións rexionais de PTEs en *Fucus* spp. mantivéronse estables ao longo do tempo.
  - **H2.2.** As concentracións de PTEs en *Fucus* spp. recollidas nos mesmos sitios non experimentaron variacións significativas entre campañas.
  - **H2.3.** Non se observaron diferenzas nas concentracións e na súa evolución temporal a nivel espacial nin entre especies.

- **H2.4.** As fontes de contaminación por PTEs mantivéronse estables ao longo do período de estudo.

- O **Estudo 3** examina as concentracións totais e as razóns isotópicas de Pb en *Fucus* spp., recollidas de forma sistemática en 173 estacións de mostraxe do noroeste da Península Ibérica (Galicia) de 1990 a 2021, co obxectivo de avaliar as tendencias temporais, identificar cambios nas fontes de contaminación e analizar o papel dos sedimentos como fonte secundaria.
  - **H3.1.** As concentracións de Pb e razóns isotópicas ($^{206}Pb/^{207}Pb$ e $^{208}Pb/^{206}Pb$) en *Fucus* spp. mantivéronse estables ao longo do tempo.
  - **H3.2.** As concentracións de Pb e razóns isotópicas ($^{206}Pb/^{207}Pb$ e $^{208}Pb/^{206}Pb$) en *Fucus* spp. recollidas nos mesmos sitios non experimentaron variacións significativas entre campañas.
  - **H3.3.** Non se observaron diferenzas nas concentracións e razóns isotópicas de Pb, nin na súa evolución temporal, a nivel espacial nin entre especies.
  - **H3.4.** As fontes de contaminación por Pb mantivéronse estables de 1990 a 2021.

- O **Estudo 4** integra a análise de concentracións de Ag en *Fucus* spp. en 173 estacións de mostraxe da costa galega de 1990 a 2021, a análise de AgNPs en dez destas estacións en diferentes momentos temporais (1990, 2005-2007 e 2021), e unha revisión global da literatura con datos entre 1952 e 2023 obxectivo de avaliar a evolución temporal e espacial das concentracións de prata e AgNPs en algas pardas.
  - **H4.1.** As concentracións de Ag en *Fucus* spp. mantivéronse estables ao longo do tempo.
  - **H4.2**. Non se observaron diferenzas nas concentracións de Ag a nivel espacial nin entre especies.
  - **H4.3.** As concentracións e distribución de tamaños das AgNPs non amosan variacións significativas ao longo do tempo.
  - **H4.4.** Non se observan cambios significativos nas concentracións de Ag nas algas pardas a nivel global ao longo do tempo.

- O **Estudo 5** combina o conxunto de datos xerados nos outros estudos e datos propios do grupo de investigación publicados con posterioridade á revisión bibliográfica co obxectivo de estudar as proporcións relativas dos elementos e caracterizar os patróns

composicionais de PTEs en algas pardas. O obxectivo é examinar as relacións entre os distintos elementos, explorar as diferenzas entre grupos taxonómicos, identificar elementos dominantes e fontes potenciais de variación, e detectar cambios temporais relevantes na composición de PTEs das algas.

- **H5.1.** Non existen diferenzas significativas na proporción relativa dos PTEs nos perfís composicionais das algas pardas.
- **H5.2.** Non se observan relacións significativas entre os distintos elementos nin patróns definidos de covariación.
- **H5.3**. A composición de PTEs non varía significativamente entre familias, xéneros nin especies de algas pardas.
- **H5.4.** Non se detectan cambios significativos na composición de PTEs en *Fucus* spp. ao longo do tempo (1990 – 2021).

3. METODOLOXÍA

3.1. Compilación de datos globais

O **Estudo 1** baseouse na recompilación de datos procedentes da literatura científica publicada entre 1952 e 2020 sobre as concentracións de Cr, Mn, Fe, Co, Cu, Zn, Cd, Hg e Pb en algas pardas a nivel global. A busca bibliográfica realizouse a través das plataformas *Scopus* e *Google Académico*, e foi complementada coa revisión das referencias incluídas nos artigos seleccionados. De cada estudo extraeuse información sobre o ano de mostraxe, a especie analizada, a localización exacta, as concentracións dos elementos e a presenza ou ausencia de presión antrópica nos puntos de mostraxe. As concentracións foron normalizadas a unidades comúns e limitadas a valores expresados en peso seco, co fin de permitir a súa comparación. En total, analizáronse 3546 rexistros procedentes de 368 estudos.

Un procedemento equivalente aplicouse no **Estudo 4** para analizar as tendencias globais da Ag, ampliando o rango temporal de busca ata o ano 2024 e incorporando todos os traballos dispoñibles ata esa data. Obtivéronse así 275 rexistros procedentes de 37 estudos.

O **Estudo 5** utilizou estas bases de datos para analizar os patróns composicionais dos elementos, engadindo ademais datos propios do grupo de investigación publicados con posterioridade, baseados en mostras recollidas en 2013, 2015-2019, 2021 e 2023[86,103,113–115].

Para o **Estudo 2** realizouse unha revisión bibliográfica exhaustiva en *Scopus, Google Académico* e nas referencias cruzadas dos artigos obtidos, co obxectivo de compilar valores de razóns isotópicas de Pb de diferentes fontes de Pb. Estes valores serviron como referencia comparativa cos datos obtidos no presente traballo e poden consultarse na **Táboa 1** dese estudo.

Finalmente, para todos os estudos incluídos nesta tese realizouse un manexo sistemático da bibliografía, fundamentalmente a través das plataformas *Scopus* e *Google Académico*, tanto para identificar lagoas de coñecemento como para contextualizar e discutir os resultados obtidos.

3.2. Mostraxe

3.2.1. Área de estudo

Os **Estudos 2, 3** e **4** utilizaron mostras recollidas en 173 localizacións ao longo da costa de Galicia, no noroeste da península ibérica, durante as campañas de mostraxe realizadas nos anos 1990, 2001, 2003, 2005, 2007 e 2021.

Galicia conta cunha singularidade xeográfica: a presenza de numerosas rías, formadas pola inundación mariña de antigos vales fluviais fai uns 10.000 anos durante o Holoceno[116,117]. Esta configuración costeira fai que Galicia represente aproximadamente un terzo da lonxitude total da costa española peninsular, malia ocupar unha proporción moito menor da súa superficie terrestre. Como resultado, a costa galega ofrece unha gran diversidade de condicións ambientais, incluíndo zonas moi expostas ao océano, áreas semi-protexidas e enclaves interiores máis resgardados, onde a constante interacción entre augas mariñas e achegas fluviais xera marcados gradientes de salinidade que condicionan a biodispoñibilidade e o comportamento dos contaminantes.

Esta diversidade combínase cun mosaico de usos do solo que inclúe espazos naturais protexidos, áreas fortemente industrializadas, zonas costeiras con elevada densidade de poboación, e rexións máis rurais e pouco urbanizadas[118,119]. Galicia constitúe, por tanto, unha área de estudo especialmente valiosa para avaliar os efectos da contaminación mariña, xa que combina presións antrópicas intensas cun marco normativo relativamente desenvolvido derivado da súa integración na Unión Europea. Esta dualidade —presións crecentes sobre o litoral xunto cun conxunto de políticas ambientais cada vez máis estritas— permite explorar tanto os impactos da actividade humana como os efectos potenciais das medidas de protección e xestión ambiental aplicadas nas últimas décadas.

3.2.2. Recollida e procesado das mostras

As especies obxecto de mostraxe foron as algas pardas *Fucus ceranoides*, *F. spiralis* e *F. vesiculosus*. Debido á alta frecuencia de hibridación entre ambas e á dificultade de diferenciación morfolóxica entre *F. spiralis* e *F. vesiculosus*, estas dúas especies foron tratadas conxuntamente (Táboa 1). Ademais, os individuos foron recollidos sen receptáculos, o que impide a súa identificación baseada no sistema reprodutivo —*F. spiralis* é hermafrodita mentres que *F. vesiculosus* é dioica—, unha das poucas características morfolóxicas útiles para a súa distinción. Por último, non se pode descartar a presenza doutros taxóns estreitamente

relacionados dentro do mesmo complexo, como *F. macroguiryi*. En conxunto, trátase dun grupo morfoloxicamente plástico no que a hibridación é habitual e está amplamente documentada[120].

Táboa 1. Número de sitios de mostraxe por ano e por especie.

	1990	2001	2003	2005	2007	2021
Fucus ceranoides	79	14	14	14	14	58
Fucus vesiculosus - F. spiralis	48	25	34	35	35	76

A mostraxe levouse a cabo no mes de xullo para todos os anos co fin de minimizar a variabilidade estacional[103]. En cada punto, recolléronse mostras compostas por varios individuos durante a marea baixa (n = 30), seguindo un patrón en zigzag en paralelo á liña de costa para asegurar unha ampla representación da variabilidade espacial. As algas foron lavadas *in situ* con auga de mar para eliminar partículas dos sedimentos e organismos adheridos, e posteriormente transportadas ao laboratorio en condicións de refrixeración[91].

No laboratorio seleccionáronse as tres dicotomías máis recentes de cada individuo, correspondentes ao tecido máis novo[103]. Estes fragmentos foron secados a 40 °C, homoxeneizados nun muíño tanxencial libre de metais pesados e almacenados en viais de vidro até o momento da súa análise. Os viais de vidro foron almacenados en escuridade e a temperatura ambiente no Banco de Especímenes Ambientais de Galicia, na Facultade de Bioloxía da USC[112].

3.3. Determinacións de PTEs

Os elementos Al, Cr, Fe, Ni, Cu, Zn, As, Ag, Cd, e Pb das mostras recollidas foron determinados con espectrometría de masas con plasma acoplado (ICP-MS, Agilent 700x) dos servizos centrais da Universidade de Santiago de Compostela previa dixestión cun 69% de HNO3 (w/w). O Hg foi analizado directamente sen dixestión previa nun analizador directo de mercurio (DMA80). A calidade analítica e a reproducibilidade dos resultados foron comprobadas a través do uso de materiais de referencia certificados (*Fucus vesiculosus* ERM-CD200), brancos e réplicas.

3.4. Determinacións de isótopos de Pb

Para caracterizar as fontes potenciais de contaminación por Pb, analizouse a composición isotópica deste metal ($^{206}Pb/^{207}Pb$ e $^{208}Pb/^{206}Pb$) tanto en mostras de algas como en materiais

representativos da contorna (rochas, sedimentos, cerámica dunha fábrica local, e petróleo e diesel procedentes dunha refinería da zona). Estas análises realizáronse mediante espectrometría de masas na Czech University of Life Sciences, Prague (Thermo Scientific™ iCAP™ Q ICP-MS). Para garantir a precisión dos cocientes isotópicos obtidos, e aplicar correccións para compensar os potenciais nesgos do instrumento de medición empregáronse estándares internacionais (NIST SRM 981).

3.5. Análise de nanopartículas de prata

Dez estacións de mostraxe que abranguían o rango de variacións de concentracións de Ag observados en Galicia foron seleccionadas para analizar AgNPs. Para cada estación, utilizáronse mostras recollidas nos anos 1990, 2005 (ou 2007, no caso dunha estación) e 2021. En cada mostra seca (25 mg), realizouse unha extracción enzimática con tampón citrato (pH 4.5), sonicación e incubación con Macerozyme R-10® a 37 °C durante 6 horas. Os extractos filtráronse (5 μm), diluíronse en glicerol ao 1% e analizáronse por SP-ICP-MS tras dilución adicional e baño ultrasónico no Departamento de Química Analítica da Universidade de Santiago de Compostela. A eficiencia de transporte determinouse con software específico, que tamén proporcionou a concentración e distribución de tamaños. Cada mostra foi extraída tres veces e cada extracto analizado entre 3 e 5 veces.

3.6. Tratamento estatístico

Os datos foron analizados empregando o software R (versións 3.6.2 a 4.4.1) e QGIS 3.36.3. As análises estatísticas incluíron estatística descritiva básica (medianas, rangos), probas de normalidade (Shapiro-Wilk) e de homoxeneidade de varianzas (Levene). Debido á non normalidade da maioría dos datos, utilizáronse métodos non paramétricos, como as probas de Mann−Whitney−Wilcoxon, Kruskal−Wallis e as correspondentes probas post-hoc (Dunn, Durbin-Conover), co axuste de p-valores mediante o método Benjamini-Hochberg. Para comparar medidas repetidas, aplicáronse tamén probas de Friedman e test de Wilcoxon emparellado. Para explorar os efectos de factores fixos (ano, especie) e aleatorios (ría), empregáronse modelos lineares mixtos (LMMs).

A evolución temporal das concentracións de PTEs nos datos obtidos a partir da literatura (Estudos 1 e 4) analizouse mediante modelos aditivos xeneralizados (GAMs). A relación entre concentracións preditas por GAMs e variables hidrográficas globais (pH, temperatura superficial, contido térmico oceánico e salinidade) analizouse mediante correlacións de

Spearman. Estas variables foron extraídas de bases de datos públicas como Copernicus Marine Environment Monitoring Service (CMEMS) e National Oceanic and Atmospheric Administration (NOAA).

Para identificar agrupamentos segundo patróns de concentracións metálicas nas principais familias de algas pardas (Dictyotaceae, Fucaceae, Laminariaceae, Sargassaceae), realizouse unha ordenación non-metric Multidimensional Scaling (nMDS) baseada en distancias de Bray-Curtis, utilizando os PTEs mellor representados (Cd, Cu, Fe, Pb, Zn). A significancia das diferenzas entre grupos avaliouse mediante Analysis of Similarities (ANOSIM).

Tamén se realizaron análises de compoñentes principais (PCA), Positive matrix factorization (PMF) e modelos de mestura isotópica bayesiana (MixSIAR) para estimar as contribucións relativas das fontes de PTEs. Para estimar as achegas sedimentarias, empregáronse trazadores xeolóxicos (Al e Fe), comparando razóns alga/sedimento para anos con datos dispoñibles.

Por último, realizouse unha análise composicional (CoDA) das concentracións de PTEs en algas pardas empregando a transformación centered-log ratio (CLR) para permitir análises estatísticas multivariantes. A análise principal incluíu Ni, Cu, Zn, Cd e Pb, mentres que As e Hg foron tratadas como variables suplementarias debido á menor dispoñibilidade de datos. Para o xénero *Fucus,* analizouse unha composición ampliada (Al, Cr, Fe, Ni, Cu, Zn, As, Cd, Pb, and Hg. Aplicáronse PCA, Permutational Multivariate Analysis of Variance (PERMANOVA) e Redudancy Analysis (RDA) para avaliar os efectos de factores taxonómicos e ambientais. Tamén se realizaron comparacións por pares entre táxons e análises temporais específicas en *Fucus* spp. mediante PERMANOVA entre os anos 1990, 2001–2007 e 2021.

4. CAPÍTULOS PUBLICADOS

4.1. Capítulo 1: Global Decrease in Heavy Metal Concentrations in Brown Algae in the Last 90 Years.

Referencia:

Aboal, J. R.*; Pacín, C.*; García-Seoane, R.†; Varela, Z.; González, A. G.; Fernández, J. A. Global Decrease in Heavy Metal Concentrations in Brown Algae in the Last 90 Years. J Hazard Mater 2023, 445, 130511. https://doi.org/10.1016/J.JHAZMAT.2022.130511.

**equal contribution*; †*corresponding author.*

Autoría e filiación:

Jesús R. Aboal[1*], Carme Pacín[1*], Rita García-Seoane[2]†, Zulema Varela[1], Aridane González[3], J. Ángel Fernández[1].

[1]CRETUS, Ecology Area, Department of Functional Biology, Faculty of Biology, Universidade de Santiago de Compostela, Santiago de Compostela, 15782, Spain

[2]Instituto Español de Oceanografía, IEO-CSIC, Centro Oceanográfico de A Coruña, 15001 A Coruña, Spain

[3]Instituto de Oceanografía y Cambio Global, IOCAG. Universidad de Las Palmas de Gran Canaria, ULPGC, Spain

Datos da publicación:

Ano: 2023

DOI: https://doi.org/10.1016/J.JHAZMAT.2022.130511

Información da revista:

Nome: Journal of Hazardous Materials ISSN: 1873-3336

Índice de impacto: 12.2 (2023)

Posición na área: 12/358 (Environmental Sciences)

Contribución da doutoranda:

Revisión bibliográfica para a recollida de datos, análise estatística, visualización, e escritura do artigo.

Autorización da revista:

Journal of Hazardous Material forma parte da editorial Elsevier, que permite que as autoras empreguen os artigos en teses de doutoramento, como se pode ver no anexo 1.

Material suplementario:

Anexado ao final do artigo a excepción do arquivo Excel con todos as referencias e datos utilizados na metanálise, que se pode descargar en:
https://doi.org/10.1016/J.JHAZMAT.2022.130511

Journal of Hazardous Materials 445 (2023) 130511

Contents lists available at ScienceDirect

Journal of Hazardous Materials

journal homepage: www.elsevier.com/locate/jhazmat

Global decrease in heavy metal concentrations in brown algae in the last 90 years

J.R. Aboal [a,1], C. Pacín [a,1], R. García-Seoane [b,*], Z. Varela [a], A.G. González [c], J.A. Fernández [a]

[a] CRETUS. Ecology Section. Universidade de Santiago de Compostela, Spain
[b] Instituto Español de Oceanografía, IEO-CSIC, Centro Oceanográfico de A Coruña, 15001 A Coruña, Spain
[c] Instituto de Oceanografía y Cambio Global, IOCAG. Universidad de Las Palmas de Gran Canaria, ULPGC, Spain

HIGHLIGHTS

- A decline in metal pollution in algae is widespread in coastal ecosystems worldwide.
- Decrease in algae concentrations may not also occur in seawater but in bioavailability.
- Decreases began from 70's coinciding with the implementation of environmental policies.
- Legislation and ocean acidification can impact on the heavy metal content in algae.

GRAPHICAL ABSTRACT

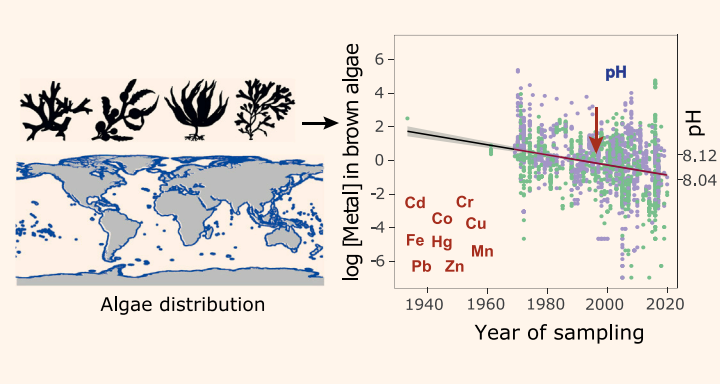

ARTICLE INFO

Editor: Lingxin Chen

Keywords:
Biomonitoring
Marine pollution
Temporal trends
Hazardous elements
Climate change

ABSTRACT

In the current scenario of global change, heavy metal pollution is of major concern because of its associated toxic effects and the persistence of these pollutants in the environment. This study is the first to evaluate the changes in heavy metal concentrations worldwide in brown algae over the last 90 years (>15,700 data across the globe reported from 1933 to 2020). The study findings revealed significant decreases in the concentrations of Cd, Co, Cr, Cu, Fe, Hg, Mn, Pb and Zn of around 60–84% (ca. 2% annual) in brown algae tissues. The decreases were consistent across the different families considered (Dictyotaceae, Fucaceae, Laminariaceae, Sargassaceae and Others), and began between 1970 and 1990. In addition, strong relationships between these trends and pH, SST and heat content were detected. Although the observed metal declines could be partially explained by these strong correlations, or by adaptions in the algae, other evidences suggest an actual reduction in metal concentrations in oceans because of the implementation of environmental policies. In any case, this study shows a reduction in metal concentrations in brown algae over the last 50 years, which is important in itself, as brown algae form the basis of many marine food webs and are therefore potential distributors of pollutants.

* Corresponding author.
E-mail address: rita.garcia@ieo.csic.es (R. García-Seoane).
[1] These authors contributed equally to this work.

https://doi.org/10.1016/j.jhazmat.2022.130511
Received 17 April 2022; Received in revised form 14 November 2022; Accepted 26 November 2022
Available online 28 November 2022

1. Introduction

Metals and metalloids have been discharged in large amounts into the marine environment as a result of human activities (e.g. agriculture, aquaculture, mining, industry, urban spills, etc.) and without adequate environmental control (Halpern et al., 2008; Islam and Tanaka, 2004; Lu et al., 2018; UNEP, 2004) since the Bronze Age (Davis Jr. et al., 2000), but especially since the industrial revolution. In addition, new sources such as 'electronic waste' have emerged (UNEP/GPA, 2006).

Chronic exposure to metals represents a real threat to marine organisms because of their high toxicity at sub-individual level and their persistence and biomagnification capacity (Tlili and Mouneyrac, 2021). Thus, the presence of high or even low concentrations for some metals (e.g. Cd, Pb and Hg) has ecological consequences for the structure and functioning of the entire ecosystem, seriously jeopardizing its integrity and undermining its ecological resilience (Halpern et al., 2008).

The potential risks associated with metallic pollution have been of particular concern for the sound management of coastal zones worldwide. States and organizations worldwide have been implementing a wide range of policies and measures for several years, trying to minimise the damage caused by metal pollution in the marine environment (Grip, 2016). However, the mitigating effects of the policies have been questioned (IPCC, 2021).

Besides metal pollution itself, other drivers of global change, interacting synergistically, can affect the bioavailability and bioaccumulation of metals by organisms, leading to a very complex scenario in the oceans. However, little attention has been paid to the impacts of these anthropogenic drivers on the oceans, and especially on the coastal environments (Duarte, 2014). The oceans are the largest reservoir in the world and have acted as sinks for around 40% of the anthropogenic CO_2 emitted in the past centuries (i.e. more than 118 ± 19 Pg), modifying the carbon dioxide-carbonate equilibrium in water and leading to ocean acidification (Broecker and Clark, 2001; Caldeira and Wickett, 2003; Sabine et al., 2004). Thus, ocean time-series observations indicate changes in the CO_2 system and the decrease in pH over years (Bates et al., 2014), and further acidification is expected in the coming years (Guinotte and Fabry, 2008; IPCC, 2021; Miller et al., 2009). Strong evidence indicates that ocean acidification increases the solubility and mobility of metals and affects their speciation in seawater (Gledhill et al., 2015; Hoffmann et al., 2012; Millero et al., 2009). However, acidification is not the only driver of global change that interacts with these pollutants: increasing water temperature, salinity and organic matter complexation can also modify the accumulation of metals by marine organisms. Based on the available data and the simulation scenario, it has been established that all of these drivers potentially contribute to increasing stress, making organisms more sensitive to even small perturbations caused by chemical stressors (Tlili and Mouneyrac, 2021).

Macroalgae are the dominant species in coastal areas worldwide and maintain the structure and integrity of these ecosystems (Smith et al., 2021). As primary producers at the base of the food webs, macroalgae are responsible for important ecosystem services such as habitat, food and shelter for a diverse community of associated organisms (Tait and Schiel, 2011; Taylor and Cole, 1994). However, macroalgae are negatively affected by metal pollution (Alestra and Schiel, 2015; Miao et al., 2013) and they can also potentially transfer contaminants to organisms that consume them, through biomagnification in marine food webs (Lee and Wang, 2001). Particularly, brown macroalgae (class Phaeophyceae) have been widely used in research studies to monitor metal pollution (e.g. Bonanno and Orlando-Bonaca, 2018; García-Seoane et al., 2018), because their high sorption capacity (Davis et al., 2003) and their ability to integrate high levels of pollutants from the environment (Phillips, 1990; Rainbow, 1995).

Globally, the Northeast Pacific is the area with the highest regional species richness of brown macroalgae of the order Laminariales, Tilopteridales and Desmanrestiales with hotspots of diversity also in the Western Pacific, the Atlantic regions from Greenland to Terranova, and along the Atlantic coast of Europe (Fragkopoulou et al., 2022). While for the order Fucales, the South Pacific is the richest area with hotspots in the Indian Ocean, in the northwest and southeast Pacific, in the North Atlantic, the southeast Mediterranean and the Black Sea. In contrast, higher latitudes such as the Arctic or the Baltic Sea, are areas with low species richness in general. Nonetheless, a study by Barrientos et al. (2020) in the Atlantic Ocean (northwest of the Iberian Peninsula) shows a decline in the number of intertidal red and brown seaweed species since 2014. Although these authors suggest that new data should be collected in the future to confirm this decreasing trend, they believe that water warming due to climate change may be affecting the distribution of seaweed at a regional scale. This conclusion was also reached by Piñeiro-Corbeira et al. (2018) who, through laboratory experiments with different macroalgae, found that water temperature is a driver of changes in abundance. Moreover, the increasing water temperature is also modifying the distribution of macroalgae, mainly in cooler-temperate waters (Kersting, 2016). Despite their worldwide distribution and ecological importance, unfortunately, few studies have reported temporal trends in metal concentrations in brown algae and have generally measured only short-term, regionally circumscribed series. Nonetheless, some authors have observed a surprising decrease in metal concentrations in brown macroalgae, under these limitations (4–7 years in a small region of the North Atlantic Ocean coast), since the beginning of the 21st century (García-Seoane et al., 2021; Viana et al., 2010).

The objective of this study was to determine whether the decrease in metal concentrations in brown algae is restricted to the aforementioned small region during the past two decades or whether it has occurred in other areas of the world at different times. Here, we present the most extensive assessment of metal concentrations in brown macroalgae sampled across the globe carried out to date (>15,700 data – sampling sites/years – from the period 1933–2020), to be used as a proxy for global long-term changes in marine metal pollution. This consistent database enables the reconstruction of detailed long-term trends (multidecadal time series) in Cd, Co, Cr, Cu, Fe, Hg, Mn, Pb and Zn concentrations in algae from observational records. Due to the scarcity of studies on the temporal trends in metal contamination in coastal ecosystems on a global scale (Lu et al., 2018), we report an important basis for global assessment of the effectiveness of environmental measures to reduce marine metal pollution. The study findings will serve to promote new governmental initiatives and environmental goals.

2. Material and methods

2.1. Literature search

Articles published worldwide concerning the metal contents of marine brown algae species (Class Phaeophyceae, Phylum Ochrophyta) were initially selected using the "Documents search" tool in the Elsevier abstract and citation database of peer-reviewed articles from scientific journals (SCOPUS; https://www.scopus.com/). Search syntax yielded articles published in English in the last 68 years (1952–2020) that met some of the following criteria in "article title, abstract and/or keywords": i) containing at least one element and/or its chemical symbol (*cadmium, chromium, cobalt, copper, iron, lead, manganese, mercury, zinc*); and ii) including some terms related to the nature of the elements (*metal, heavy metal*), to pollution monitoring (*bioaccumulation, accumulation, biomonitoring, monitoring, pollution, contamination*), and to algae (*algae, brown algae, macroalgae, macroalgal, seaweed*). The search result (9006 articles) was manually screened by reading the titles and abstracts, and 161 articles were finally selected. Additional publications were searched in the Google Scholar database (http://www.scholar.google.com/) by using the keywords "*metal, monitoring, pollution, brown algae*". Finally, reference lists of the selected articles were also checked. After discarding several studies that did not meet the desired criteria, e.g. they did not

report the concentrations of the elements or the exact location of the sampling sites (either indicating the coordinates, place names or locations on a map or in the text), a total of 368 articles were finally accessed through the search platform, library exchange or by requests to the authors, and included in the database. Data published in annual reports, thesis and others were not considered.

2.2. Data collection

The information of interest for building the database, including "Year of sampling", "Species", "Locations (geographical coordinates)", "Element concentrations" and "Anthropogenic pressure of the sampling stations", was recorded in a data set, which is accessible in a Supplementary file. Some guidelines, described below, were considered for screening the information included in the articles.

2.2.1. Year of sampling

Most of the studies indicated the year when the samples were collected, but when omitted, the year of publication of the article was recorded. In some studies, several sampling surveys were carried out over the years but only a single mean value of the concentrations was reported. In this case, if the same sampling frequency was used over the years (i.e. sampling the same number of days/months in each year), a year in the middle of the time series was taken as the reference year (the latter in two-year sampling campaigns). In the same situation, but with a different sampling frequency, the year most frequently sampled was selected. In the studies with independent monthly values, the annual mean value was recorded.

2.2.2. Species

Scientific names of the species reported in the studies were checked against the taxonomic information included in the global algal database AlgaeBase (AlgaeBase, 2021; http://www.algaebase.org/), and the taxonomically accepted names were recorded. Information about scientific names of the species used in the literature consulted and scientific names currently accepted taxonomically is given in detail in a Supplementary file.

2.2.3. Geographical location

Most of the studies detailed the exact location of the sampling sites, either indicating the coordinates, the name of the sites or including a map. The geographical information programme Google Earth Pro (7.3.2 version) was used to map the points. The coordinate system used was Geographical Coordinates WGS84 (World Geodetic System 84). When sampling locations were indicated by the names of the locations (neither coordinates nor a map were shown), toponyms were searched in Google Earth Pro. When the studies provided sampling locations on land, the closest intertidal zone where brown algae could be found was recorded. When several locations were sampled in the same area but only a single mean concentration was given for all of them, the assigned location corresponded to a mean value of all the point coordinates. If the midpoint was located on land, the closest intertidal location was chosen. Exceptionally, in two of the articles reviewed (Carral et al., 1995; Viana et al., 2010), regional studies covering more than 100 sampling points were carried out in each case, but only regional global results were reported. Information on sampling points was therefore requested directly from the authors.

2.2.4. Element concentrations

In order to enable comparability between data within and between sampling sites, the basis on which the elemental concentrations are expressed must be stated. The choice of the basis was intended to satisfy several considerations: scientific validity, uniformity in groups of contaminants and minimum loss of data. As most of the studies expressed the elemental concentrations in μg g^{-1}, this unit was chosen to present the results in the database. In some cases (e.g. those using nmol g^{-1}), the original data were converted to the reference unit when possible. Only those concentrations expressed on a dry weight basis (DW) were considered. Data was extracted from figures using the WebPlotDigitizer web tool (Version 4.3, https://automeris.io/WebPlotDigitizer/). For concentrations expressed as a range (minimum value–maximum value), the mean value was used. For concentrations indicated as being below the limit of quantification of the analytical technique used (LOQ), the value given was replaced by 0.5 LOQ (Real et al., 2011). When concentrations for the same element were obtained by different analytical methods, a single mean value was recorded. In studies reporting disaggregated concentration values of different sections of the algae thallus, the mean value for all sections was recorded. The bulk data analysis includes the global available data and the statistical analysis confirmed their validity.

2.2.5. Anthropogenic pressure on the sampling sites

In order to prevent erroneous conclusions regarding overall trends in algal contamination, the different sampling sites were classified as belonging to areas affected by anthropogenic pressure (a priori polluted) and areas not affected by anthropogenic pressure (presumed to be free of contamination) on the basis of statements made by the authors or the presence of obvious nearby pollution sources such as urban settlements or power plants.

2.3. Data treatment and statistical analysis

Classification of areas affected and not affected by anthropogenic pressure is subject to some subjectivity, as there are no standardized criteria available for this purpose. The Mann−Whitney−Wilcoxon test was used to assess whether the classification was meaningful by comparing the concentrations of the main hazardous metals (i.e. Cd, Co, Cr, Cu, Fe, Hg, Mn, Pb and Zn) in algae collected in areas affected by anthropogenic pressure and those in algae collected in areas not affected by anthropogenic pressure. Significant differences were obtained for most of the elements in the different families of algae (i.e. Dictyotaceae, Fucaceae, Laminariaceae, Sargassaceae and Others), and generalized additive models (GAMs) were then used to analyse the temporal evolution of the ratio between sampling areas with anthropogenic pressure and the total number of sampled areas. Association between records of algae families and the different oceans was assessed with a chi-square test. To study global trends in algal pollution, GAMs of the logarithmic concentrations of these metals in the different families over the years were also used. The difference between the highest concentration value predicted by the model (excluding the last predicted point and those initial periods of ten years with less than five records) and the value at the last predicted point divided by the former was calculated, providing percentages of variation in metal concentrations for these periods that were considered significant if the 95% confidence intervals of the two points did not overlap. In addition, these values were divided by the number of years of these periods obtaining the percentage of annual variation.

As the trend of climate change related variables can affect the metal speciation, availability and mobility, metal concentrations in brown algae predicted by GAMs over the periods studied were obtained to allow comparison of the time series of each metal with the observed trends for different hydrographic variables over the entire water column (annual values), i.e.: global surface ocean pH (1985–2020), global average sea surface temperature (SST) anomalies (1993–2020), global heat content (1970–2017), and global vertical mean salinity anomalies (PSS) (1970–2017). Hydrographic data are available online from the Copernicus Marine Environment Monitoring Service (CMEMS, https://marine.copernicus.eu/) for pH and SST anomalies, and from the National Oceanic and Atmospheric Administration, National Centers for Environmental Information (NOAA, https://marine.copernicus.eu/) for heat and PSS. Non-parametric Spearman's rank correlation coefficients (ρ) were also calculated in order to determine the relationship between

elemental concentrations predicted by GAMs and hydrographic data.

Finally, a non-metric multidimensional scaling (nMDS) ordination was conducted to explore groupings between the most represented families of brown algae (Dictyotaceae, Fucaceae, Laminariaceae and Sargassaceae) based on the patterns of similarity in metal concentrations. Because of the existence of missing values for the elements included in our data set in a significant number of records, the nMDS was performed maximizing the number of data for the elements more consistently measured across these families, based on the Bray-Curtis dissimilarity matrix constructed from non-transformed metal concentrations for Cd, Cu, Fe, Pb and Zn (n = 1013 records, 5065 individual data). The significance of dissimilarity in metal concentrations between the different assemblage clusters was assessed with ANOSIM statistics. Statistical analysis was carried out using R Software, version 3.6.2 (R Development Core Team, 2008). The "mgcv" (Wood, 2017) and the "vegan" (Oksanen et al., 2020) packages were used to derive the GAMs and compute the nMDS, respectively; "ggplot2" (Wickham, 2009) package was used to plot them. The "PerformanceAnalytics" (Peterson and Carl, 2018) package was used to calculate Spearman's correlations. ArcGIS 10.8 software was used to plot the maps.

3. Results

3.1. Distribution of algae families

Association between various families of brown algae and different oceans is shown in Fig. 1. The Dictyotaceae family is significantly linked to the Indian Ocean, the Mediterranean Sea and the South Atlantic Ocean (Fig. 1A), whereas the Fucaceae family is significantly linked to the North Atlantic Ocean (Fig. 1B); Laminariaceae family is significantly linked to the Pacific Ocean and the Antarctic Ocean (Fig. 1C) and the Sargassaceae family to the Indian Ocean, the Mediterranean Sea and the North Pacific Ocean (Fig. 1D). The other families are mainly associated with the Pacific Ocean, the Antarctic Ocean and the Arctic Ocean (Others in Fig. 1E). The previous associations will be considered in the following analysis, and the trends identified for the different families will be restricted to the afore-mentioned oceans.

3.2. Global trends in metal concentrations

The obtained GAMs for concentrations over time for the different metals and algae families are shown in Figs. 2–5 and Figs. S1–S5. In general, despite some oscillations over time, the concentrations of all metals tended to decrease, although these declines were not always linear or significant in all families. Thus, considering all the families together, significant decreases in concentrations of Pb (84%), Zn (79%), Cd (77%) and Cu (72%) have occurred since the 1970 s (Figs. 2-4, Fig. S2, Table S1), while decreases in concentrations of Mn (75%) and Hg (65%) occurred since the 1980 s (Figs. S1 and S4; Table S1), and in those of Cr (66%), Fe (64%) and Co (60%) since the 1990 s (Fig. 5; Figs. S3 and S5, Table S1). This represents an annual global decrease between 1.4% (in Cu) and 2.6% (in Fe). The order obtained by ranking the metals according to the overall percentage decrease did not correspond to the order based on the annual rates of decrease, as the lag in the period of decrease differs for the various elements considered.

The ratio between sampled areas affected by anthropogenic activities and the total area sampled was very variable and was not consistent with the decrease in metal concentrations (Fig. S6).

3.3. Climate change drivers related to global metal trends

Spearman's rank correlation coefficients between metal concentrations in brown algae predicted by GAMs and pH, SST, heat content and salinity are shown in Table 1 and Fig. 6. A strong significant positive correlation was observed between all elements and pH since 1985. Fig. 6A shows that after normalising the metal concentration values predicted by the GAMs and pH values, when plotted against time, the resulting shape for pH is extremely similar to that of Cd, Co, Cu, Mn and Pb (ρ ca. 1.00), while the trend for Fe and Cr is slightly concave (with lower ρ values, 0.91 and 0.94, respectively), and that of Zn and Hg is convex (with the lowest ρ values, 0.77 and 0.83, respectively) with respect to pH. In turn, since 1993, significant negative correlations were observed with SST, with most metals clearly following the same decreasing trend (ρ between −0.91 and −0.94), although without reacting to small variations of SST over time. However, correlation adjustment for Zn and Hg (ρ = −0.49 and −0.62, respectively) is again weaker because of the convex trend (Table 1, Fig. 6B). Regarding heat content, despite increasing the time window (1970–2017), the results obtained were similar to those for SST, showing a negative relationship with a good fit for most metals (ρ between −0.90 and −0.99), weaker for Fe, Hg, Zn and Cr (ρ between −0.31 and −0.89) (Table 1, Fig. 6D). However, salinity displayed a less clear pattern over time and, thus, the relationship between salinity and metal concentrations obtained were weaker. In addition, this relationship showed variable results, with some metals being positively (i.e. Pb, Cd, and Zn, ρ between 0.33 and 0.52) and others being negatively (Fe and Cr, ρ between −0.52 and −0.40) correlated with salinity since 1970, while Cu, Hg, Co and Mn showed no significant correlation (Table 1, Fig. 6C). These results suggest that ocean acidification and increasing seawater temperatures could be decreasing the bioconcentrated metals in brown algae tissues.

3.4. Trends in metal concentrations by algae family

Considering each individual algae family separately, no consistent pattern was observed when comparing the extent of decrease in element concentrations between families (see Figs. 2–5, Figs. S1–S5, Table S1). In the Dictyotaceae family there has been a significant decrease in concentrations of all metals considered (from 75% in Cu to 88% in Fe), except for Hg; since the early 2000 s, except for Cr and Mn, for which they began in the late 1970 s–early 1980 s (annual declines between 2.0% in Mn and 5.7% in Co). The Fucaceae family has also experienced significant decreases in concentrations of the metals considered, except Mn; however, these decreases began in the 1970–1990 s, ranging from 45% (Fe) to 91% (Co) (annual decreases ranging from 1.3% in Zn to 3.6% in Cr). In the Laminariaceae family, significant decreases were observed in concentrations of Fe, Zn, Cu and Pb, since 1947, and in Co and Cd, since the 1980 s and 2000 s, respectively. The decreases in concentrations range from 75% for Fe to 96% for Cu (with annual decreases ranging from 1.0% for Zn to 4.5% for Cd). In the Sargassaceae family, significant decreases were only observed for Fe (78%), Mn (79%) and Zn (46%) (annual decreases ranging from 1.7% for Mn to 4.6% for Fe). In the other families (Others), significant decreases were only observed in Mn concentrations (80%) (annual decrease of 1.6%).

Fig. S7 shows the result of the non-metric multidimensional scaling (nMDS) based on the concentrations of Cd, Cu, Fe, Pb and Zn found in the algae from the families Dictyotaceae, Fucaceae, Laminariaceae and Sargassaceae. Although no clear separation between clusters was observed due to the overlapping of the groups, the existence of higher concentrations of these metals in Laminariaceae, but especially in Fucaceae, could be observed. However, the ANOSIM results (Global R statistic = 0.151, $p > 0.05$) indicated that the metal composition was not significantly different among families.

4. Discussion

4.1. Global trends in metal concentrations

Long-term time series data revealed a significant global decrease (ranging from 60% to 84%) in the concentration of all metals considered since the early 1970 s, with annual rates of decline around 2%. However, these declines were not always linear and, in some cases, after an initial sharp decrease, a stabilisation or "damping" effect (Jepson et al.,

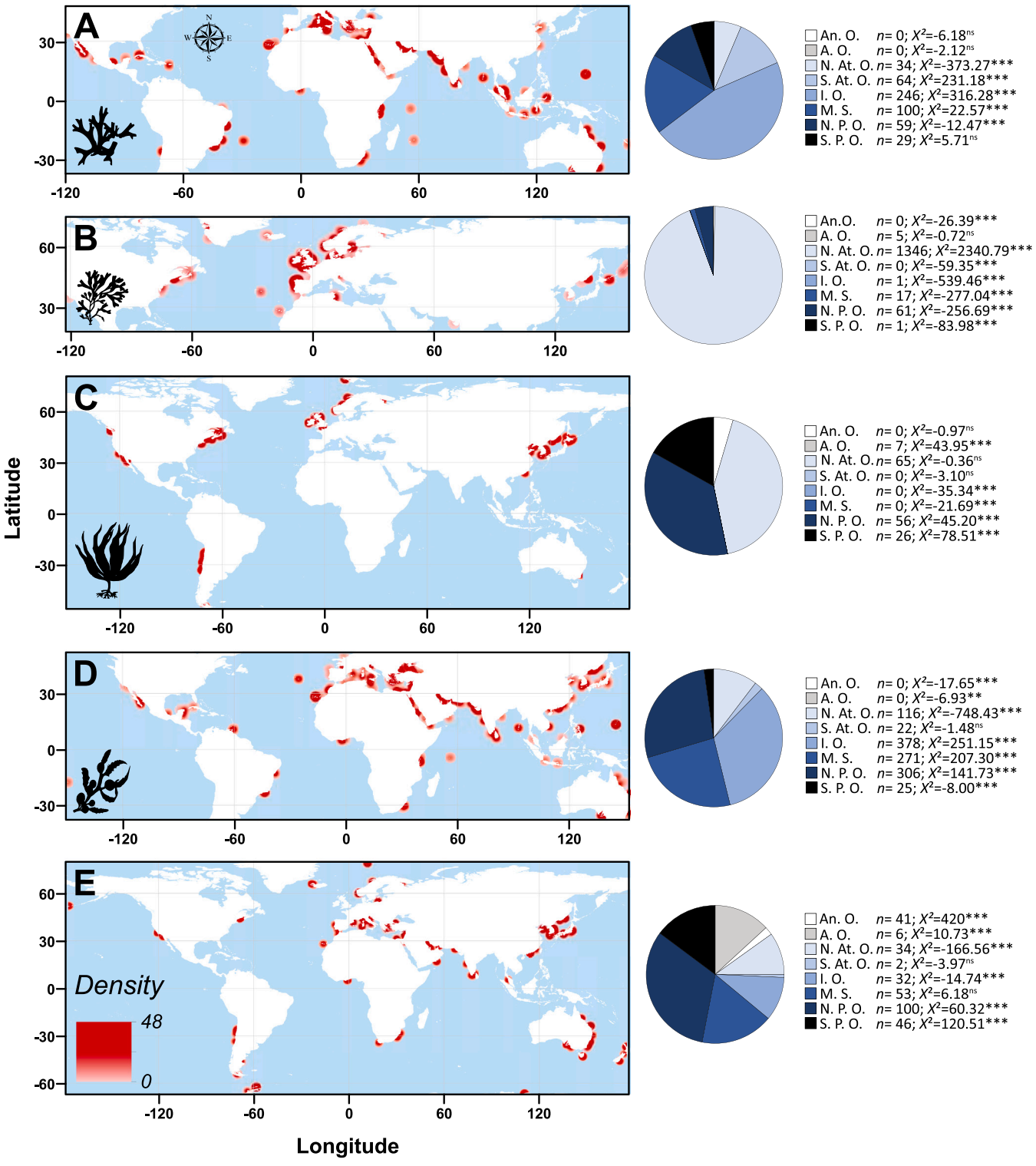

Fig. 1. Distribution of records in the seas and oceans for the different families of brown algae. Left: Kernel density maps of the sampling sites (sites / 0.01 geographic degree) where algae belonging to the following families were collected: A) Dictyotaceae (n, 532), B) Fucaceae (n, 1431), C) Laminariaceae (n, 154), D) Sargassaceae (n, 1118), and E) Others (Adenocystaceae, n = 7; Agaraceae, n = 4, Alariaceae, n = 46; Ascoseiraceae, n = 6; Bachelotiaceae, n = 2; Chordaceae, n = 15; Chordariaceae, n = 7; Cladostephaceae, n = 2; Desmarestiaceae, n = 36; Durvillaeaceae, n = 3; Ectocarpaceae, n = 8; Halosiphonaceae, n = 3; Hormosiraceae, n = 7; Ishigeaceae, n = 3; Lessoniaceae, n = 32; Neoralfsiaceae, n = 1; Phyllariaceae, n = 1; Ralfsiaceae, n = 1; Scytosiphonaceae, n = 106; Seirococcaceae, n = 2; and Stypocaulaceae, n = 19). Right: Pie charts for each family (see above), representing the number of sampling sites in each ocean/sea (An.O.: Antarctic Ocean; A.O.: Arctic Ocean; N.At.O.: North Atlantic Ocean; S.At.O.: South Atlantic Ocean; I.O.: Indian Ocean; M.S.: Mediterranean Sea; N.P.O.: North Pacific Ocean; and S.P.O.: South Pacific Ocean) and the $\chi 2$ value of the null hypothesis of an independent distribution of the families in the different oceans and their significance ($p > 0.01$: ns; $p < 0.01$: **; and $p < 0.001$: ***) obtained in each case. A negative sign before the $\chi 2$ value indicates a negative association, and no sign indicates a positive association. ns: not significant.

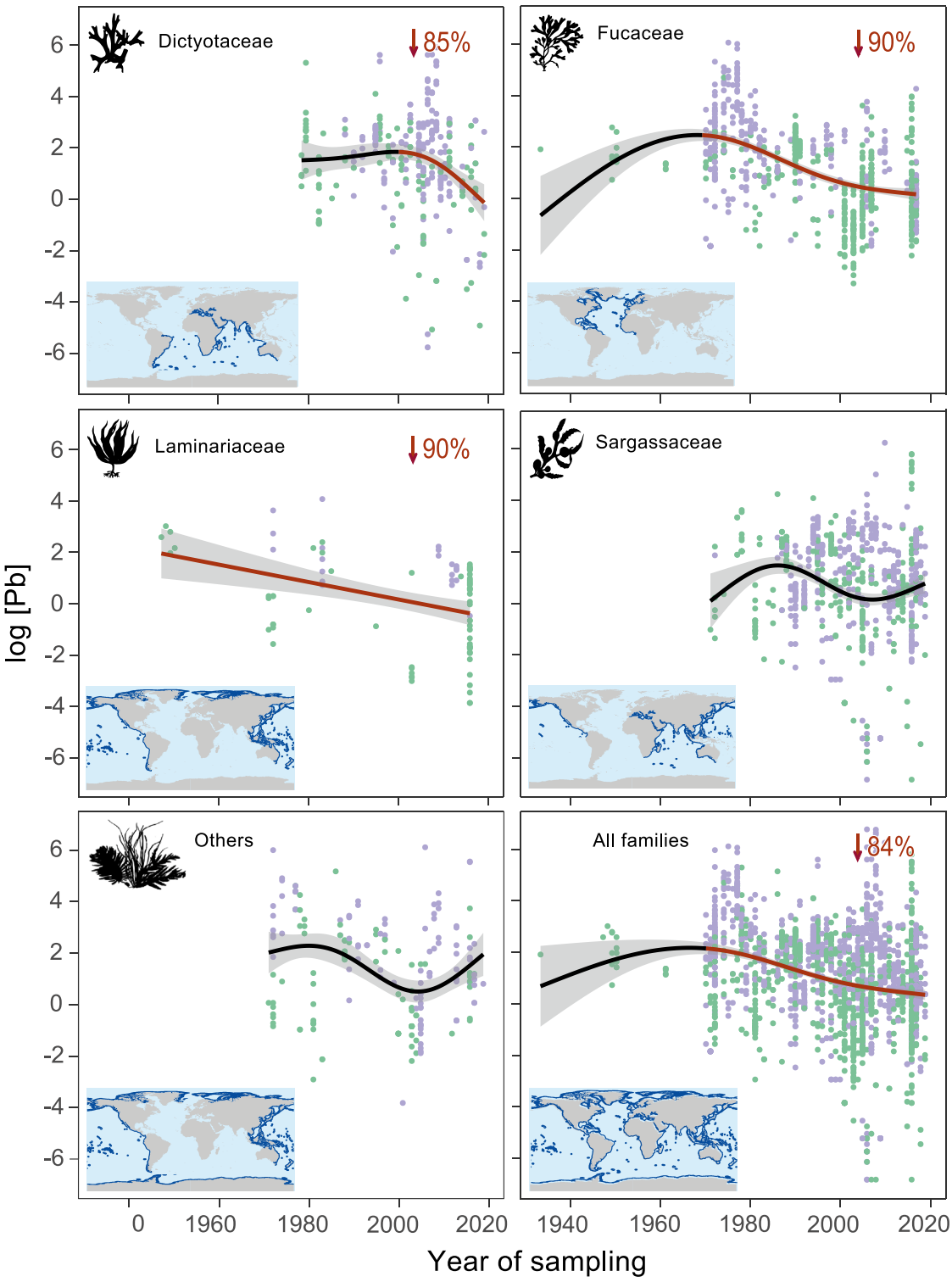

Fig. 2. Temporal changes in log Pb concentrations. Worldwide temporal changes in log Pb concentrations (μg g^{-1} DW) in samples of different families or group of families of brown algae (for Others; see Fig. 1 for more details), and those corresponding to all of the families together. The map inside each graph corresponds to the main area of distribution of each family in the compiled data set (see Fig. 1 for more details). The area coloured in dark blue on the map inside each graph corresponds to the main area of distribution of each family in the compiled data set. The solid black line represents the GAM fit, and the grey area represents the limits of the confidence intervals at 95%. Green dots indicate algae samples collected in areas without any anthropogenic pressure; purple dots indicate areas subjected to anthropogenic pressure. The red lines indicate the period of decline considered to calculate the percentage decline in concentrations, also shown in the figure with a downward arrow.

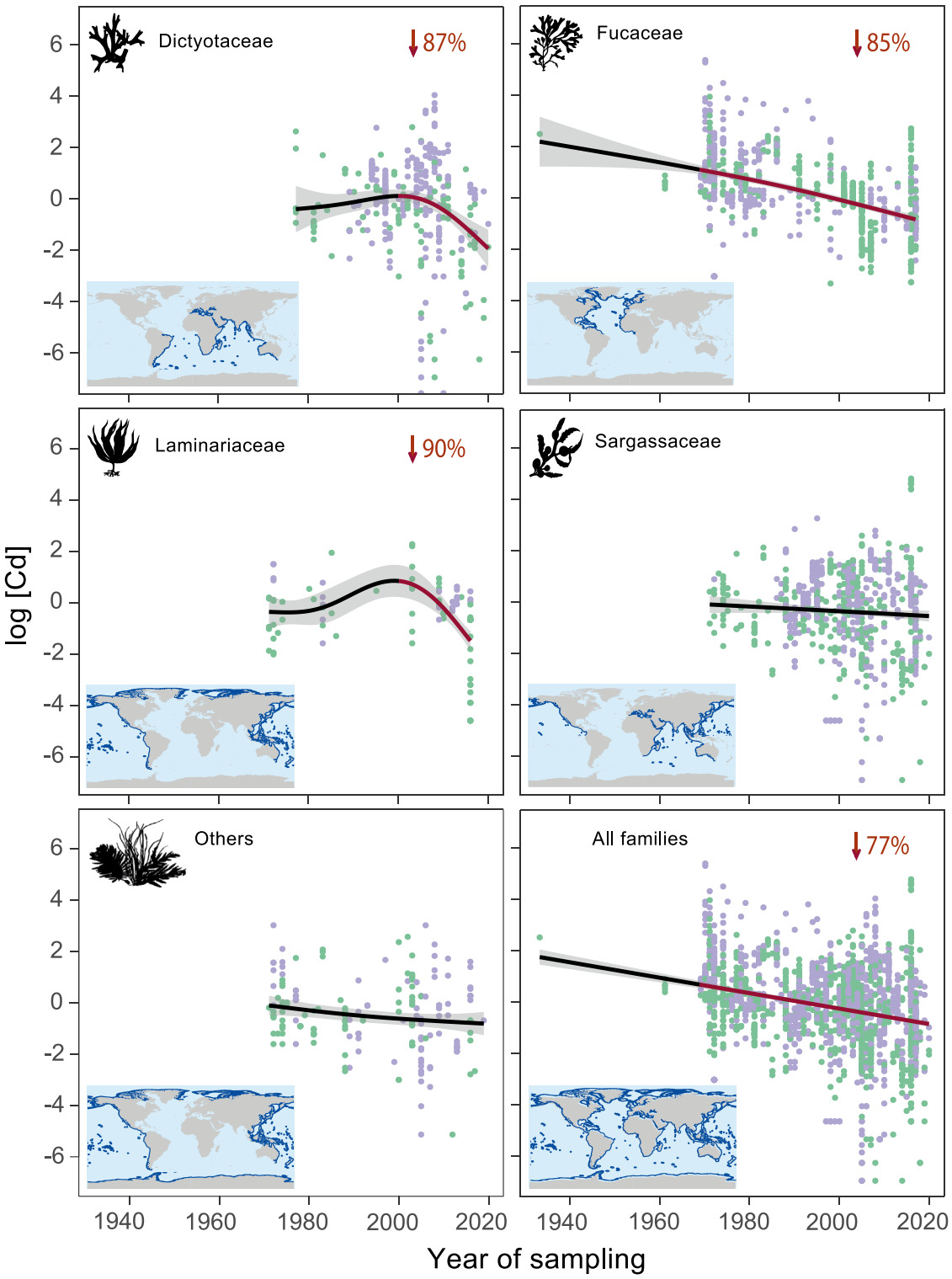

Fig. 3. Temporal changes in log Cd concentrations. Worldwide temporal changes in log Cd concentrations (μg g^{-1} DW) in samples of different families or group of families of brown algae (for Others; see Fig. 1 for more details), and those corresponding to all of the families together. The map inside each graph corresponds to the main area of distribution of each family in the compiled data set (see Fig. 1 for more details). The area coloured in dark blue on the map inside each graph corresponds to the main area of distribution of each family in the compiled data set. The solid black line represents the GAM fit, and the grey area represents the limits of the confidence intervals at 95%. Green dots indicate algae samples collected in areas without any anthropogenic pressure; purple dots indicate areas subjected to anthropogenic pressure. The red lines indicate the period of decline considered to calculate the percentage decline in concentrations, also shown in the figure with a downward arrow.

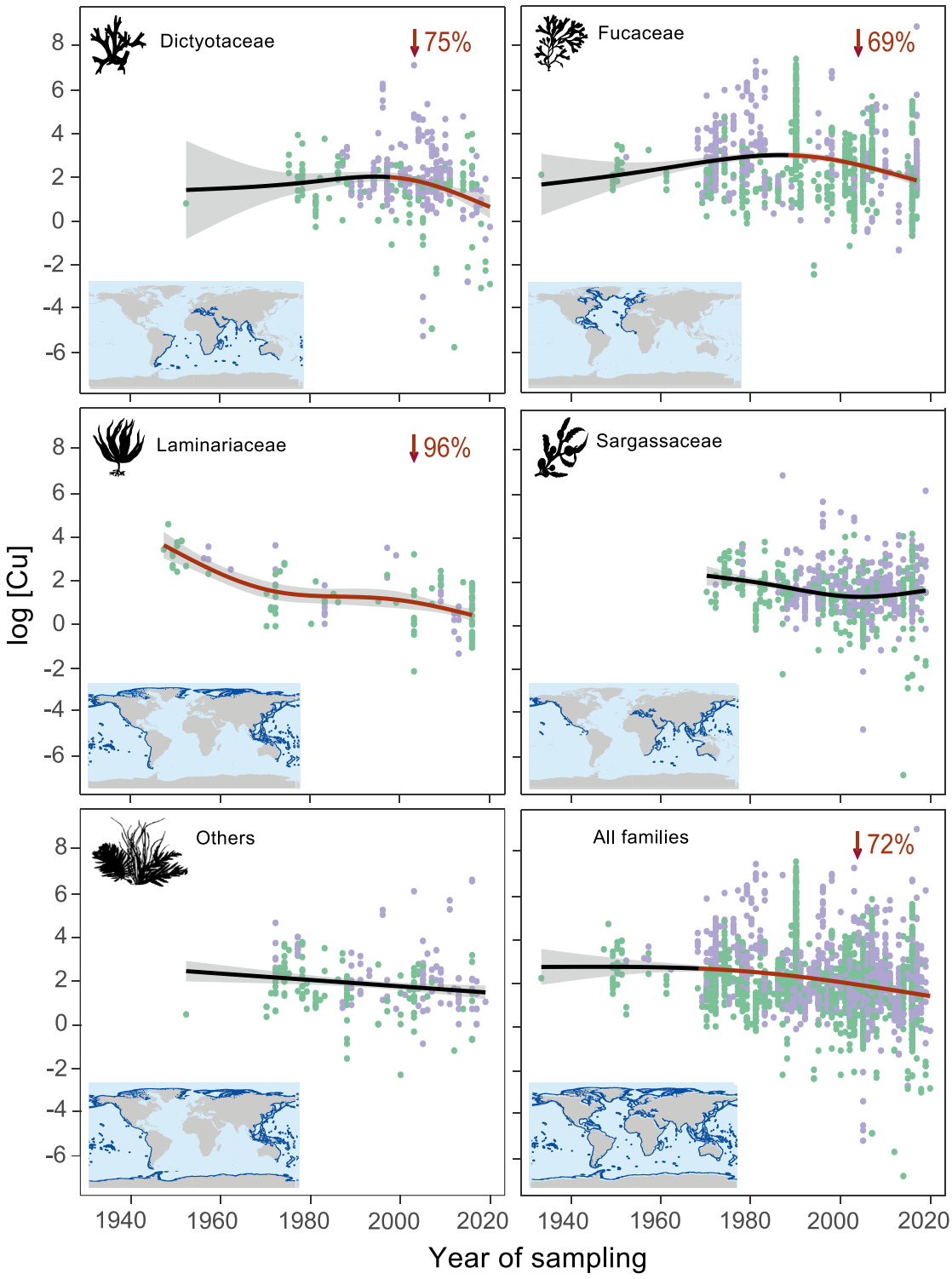

Fig. 4. Temporal changes in log Cu concentrations. Worldwide temporal changes in log Cu concentrations (μg g^{-1} DW) in samples of different families or group of families of brown algae (for Others; see Fig. 1 for more details), and those corresponding to all of the families together. The map inside each graph corresponds to the main area of distribution of each family in the compiled data set (see Fig. 1 for more details). The area coloured in dark blue on the map inside each graph corresponds to the main area of distribution of each family in the compiled data set. The solid black line represents the GAM fit, and the grey area represents the limits of the confidence intervals at 95%. Green dots indicate algae samples collected in areas without any anthropogenic pressure; purple dots indicate areas subjected to anthropogenic pressure. The red lines indicate the period of decline considered to calculate the percentage decline in concentrations, also shown in the figure with a downward arrow.

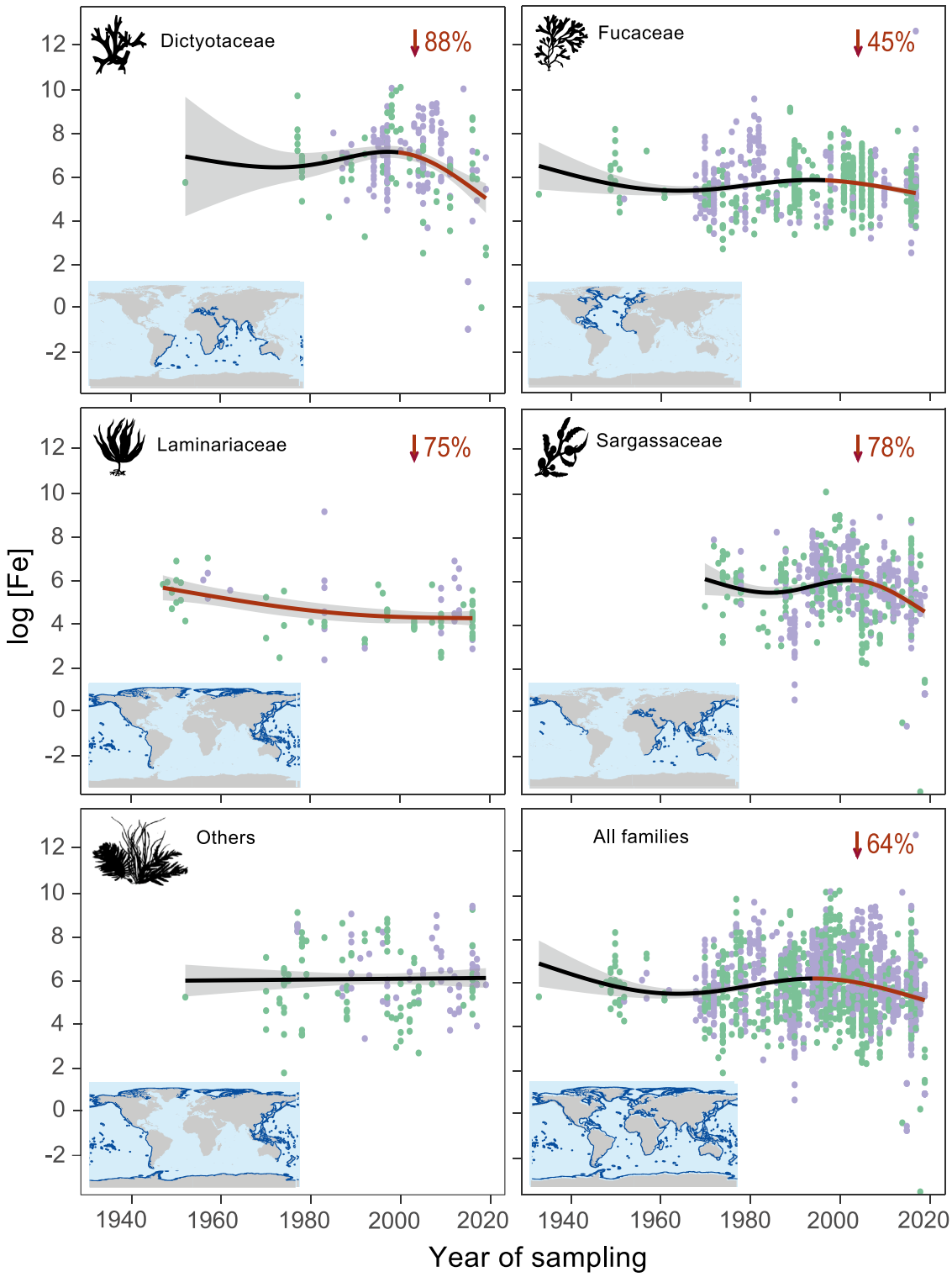

Fig. 5. Temporal changes in log Fe concentrations. Worldwide temporal changes in log Fe concentrations (μg g^{-1} DW) in samples of different families or group of families of brown algae (for Others; see Fig. 1 for more details), and those corresponding to all of the families together. The map inside each graph corresponds to the main area of distribution of each family in the compiled data set (see Fig. 1 for more details). The area coloured in dark blue on the map inside each graph corresponds to the main area of distribution of each family in the compiled data set. The solid black line represents the GAM fit, and the grey area represents the limits of the confidence intervals at 95%. Green dots indicate algae samples collected in areas without any anthropogenic pressure; purple dots indicate areas subjected to anthropogenic pressure. The red lines indicate the period of decline considered to calculate the percentage decline in concentrations, also shown in the figure with a downward arrow.

Table 1
Non-parametric Spearman's rank correlations between metal concentrations in brown algae predicted by GAMs over the periods studied and four hydrographic variables. pH: global annual surface ocean pH (yr^{-1}) relative to the period 1985–2020. SST: global annual average sea surface temperature anomalies (ºC. yr^{-1}) relative to the period 1993–2020. Heat: global annual heat content (Joules) relative to the period 1970–2017. Salinity: global annual vertical mean salinity anomaly (PSS) relative to the period 1970–2017. The values of the Spearman's correlation coefficient (ρ) along with the significance level are shown: ($p < 0.001$, "***"); ($p < 0.01$, "**"); ($p < 0.05$, "*").

	Hydrographic variables			
Elements	pH	SST	Heat	Salinity
Cd	1.00 * **	-0.94 * **	-0.97 * **	0.33 * **
Co	0.99 * **	-0.94 * **	-0.90 * **	-0.02
Cr	0.94 * **	-0.94 * **	-0.53 * **	-0.40 * **
Cu	1.00 * **	-0.94 * **	-0.99 * **	0.26
Fe	0.91 * **	-0.91 * **	-0.31 *	-0.52 * **
Hg	0.83 * **	-0.62 * **	-0.89 * **	0.24
Mn	0.99 * **	-0.94 * **	-0.95 * **	0.06
Pb	0.97 * **	-0.94 * **	-0.94 * **	0.40 * **
Zn	0.77 * **	-0.49 *	-0.83 * **	0.52 * **

2016; Jepson and Law, 2016) has been identified from 1990 onwards (e.g. Hg, Zn). These variations were independent for each family, and it was not possible to identify any common pattern by ordering the elements according to the percentage decrease in concentration. This lack of a common pattern may be attributed to the narrow ranges of variability in the concentrations observed (e.g. in Dyctiotaceae, the decrease in the concentration of 7 elements, except for Cu and Hg, ranged between 82% and 88%).

Accordingly, other studies using brown algae showed the same trends. Kozhenkova et al. (2021) reported decreasing trends in metal concentrations in *Sargassum miyabei* and *S. pallidum* in the Sea of Japan. Likewise, significant decreases in *Fucus vesiculosus* (Fucaceae) on the NW Iberian coast, between 2001 and 2007, specifically for Al, Cd, Co, Fe, Hg, Ni and Zn (annual decrease from 5% to 10%) were detected (Viana et al., 2010); and even greater annual decreases (between 10% and 20%) were observed for Co, Fe, Hg, Ni and Zn between 2015 and 2019 (García--Seoane et al., 2021). Thus, the findings of the present study are consistent with these previous observations, despite the different nature of the approaches compared, i.e. large spatial-temporal scale with low resolution and non-standardized methodologies (present study) versus small spatial-temporal scale with high resolution using standard methods

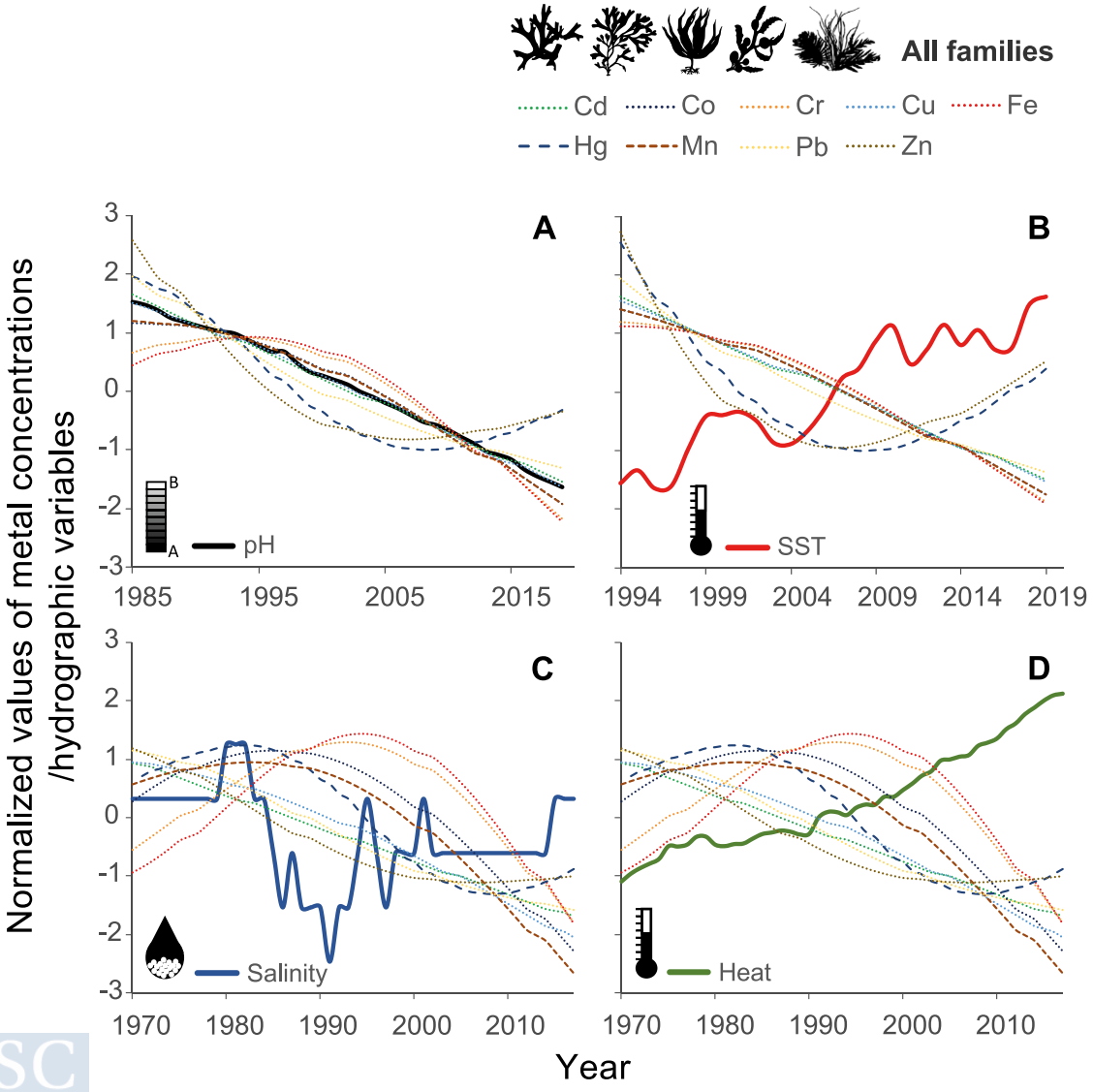

Fig. 6. Metal concentration values obtained in the GAM adjustments and subsequently normalised, and water variable data according to the periods of years available for these variables: A) pH: annual global surface ocean pH (yr^{-1}) from 1985 to 2020; B) SST: global annual average sea surface temperature anomalies (ºC yr^{-1}) from 1993 to 2020; C) Salinity: annual global vertical mean salinity anomaly from 1970 to 2017; D) Heat: global annual heat content (Joules) from 1970 to 2017.

(regional studies).

However, in other organisms and in abiotic components of the oceans the results obtained were not homogeneous. Thus, significant decreasing trends in metal concentrations have been detected in bivalves and fish in the European Economic Area (EEA, 2003), in offshore sediments in the Cantabrian Sea (Garmendia et al., 2019), the China Sea (Yang et al., 2021), the North Sea (except for Zn, Le et al., 2021), and in coastal waters of South Africa (Wepener and Degger, 2012). In contrast, Dong et al. (2021) found that, globally, the levels of metals in sediments have not changed significantly over time, and those of Cd and Hg have even increased. Increases in metal concentrations have also been reported in mussel tissues in the North Sea (Mubiana, 2005), in marine sediments of the Aegean Sea (Sert, 2018) and in coral reefs in the China Sea and the Persian Gulf (Chen et al., 2010; Jafarabadi et al., 2017; Song et al., 2014). Finally, other studies found different direction trends depending on the metals and locations studied, as in the case of offshore sediments in the Persian Gulf (Nicolaus et al., 2022) or the franciscana dolphins in South America (Garcia-Garin, 2021). Although these results differ from those obtained in the present study, the different environmental compartments studied (i.e. sediment, animals, etc.) and the reduced spatial scale of most of them make these results compatible with the global downward trend and the high variability observed in our study.

4.2. Trends in metal concentrations by algae family and region

Regarding the different algae families, the detailed evaluation of the trends revealed some differences between groups, with the highest annual rates of decrease reached in the Dyctiotaceae family (from over 3–6%), almost doubling the rates in other families for elements such as Co, Cu, Pb and Zn. These differences may be explained by different reasons; firstly, the different bioconcentration capacity among species and/or genera. For example, the genus *Padina* (which accounts for >70% of our database records for the family Dyctiotaceae), includes some of the species with the highest capacity to concentrate metals (Jalali et al., 2002; Sheng et al., 2005) and may be somewhat more sensitive to major changes in environmental metals than other brown species. However, the nMDS performed in this study testing the different uptake capacities of the families considered (see Supplementary Fig. 7) was not significant. Secondly, since the families considered are restricted to certain oceans and seas, the different decreasing trends between families may reflect different changes in metal concentrations in the marine environment depending on where they are located.

4.3. Underlying causes of the observed trends

Previous sections showed a decrease in metal concentrations in brown algae consistent with findings in the existing literature. This decline can be explained by different causes such as a decrease in the ions bioavailability, adaptive mechanisms of the algae that diminish their ability to bioconcentrate metals, or a global reduction in metal concentrations in oceans.

4.3.1. Climate change drivers

Climate change invokes the increase of surface seawater temperature, salinity, heat content and ocean acidification, which rules the metals speciation and mobility. In this sense, strong significant correlations between pH and metals considered were found in this study (Fig. 6A, Table 1). Decreasing pH causes changes in the hydrogen, carbonate, and hydroxide ion concentrations in seawater, which affects: i) the adsorption of the ions by the protonation of chemical active sites of the algae cell walls, decreasing the number of available sites for the metals (González and Pokrovsky, 2014; Yee and Fein, 2001), and could explain the relationship between pH and the adsorption and uptake of metals found in brown algae (Haug, 1961; Lu et al., 2009); ii) the speciation of metals in solution (González-Dávila et al., 1995; González and Pokrovsky, 2014; Gledhill et al., 2015; Miller et al., 2014; Millero et al., 2009; Stockdale et al., 2016), increasing the free, bioavailable species of metals whose speciation is related to the above-mentioned ions; iii) complexation with organic matter as previously exposed in i) (Calace and Petronio, 2004; Cheng et al., 2020); iv) the sediment-water exchange of metals mainly reducing the metal sorption of metals to sediments (López et al., 2010); and v) the organism's metabolism and functioning that may modify the uptake of metals (e.g. changes in membrane permeability), although to our knowledge these changes are not properly studied in brown algae (Roleda and Hurd, 2012). While the first pH effect would reduce the levels of metals in the algae, the second, the third and the fourth would increase them, and the fifth is difficult to predict. Hence, the final effect of ocean acidification in metal concentrations in brown algae over time remains uncertain and will depend on the algae species and the metals considered, the pollution source and the geological composition of the sediments. Therefore, although the results suggest a strong relationship between pH and algae metal concentrations (Table 1, Fig. 6A), there is not enough information to state which fraction of the obtained decrease in metal concentration can be attributed to the observed decrease in pH (which in fact was limited, ca. 0.002 units.yr^{-1}, during the studied period). Other variables showing collinearity with pH, not considered here, could be also responsible for the decrease in metal concentrations in the algae.

Likewise, SST anomalies and heat content resulted significantly correlated with metal concentrations trends (Table 1, Figs. 6B and 6D). Temperature affects metal-algae interactions by changes in their metabolism and in the bioavailability of metals. Thus, increasing temperatures impact the particle residence in the euphotic zone and the redox chemistry of metals by implication of photooxidation (Breitbarth et al., 2010). However, robust studies and predictions are not yet available on this regard (Hoffmann et al., 2012).

Finally, vertical mean salinity anomalies displayed different correlations with algae metal concentrations, some of them being not significant (Table 1, Fig. 6C). Salinity can reduce the bioavailability of metals as they strongly bind to salts, a phenomenon known as "salting out effect" (Noyes et al., 2009). However, the salinity pattern over time was not clear and it is difficult to extract preliminary conclusions regarding this variable.

4.3.2. Algae adaptive responses to metal pollution

Another possible factor influencing the decreasing pattern of metal concentrations in algae could be the continued exposure to high metal concentrations in the environment. Thus, García-Seoane et al. (2020) have demonstrated that some *F. vesiculosus* populations exposed to long-term pollution show limited heavy metal uptake because of the adaptive response to metallic toxicity. This response includes the reduction of (García-Seoane et al., 2020): i) their growing speed which limits the concentration dilution by growth; ii) specific leaf area of algae causing the diminishing of the adsorption surface related to the algae mass; iii) alginate concentrations, which are the main compounds involved in algae bioconcentration capacity; and iv) the number or activity of cell membrane cation transporters. Moreover, exudation of organic compounds that complex metals decrease their concentration in brown algae (Andrade et al., 2006; Davis et al., 2003). Finally, it must be taken into account that changes in response to polluted-induced stress can operate in algae living in highly polluted sites, so it is unclear whether this fact could be important enough throughout the entire globe to explain the global decreases detected.

4.3.3. Environmental policies affecting metal concentrations

The observed decrease in metal concentrations in brown algae may reflect a decrease in marine metal pollution as a result of the environmental policies implemented to date. Indeed, the beginning of the decrease coincides with the first measures adopted in the Stockholm Convention (1972) (UN, 1972) and the International Convention for the Prevention of Pollution From Ships (1973) (IMO, 1973). Since then, a

wide range of policies has been established, particularly since the 1990–2000 s, by the major global marine-related organizations and conventions within the United Nations system, coordinating intergovernmental responses against metal pollution, via environmental programmes and actions. Implemented measures include those taken by the UN Conference on Environment and Development (UNCED), the UN Convention on Law of the Sea (UNCLOS), the Intergovernmental Oceanographic Commission of UNESCO (IOC), the International Maritime Organization (IMO) and the United Nations Environment Programme (UNEP) (UN, 2013, 1992, 1982). Moreover, other regional marine-related organizations collaborate, especially in developed countries: the European Environment Agency (EEA), the U.S. Environmental Protection Agency (US-EPA) or the China State Environmental Protection Administration (SEPA).

Metal-specific measures implemented have been mostly developed for Cd and Pb (e.g. Battery Directive and Directive 2006/66/EC of the EU) and for Hg (e.g. Mercury Export Ban act -US EPA, 2008, EU Regulation 2017/852 and Minamata Convention on Mercury, 2013). In addition, the closure of most of the non-ferrous refining and smelting industries and coal-fired electricity generation plants together with the decrease in coal consumption and the implementation of effective waste treatment in developed countries have been produced. As a result, a 34% reduction in the release of trace metals to water from Europe's industries in the period 2010–2016 has been reported (EEA, 2018). Likewise, Canada has registered a decrease of Pb by 89% (907 t) between 1990 and 2020 and, in China, emissions of metals in waste water decreased 28% between 2016 and 2019. Moreover, the MSC-E Technical Report 1/2015 reported a total reduction of 78% in Pb, 53% in Cd and 23% in Hg between 1990 and 2012 for the EMEP region (Europe, Caucasus and Central Asia). Thus, it seems that the results obtained in this study can be explained to a large extent by the real reduction of metal pollution observed in the marine environment in developed countries. However, at the global scale, this reduction does not seem to be as clear, and there are even indications of an increase in pollution (e.g. Emissions Database for Global Atmospheric Research reported a significant global increase in Hg air emissions between 1970 and 2012). Since the vast majority of the data recorded in this study were collected in developed countries, an increase in the sampling effort in both developing and underdeveloped countries is essential.

5. Final remarks

The meta-analysis conducted showed robust decreases in metal concentrations (45–96%) for all the brown algae families considered, distributed throughout the World's oceans. Thus, the high variability obtained did not prevent the detection of consistent temporal changes. This variability is not only explained by differences in metal concentrations in the environment or by changing physico-chemical parameters such as pH, but also by the use of non-standardised methodologies within the collected studies (i.e. different algal species with varying size/age, different sampling times, different analytical techniques, lower analytical quality and lower number of samples in previous studies, etc.). The trends were quite synchronous and post-date global marine environmental protection actions, which could be the main cause of these temporal patterns, although decreasing pH and increasing SST and heat content could also explain them partially. Therefore, this study found, for the first time, a decline in the bioconcentrated metal levels of brown macroalgae for the last 40–50 years, and with it, a potential decline of metal concentrations in world's intertidal habitats. However, most of the records were located in North Atlantic Ocean, with other oceans such as the Arctic Ocean or the South Atlantic Ocean poorly represented (18 and 88 records respectively). Thus, conclusions drawn here must be applied primarily to the North Atlantic Ocean and monitoring efforts in other oceans should be increased. This data can be used as a starting point for future emission scenarios and to inform management decisions.

Competing Interest Declaration

The authors declare that they have no competing financial or non-financial interests that could have influence the work reported in this paper.

CRediT authorship contribution statement

J.R. Aboal, J.A. Fernández: Study conception and design. **J.R. Aboal, C. Pacín, R. García-Seoane, Z. Varela, J.A. Fernández**: Data mining. **J.R. Aboal, C. Pacín, R. García-Seoane**: Data analysis and figure design. **J.R. Aboal, C. Pacín, R. García-Seoane, Z. Varela, A.G. González, J.A. Fernández**: Interpretation and wrote the manuscript. All authors reviewed and approved the final version of the manuscript.

Declaration of Competing Interest

The authors declare that they have no known competing financial interests or personal relationships that could have appeared to influence the work reported in this paper.

Data availability

All data are provided in a Supplementary file.

Acknowledgements

C. Pacín was partly supported by funding from the "Bolsa de Investigación Deputación da Coruña". R. García-Seoane was supported by a postdoctoral research grant awarded by the Juan de la Cierva-Formación (FJC2019–040921-I), funded by MCIN/AEI /10.13039/501100011033 (Spain) and EU NextGenerationEU/PRTR programmes. Z. Varela was supported by a postdoctoral research grant awarded by the autonomous government of Galicia (Xunta de Galicia, Spain).

Statement of "environmental implication"

Metallic pollution is of major concern because of the toxic effects and persistence of these pollutants in the environment. This contribution provides the first extensive meta-analysis of metal concentrations and their evolution (15,758 data compiled from 368 studies worldwide over the last century) in brown macroalgae. The findings revealed significant global decreases of Cd, Co, Cr, Cu, Fe, Hg, Mn, Pb and Zn since 1970, coinciding with the implementation of environmental policies. This information is essential to work on future legal regulations and provides some hope about the evolution of metal pollution in the oceans, severely threatened by global change.

Appendix A. Supporting information

Supplementary data associated with this article can be found in the online version at doi:10.1016/j.jhazmat.2022.130511.

References

Alestra, T., Schiel, D.R., 2015. Impacts of local and global stressors in intertidal habitats: Influence of altered nutrient, sediment and temperature levels on the early life history of three habitat-forming macroalgae. J. Exp. Mar. Bio. Ecol. 468, 29–36. https://doi.org/10.1016/j.jembe.2015.03.017.

Andrade, S., Medina, M.H., Moffett, J.W., Correa, J.A., 2006. Cadmium–copper antagonism in seaweeds inhabiting coastal areas affected by copper mine waste disposals. Environ. Sci. Technol. 40 (14), 4382–4387. https://doi.org/10.1021/ES060278C.

Barrientos, S., Barreiro, R., Cremades, J., Piñeiro-Corbeira, C., 2020. Setting the basis for a long-term monitoring network of intertidal seaweed assemblages in northwest Spain. Mar. Environ. Res. 160, 105039 https://doi.org/10.1016/j.marenvres.2020.105039.

Bates, N.R., Astor, Y.M., Church, M.J., Currie, K., Dore, J.E., González-Dávila, M., Lorenzoni, L., Muller-Karger, F., Olafsson, J., Santana-Casiano, J.M., 2014. A time-

series view of changing surface ocean chemistry due to ocean uptake of anthropogenic CO_2 and ocean acidification. Oceanography 27 (1), 126–141. https://doi.org/10.5670/oceanog.2014.16.
Bonanno, G., Orlando-Bonaca, M., 2018. Perspectives on using marine species as bioindicators of plastic pollution. Mar. Pollut. Bull. 137, 209–221. https://doi.org/10.1016/j.marpolbul.2018.10.018.
Breitbarth, E., Achterberg, E.P., Ardelan, M.V., Baker, A.R., Bucciarelli, E., Chever, F., Croot, P.L., Duggen, S., Gledhill, M., Hassellöv, M., Hassler, C., Hoffmann, L.J., Hunter, K.A., Hutchins, D.A., Ingri, J., Jickells, T., Lohan, M.C., Nielsdóttir, M.C., Sarthou, G., Schoemann, V., Trapp, J.M., Turner, D.R., Ye, Y., 2010. Iron biogeochemistry across marine systems - progress from the past decade. Biogeosciences 7, 1075–1097. https://doi.org/10.5194/BG-7-1075-2010.
Broecker, W.S., Clark, E., 2001. Glacial-to-holocene redistribution of carbonate ion in the deep sea. Science 294 (5549), 2152–2155. https://doi.org/10.1126/science.1064171.
Calace, N., Petronio, B.M., 2004. The role of organic matter on metal toxicity and bio-availability. Ann. di Chim. 94 (7–8), 487–493. https://doi.org/10.1002/adic.200490062.
Caldeira, K., Wickett, M.E., 2003. Anthropogenic carbon and ocean pH. Nature 425 (6956), 365. https://doi.org/10.1038/425365a.
Carral, E., Puente, X., Villares, R., Carballeira, A., 1995. Background heavy metal levels in estuarine sediments and organisms in Galicia (northwest Spain) as determined by modal analysis. Sci. Total Environ. 172 (2–3), 175–188. https://doi.org/10.1016/0048-9697(95)04788-3.
Chen, T.R., Yu, K.F., Li, S., Price, G.J., Shi, Q., Wei, G.J., 2010. Heavy metal pollution recorded in Porites corals from Daya Bay, northern South China Sea. Mar. Environ. Res. 70 (3–4), 318–326. https://doi.org/10.1016/j.marenvres.2010.06.004.
Cheng, X., Zheng, M., Zhang, G., Li, F., Chen, H., Leng, Y., 2020. The nature of dissolved organic matter determines the biosorption capacity of Cu by algae. Chemosphere 252, 126465. https://doi.org/10.1016/j.chemosphere.2020.126465.
Davis Jr., R.A., Welty, A.T., Borrego, J., Morales, J.A., Pendon, J.G., Ryan, J.G., 2000. Rio Tinto estuary (Spain): 5000 years of pollution. Environ. Geol. 39 (10), 1107–1116. https://doi.org/10.1007/s002549900096.
Davis, T.A., Volesky, B., Mucci, A., 2003. A review of the biochemistry of heavy metal biosorption by brown algae. Water Res 37 (18), 4311–4330. https://doi.org/10.1016/S0043-1354(03)00293-8.
Dong, M., Chen, W., Chen, X., Xing, X., Shao, M., Xiong, X., Luo, Z., 2021. Geochemical markers of the Anthropocene: Perspectives from temporal trends in pollutants. Sci. Total Environ. 763, 142987 https://doi.org/10.1016/j.scitotenv.2020.142987.
Duarte, C.M., 2014. Global change and the future ocean: a grand challenge for marine sciences. Front. Mar. Sci. 0, 63. https://doi.org/10.3389/fmars.2014.00063.
European Environment Agency (EEA). Environmental management (EMAS). ⟨https://www.eea.europa.eu/about-us/emas⟩ (accessed 11.9.21).
European Environment Agency (EEA), 2003, Topic report No 2/2003. Hazardous substances in the European marine environment: Trends in metals and persistent organic pollutants. ⟨https://www.eea.europa.eu/publications/topic_report_2003_2/⟩.
European Environment Agency (EEA), 2018, Environmental pressures of heavy metal releases from Europe's industry.
Fragkopoulou, E., Serrão, E.A., De Clerck, O., Costello, M.J., Araújo, M.B., Duarte, C.M., Krause-Jensen, D., Assis, J., 2022. Global biodiversity patterns of marine forests of brown macroalgae. Glob. Ecol. Biogeogr. 31 (4), 636–648. https://doi.org/10.1111/geb.13450.
Garcia-Garin, O., Borrell, A., Vighi, M., Aguilar, A., Valdivia, M., González, E.M., Drago, M., 2021. Long-term assessment of trace elements in franciscana dolphins from the Río de la Plata estuary and adjacent Atlantic waters. Science of The Total Environment 788 (147797). https://doi.org/10.1016/j.scitotenv.2021.147797.
García-Seoane, R., Aboal, J.R., Boquete, M.T., Fernández, J.A., 2018. Biomonitoring coastal environments with transplanted macroalgae: A methodological review. Mar. Pollut. Bull. 135, 988–999. https://doi.org/10.1016/j.marpolbul.2018.08.027.
García-Seoane, R., Aboal, J.R., Boquete, M.T., Fernández, J.A., 2020. Phenotypic differences in heavy metal accumulation in populations of the brown macroalgae *Fucus vesiculosus*: A transplantation experiment. Ecol. Indic. 111, 105978 https://doi.org/10.1016/j.ecolind.2019.105978.
García-Seoane, R., Fernández, J.A., Boquete, M.T., Aboal, J.R., 2021. Analysis of intra-thallus and temporal variability of trace elements and nitrogen in *Fucus vesiculosus*: Sampling protocol optimization for biomonitoring. J. Hazard. Mater. 412, 125268 https://doi.org/10.1016/j.jhazmat.2021.125268.
Garmendia, M., de Vallejuelo, Fdez-Ortiz, Liñero, S., Gredilla, O., Arana, A., Soto, G., de Diego, A, M., 2019. Long term monitoring of metal pollution in sediments as a tool to investigate the effects of engineering works in estuaries. A case study, the Nerbioi-Ibaizabal estuary (Bilbao, Basque Country). Mar. Pollut. Bull. 145, 555–563. https://doi.org/10.1016/J.MARPOLBUL.2019.06.051.
Gledhill, M., Achterberg, E.P., Li, K., Mohamed, K.N., Rijkenberg, M.J.A., 2015. Influence of ocean acidification on the complexation of iron and copper by organic ligands in estuarine waters. Mar. Chem. 177, 421–433. https://doi.org/10.1016/j.marchem.2015.03.016.
González, A.G., Pokrovsky, O.S., 2014. Metal adsorption on mosses: Toward a universal adsorption model. J. Colloid Interface Sci. 415, 169–178. https://doi.org/10.1016/j.jcis.2013.10.028.
González-Dávila, M., Santana-Casiano, J.M., Perez-Pena, J., Millero, F.J., 1995. Binding of Cu(II) to the Surface and Exudates of the Alga *Dunaliella tertiolecta* in Seawater. Environ. Sci. Technol. 29 (2), 289–301. https://doi.org/10.1021/es00002a004.
Grip, K., 2016. International marine environmental governance: A review. Ambio 46 (4), 413–427. https://doi.org/10.1007/s13280-016-0847-9.
Guinotte, J.M., Fabry, V.J., 2008. Ocean acidification and its potential effects on marine ecosystems. Ann. N. Y. Acad. Sci. 1134 (1), 320–342. https://doi.org/10.1196/annals.1439.013.
Halpern, B.S., Walbridge, S., Selkoe, K.A., Kappel, C.V., Micheli, F., D'Agrosa, C., Bruno, J.F., Casey, K.S., Ebert, C., Fox, H.E., Fujita, R., Heinemann, D., Lenihan, H.S., Madin, E.M.P., Perry, M.T., Selig, E.R., Spalding, M., Steneck, R., Watson, R., 2008. A global map of human impact on marine ecosystems. Science 319 (5865), 948–952. https://doi.org/10.1126/science.1149345.
Haug, A., 1961. The affinity of some divalent metals to different types of alginates. Acta Chem. Scand. 15 (8), 1794–1795.
Hoffmann, L.J., Breitbarth, E., Boyd, P.W., Hunter, K.A., 2012. Influence of ocean warming and acidification on trace metal biogeochemistry. Mar. Ecol. Prog. Ser. 470, 191–205. https://doi.org/10.3354/meps10082.
Intergovernmental Panel on Climate Change (IPCC), 2021, Climate Change 2021: The Physical Science Basis. Contribution of Working Group I to the Sixth Assessment Report of the Intergovernmental Panel on Climate Change. ⟨https://www.ipcc.ch/report/ar6/wg1/⟩.
International Maritime Organization (IMO). Pollution Prevention. ⟨https://www.imo.org/en/OurWork/Environment/Pages/Pollution-Prevention.aspx⟩ (accessed 11.9.21).
International Maritime Organization (IMO), 1973, International Convention for the Prevention of Pollution from Ships (MARPOL).
IOC-UNESCO. Our Work. ⟨https://ioc.unesco.org/index.php/our-work⟩ (accessed 11.9.21).
Islam, M.S., Tanaka, M., 2004. Impacts of pollution on coastal and marine ecosystems including coastal and marine fisheries and approach for management: A review and synthesis. Mar. Pollut. Bull. 48 (7–8), 624–649. https://doi.org/10.1016/j.marpolbul.2003.12.004.
Jafarabadi, A.R., Bakhtiyari, A.R., Toosi, A.S., Jadot, C., 2017. Spatial distribution, ecological and health risk assessment of heavy metals in marine surface sediments and coastal seawaters of fringing coral reefs of the Persian Gulf, Iran. Chemosphere 185, 1090–1111. https://doi.org/10.1016/j.chemosphere.2017.07.110.
Jalali, R., Ghafourian, H., Asef, Y., Davarpanah, S., Sepehr, S., 2002. Removal and recovery of lead using nonliving biomass of marine algae. J. Hazard. Mater. 92 (3), 253–262. https://doi.org/10.1016/S0304-3894(02)00021-3.
Jepson, P.D., Law, R.J., 2016. Persistent pollutants, persistent threats. Science 352 (6292), 1388–1389. https://doi.org/10.1126/science.aaf9075.
Jepson, P.D., Deaville, R., Barber, J.L., Aguilar, À., Borrell, A., Murphy, S., Barry, J., Brownlow, A., Barnett, J., Berrow, S., Cunningham, A.A., Davison, N.J., ten Doeschate, M., Esteban, R., Ferreira, M., Foote, A.D., Genov, T., Giménez, J., Loveridge, J., Llavona, Á., Martin, V., Maxwell, D.L., Papachlimitzou, A., Penrose, R., Perkins, M.W., Smith, B., de Stephanis, R., Tregenza, N., Verborgh, P., Fernandez, A., Law, R.J., 2016. PCB pollution continues to impact populations of orcas and other dolphins in European waters. Sci. Rep. 6 (1), 18573. https://doi.org/10.1038/srep18573.
Kersting, D.K., 2016, Cambio Climático en el medio marino español: impactos, vulnerabilidad y adaptación. Oficina de Cambio Climático, Ministerio de Agricultura, Alimentación y Medio Ambiente, Madrid.
Kozhenkova, S.I., Khristoforova, N.K., Chernova, E.N., Kobzar, A.D., 2021. Long-Term Biomonitoring of Heavy Metal Pollution of Ussuri Bay, Sea of Japan. Russ. J. Mar. Biol. 47 (4), 256–264. https://doi.org/10.1134/S106307402104009X.
Le, H.M., Bekaert, K., Lagring, R., Ampe, B., Ruttens, A., De Cauwer, K., Hostens, K., De Witte, B., 2021. 4DEMON: Integrating 40 Years of Data on PCB and Metal Contamination in Marine Sediments of the Belgian Part of the North Sea. Front. Mar. Sci. 8, 588. https://doi.org/10.3389/FMARS.2021.681901/BIBTEX.
Lee, W.Y., Wang, W.X., 2001. Metal accumulation in the green macroalga *Ulva fasciata*: effects of nitrate, ammonium and phosphate. Sci. Total Environ. 278 (1–3), 11–22. https://doi.org/10.1016/S0048-9697(00)00884-6.
López, I.R., Kalman, J., Vale, C., Blasco, J., 2010. Influence of sediment acidification on the bioaccumulation of metals in *Ruditapes philippinarum*. Environ. Sci. Pollut. Res. 17 (9), 1519–1528. https://doi.org/10.1007/s11356-010-0338-7.
Lu, Y., Yuan, J., Lu, X., Su, C., Zhang, Y., Wang, C., Cao, X., Li, Q., Su, J., Ittekkot, V., Garbutt, R.A., Bush, S., Fletcher, S., Wagey, T., Kachur, A., Sweijd, N., 2018. Major threats of pollution and climate change to global coastal ecosystems and enhanced management for sustainability. Environ. Pollut. 239, 670–680. https://doi.org/10.1016/j.envpol.2018.04.016.
Miao, L., Yan, W., Zhong, L., Xu, W., 2013. Effect of heavy metals (Cu, Pb, and As) on the ultrastructure of *Sargassum pallidum* in Daya Bay, China. Environ. Monit. Assess. 186 (1), 87–95. https://doi.org/10.1007/s10661-013-3358-1.
Miller, A.W., Reynolds, A.C., Sobrino, C., Riedel, G.F., 2009. Shellfish face uncertain future in high CO_2 world: Influence of acidification on oyster larvae calcification and growth in estuaries. PLoS One 4 (5), e5661. https://doi.org/10.1371/journal.pone.0005661.
Miller, L.A., Macdonald, R.W., McLaughlin, F., Mucci, A., Yamamoto-Kawai, M., Giesbrecht, K.E., Williams, W.J., 2014. Changes in the marine carbonate system of the western Arctic: patterns in a rescued data set. Pol. Res 33 (1), 20577. https://doi.org/10.3402/polar.v33.20577.
Millero, F.J., Woosley, R., Ditrolio, B., Waters, J., 2009. Effect of ocean acidification on the speciation of metals in seawater. Oceanography 22 (4), 72–85. https://doi.org/10.5670/oceanog.2009.98.
Mubiana, V.K., Qadah, D., Meys, J., Blust, R., 2005. Temporal and spatial trends in heavy metal concentrations in the marine mussel *Mytilus edulis* from the Western Scheldt estuary (The Netherlands). Hydrobiologia 540, 169–180. https://doi.org/10.1007/s10750-004-7134-7.
Nicolaus, E.E.M., Maxwell, D.L., Khamis, A.S., Abdulla, K.H., Harrod, R.P., Devlin, M.J., Lyons, B.P., 2022. Spatial and temporal analysis of the risks posed by metal

contamination in coastal and marine sediments of Bahrain. Environ. Monit. Assess. 194, 62. https://doi.org/10.1007/S10661-021-09722-7.
Noyes, P.D., McElwee, M.K., Miller, H.D., Clark, B.W., Van Tiem, L.A., Walcott, K.C., Erwin, K.N., Levin, E.D., 2009. The toxicology of climate change: Environmental contaminants in a warming world. Environ. Int. 35 (6), 971–986. https://doi.org/10.1016/J.ENVINT.2009.02.006.
Oksanen, J., Blanchet, F.G., Friendly, M., Kindt, R., Legendre, P., McGlinn, D., Minchin, P.R., O'hara, R.B., Simpson, G.L., Solymos, P., Stevens, M.H., Szoecs, E., Wagner, H., 2020. vegan: Community Ecology Package. R. Package Version 2, 5–7. ⟨https://CRAN.R-project.org/package=vegan/⟩.
Peterson, B.G., Carl, P., 2018, PerformanceAnalytics: Econometric Tools for Performance. ⟨https://cran.r-project.org/web/packages/PerformanceAnalytics/index.html⟩.
Phillips, D.J.H., 1990. Use of Macroalgae and Invertebrates as Monitors of Metal Levels in Estuaries and Coastal Waters. In: Heavy Metals in the Marine Environment. CRC Press, pp. 81–99.
Piñeiro-Corbeira, C., Barreiro, R., Cremades, J., Arenas, F., 2018. Seaweed assemblages under a climate change scenario: Functional responses to temperature of eight intertidal seaweeds match recent abundance shifts. Sci. Rep. 8 (1), 1–9. https://doi.org/10.1038/s41598-018-31357-x.
R Development Core Team, 2008, R: A Language and Environment for Statistical Computing. R Foundation for Statistical Computing, Vienna, Austria. ISBN 3–900051-07–0. ⟨https://www.R-project.org/⟩.
Rainbow, P.S., 1995. Biomonitoring of heavy metal availability in the marine environment. Mar. Pollut. Bull. 31 (4–12), 183–192. https://doi.org/10.1016/0025-326X(95)00116-5.
Real, C., Ángel Fernández, J., Aboal, J.R., Carballeira, A., 2011. Substituting missing data in compositional analysis. Environ. Pollut. 159 (10) https://doi.org/10.1016/j.envpol.2011.05.006.
Roleda, M.Y., Hurd, C.L., 2012. Seaweed responses to ocean acidification. Seaweed Biology Ecological Studies. Springer,, Berlin, Heidelberg. https://doi.org/10.1007/978-3-642-28451-9_19.
Sabine, C.L., Feely, R.A., Gruber, N., Key, R.M., Lee, K., Bullister, J.L., Wanninkhof, R., Wong, C.S., Wallace, D.W.R., Tilbrook, B., Millero, F.J., Peng, T.-H., Kozyr, A., Ono, T., Rios, A.F., 2004. The Oceanic Sink for Anthropogenic CO_2. Science 305 (5682), 367–371. https://doi.org/10.1126/science.1097403.
Sert, I., 2018. Temporal evolution of lead isotope ratios and metal concentrations in sediments of the north Aegean Sea, in Turkish coast. JRNC 317, 825–840. https://doi.org/10.1007/s10967-018-5947-5.
Sheng, P.X., Tan, L.H., Chen, J.P., Ting, Y.P., 2005. Biosorption Performance of Two Brown Marine Algae for Removal of Chromium and Cadmium. J. Dispers. Sci. Technol. 25 (5), 679–686. https://doi.org/10.1081/DIS-200027327.
Smith, J.G., Tomoleoni, J., Staedler, M., Lyon, S., Fujii, J., Tinker, M.T., 2021. Behavioral responses across a mosaic of ecosystem states restructure a sea otter–urchin trophic cascade. Proc. Natl. Acad. Sci. 118 (11), e2012493118 https://doi.org/10.1073/pnas.2012493118.
Song, Y., Yu, K., Zhao, J., Feng, Y., Shi, Q., Zhang, H., Ayoko, G.A., Frost, R.L., 2014. Past 140-year environmental record in the northern South China Sea: evidence from coral skeletal trace metal variations. Environ. Pollut. 185, 97–106. https://doi.org/10.1016/j.envpol.2013.10.024.
Stockdale, A., Tipping, E., Lofts, S., Mortimer, R.J.G., 2016. Effect of Ocean Acidification on Organic and Inorganic Speciation of Trace Metals. Environ. Sci. Technol. 50 (4), 1906–1913. https://doi.org/10.1021/ACS.EST.5B05624.
Tait, L.W., Schiel, D.R., 2011. Dynamics of productivity in naturally structured macroalgal assemblages: importance of canopy structure on light-use efficiency. Mar. Ecol. Prog. Ser. 421, 97–107. https://doi.org/10.3354/meps08909.
Taylor, R.B., Cole, R.G., 1994. Mobile epifauna on subtidal brown seaweeds in northeastern New Zealand. Mar. Ecol. Prog. Ser. 115, 271–282. https://doi.org/10.3354/meps115271.
Tlili, S., Mouneyrac, C., 2021. New challenges of marine ecotoxicology in a global change context. Mar. Pollut. Bull. 166, 112242 https://doi.org/10.1016/j.marpolbul.2021.112242.
United Nations (UN), 1972, United Nations Conference on the Human Environment. ⟨https://www.un.org/en/conferences/environment/stockholm1972⟩.
United Nations (UN), 1982, United Nations Convention on the Law of the Sea (UNCLOS).
United Nations (UN), 1992, United Nations Conference on Environment and Development (UNCED), in: Earth Summit. ⟨https://www.un.org/en/conferences/environment/rio1992⟩.
United Nations (UN), 2013, Minamata Convention on Mercury.
United Nations Environment Program (UNEP) /Global Programme of Action for the Protection of the Marine Environment from Land-based Activities (GPA), 2006. The state of the marine environment: Trends and processes. ⟨https://www.unep.org/resources/report/state-marine-environment-trends-and-processes⟩.
United Nations Environment Programme (UNEP) . Environmental rights and governance. ⟨https://www.unep.org/explore-topics/environmental-rights-and-governance⟩ (accessed 11.9.21).
United Nations Environment Programme (UNEP), 2004, Annual Evaluation Report. ⟨https://www.unep.org/resources/synthesis-reports/unep-annual-evaluation-report-2004⟩.
United States Environmental Protection Agency (US EPA), 1972, Report Environmental Violations. ⟨https://echo.epa.gov/report-environmental-violations#:~:text=Stop-,Stop,-800–424-8802⟩ (accessed 11.9.21).
Viana, I.G., Aboal, J.R., Fernández, J.A., Real, C., Villares, R., Carballeira, A., 2010. Use of macroalgae stored in an Environmental Specimen Bank for application of some European Framework Directives. Water Res 44 (6), 1713–1724. https://doi.org/10.1016/j.watres.2009.11.036.
Wepener, V., Degger, N., 2012. Status of marine pollution research in South Africa (1960–present. Mar. Pollut. Bull. 64 (7), 1508–1512. https://doi.org/10.1016/J.MARPOLBUL.2012.05.037.
Wickham, H., 2009, ggplot2: Elegant Graphics for Data Analysis. ⟨https://doi.org/10.1007/978–0-387–98141-3⟩.
Wood, S.N., 2017, Generalized additive models: An introduction with R, second edition. 1–476. Chapman and Hall/CRC. ⟨https://cran.r-project.org/web/packages/mgcv/index.html⟩.
Yang, L., Ma, X., Luan, Z., Yan, J., 2021. The spatial-temporal evolution of heavy metal accumulation in the offshore sediments along the Shandong Peninsula over the last 100 years: Anthropogenic and natural impacts. Environ. Pollut. 289, 117894 https://doi.org/10.1016/J.ENVPOL.2021.117894.
Yee, N., Fein, J., 2001. Cd adsorption onto bacterial surfaces: A universal adsorption edge. GCA 65 (13), 2037–2042. https://doi.org/10.1016/S0016-7037(01)00587-7.

Supplementary Information

Global decrease in heavy metal concentrations in brown algae in the last 90 years

Aboal, J.R.[+1], Pacín, C.[+1], García-Seoane, R.[*2], Varela, Z.[1], González, A.G.[3], Fernández, J.A.[1]

[1]CRETUS. Ecology Section. Universidade de Santiago de Compostela.

[2]Instituto Español de Oceanografía, IEO-CSIC, Centro Oceanográfico de A Coruña, 15001 A Coruña, Spain.

[3]Instituto de Oceanografía y Cambio Global, IOCAG. Universidad de Las Palmas de Gran Canaria, ULPGC.

[+]These authors contributed equally to this work.

[*]Corresponding author: rita.garcia@ieo.csic.es

Supplementary Figures

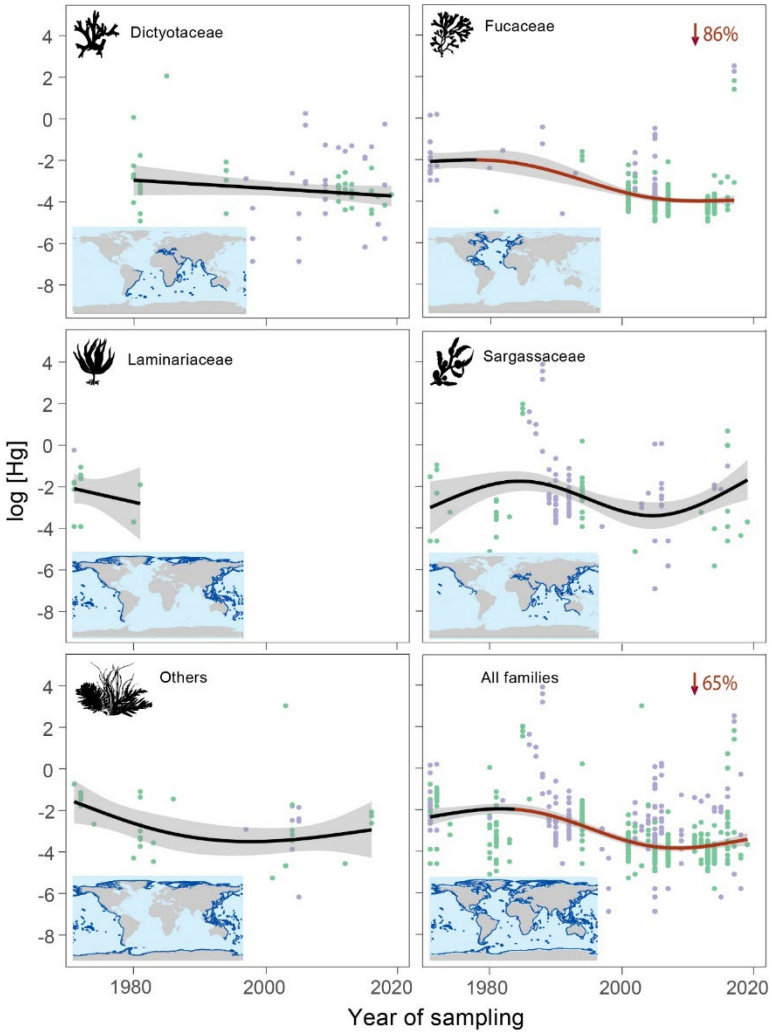

Supplementary Fig. 1. Temporal changes in log Hg concentrations. Worldwide temporal changes in log Hg concentrations (μg g^{-1} DW) in samples of different families or group of families of brown algae (for Others; see Fig. 1 for more details), and those corresponding to all of the families together. The map inside each graph corresponds to the main area of distribution of each family in the compiled data set (see Fig. 1 for more details). The area coloured in dark blue on the map inside each graph corresponds to the main area of distribution of each family in the compiled data set. The solid black line represents the GAM fit, and the grey area represents the limits of the confidence intervals at 95%. Green dots indicate algae samples collected in areas without any anthropogenic pressure; purple dots indicate areas subjected to anthropogenic pressure. The red lines indicate the period of

decline considered to calculate the percentage decline in concentrations, also shown in the figure with a downward arrow.

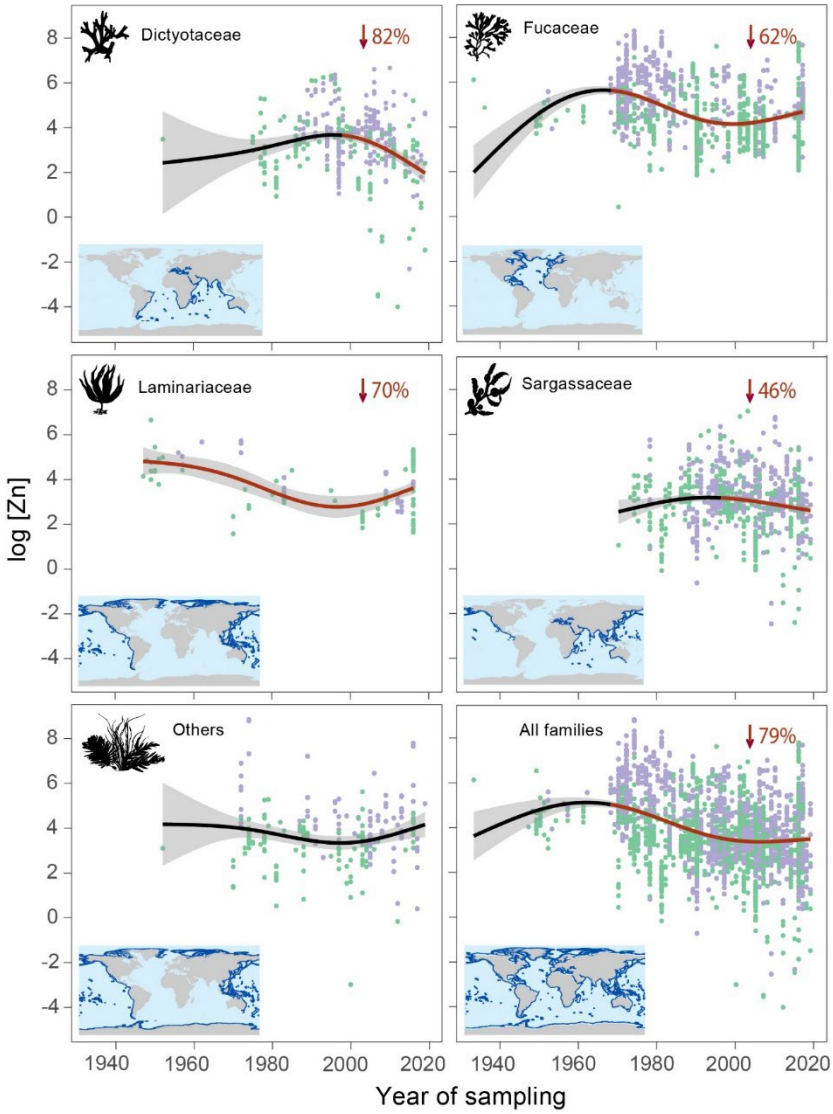

Supplementary Fig. 2. Temporal changes in log Zn concentrations. Worldwide temporal changes in log Zn concentrations (μg g^{-1} DW) in samples of different families or group of families of brown algae (for Others; see Fig. 1 for more details), and those corresponding to all of the families together. The map inside each graph corresponds to the main area of distribution of each family in the compiled data set (see Fig. 1 for more details). The area coloured in dark blue on the map inside each graph corresponds to the main area of distribution of each family in the compiled data set. The solid black line represents the GAM

fit, and the grey area represents the limits of the confidence intervals at 95%. Green dots indicate algae samples collected in areas without any anthropogenic pressure; purple dots indicate areas subjected to anthropogenic pressure. The red lines indicate the period of decline considered to calculate the percentage decline in concentrations, also shown in the figure with a downward arrow.

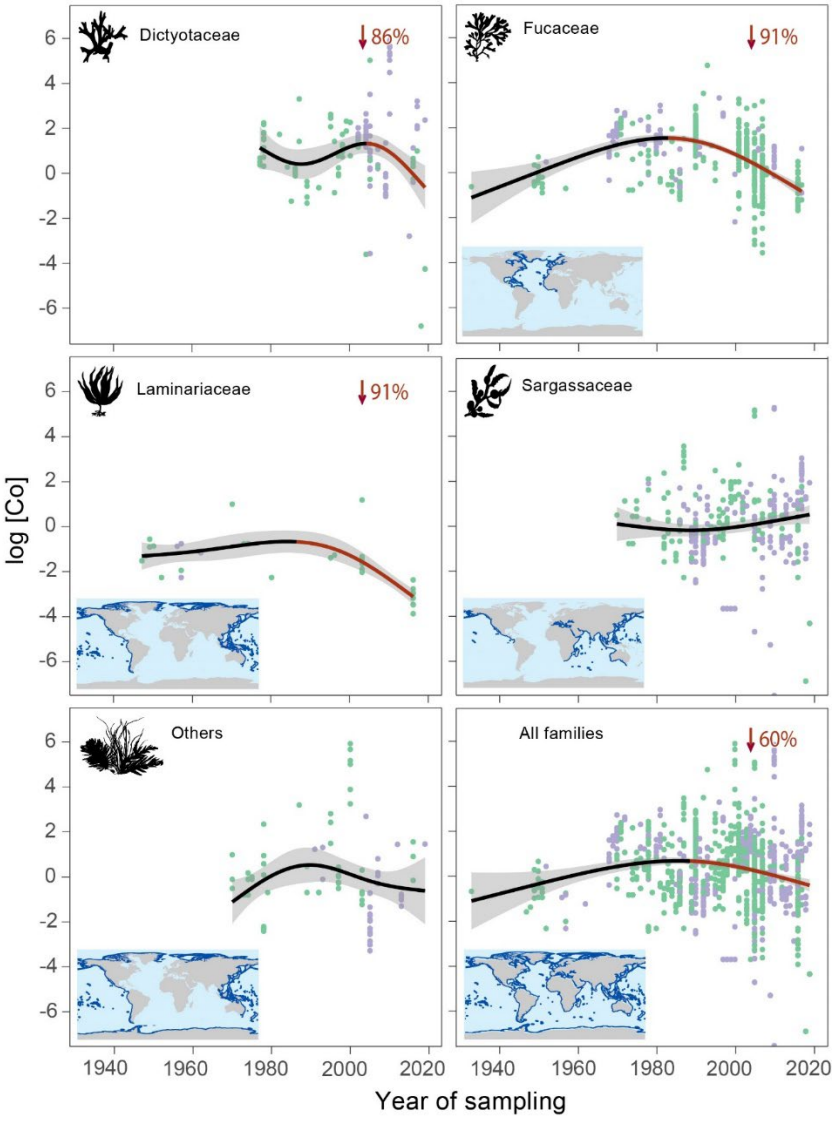

Supplementary Fig. 3. Temporal changes in log Co concentrations. Worldwide temporal changes in log Co concentrations (μg g^{-1} DW) in samples of different families or group of families of brown algae (for Others; see Fig. 1 for more details), and those corresponding to all of the families together. The map inside each graph corresponds to the main area of

distribution of each family in the compiled data set (see Fig. 1 for more details). The area coloured in dark blue on the map inside each graph corresponds to the main area of distribution of each family in the compiled data set. The solid black line represents the GAM fit, and the grey area represents the limits of the confidence intervals at 95%. Green dots indicate algae samples collected in areas without any anthropogenic pressure; purple dots indicate areas subjected to anthropogenic pressure. The red lines indicate the period of decline considered to calculate the percentage decline in concentrations, also shown in the figure with a downward arrow.

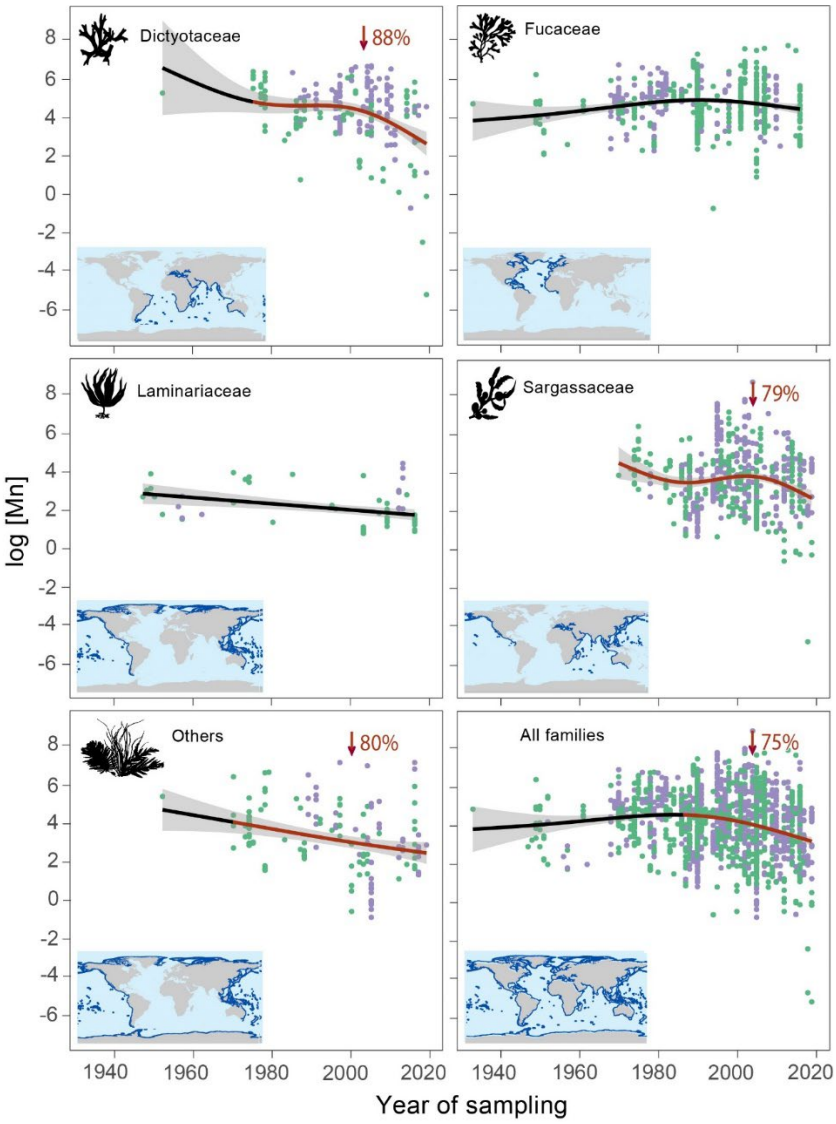

Supplementary Fig. 4. Temporal changes in log Mn concentrations. Worldwide temporal changes in log Mn concentrations (μg g^{-1} DW) in samples of different families or group of families of brown algae (for Others; see Fig. 1 for more details), and those corresponding to all of the families together. The map inside each graph corresponds to the main area of distribution of each family in the compiled data set (see Fig. 1 for more details). The area coloured in dark blue on the map inside each graph corresponds to the main area of distribution of each family in the compiled data set. The solid black line represents the GAM fit, and the grey area represents the limits of the confidence intervals at 95%. Green dots indicate algae samples collected in areas without any anthropogenic pressure; purple dots indicate areas subjected to anthropogenic pressure. The red lines indicate the period of decline considered to calculate the percentage decline in concentrations, also shown in the figure with a downward arrow.

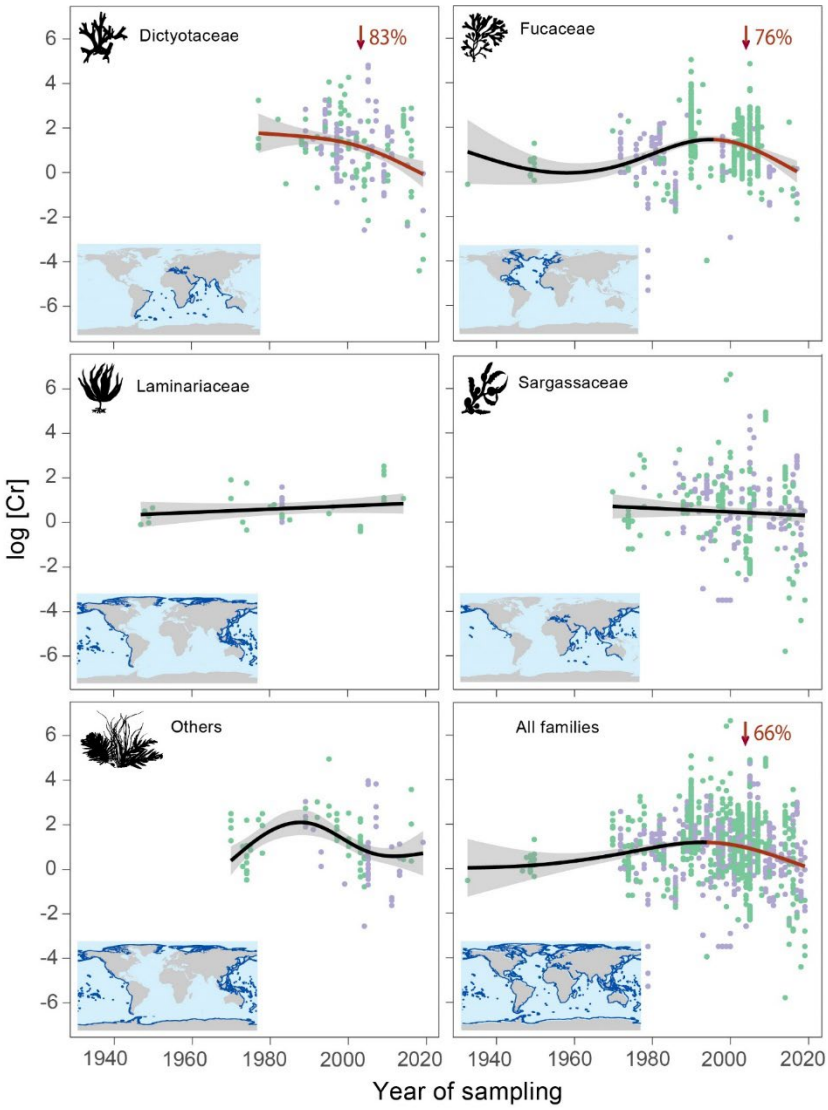

Supplementary Fig. 5. Temporal changes in log Cr concentrations. Worldwide temporal changes in log Cr concentrations (μg g^{-1} DW) in samples of different families or group of families of brown algae (for Others; see Fig. 1 for more details), and those corresponding to all of the families together. The map inside each graph corresponds to the main area of distribution of each family in the compiled data set (see Fig. 1 for more details). The area coloured in dark blue on the map inside each graph corresponds to the main area of distribution of each family in the compiled data set. The solid black line represents the GAM fit, and the grey area represents the limits of the confidence intervals at 95%. Green dots indicate algae samples collected in areas without any anthropogenic pressure; purple dots indicate areas subjected to anthropogenic pressure. The red lines indicate the period of

decline considered to calculate the percentage decline in concentrations, also shown in the figure with a downward arrow.

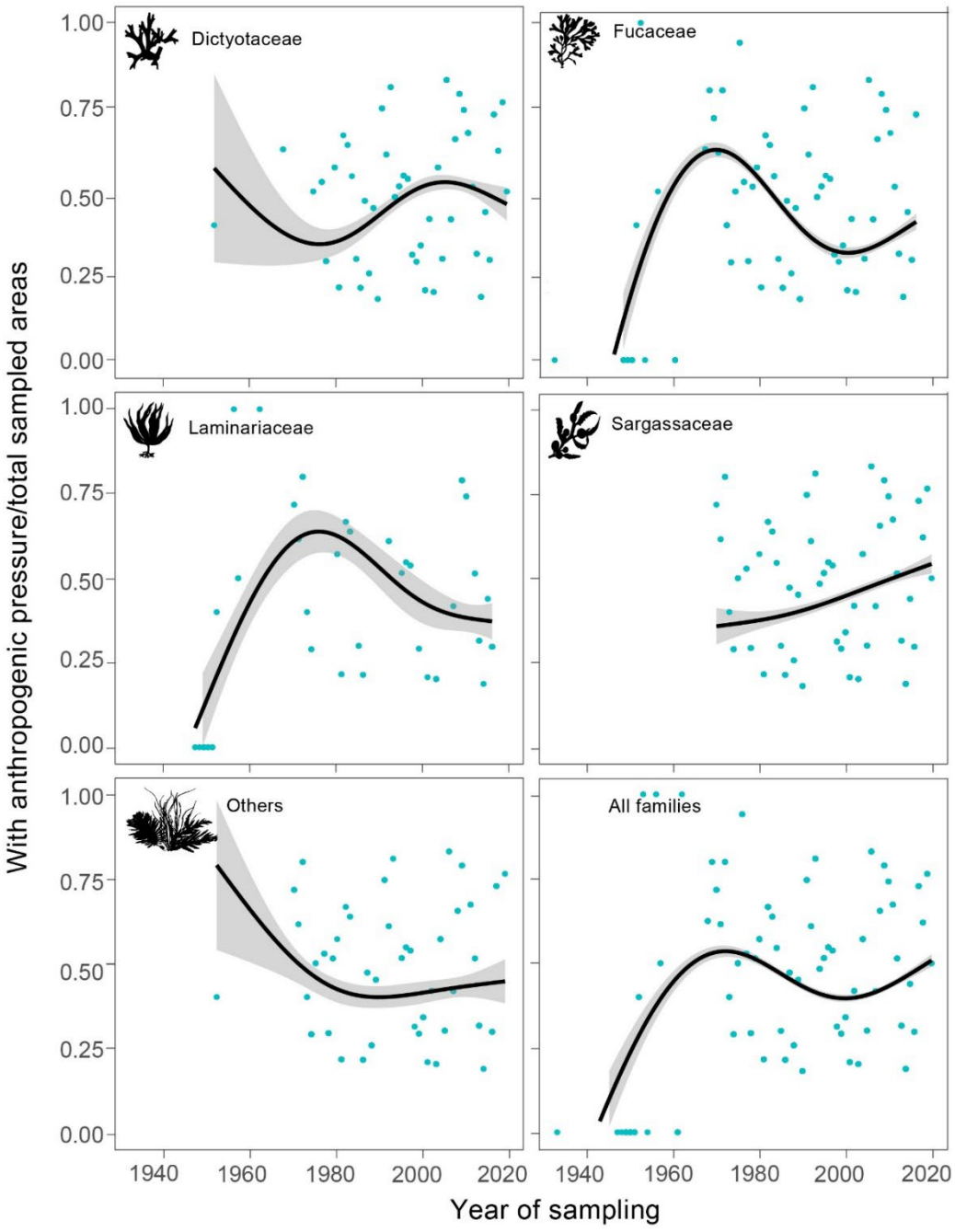

Supplementary Fig. 6. Worldwide temporal changes in the ratio between sampling areas affected by anthropogenic pressure respect to the total number of sampled areas where brown algae samples belonging to different families or group of families (for Others; see Fig. 1 for more details), and all families, were collected. Each point represents this ratio annually.

The solid black line represents the GAM fit, and the grey area the limits of the confidence intervals at 95%.

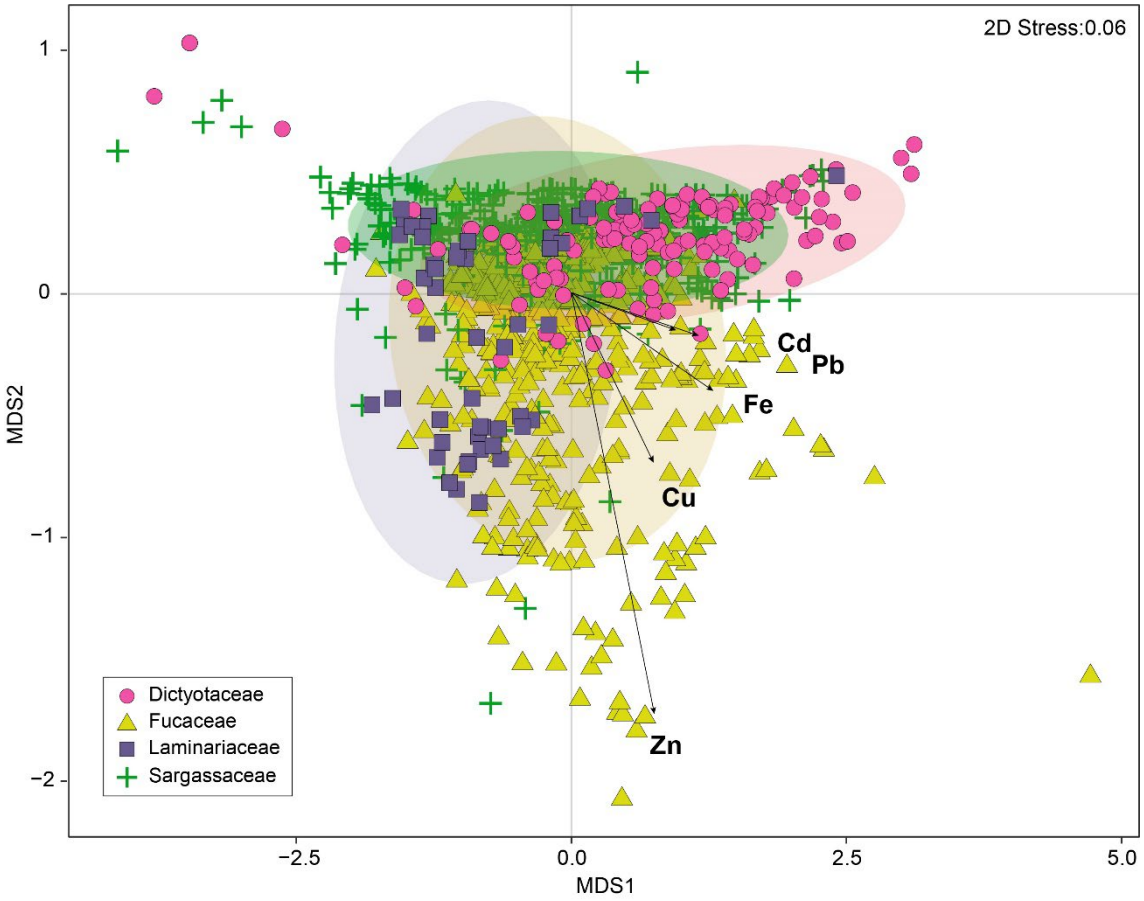

Supplementary Fig. 7. Non-metric multidimensional scaling (nMDS) ordination plot illustrating differences among the families of brown algae based on the Bray-Curtis dissimilarity matrix computed from metal concentrations of Cd, Cu, Fe, Pb and Zn (n = 1013 records). Ellipses represent the 95% confidence intervals of each group. Arrows represent the direction (increase) and strength (length) of quantitative explanatory variables. Stress of the nMDS is also shown.

Supplementary Tables

Supplementary Table 1. Metal concentrations (μg g^{-1}, DW) in the different families of brown algae predicted by GAMs and its variation over the periods studied. Periods range from the predicted point of highest concentration (excluding last point and those initial periods of ten years with less than five records) to the last predicted point. ns: not significant, i.e. the 95% confidence intervals of the two predicted points overlap.

Element	Family	Period	Initial concentration (μg g^{-1})	Final concentration (μg g^{-1})	Concentration variation (%)	Annual rate diminution (%)
Pb	Dyctiotaceae	1999-2019	6.120	0.924	-84.9	4.2
Pb	Fucaceae	1970-2017	11.315	1.136	-90.0	1.9
Pb	Laminariaceae	1947-2016	6.874	0.664	-90.3	1.3
Pb	Sargassaceae	1987-2019	4.251	2.124	-50.0	(ns)
Pb	Others	1981-2019	9.209	6.647	-27.8	(ns)
Pb	All	1968-2019	8.544	1.369	-84.0	1.6
Cd	Dyctiotaceae	2000-2020	1.131	0.147	-87.0	4.4
Cd	Fucaceae	1970-2017	2.991	0.456	-84.7	1.8
Cd	Laminariaceae	2000-2020	2.239	0.220	-90.2	4.5
Cd	Sargassaceae	1971-2020	0.901	0.577	-35.9	(ns)
Cd	Others	1971-2019	0.894	0.443	-50.5	(ns)
Cd	All	1970-2020	1.906	0.436	-77.1	1.6
Cu	Dyctiotaceae	1995-2020	7.381	1.846	-75.0	3.0
Cu	Fucaceae	1987-2017	19.783	6.186	-68.7	2.3
Cu	Laminariaceae	1947-2016	36.434	1.497	-95.9	1.4
Cu	Sargassaceae	1970-2019	9.034	4.475	-50.5	(ns)
Cu	Others	1970-2019	8.609	4.239	-50.8	(ns)
Cu	All	1968-2020	12.540	3.566	-71.6	1.4
Fe	Dyctiotaceae	1998-2019	1223.729	149.219	-87.8	4.2
Fe	Fucaceae	1995-2017	341.739	188.201	-44.9	2.0
Fe	Laminariaceae	1947-2016	269.022	67.003	-75.1	1.1
Fe	Sargassaceae	2002-2019	382.692	85.699	-77.6	4.6
Fe	Others	1970-2019	386.781	422.412	9.2	(ns)
Fe	All	1994-2019	413.805	149.427	-63.9	2.6
Hg	Dyctiotaceae	1980-2019	0.050	0.023	-53.2	(ns)
Hg	Fucaceae	1978-2017	0.133	0.019	-85.7	2.2
Hg	Laminariaceae	–	–	–	–	–
Hg	Sargassaceae	1985-2019	0.196	0.196	-0.1	(ns)
Hg	Others	1971-2016	0.197	0.051	-74.2	(ns)
Hg	All	1983-2019	0.094	0.033	-65.1	1.8
Zn	Dyctiotaceae	1996-2019	40.833	7.349	-82.0	3.6
Zn	Fucaceae	1968-2017	301.969	115.885	-61.6	1.3
Zn	Laminariaceae	1947-2016	116.001	34.933	-69.9	1.0
Zn	Sargassaceae	1994-2019	22.914	12.377	-46.0	1.8
Zn	Others	1970-2019	58.083	65.632	13.0	(ns)
Zn	All	1968-2019	161.715	33.612	-79.2	1.6
Co	Dyctiotaceae	2004-2019	3.639	0.506	-86.1	5.7
Co	Fucaceae	1983-2017	4.660	0.426	-90.9	2.7
Co	Laminariaceae	1984-2016	0.494	0.043	-91.4	2.9
Co	Sargassaceae	1970-2019	1.076	1.635	52.0	(ns)
Co	Others	1990-2019	1.710	0.539	-68.5	(ns)
Co	All	1990-2019	1.710	0.689	-59.7	2.1

Mn	Dyctiotaceae	1975-2019	112.409	13.019	-88.4		2.0
Mn	Fucaceae	1991-2016	126.869	79.377	-37.4	(ns)	
Mn	Laminariaceae	1947-2016	17.712	5.863	-66.9	(ns)	
Mn	Sargassaceae	1973-2019	66.277	14.062	-78.8		1.7
Mn	Others	1970-2019	53.574	10.805	-79.8		1.6
Mn	All	1985-2019	77.977	19.731	-74.7		2.2
Cr	Dyctiotaceae	1978-2019	5.482	0.925	-83.1		2.0
Cr	Fucaceae	1996-2017	4.390	1.037	-76.4		3.6
Cr	Laminariaceae	1947-2014	1.411	2.305	63.4	(ns)	
Cr	Sargassaceae	1973-2019	1.981	1.358	-31.5	(ns)	
Cr	Others	1989-2019	7.927	1.983	-75.0	(ns)	
Cr	All	1993-2019	3.253	1.105	-66.0		2.5

4.2. Capítulo 2: Three Decades of Change in Potentially Toxic Elements in Brown Algae in the Northeast Atlantic Ocean.

Referencia:

Pacín, C.*; Fernández, J. A.; Conde-Amboage, M.; Lazzari, M.; García-Seoane, R.; Viana, I. G.; Varela, Z.; Real, C.; Villares, R.; Aboal, J. R. Three Decades of Change in Potentially Toxic Elements in Brown Algae in the Northeast Atlantic Ocean. Environ Sci Technol 2025, 59(21), 10476-10487. https://doi.org/10.1021/acs.est.4c14013.

**corresponding author.*

Autoría e filiación:

Carme Pacín[1,2]; J. Ángel Fernández[1]; Mercedes Conde-Amboage[3]; Massimo Lazzari[2]; Rita García-Seoane[4,5]; Inés G. Viana[4]; Zulema Varela[1]; Carlos Real[6]; Rubén Villares[6]; Jesús R. Aboal[1].

[1]CRETUS, Ecology Area, Department of Functional Biology, Faculty of Biology, Universidade de Santiago de Compostela, Santiago de Compostela, 15782, Spain

[2]CIQUS Centre, Department of Physical Chemistry, Universidade de Santiago de Compostela, Santiago de Compostela 15782, Spain

[3]Department of Statistics, Mathematical Analysis and Optimization, Universidade de Santiago de Compostela, Santiago de Compostela 15782, Spain

[4]Instituto Espanol de Oceanografía (IEO−CSIC), Centro Oceanográfico de A Coruna, A Coruna 15001, Spain

[5]Department of Earth Sciences, University of Hawaii at Manoa, Honolulu, Hawaii 96822, United States

[6]Department of Functional Biology, Ecology Unit, Universidade de Santiago de Compostela, Escola Politécnica Superior de Enxenaría, Lugo 27002, Spain

Datos da publicación:

Ano: 2025

DOI: https://doi.org/10.1021/acs.est.4c14013

Información da revista:

Nome: Environmental Science & Technology ISSN: 1520-5851

Índice de impacto: 11.3 (2024)

Posición na área: 5/83 (Engineering, Environmental), 19/374 (Environmental Sciences)

Contribución da doutoranda:

Recollida de mostras para o ano 2021, determinación analítica, análise estatística, visualización, e escritura do artigo.

Autorización da revista:

Environmental Science & Technology forma parte da editorial ACS, que permite que as autoras empreguen os artigos en teses de doutoramento, como se pode ver no anexo 1.

Material suplementario:

Anexado ao final do artigo a excepción da Táboa S4, que se pode descargar en: https://doi.org/10.1016/J.JHAZMAT.2022.130511

Environmental Science & Technology

pubs.acs.org/est

Article

Three Decades of Change in Potentially Toxic Elements in Brown Algae in the Northeast Atlantic Ocean

Published as part of Environmental Science & Technology special issue "Ocean Health".

Carme Pacín,* J. Ángel Fernández, Mercedes Conde-Amboage, Massimo Lazzari, Rita García-Seoane, Inés G. Viana, Zulema Varela, Carlos Real, Rubén Villares, and Jesús R. Aboal

Cite This: *Environ. Sci. Technol.* 2025, 59, 10476−10487

Read Online

ACCESS | Metrics & More | Article Recommendations | Supporting Information

ABSTRACT: Marine pollution from potentially toxic elements (PTEs) threatens coastal ecosystems, making long-term assessments essential. This study analyzes trends in Al, Cr, Fe, Ni, Cu, Zn, As, Cd, and Hg using 446 samples of *Fucus ceranoides*, *F. spiralis*, and *F. vesiculosus* collected between 1990 and 2021 at 173 coastal sites in NW Spain. A consistent resampling approach revealed significant declines in most anthropogenic PTEs, including Cu (−84.7%), Cr (−84.6%), Hg (−49.6%), and Cd (−36.7%) over time. In contrast, arsenic increased by 36.1%, but the underlying causes remain unclear, with potential factors including changes in sediment inputs, bioavailability, or emerging sources such as groundwater discharges. Higher PTE levels were detected in inner estuarine areas, but no consistent latitudinal patterns emerged. Overall, the results suggest effective mitigation of coastal pollution, with reduced bioavailable PTEs entering the food web via *Fucus* spp. However, rising As levels and complex contamination dynamics underscore the need for continued monitoring. This study offers the most comprehensive standardized assessment of long-term PTE trends in brown algae to date, providing valuable insights for environmental policy and coastal management.

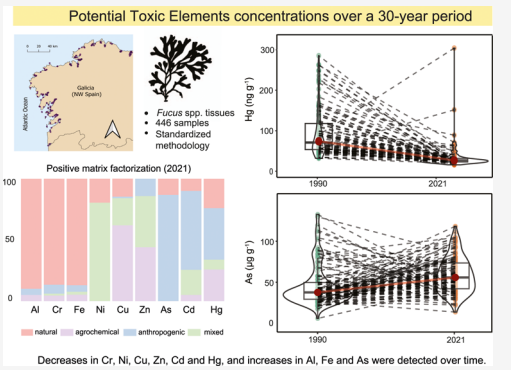

KEYWORDS: *Heavy metals, Seaweed, Biomonitoring, Marine pollution, Hazardous elements, Temporal trends*

INTRODUCTION

Pollution from Potentially Toxic Elements (PTEs) poses a significant threat to marine environments. PTEs are naturally occurring elements in the Earth's crust that can be released into the marine environment through geological processes (e.g., volcanoes, erosion) and human activities (e.g., industry, mining, and fossil fuel combustion).[1] The latter has intensified significantly since the Industrial Revolution, increasing discharges of these compounds.[2] Some PTEs have metabolic importance and become toxic at high concentrations (e.g., Cu, Ni, and Zn), but others can be toxic even at trace levels (e.g., Hg and Cd).[3,4]

Brown algae (Phaeophyceae) accumulate PTEs at concentrations that often exceed those in seawater,[5,6] leading to reduced reproduction and survival rates, and increased oxidative damage.[7−9] This is critical given their role as ecosystem engineers in temperate coastal ecosystems, with *Fucus* species shaping intertidal habitats, acting as carbon sinks, and contributing to climate change mitigation.[10] As primary producers, they transfer PTEs through the marine food web, potentially leading to biomagnification.[11−15] The study of PTE concentrations in algae therefore holds intrinsic value due to their ecological significance.

Since the 1950s, PTE concentrations in brown algae have been used to assess marine pollution. Unlike water samples, which provide snapshots, and sediments, which record historical pollution, algal tissues reflect bioavailable PTEs and are therefore more indicative of ecological risk. Accordingly, comparisons of PTE concentrations in seawater and sediment with those in algae have often shown limited correlations.[16] *Fucus* spp. have been especially valuable in the Northern Hemisphere because of their high accumulation capacity, wide distribution, and simple tissue structure.[17]

The use of brown algae as biomonitors has provided valuable insights into temporal trends in PTE pollution at global, regional, and local scales.[18−21] However, these studies have often been compromised by the use of nonstandardized methodologies, the inclusion of different species, and inconsistent sampling seasons.[20] Even studies applying stand-

Received: December 23, 2024
Revised: May 10, 2025
Accepted: May 12, 2025
Published: May 22, 2025

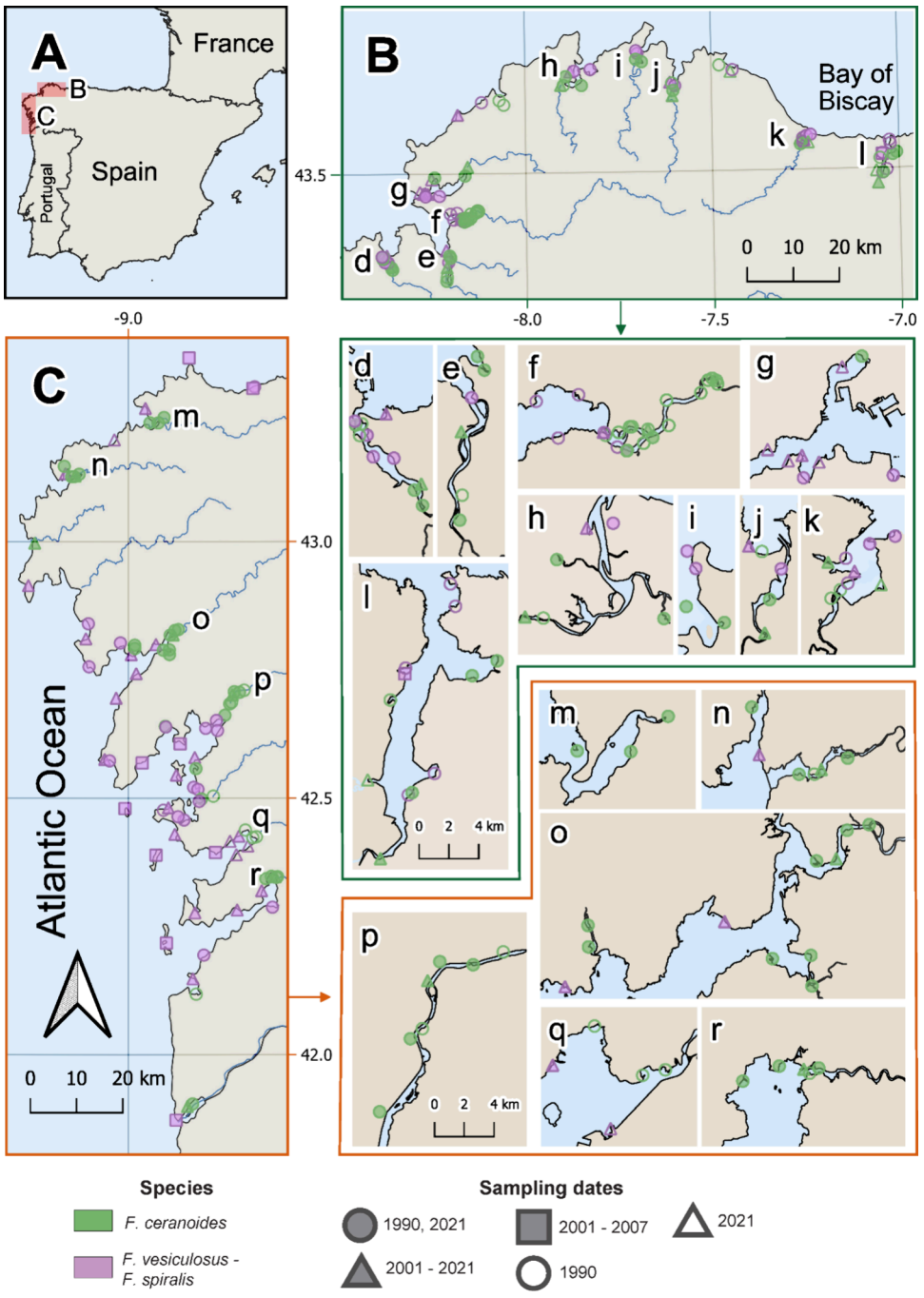

Figure 1. Map of the study area in NW Spain. Panels A–C display an overview of the region, with B and C showing the sampling sites. Panels d–l and m–r present detailed views of coastal inlets that cannot be distinguished in B and C, respectively. Colors represent the species sampled (*Fucus ceranoides* and *F. vesiculosus* − *F. spiralis*), while symbols indicate the sampling dates: circles for sites sampled in both 1990 and 2021, triangles for the 2001–2021 series (2001, 2003, 2005, 2007, 2021), rectangles for the 2001–2007 subset (2001, 2003, 2005, 2007), and unfilled circles and triangles for sites sampled in 1990 and 2021, respectively. To reduce clutter, incomplete samplings from 2001, 2003, 2005, and 2007 are grouped under the 2001–2007 symbol.

ardized methodologies[22,23] have often been limited by short observation periods and inconsistent or limited sampling sites.

Given the importance of identifying temporal trends for assessing the environmental impact of PTE pollution and the effectiveness of regulations, such as the Marine Strategy Framework Directive,[24] comprehensive long-term studies using standardized methodologies are essential. For this purpose, environmental specimen banks, through the retrospective analysis of preserved samples, are a critical resource.[23,25]

This study aims to fill this gap in long-term pollution assessments of brown algae using standardized methodologies and a representative number of sampling sites by analyzing concentrations of Al, Cr, Fe, Ni, Cu, Zn, As, Cd, and Hg in the tissues of *Fucus ceranoides, F. spiralis*, and *F. vesiculosus* that were systematically collected from consistent sites in NW Spain over three decades (1990–2021). The samples, stored in the Galician Environmental Specimen Bank (Universidade de Santiago de Compostela), were analyzed (or reanalyzed) using

https://doi.org/10.1021/acs.est.4c14013
Environ. Sci. Technol. 2025, 59, 10476−10487

consistent methodologies. The NW Spanish coast, a heavily navigated maritime route, has faced significant industrial development and pollutant discharge,[26,27] but has also been subjected to European environmental policies aimed at reducing pollution.[28] This combination of historical pressures and progressive management makes it an ideal study area, with findings potentially applicable to other coastal regions facing similar challenges. We hypothesized that a) regional PTE concentrations in *Fucus* spp. tissues will remain unchanged over time; b) PTE concentrations in *Fucus* spp. tissues collected from the same sites will remain unchanged over time; and c) PTE pollution sources, inferred from *Fucus* spp. PTE concentrations, will be stable over time.

MATERIAL AND METHODS

2.1. Study Area. Galicia region (NW Spain) features 1498 km of coastline dominated by rías, coastal inlets where the oceanic influence dominates, except in the inner estuarine zones (see Figure 1). The region has an oceanic climate with mild temperatures and consistent rainfall. Coastal industries include automotive, naval, energy, ceramics, metallurgy, and paper production.[29] The region's geology is predominantly granitic.[30,31]

2.2. Sampling. A total of 446 samples of *Fucus ceranoides, F. spiralis*, and *F. vesiculosus* were collected from 173 sites in 1989−1990 (1990 from now on), 2001, 2003, 2005, 2007, and 2021 (Figure 1, Table S1). Most sites sampled in 1990 were resampled in 2021, and those sampled in 2001 were revisited in 2003, 2005, 2007, and 2021.

Due to uncertainties in distinguishing *F. spiralis* from *F. vesiculosus*, including potential hybridization and misidentification with *F. macroguiryi*,[32] these taxa were treated as a single group, while *F. ceranoides* was categorized separately.

Sampling was conducted in July to minimize seasonal effects.[22] At each site, a minimum of 30 thalli were collected at low tide in a zigzag pattern along a 50 m transect, rinsed on-site with seawater, combined into a composite sample, and transported to the laboratory in a cooler. Detailed sampling protocols were described elsewhere.[17]

2.3. Sample Processing. To minimize intrathallus variability in PTE concentrations,[22] apical tissues corresponding to 3 dichotomous sections, which represent the recent growth period of the algae,[33] were selected excluding receptacles and tissues with epiphytes. Samples were dried in a forced-air oven at 40 °C until constant weight, homogenized in a tangential mixer mill with zirconium oxide vessels (Retsch MM400), and stored in sealed glass vessels at room temperature, protected from light in the Galician Environmental Specimen Bank at Universidade de Santiago de Compostela until chemical analysis.

2.4. Chemical Analysis. Samples were dried again at 100 °C (Al, Cr, Fe, Ni, Cu, Zn, As, and Cd) or 40 °C (Hg). Samples from 1990, 2001, 2003, 2005, and 2007 were reanalyzed,[23] while 2021 samples were analyzed for the first time. This approach allowed us to apply consistent and up-to-date methodology across the entire data set. Al, Cr, Fe, Ni, Cu, Zn, As, and Cd concentrations were determined by inductively coupled plasma mass spectrometry (ICP−MS, Agilent 7700x) at the Research Support Services Unit of the Universidade de Santiago de Compostela. Hg concentrations were measured in an elemental analyzer (Milestone DMA 80) at the Ecology unit in the same university.

Certified reference material (Bladderwrack-*Fucus vesiculosus*, ERM-CD200, Belgium), analytical blanks, and replicates were included every 30 samples for all PTEs, except for Hg, whose controls were included every 15. Recoveries ranged from 90% (for Cu) to 110% (for As), with Relative Percent Differences below 9% for all PTEs. Determinations were above the limit of quantification except for one sample for Cu and Al, and 19 samples for Cr (i.e., 4% of the total). Detailed analytical quality results are shown in Table S2.

2.5. Statistical Analysis and Visualization. Descriptive statistics and tests were conducted using R v4.1.1,[34] including normality assessment (Shapiro-Wilk test), and variance homogeneity testing (Levene test from the 'car' package[35]). Data visualization was performed using the 'ggplot2' and 'ggstatsplot' packages.[36,37] Species PTE content was compared with the Wilcoxon rank-sum test (*'wilcox.test'* function), while Kruskal−Wallis (*'kruskal.test'* function) and Dunn's ('FSA' package[38]) tests compared temporal PTE trends across all *Fucus* spp. and samples (n = 446). Paired comparisons (1990 vs 2021) used Wilcoxon paired tests (*'wilcox.test'* function), while Friedman (*'friedman.test'* function) and Durbin-Conover ('PMCMRplus' package[39]) tests were applied to analyze repeated measures data from 2001, 2003, 2005, 2007, and 2021. For sites where two species were present in a given year, comparisons were made between them in that year and across years. All posthoc p-values were adjusted via Benjamini-Hochberg (BH, p.adjust function).

Linear Mixed Models (LMMs) were applied ('lme4' package[40]) to account for fixed (year, species) and random (ría) effects on the PTE concentrations, and to properly model the potential correlations arising from the use of repeated measures. Data were grouped by ría due to the limited number of observations per site, typically from 1 to 3. Best-fitting models were selected based on Akaike Information Criterion (AIC) and Bayesian Information Criterion (BIC) values. Detailed information on the LMMs can be found in the Supporting Information.

Spearman correlation analyses (*'cor.test'* function from 'Hmisc' package,[41] and 'polycor',[42] and 'ggcorrplot'[43] packages for visualization) on PTE data, with p-values adjusted using the BH method, and Principal Component Analysis (PCA) on log-transformed PTE values ('FactoMineR' package[44]), were conducted[44] to assess relationships between PTEs. Additionally, because three time periods (i.e., 1990, 2001−2007, and 2021) were found to have significantly different values for PTE concentrations (see section 3.2), positive matrix factorization models (PMF) were performed separately for each period to estimate PTE sources and contributions (PMF5 software[45]). Twenty base models were run for each period, and the model with the lowest q-robust value was selected. Factor numbers were determined through Bootstrap.

Spatial variation of PTE concentrations was mapped with QGIS 3.36.3.[46] Percentage change over time was calculated as the difference between the oldest and latest available concentrations at each site. In addition, overall median percentage changes were calculated, along with median concentrations at each site for each element. Bioconcentration factors (BCFs) were calculated to compare PTE concentrations in seawater and algae samples. Since seawater concentration data were only available for Al, Cd, Cr, Cu, Fe, Ni, and Zn in 2023,[16] BCFs for these elements were derived by pairing the 2023 seawater data with the 2021 algae data, as follows:

61
https://doi.org/10.1021/acs.est.4c14013
Environ. Sci. Technol. 2025, 59, 10476−10487

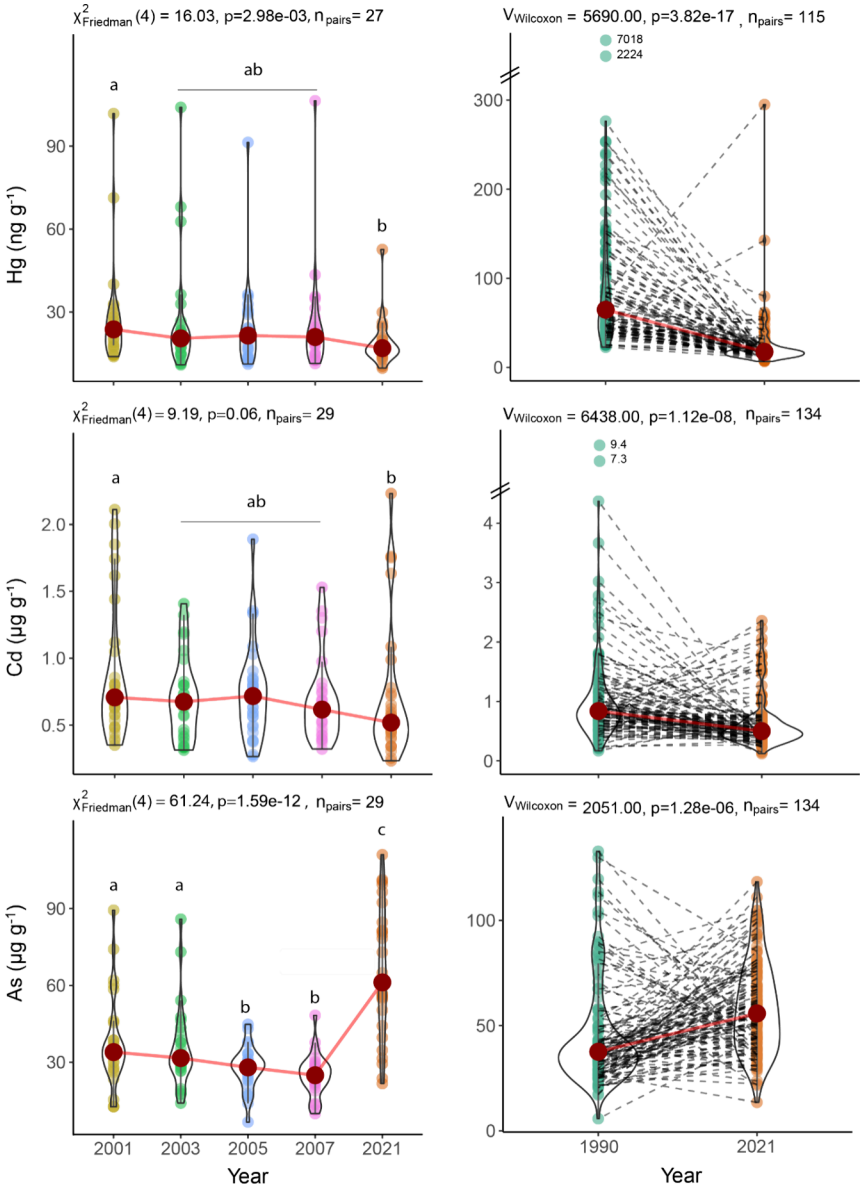

Figure 2. Temporal trends of Hg (ng g^{-1}), Cd ($\mu g\ g^{-1}$), and As ($\mu g\ g^{-1}$) concentrations in *Fucus* spp. Left panel: Repeated measures (2001−2021) analyzed by Friedman test with Durbin−Conover posthoc comparisons. Right panel: Paired 1990 vs 2021 comparisons (Wilcoxon test). Distinct lowercase letters indicate significant differences between years (no shared letters = significant). Note: For Cd, the Kruskal−Wallis test was marginal nonsignificant (p = 0.06); however, Dunn's posthoc test was conducted for exploratory purposes.

$$\mathrm{BCF} = \frac{median[PTE]_{algae}}{median[PTE]_{seawater}} \quad (1)$$

Sediment contributions to PTE concentrations in algae were estimated using Al as a geological tracer,[47] with PTE and Al ratios calculated from published sediment data,[23,48] and corresponding algae measurements. Due to the unavailability of sediment data for 2021, this analysis was limited to the years 1990, 2001, 2003, 2005, and 2007. Sediment contributions were determined for each sampling site and year[23,48] using the following equation:

$$\text{sediment contribution} = \frac{\frac{[PTE]_{sediment}}{[PTE]_{algae}}}{\frac{[Al]_{sediment}}{[Al]_{algae}}} \quad (2)$$

The median sediment contribution was calculated for each available PTE and year.

3. RESULTS

3.1. Data Contextualization. PTE concentrations were non-normally distributed and skewed to the right. Median PTE concentrations ranged from 0.023 to 290 $\mu g\ g^{-1}$, following the sequence: Hg < Cd < Cr < Ni < Cu < As < Zn < Al < Fe (Table S3). Detailed PTE concentrations by species, site, and year are presented in Table S4.

PTE concentrations varied significantly between species, with the exception of Cd. *Fucus ceranoides* exhibited higher concentrations of all PTEs ($p < 0.01$), with the exception of As, which was higher in *F. vesiculosus* − *F. spiralis* ($p < 0.05$) (Table S3). Spatially, PTE concentrations were usually higher in the inner part of the rías (Figures S4−S9), although this pattern was less pronounced for Hg and absent for Cd and As

https://doi.org/10.1021/acs.est.4c14013
Environ. Sci. Technol. 2025, 59, 10476−10487

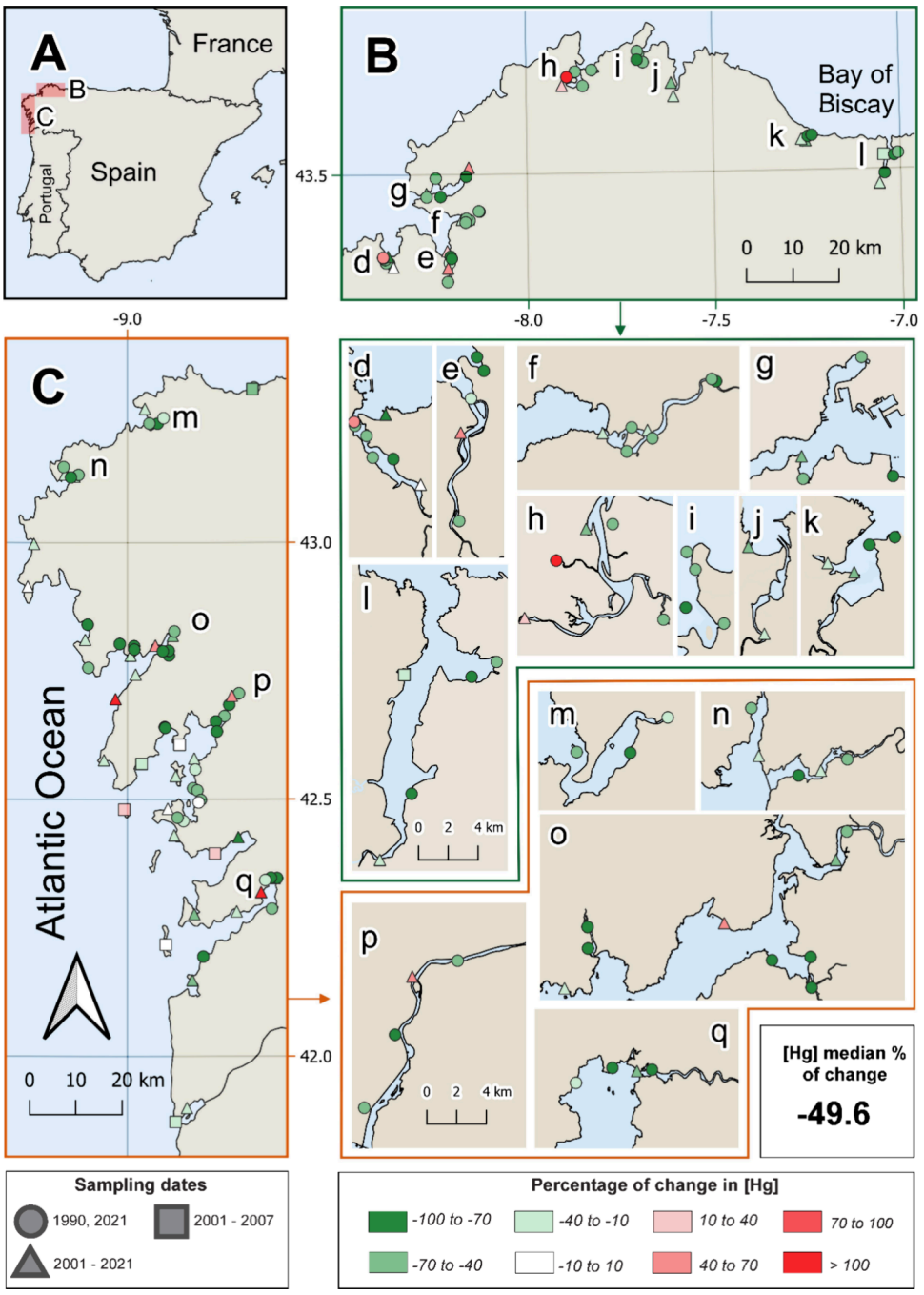

Figure 3. Map of percentage changes in Hg concentrations over time. Panels A−C provide a regional overview, with B and C showing the differences between the final and initial Hg concentrations (in %) at each sampling station. Panels d−l and m−q offer detailed views of sampling sites that are densely clustered and hard to distinguish in B and C, respectively. Different colors represent the percentage changes in Hg concentrations, while distinct symbols indicate the sampling dates: 1990 and 2021, 2001−2021, and 2001−2007. The total median percentage change, calculated as the median of the percentage changes across all sampling sites, is displayed below.

(Figures S1−S3). Only Ni concentrations exhibited latitudinal differences, with higher values in the northern rías (Figure S7B). Nearby rías did not show similar PTE concentrations. Some rías showed elevated levels of specific elements (e.g., rías 'e', 'k', and 'o' for Hg in Figure S1, or 'i', 'j', and 'o' for Cd in Figure S2), while others exhibited high within-ría variability, especially for As (Figure S3). Accordingly, the coefficient of dispersion (COD; i.e., median absolute deviation divided by the median) was elevated for all the PTEs (Table S3). Additionally, high concentrations in certain rías were not consistent across all elements, indicating substantial interelement variability (e.g., ría 'p' for Hg and Zn in Figures S1 and S9).

BCFs indicated that *Fucus* spp. concentrations were much higher than those in seawater, with the exception of Zn. Sediment contributions varied among PTEs and increased significantly since 1990 (Table S5).

3.2. Long-Term Trends. Median PTE concentrations exhibited decreasing Cr, Ni, Cu, Zn, Cd, and Hg, and increasing Al, Fe, and As levels over the study period (Table

https://doi.org/10.1021/acs.est.4c14013
Environ. Sci. Technol. 2025, 59, 10476−10487

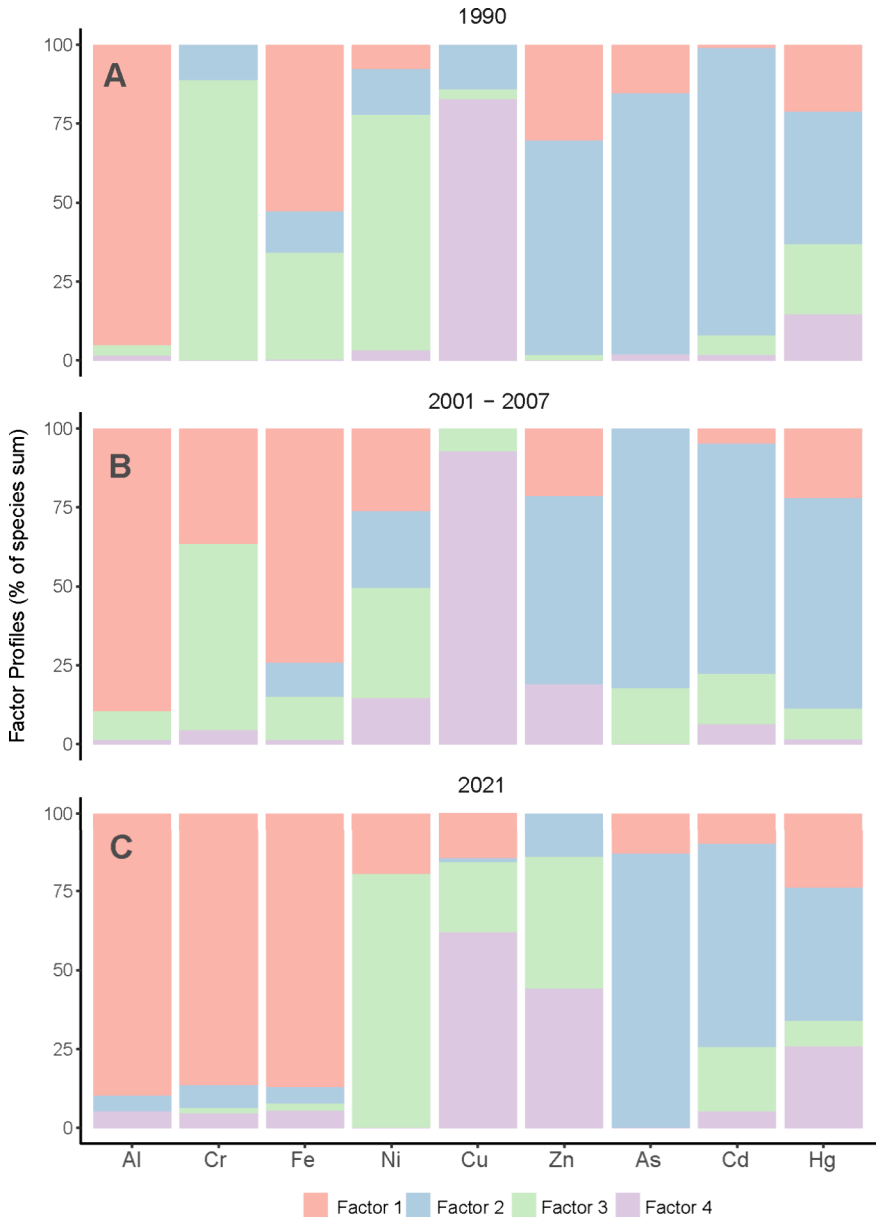

Figure 4. PMF results. Percentage contribution of each element to the factors identified using the Positive Matrix Factorization method. Panel A shows the results for 1990, panel B for 2001−2007, and panel C for 2021.

S3). These trends were supported by Kruskal−Wallis tests with Dunn's posthoc comparisons, which revealed significant changes for all PTEs between 1990 and 2021. Concentrations remained largely stable during 2001−2007, with minimal intraperiod variation. Comparisons between 1990 and 2007 and 2001−2021 periods showed fewer but still notable significant differences (Table S3). Complementary analyses using Friedman tests with Durbin-Conover posthoc comparisons (2001−2021), and Wilcoxon paired tests (1990 and 2021), restricted to sites with repeated sampling across years, were very similar, confirming these patterns (Figure 2, Figures S10−S11). Friedman tests were insignificant for Al ($p = 0.42$) and near significant for Cd ($p = 0.06$), prompting exploratory Dunn's tests for Cd.

Spatial-temporal interactions were further assessed using LMMs, which confirmed significant decreases in all PTEs except Al, Fe, and As, which increased. Best-fit models (based on AIC/BIC) varied by element: random slopes (year|ría) were included for Hg, Cr, Ni, Cu, Zn, and As; Al, Fe, and Cd models used ría as a random intercept (1|ría), and all of them except Cd included species as a fixed effect. Detailed LMM outputs are shown in Table S6. Median percentage changes, derived from site-level changes from the first to last survey, showed decreases in Cr (−84.7%), Ni (−72.4%), Cu (−84.7%), Zn (−24.4%), Cd (−36.7%), and Hg (−49.6%), while Al (+367.9%), Fe (+105.2%), and As (+36.1%) increased (Figure 3 and Figures S12−S19). No consistent latitudinal or inner-outer rías patterns emerged, though localized substantial increases were detected in certain rías (e.g., Cd for ría 'm' and Cr for ría 'h', Figures S12 and S15), and specific sites from 1990 to 2021 (e.g., Cd, As, Ni, and Cu in ría 'h'; Zn, Cd, Cr, As in ría 'm'; and Hg in rías 'h' and 'd').

3.3. Identification of Potential Sources. Correlation analysis revealed strong positive relationships between Al−Fe, Cr−Ni, Cu−Cr, and Cu−Ni ($r > 0.55$), while As showed a moderate positive correlation with Al ($r = 0.23$), but negative

64
https://doi.org/10.1021/acs.est.4c14013
Environ. Sci. Technol. 2025, 59, 10476−10487

correlations with Cu, Cr, and Ni ($r \approx -0.25$) (Figure S20A). PCA supported these patterns, with PC1 dominated by Cr, Ni, Cu, Zn, and Hg and PC2 by Fe and Al, explaining 58.4% of the variance. As and Cd clustered separately (Figure S20B). PMF models identified four consistent factors across 1990, 2001−2007, and 2021, with shifts in element allocation, especially in 2021. In 1990 and 2001−2007, Factor 1 represented Al and Fe, Factor 2 Zn, As, Cd, and Hg, Factor 3 Cr and Ni (though Ni showed mixed contributions in 2001−2007), and Factor 4 Cu. In 2021, Factor 1 included Fe, Al, and Cr, Ni shifted to Factor 3, As, Cd, and Hg remained in Factor 3, Zn was distributed between Factors 3 and 4, and Cu remained primarily associated with Factor 4, with contributions from Factors 1 and 3 (Figure 4, Table S7).

4. DISCUSSION

4.1. PTE Concentrations and Spatial Patterns. Median PTE concentrations in *Fucus* spp. were largely consistent with values from a global meta-analysis,[20] suggesting potential physiological regulation of metal composition. However, the observed higher levels of Cu (+66%) and As (+21%), and lower levels of Cd (−28%) compared to the global medians suggest potential regional differences in bioavailability and anthropogenic influences. Overall, these findings suggest moderate pollution levels in the area, with Cd and Hg medians within EU limits for seaweed consumption.[49,50] *Fucus* spp. showed significantly higher PTE concentrations than regional seawater (except Zn), confirming their role as bioconcentrators of metals.[51] Sediment contributions varied among PTEs and were higher in 2001−2007 than in 1990 (Table S5).

Interspecific comparisons revealed higher PTE concentrations in *F. ceranoides*, except for Cd and As (Table S3, Figures S1−S9). This pattern may reflect habitat-related factors rather than intrinsic differences in accumulation capacity.[47,48] The observed spatial segregation (Figure 1), with *F.* ceranoides inhabiting sediment-rich estuarine environments and *F. vesiculosus* − *F. spiralis* occupying rocky marine substrates,[52,53] likely contributes to greater sediment-derived inputs (as evidenced by elevated Al and Fe concentrations) and increased exposure to anthropogenic discharges typical of estuarine zones. Additionally, lower salinity and pH in these areas may enhance PTE bioavailability.[54,55] In contrast, higher As levels in *F. vesiculosus* − *F. spiralis* likely reflect the naturally higher As concentrations in marine environments.[56,57] Estuarine areas may exhibit lower As due to freshwater dilution and sedimentation.[58]

No clear spatial trend in PTE concentrations was found, with high variability among rías reflecting localized natural and anthropogenic influences (COD in Table S3; Figures S1−S9). Within-ria variability was marked, with no single ria consistently exhibiting high levels across all PTEs or sites. However, despite this variability, LMMs (Table S6), with ría included as a significant random effect, confirmed that each ría has a distinct PTE signature. For Al and Fe, random slopes for Year were not supported, likely because their concentrations, of lithogenic origin, are mainly driven by relatively stable sediment inputs, showing less interannual variability within rías. In the case of Cd, species was not included as a random slope, consistent with the lack of significant differences among species. This suggests a uniform accumulation pattern, with no additional species driven variation complicating spatial or temporal trends. Such homogeneity stabilizes Cd's signal across *rías* and years, obviating the need for random slopes in the model.

4.2. Long-Term Trends and Source Apportionment. Temporal trends revealed significant decreases in Cr, Ni, Cu, Zn, Cd, and Hg with reductions ranging from −84.7% for Cu to −24.4% for Zn, alongside notable increases in Al (367.9%), Fe (105.2%), and As (36.1%). The most pronounced shifts occurred between 1990 and 2021, while concentrations remained relatively stable between1990−2001, 2001−2007, and 2001−2021 (Table S3, Figure 2, Figures S10 and S11). This underscores the critical role of long-term monitoring in detecting gradual trends that short-term studies may overlook. These trends are consistent with global declines in PTE concentrations in brown algae,[20] as well as previous reports from the same study area on *Fucus* spp.,[22,23] and other regional observations in these organisms.[18,21,59] Despite the absence of latitudinal or inner-outer ría patterns, localized PTE increases emerged between 1990 and 2021, with Hg increasing in rías 'h' and 'd', Cd in ría 'm', and Cr in ría 'h' (Figure 3 and Figures S12 and S15). Specific sites showed multielement spikes (Cu, Ni, Zn, and As in ría 'h', and Zn, Cd, Cr in ría 'm') near wastewater treatment plants, spill zones, and major roads,[60] suggesting the ongoing influence of anthropogenic impacts. In contrast, ría 'd' (Ría O Burgo), previously considered one of the most polluted rías in Europe, showed substantial PTE decreases across most sites (Figure 3 and Figures S12−S19).

Elemental correlations and PCA identified two major groupings: Al−Fe and Cu−Cr−Ni−Zn-Hg, while Cd and As showed independent patterns (Figure S20). PMF further resolved four pollution sources: a potential natural source dominated by Al and Fe,[61,62] a combined natural and industrial source for Ni and Cr[63−65] (with Cr shifting toward natural sources in 2021, possibly due to increased runoff from land degradation[66]), and a consistent grouping of Zn, As, Cd, and Hg, which may reflect industrial, agricultural, and mining activities.[67−69] Cu, initially separate in 1990 and 2001−2007, evolved from potential agricultural use, especially in vineyards,[70,71] to association with Zn in 2021, suggesting modern agrochemicals or antifouling paint inputs[72,73] (Figure 4).

4.3. Underlying Drivers of Long-Term PTE Trends. Several factors likely contributed to the observed trends. Notably, the decrease in PTE levels in *Fucus* spp. aligns with the implementation of significant environmental policies and international agreements, including the Urban Waste Water Treatment Directive,[28] the OSPAR Convention,[74] the Water Framework Directive,[75] and the Marine Strategy Framework Directive.[24] These initiatives collectively improved wastewater treatment systems and limited metal discharges into marine ecosystems. Specifically, the Urban Waste Water Treatment Directive played a crucial role by driving the construction of treatment plants and modernization of existing facilities, with 21 new treatment plants by 2000, 34 by 2010, and 11 more by 2020, in the study area.[60,76] Complementary regulations such as the Integrated Pollution Prevention and Control Directive,[77] the Industrial Emissions Directive,[78] and the Minamata Convention on Mercury[79] targeted metal emissions, while waste valorization practices may have reduced direct metal releases (Figure 5).[80,81]

These measures may have collectively lowered anthropogenic metal inputs in marine ecosystems, aligning with both reported emission declines[82] and the PTE levels reductions observed in this study. PMF analysis confirmed this link, attributing most PTEs (excluding Al and Fe, and partially Ni

https://doi.org/10.1021/acs.est.4c14013
Environ. Sci. Technol. 2025, 59, 10476−10487

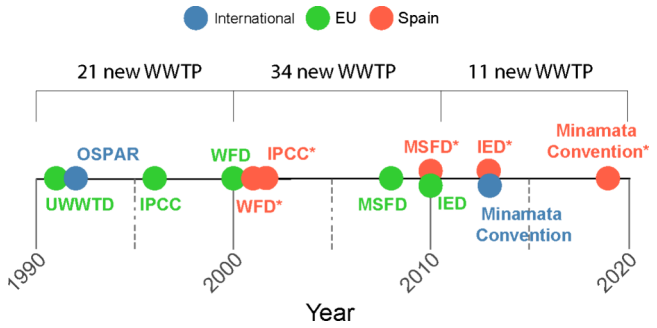

Figure 5. Timeline of key environmental regulations impacting marine environment. Asterisks (∗) denote Spanish legislation implemented in response to prior international or European agreements. UWWTD: Urban Waste Water Treatment Directive. OSPAR: Oslo and Paris Convention for the Protection of the Marine Environment of the North-East Atlantic. IPCC: Integrated Pollution Prevention and Control Directive. WFD: Water Framework Directive. MSFD: EU Marine Strategy Framework Directive. IED: Industrial Emissions Directive. WWTP: Wastewater Treatment Plant (numbers indicate newly constructed WWTPs discharging into the rías within the study area).[60]

and Cr) to human activities. Additionally, the detected PTE increases near wastewater treatment outfalls suggest that *Fucus* spp. may effectively capture anthropogenic pollution.

The observed trends may reflect not only decreasing metal concentrations in the marine environment but also reduced metal bioavailability, supported by weak correlations between seawater and algae PTE levels.[83−85] Environmental drivers, like ocean acidification, temperature, and salinity shifts can alter PTEs speciation,[86,87] while organic matter may affect bioavailability through chelation and particulate adsorption.[88,89] However, the exact mechanisms require further study. Sediment dynamics further complicate the interpretation, as elevated Al and Fe, which are established sediment tracers, have increased in 2021 compared to 1990, suggesting higher sediment influence. Since Al correlated positively with Cr, Zn, and Hg, the measured declines in these metals may underestimate true reductions in bioavailable fractions, as sediment inputs likely masked anthropogenic decreases.

Additionally, physiological traits may influence PTE concentrations in *Fucus*. For instance, faster growth rates and nutrient limitation can increase metal uptake,[90] while variations in cell wall polysaccharide composition may affect metal binding through their functional groups.[91] Differences in the abundance of physodes, vesicles that contain phlorotannins with known metal-binding properties, may also play a role.[92,93] Epiphytic microbiomes[94] and potential genetic or epigenetic adaptations,[95] add further complexity. Despite considerable efforts, the specific effects and temporal dynamics of these physiological factors remain unclear. However, preliminary, unpublished data from the algae samples in this study suggest temporal variations in cell wall composition, which may partly explain the observed trends.

This study also revealed increasing concentrations of Al, Fe, and As. Al and Fe, considered low-toxicity sediment tracers, likely reflect greater sediment contributions,[47] as supported by correlations, PCA, and PMF analyses. In contrast, the increase in As appears to result from a combination of factors. Its positive correlation with Al ($r = 0.23$) and Fe ($r = 0.11$) suggests a sediment influence, yet this does not explain why similarly correlated elements such as Cr, Zn, Hg did not show comparable trends. The distinct behavior of As, evident in its PCA separation and its higher concentrations in *F. vesiculosus* and *F. spiralis* relative to *F. ceranoides*, suggests additional dynamics.

Environmental variables such as temperature, salinity, and organic matter likely modulate As mobility and bioavailability.[58,96] While reported anthropogenic As emissions have declined in the EU,[97,98] rising concentrations in this study and in other organisms and environmental compartments,[99,100] though scarcely discussed, point to overlooked emerging sources such as groundwater discharges.[101,102] The complexity and persistence of As in coastal ecosystems underscore the need for further investigation into its sources and accumulation pathways in coastal ecosystems.

4.4. Limitations and Implications. This study has several limitations. Variability in sediment input, reflected in fluctuating Fe and Al concentrations, complicates the interpretation of temporal trends, particularly for As, which showed associations with these elements while increasing significantly. The complex interplay of pollution with physicochemical and biological factors also makes it challenging to fully attribute changes in PTE concentrations to reduced pollution following environmental regulations. Consequently, the combined effects of factors affecting PTE concentrations in algae remain poorly understood and need further investigation. Although this may appear to limit the utility of *Fucus* as a biomonitor, it actually highlights a key strength: *Fucus* spp. concentrates bioavailable metal fractions over time, capturing contamination dynamics that water or sediment samples cannot, highlighting the importance of continued seaweed monitoring for assessing coastal metal pollution.

Taxonomic challenges, such as distinguishing *F. spiralis* from *F. vesiculosus*, and the lack of overlapping sites for all three species, limited interspecific comparisons of bioconcentration capacity. Although the toxic effects of PTEs on algae are documented,[103,104] our understanding of the underlying mechanisms is still limited,[105,106] particularly regarding subcellular distribution and metal speciation.[51] While highly toxic forms like arsenite and methylmercury are believed to be less prevalent in brown algae,[107−109] their specific contributions and risks remain unclear. Some *Fucus* populations may have evolved mechanisms to limit PTE uptake,[110] but climate-related stressors like ocean acidification may increase their vulnerability, as seen in recent declines linked to heatwaves and increased wave action.[111,112] Understanding the combined effects of PTE exposure and environmental stressors is critical for predicting the future of these species.

Despite these challenges, our results show clear long-term changes in PTE concentrations in *Fucus* spp., consistent with declining contamination inputs across the EU. The consistency of patterns across multiple metals supports our conclusions and reinforces the suitability of *Fucus* as a biomonitor at decadal scales. These findings are ecologically relevant, given the importance of *Fucus* spp. in coastal ecosystems, and provide reference values for PTE concentrations in the study area. This study underscores the importance of sustained, long-term monitoring, as such trends would remain unnoticed without multidecade observations.

■ ASSOCIATED CONTENT

Supporting Information

The Supporting Information is available free of charge at https://pubs.acs.org/doi/10.1021/acs.est.4c14013.

https://doi.org/10.1021/acs.est.4c14013
Environ. Sci. Technol. 2025, 59, 10476−10487

Additional information for Linear Mixed Models (LMM). Table S1 (Number of sampling sites per year and species). Table S2 (Quality analysis results). Table S3 (Median PTE concentrations per year and species, and significant interannual Dunn's test results). Table S5 (Bioconcentration factors and sediment contribution). Table S6 (Summary of key outputs from LMMs). Table S7 (Percentage of variability explained by each factor in PMF models). Figures S1−S9 (Overview of PTEs concentrations on the sampling sites). Figures S10−S11 (Overview of PTEs concentrations over time). Figures S12−S19 (Maps of percentage changes in PTES concentrations). Figure S20 (Correlation matrix and PCA). (PDF)

Table S4 (Detailed PTE concentrations per sampling site and sampling campaign) (XLSX)

AUTHOR INFORMATION

Corresponding Author

Carme Pacín − *CRETUS Centre, Department of Functional Biology, Ecology Unit, Universidade de Santiago de Compostela, Santiago de Compostela 15782, Spain; CIQUS Centre, Department of Physical Chemistry, Universidade de Santiago de Compostela, Santiago de Compostela 15782, Spain;* orcid.org/0000-0002-2566-9259; Email: mcarme.pacin@usc.es

Authors

J. Ángel Fernández − *CRETUS Centre, Department of Functional Biology, Ecology Unit, Universidade de Santiago de Compostela, Santiago de Compostela 15782, Spain*

Mercedes Conde-Amboage − *Department of Statistics, Mathematical Analysis and Optimization, Universidade de Santiago de Compostela, Santiago de Compostela 15782, Spain*

Massimo Lazzari − *CIQUS Centre, Department of Physical Chemistry, Universidade de Santiago de Compostela, Santiago de Compostela 15782, Spain;* orcid.org/0000-0003-1300-6711

Rita García-Seoane − *Instituto Español de Oceanografía (IEO−CSIC), Centro Oceanográfico de A Coruña, A Coruña 15001, Spain; Department of Earth Sciences, University of Hawaii at Mānoa, Honolulu, Hawaii 96822, United States*

Inés G. Viana − *Instituto Español de Oceanografía (IEO−CSIC), Centro Oceanográfico de A Coruña, A Coruña 15001, Spain*

Zulema Varela − *CRETUS Centre, Department of Functional Biology, Ecology Unit, Universidade de Santiago de Compostela, Santiago de Compostela 15782, Spain;* orcid.org/0000-0002-4751-7686

Carlos Real − *Department of Functional Biology, Ecology Unit, Universidade de Santiago de Compostela, Escola Politécnica Superior de Enxeñaría, Lugo 27002, Spain*

Rubén Villares − *Department of Functional Biology, Ecology Unit, Universidade de Santiago de Compostela, Escola Politécnica Superior de Enxeñaría, Lugo 27002, Spain*

Jesús R. Aboal − *CRETUS Centre, Department of Functional Biology, Ecology Unit, Universidade de Santiago de Compostela, Santiago de Compostela 15782, Spain;* orcid.org/0000-0001-8310-2907

Complete contact information is available at: https://pubs.acs.org/10.1021/acs.est.4c14013

Author Contributions

The manuscript was written through contributions of all authors. All authors have given approval to the final version of the manuscript. Carme Pacín: Formal analysis, Writing - Original Draft, Writing - Review & Editing. J. Ángel Fernández: Funding acquisition, Conceptualization, Writing - Review & Editing. Mercedes Conde-Amboage: Formal analysis. Massimo Lazzari: Writing - Review & Editing. Rita García-Seoane: Writing - Review & Editing. Inés G. Viana: Writing - Review & Editing. Zulema Varela: Writing - Review & Editing. Carlos Real: Writing - Review & Editing. Rubén Villares: Writing - Review & Editing. Jesús R. Aboal: Funding acquisition, Conceptualization, Writing - Review & Editing.

Notes

The authors declare no competing financial interest.

ACKNOWLEDGMENTS

C. Pacín received a predoctoral grant from Xunta de Galicia (ED481A 2022/374). R. García-Seoane was supported by the postdoctoral research grant Juan de la Cierva-Formación (FJC2019-040921-I) from MCIN/AEI/10.13039/501100011033 (Spain) and EU NextGenerationEU/PRTR programmes and is currently supported by a Marie Skłodowska-Curie Postdoctoral Fellowship (101150001-Pel-Con). I. G. Viana was funded by the Juan de la Cierva-Incorporación programme (IJC2019-040554-I) and Z. Varela by the María Zambrano Programme from the Spanish Ministry of Universities. We thank Julia Bairstrow for her valuable contributions to the English language editing of this manuscript.

REFERENCES

(1) Vareda, J. P.; Valente, A. J. M.; Durães, L. Assessment of Heavy Metal Pollution from Anthropogenic Activities and Remediation Strategies: A Review. *J. Environ. Manage* **2019**, *246*, 101−118.

(2) Lu, Y.; Yuan, J.; Lu, X.; Su, C.; Zhang, Y.; Wang, C.; Cao, X.; Li, Q.; Su, J.; Ittekkot, V.; Garbutt, R. A.; Bush, S.; Fletcher, S.; Wagey, T.; Kachur, A.; Sweijd, N. Major Threats of Pollution and Climate Change to Global Coastal Ecosystems and Enhanced Management for Sustainability. *Environ. Pollut.* **2018**, *239*, 670−680.

(3) Nieder, R.; Benbi, D. K. Integrated Review of the Nexus between Toxic Elements in the Environment and Human Health. *AIMS Public Health* **2022**, *9* (4), 758.

(4) Fakhri, Y.; Djahed, B.; Toolabi, A.; Raoofi, A.; Gholizadeh, A.; Eslami, H.; Taghavi, M.; Alipour, M. r.; Mousavi Khaneghah, A. Potentially Toxic Elements (PTEs) in Fillet Tissue of Common Carp (Cyprinus Carpio): A Systematic Review, Meta-Analysis and Risk Assessment Study. *Toxin Rev.* **2021**, *40* (4), 1505−1517.

(5) Henriques, B.; Lopes, C. B.; Figueira, P.; Rocha, L. S.; Duarte, A. C.; Vale, C.; Pardal, M. A.; Pereira, E. Bioaccumulation of Hg, Cd and Pb by Fucus Vesiculosus in Single and Multi-Metal Contamination Scenarios and Its Effect on Growth Rate. *Chemosphere* **2017**, *171*, 208−222.

(6) Sundhar, S.; Arisekar, U.; Shakila, R. J.; Shalini, R.; Al-Ansari, M. M.; Al-Dahmash, N. D.; Mythili, R.; Kim, W.; Sivaraman, B.; Jenishma, J. S.; Karthy, A. Potentially Toxic Metals in Seawater, Sediment and Seaweeds: Bioaccumulation, Ecological and Human Health Risk Assessment. *Environ. Geochem Health* **2024**, *46* (2), 1−21.

(7) Andrade, L. R.; Leal, R. N.; Noseda, M.; Duarte, M. E. R.; Pereira, M. S.; Mourão, P. A. S.; Farina, M.; Amado Filho, G. M. Brown Algae Overproduce Cell Wall Polysaccharides as a Protection Mechanism against the Heavy Metal Toxicity. *Mar. Pollut. Bull.* **2010**, *60* (9), 1482−1488.

(8) Stankovic, S.; Kalaba, P.; Stankovic, A. R. Biota as Toxic Metal Indicators. *Environ. Chem. Lett.* **2014**, *12*, 63−84.
(9) Mamboya, F. A.; Pratap, H. B.; Mtolera, M.; Björk, M. Accumulation of Copper and Zinc and Their Effects on Growth and Maximum Quantum Yield of the Brown Macroalga Padina Gymnospora. *Western Indian Ocean J. Mar. Sci.* **2009**, *6*, 17−28.
(10) Mineur, F.; Arenas, F.; Assis, J.; Davies, A. J.; Engelen, A. H.; Fernandes, F.; Malta, E.-j.; Thibaut, T.; Van Nguyen, T.; Vaz-Pinto, F.; Vranken, S.; Serrao, E. A.; De Clerck, O. European Seaweeds under Pressure: Consequences for Communities and Ecosystem Functioning. *J. Sea Res.* **2015**, *98*, 91−108.
(11) Coelho, J. P.; Mieiro, C. L.; Pereira, E.; Duarte, A. C.; Pardal, M. A. Mercury Biomagnification in a Contaminated Estuary Food Web: Effects of Age and Trophic Position Using Stable Isotope Analyses. *Mar. Pollut. Bull.* **2013**, *69* (1−2), 110−115.
(12) Córdoba-Tovar, L.; Marrugo-Negrete, J.; Barón, P. R.; Díez, S. Drivers of Biomagnification of Hg, As and Se in Aquatic Food Webs: A Review. *Environ. Res.* **2022**, *204*, 112226.
(13) Vardhan, K. H.; Kumar, P. S.; Panda, R. C. A Review on Heavy Metal Pollution, Toxicity and Remedial Measures: Current Trends and Future Perspectives. *J. Mol. Liq.* **2019**, *290*, 111197.
(14) Tlili, S.; Mouneyrac, C. New Challenges of Marine Ecotoxicology in a Global Change Context. *Mar. Pollut. Bull.* **2021**, *166*, 112242.
(15) Goutam Mukherjee, A.; Ramesh Wanjari, U.; Renu, K.; Vellingiri, B.; Valsala Gopalakrishnan, A. Heavy Metal and Metalloid - Induced Reproductive Toxicity. *Environ. Toxicol Pharmacol* **2022**, *92*, 103859.
(16) Vázquez-Arias, A.; Boquete, M. T.; Fernández, J. Á.; Aboal, J. R. Assessing the Effectiveness of Seaweed Transplants in Reflecting Seawater Pollution Levels. *Environmental Pollution* **2025**, *na*, 126456.
(17) García-Seoane, R.; Fernández, J. A.; Villares, R.; Aboal, J. R. Use of Macroalgae to Biomonitor Pollutants in Coastal Waters: Optimization of the Methodology. *Ecological Indicators.* **2018**, *84*, 710−726.
(18) Kozhenkova, S. I.; Khristoforova, N. K.; Chernova, E. N.; Kobzar, A. D. Long-Term Biomonitoring of Heavy Metal Pollution of Ussuri Bay, Sea of Japan. *Russ J. Mar Biol.* **2021**, *47* (4), 256−264.
(19) Søndergaard, J.; Mosbech, A. Mining Pollution in Greenland - the Lesson Learned: A Review of 50 Years of Environmental Studies and Monitoring. *Sci. Total Environ.* **2022**, *812*, 152373.
(20) Aboal, J. R.; Pacín, C.; García-Seoane, R.; Varela, Z.; González, A. G.; Fernández, J. A. Global Decrease in Heavy Metal Concentrations in Brown Algae in the Last 90 Years. *J. Hazard Mater.* **2023**, *445*, 130511.
(21) Chalkley, R.; Child, F.; Al-Thaqafi, K.; Dean, A. P.; White, K. N.; Pittman, J. K. Macroalgae as Spatial and Temporal Bioindicators of Coastal Metal Pollution Following Remediation and Diversion of Acid Mine Drainage. *Ecotoxicol Environ. Saf* **2019**, *182*, 109458.
(22) García-Seoane, R.; Fernández, J. A.; Boquete, M. T.; Aboal, J. R. Analysis of Intra-Thallus and Temporal Variability of Trace Elements and Nitrogen in Fucus Vesiculosus: Sampling Protocol Optimization for Biomonitoring. *J. Hazard Mater.* **2021**, *412*, 125268.
(23) Viana, I. G.; Aboal, J. R.; Fernández, J. A.; Real, C.; Villares, R.; Carballeira, A. Use of Macroalgae Stored in an Environmental Specimen Bank for Application of Some European Framework Directives. *Water Res.* **2010**, *44* (6), 1713−1724.
(24) Marine Strategy Framework Directive 2008/56/EC, 2008. *European Environment Agency*. https://www.eea.europa.eu/policy-documents/2008-56-ec.
(25) Tanabe, S.; Ramu, K. Monitoring Temporal and Spatial Trends of Legacy and Emerging Contaminants in Marine Environment: Results from the Environmental Specimen Bank (Es-BANK) of Ehime University, Japan. *Mar. Pollut. Bull.* **2012**, *64* (7), 1459−1474.
(26) Beiras, R.; Bellas, J.; Fernández, N.; Lorenzo, J. I.; Cobelo-García, A. Assessment of Coastal Marine Pollution in Galicia (NW Iberian Peninsula); Metal Concentrations in Seawater, Sediments and Mussels (Mytilus Galloprovincialis) versus Embryo-Larval Bioassays Using Paracentrotus Lividus and Ciona Intestinalis. *Mar Environ. Res.* **2003**, *56* (4), 531−553.
(27) Bellas, J.; Fernández, N.; Lorenzo, I.; Beiras, R. Integrative Assessment of Coastal Pollution in a Ría Coastal System (Galicia, NW Spain): Correspondence between Sediment Chemistry and Toxicity. *Chemosphere* **2008**, *72* (5), 826−835.
(28) Council Directive. *Urban Wastewater Treatment Directive (91/271/EEC)*.
(29) PRTR España. *Registro Estatal de Emisiones y Fuentes Contaminantes*.
(30) Taboada, T.; Martínez Cortizas, A.; García, C.; García-Rodeja, E. Uranium and Thorium in Weathering and Pedogenetic Profiles Developed on Granitic Rocks from NW Spain. *Science of The Total Environment* **2006**, *356* (1−3), 192−206.
(31) Romaní, J. R. V. Introduction to the Geology of Galicia. *Environment in Galicia: A Book of Images: Galician Environment Through Images* **2023**, 21−35.
(32) Wallace, A. L.; Klein, A. S.; Mathieson, A. C. Determining the Affinities of Salt Marsh Fucoids Using Microsatellite Markers: Evidence of Hybridization and Introgression between Two Species of Fucus (Phaeophyta) in a Maine Estuary. *J. Phycol* **2004**, *40* (6), 1013−1027.
(33) Viana, I. G.; Bode, A. Variability in Δ15N of Intertidal Brown Algae along a Salinity Gradient: Differential Impact of Nitrogen Sources. *Science of The Total Environment* **2015**, *512−513*, 167−176.
(34) R Core Team. *R: A Language and Environment for Statistical Computing, Version 4.4.1*; R Foundation for Statistical, 2024.
(35) Fox, J.; Weisberg, S. *An R Companion to Applied Regression*, Third ed.; Sage: Thousand Oaks CA, 2019.
(36) Wickham, H. *Ggplot2: Elegant Graphics for Data Analysis*; Springer-Verlag: New York, 2016.
(37) Patil, I. Visualizations with Statistical Details: The "ggstatsplot" Approach. *J. Open Source Softw* **2021**, *6* (61), 3167.
(38) Ogle, D. H.; Doll, J. C.; Powell Wheeler, A.; Dinno, A. *FSA: Simple Fisheries Stock Assessment Methods*, 2023.
(39) Pohlert, T. *PMCMRplus: Calculate Pairwise Multiple Comparisons of Mean Rank Sums Extended*, 2023.
(40) Bates, D.; Mächler, M.; Bolker, B.; Walker, S. Fitting Linear Mixed-Effects Models Using Lme4. *J. Stat Softw* **2015**, *67* (1), na DOI: 10.18637/jss.v067.i01.
(41) Harrell, F. E., Jr. *Hmisc: Harrell Miscellaneous*, **2003**. DOI: 10.32614/CRAN.package.Hmisc.
(42) Fox, J. *Polycor: Polychoric and Polyserial Correlations*; CRAN: Contributed Packages, 2004. DOI: 10.32614/CRAN.package.polycor.
(43) Kassambara, A. *Ggcorrplot: Visualization of a Correlation Matrix Using "Ggplot2"*; CRAN: Contributed Packages, 2016. DOI: 10.32614/CRAN.package.ggcorrplot.
(44) Le, S.; Josse, J.; Husson, F. *FactoMineR: Multivariate Exploratory Data Analysis and Data Mining*, 2006. DOI: 10.32614/CRAN.package.FactoMineR.
(45) *EPA Positive Matrix Factorization (PMF) 5.0*; U.S. Environmental Protection Agency: Washington, DC, 2014.
(46) QGIS Development Team, 2024. QGIS Geographic Information System, Version 3.36.3, 2024. https://www.qgis.org.
(47) Barreiro, R.; Picado, L.; Real, C. Biomonitoring Heavy Metals in Estuaries: A Field Comparison of Two Brown Algae Species Inhabiting Upper Estuarine Reaches. *Environmental Monitoring and Assessment 2002 75:2* **2002**, *75* (2), 121−134.
(48) Carballeira, A.; Carral, E.; Puente, X.; Villares, R. Regional-Scale Monitoring of Coastal Contamination. Nutrients and Heavy Metals in Estuarine Sediments and Organisms on the Coast of Galicia (Northwest Spain). *Int. J. Environ. Pollut* **2000**, *13* (1/2/3/4/5/6), 534.
(49) Council Directive. *Regulation (EC) No 396/2005 on Maximum Residue Levels of Pesticides in or on Food and Feed of Plant and Animal Origin and Amending Council Directive 91/414/EEC*, 2005. eur-lex.europa.eu/legal-content/EN/ALL/?uri=celex%3A32005R0396.

(50) Council Directive. *COMMISSION REGULATION (EU) 2023/915 on Maximum Levels for Certain Contaminants in Food and Repealing Regulation (EC) No 1881/2006*, 2023. https://eur-lex.europa.eu/legal-content/es/TXT/?uri=CELEX%3A32023R0915.
(51) Vázquez-Arias, A.; Pacín, C.; Ares, Á.; Fernández, J. Á.; Aboal, J. R. Do We Know the Cellular Location of Heavy Metals in Seaweed? An up-to-Date Review of the Techniques. *Sci. Total Environ.* **2023**, *856*, 159215.
(52) Billard, E.; Daguin, C.; Pearson, G.; Serrão, E.; Engel, C.; Valero, M. Genetic Isolation between Three Closely Related Taxa: Fucus Vesiculosus, F. Spiralis, and F. Ceranoides (Phaophyceae). *J. Phycol* **2005**, *41* (4), 900−905.
(53) Neiva, J.; Pearson, G. A.; Valero, M.; Serrão, E. A. Fine-Scale Genetic Breaks Driven by Historical Range Dynamics and Ongoing Density-Barrier Effects in the Estuarine Seaweed Fucus Ceranoides L. *BMC Evol Biol.* **2012**, *12* (1), 78.
(54) Kennish, M. J. Environmental Threats and Environmental Future of Estuaries. *Environ. Conserv* **2002**, *29* (1), 78−107.
(55) Pan, K.; Wang, W. X. Trace Metal Contamination in Estuarine and Coastal Environments in China. *Science of The Total Environment* **2012**, *421*−*422*, 3−16.
(56) Smedley, P. L.; Kinniburgh, D. G. A Review of the Source, Behaviour and Distribution of Arsenic in Natural Waters. *Appl. Geochem.* **2002**, *17* (5), 517−568.
(57) Missimer, T. M.; Teaf, C. M.; Beeson, W. T.; Maliva, R. G.; Woolschlager, J.; Covert, D. J. Natural Background and Anthropogenic Arsenic Enrichment in Florida Soils, Surface Water, and Groundwater: A Review with a Discussion on Public Health Risk. *Int. J. Environ. Res. Public Health* **2018**, *15* (10), 2278.
(58) Jin, X.; Liu, J.; Wang, L.; Yu, X.; Wang, J.; Jin, Y.; Qiu, S.; Liu, J.; Zhao, Y.; Sun, S. Distribution Characteristics and Ecological Risk Assessment of Heavy Metal Pollution in Seawater near the Yellow River Estuary of Laizhou Bay. *Mar Environ. Res.* **2025**, *203*, 106776.
(59) Søndergaard, J.; Mosbech, A. Mining Pollution in Greenland - the Lesson Learned: A Review of 50 Years of Environmental Studies and Monitoring. *Science of The Total Environment* **2022**, *812*, 152373.
(60) *Censo Nacional de Vertidos (CNV)*. https://www.miteco.gob.es/es/cartografia-y-sig/ide/descargas/agua/censo-nacional-vertidos.html.
(61) Liu, L.; Wang, Z.; Ju, F.; Zhang, T. Co-Occurrence Correlations of Heavy Metals in Sediments Revealed Using Network Analysis. *Chemosphere* **2015**, *119*, 1305−1313.
(62) Ranjbar Jafarabadi, A.; Raudonytė-Svirbutavičienė, E.; Shadmehri Toosi, A.; Riyahi Bakhtiari, A. Positive Matrix Factorization Receptor Model and Dynamics in Fingerprinting of Potentially Toxic Metals in Coastal Ecosystem Sediments at a Large Scale (Persian Gulf, Iran). *Water Res.* **2021**, *188*, 116509.
(63) Cai, P.; Cai, G.; Yang, J.; Li, X.; Lin, J.; Li, S.; Zhao, L. Distribution, Risk Assessment, and Quantitative Source Apportionment of Heavy Metals in Surface Sediments from the Shelf of the Northern South China Sea. *Mar. Pollut. Bull.* **2023**, *187*, 114589.
(64) Huang, P.; Li, T.; Li, A.; Yu, X.; Hu, N.-J. Distribution, Enrichment and Sources of Heavy Metals in Surface Sediments of the North Yellow Sea. *Cont Shelf Res.* **2014**, *73*, 1−13.
(65) Song, Y.; Ji, J.; Yang, Z.; Yuan, X.; Mao, C.; Frost, R. L.; Ayoko, G. A. Geochemical Behavior Assessment and Apportionment of Heavy Metal Contaminants in the Bottom Sediments of Lower Reach of Changjiang River. *Catena (Amst)* **2011**, *85* (1), 73−81.
(66) Tumolo, M.; Ancona, V.; De Paola, D.; Losacco, D.; Campanale, C.; Massarelli, C.; Uricchio, V. F. Chromium Pollution in European Water, Sources, Health Risk, and Remediation Strategies: An Overview. *Int. J. Environ. Res. Public Health* **2020**, *17* (15), 5438.
(67) Kuang, Z.; Wang, H.; Han, B.; Rao, Y.; Gong, H.; Zhang, W.; Gu, Y.; Fan, Z.; Wang, S.; Huang, H. Coastal Sediment Heavy Metal(Loid) Pollution under Multifaceted Anthropogenic Stress: Insights Based on Geochemical Baselines and Source-Related Risks. *Chemosphere* **2023**, *339*, 139653.
(68) Mao, L.; Kong, H.; Li, F.; Chen, Z.; Wang, L.; Lin, T.; Lu, Z. Improved Geochemical Baseline Establishment Based on Diffuse Sources Contribution of Potential Toxic Elements in Agricultural Alluvial Soils. *Geoderma* **2022**, *410*, 115669.
(69) Huang, F.; Xu, Y.; Tan, Z.; Wu, Z.; Xu, H.; Shen, L.; Xu, X.; Han, Q.; Guo, H.; Hu, Z. Assessment of Pollutions and Identification of Sources of Heavy Metals in Sediments from West Coast of Shenzhen, China. *Environmental Science and Pollution Research* **2018**, *25* (4), 3647−3656.
(70) Brunetto, G.; Bastos de Melo, G. W.; Terzano, R.; Del Buono, D.; Astolfi, S.; Tomasi, N.; Pii, Y.; Mimmo, T.; Cesco, S. Copper Accumulation in Vineyard Soils: Rhizosphere Processes and Agronomic Practices to Limit Its Toxicity. *Chemosphere* **2016**, *162*, 293−307.
(71) Seiler, C.; Berendonk, T. U. Heavy Metal Driven Co-Selection of Antibiotic Resistance in Soil and Water Bodies Impacted by Agriculture and Aquaculture. *Front Microbiol* **2012**, *3*, na DOI: 10.3389/fmicb.2012.00399.
(72) Soroldoni, S.; Abreu, F.; Castro, Í. B.; Duarte, F. A.; Pinho, G. L. L. Are Antifouling Paint Particles a Continuous Source of Toxic Chemicals to the Marine Environment? *J. Hazard Mater.* **2017**, *330*, 76−82.
(73) Imfeld, G.; Meite, F.; Wiegert, C.; Guyot, B.; Masbou, J.; Payraudeau, S. Do Rainfall Characteristics Affect the Export of Copper, Zinc and Synthetic Pesticides in Surface Runoff from Headwater Catchments? *Science of The Total Environment* **2020**, *741*, 140437.
(74) OSPAR Commission. *OSPAR Convention*. https://www.ospar.org/convention.
(75) European Commission. *Water Framework Directive*. https://environment.ec.europa.eu/topics/water/water-framework-directive_en.
(76) Kemp, R. Implementation of the Urban Waste Water Treatment Directive (91/271/EEC) in Germany, the Netherlands, Spain, England and Wales. The Tangible Results. *European Environment* **2001**, *11* (5), 250−264.
(77) Council Directive. *Directive 96/61*. https://eur-lex.europa.eu/eli/dir/1996/61/oj/eng.
(78) Council Directive. *Directive 2010/75*. https://eur-lex.europa.eu/eli/dir/2010/75/oj/eng.
(79) United Nations. *Minamata Convention on Mercury*; 2013. https://treaties.un.org/doc/Treaties/2013/10/20131010%2011-16%20AM/CTC-XXVII-17.pdf.
(80) Birat, J. P. Life-Cycle Assessment, Resource Efficiency and Recycling. *Metallurgical Research & Technology* **2015**, *112* (2), 206.
(81) Reck, B. K.; Graedel, T. E. Challenges in Metal Recycling. *Science* **2012**, *337* (6095), 690−695.
(82) European Environment Agency. *Heavy metal emissions in Europe*. https://www.eea.europa.eu/data-and-maps/indicators/eea32-heavy-metal-hm-emissions-2/assessment.
(83) Akcali, I.; Kucuksezgin, F. A Biomonitoring Study: Heavy Metals in Macroalgae from Eastern Aegean Coastal Areas. *Mar. Pollut. Bull.* **2011**, *62* (3), 637−645.
(84) Bonanno, G.; Veneziano, V.; Raccuia, S. A.; Orlando-Bonaca, M. Seagrass Cymodocea Nodosa and Seaweed Ulva Lactuca as Tools for Trace Element Biomonitoring. A Comparative Study. *Mar. Pollut. Bull.* **2020**, *161*, 111743.
(85) Chernova, E. N.; Shulkin, V. M. Concentrations of Metals in the Environment and in Algae: The Bioaccumulation Factor. *Russ J. Mar Biol.* **2019**, *45* (3), 191−201.
(86) Romero-Freire, A.; Lassoued, J.; Silva, E.; Calvo, S.; Pérez, F. F.; Bejaoui, N.; Babarro, J. M. F.; Cobelo-García, A. Trace Metal Accumulation in the Commercial Mussel M. Galloprovincialis under Future Climate Change Scenarios. *Mar Chem.* **2020**, *224*, 103840.
(87) Stockdale, A.; Tipping, E.; Lofts, S.; Mortimer, R. J. G. Effect of Ocean Acidification on Organic and Inorganic Speciation of Trace Metals. *Environ. Sci. Technol.* **2016**, *50* (4), 1906−1913.
(88) De la Rosa, J. M.; Santos, M.; Araújo, M. F. Metal Binding by Humic Acids in Recent Sediments from the SW Iberian Coastal Area. *Estuar Coast Shelf Sci.* **2011**, *93* (4), 478−485.

(89) Jokinen, S. A.; Jilbert, T.; Tiihonen-Filppula, R.; Koho, K. Terrestrial Organic Matter Input Drives Sedimentary Trace Metal Sequestration in a Human-Impacted Boreal Estuary. *Science of The Total Environment* **2020**, *717*, 137047.
(90) Malea, P.; Chatziapostolou, A.; Kevrekidis, T. Trace Element Seasonality in Marine Macroalgae of Different Functional-Form Groups. *Mar Environ. Res.* **2015**, *103*, 18−26.
(91) He, J.; Chen, J. P. A Comprehensive Review on Biosorption of Heavy Metals by Algal Biomass: Materials, Performances, Chemistry, and Modeling Simulation Tools. *Bioresour. Technol.* **2014**, *160*, 67−78.
(92) Gómez, I.; Huovinen, P. Brown Algal Phlorotannins: An Overview of Their Functional Roles. *Antarctic Seaweeds: Diversity, Adaptation and Ecosystem Services* **2020**, 365−388.
(93) Vázquez-Arias, A.; Boquete, M. T.; Martín-Jouve, B.; Tucoulou, R.; Rodríguez-Prieto, C.; Fernández, J. Á.; Aboal, J. R. Nanoscale Distribution of Potentially Toxic Elements in Seaweeds Revealed by Synchrotron X-Ray Fluorescence. *J. Hazard Mater.* **2024**, *480*, 136454.
(94) Paix, B.; Layglon, N.; Le Poupon, C.; D'Onofrio, S.; Misson, B.; Garnier, C.; Culioli, G.; Briand, J. F. Integration of Spatio-Temporal Variations of Surface Metabolomes and Epibacterial Communities Highlights the Importance of Copper Stress as a Major Factor Shaping Host-Microbiota Interactions within a Mediterranean Seaweed Holobiont. *Microbiome* **2021**, *9* (1), 1−19.
(95) García-Seoane, R.; Richards, C. L.; Aboal, J. R.; Fernández, J. Á.; Schmid, M. W.; Boquete, M. T. A Field Study of the Molecular Response of Brown Macroalgae to Heavy Metal Exposure: An (Epi)Genetic Approach. *J. Hazard Mater.* **2024**, *480*, 136304.
(96) Simou, A.; Mrabet, A.; Abdelfattah, B.; Bougrine, O.; Khaddor, M.; Allali, N. Distribution, Ecological, and Health Risk Assessment of Trace Elements in the Surface Seawater along the Littoral of Tangier Bay (Southwestern Mediterranean Sea). *Mar. Pollut. Bull.* **2024**, *202*, 116362.
(97) European Environmental Agency. *Air quality in Europe 2022, Report 05/2022*. https://www.eea.europa.eu/publications/air-quality-in-europe-2022.
(98) Zhang, L.; Gao, Y.; Wu, S.; Zhang, S.; Smith, K. R.; Yao, X.; Gao, H. Global Impact of Atmospheric Arsenic on Health Risk: 2005 to 2015. *Proc. Natl. Acad. Sci. U. S. A.* **2020**, *117* (25), 13975−13982.
(99) Wang, L.; Wang, X.; Chen, H.; Wang, Z.; Jia, X. Oyster Arsenic, Cadmium, Copper, Mercury, Lead and Zinc Levels in the Northern South China Sea: Long-Term Spatiotemporal Distributions, Combined Effects, and Risk Assessment to Human Health. *Environmental Science and Pollution Research* **2022**, *29* (9), 12706−12719.
(100) Knopf, B.; Fliedner, A.; Radermacher, G.; Rüdel, H.; Paulus, M.; Pirntke, U.; Koschorreck, J. Seasonal Variability in Metal and Metalloid Burdens of Mussels: Using Data from the German Environmental Specimen Bank to Evaluate Implications for Long-Term Mussel Monitoring Programs. *Environ. Sci. Eur.* **2020**, *32* (1), 1−13.
(101) Chung, J.-Y.; Yu, S.-D.; Hong, Y.-S. Environmental Source of Arsenic Exposure. *Journal of Preventive Medicine and Public Health* **2014**, *47* (5), 253−257.
(102) Podgorski, J.; Berg, M. Global Threat of Arsenic in Groundwater. *Science (1979)* **2020**, *368* (6493), 845−850.
(103) Maharana, D.; Jena, K.; Pise, N. M.; Jagtap, T. G. Assessment of Oxidative Stress Indices in a Marine Macro Brown Alga Padina Tetrastromatica (Hauck) from Comparable Polluted Coastal Regions of the Arabian Sea, West Coast of India. *Journal of Environmental Sciences* **2010**, *22* (9), 1413−1417.
(104) Zhang, A.; Xu, T.; Zou, H.; Pang, Q. Comparative Proteomic Analysis Provides Insight into Cadmium Stress Responses in Brown Algae Sargassum Fusiforme. *Aquatic Toxicology* **2015**, *163*, 1−15.
(105) Lü, F.; Dind, G.; Liu, W.; Zhan, D.; Wu, H.; Guo, W. Comparative Study of Responses in the Brown Algae Sargassum Thunbergii to Zinc and Cadmium Stress. *J. Oceanol Limnol* **2018**, *36* (3), 933−941.
(106) Connan, S.; Stengel, D. B. Impacts of Ambient Salinity and Copper on Brown Algae: 2. Interactive Effects on Phenolic Pool and Assessment of Metal Binding Capacity of Phlorotannin. *Aquatic Toxicology* **2011**, *104* (1−2), 1−13.
(107) Coelho, J. P. Arsenic Speciation in Algae: Case Studies in Europe. *Arsenic Speciation in Algae*2019, *85*179−198. .
(108) Jinadasa, K. K.; Herbello-Hermelo, P.; Peña-Vázquez, E.; Bermejo-Barrera, P.; Moreda-Piñeiro, A. Mercury Speciation in Edible Seaweed by Liquid Chromatography - Inductively Coupled Plasma Mass Spectrometry after Ionic Imprinted Polymer-Solid Phase Extraction. *Talanta* **2021**, *224*, 121841.
(109) Al-Soufi, S.; García, J.; Muíños, A.; Pereira, V.; Piñeiro, V.; Miranda, M.; García-Vaquero, M.; López-Alonso, M. Assessment of Macroalgae and Macroalgal Extracts as a Source of Minerals in Need of Fine-Tuning in Multiple Livestock Production Systems. *Anim Feed Sci. Technol.* **2025**, *319*, 116154.
(110) García-Seoane, R.; Aboal, J. R.; Boquete, M. T.; Fernández, J. A. Phenotypic Differences in Heavy Metal Accumulation in Populations of the Brown Macroalgae Fucus Vesiculosus: A Transplantation Experiment. *Ecol Indic* **2020**, *111*, 105978.
(111) Piñeiro-Corbeira, C.; Barreiro, R.; Cremades, J.; Arenas, F. Seaweed Assemblages under a Climate Change Scenario: Functional Responses to Temperature of Eight Intertidal Seaweeds Match Recent Abundance Shifts. *Scientific Reports 2018 8:1* **2018**, *8* (1), 1−9.
(112) Piñeiro-Corbeira, C.; Barreiro, R.; Cremades, J. Decadal Changes in the Distribution of Common Intertidal Seaweeds in Galicia (NW Iberia). *Mar Environ. Res.* **2016**, *113*, 106−115.

70
https://doi.org/10.1021/acs.est.4c14013
Environ. Sci. Technol. 2025, 59, 10476−10487

Three Decades of Change in Potentially Toxic Elements in Brown Algae in the Northeast Atlantic Ocean

Carme Pacín[1,2*], J. Ángel Fernández[1], Mercedes Conde-Amboage[3], Massimo Lazzari[2], Rita García-Seoane[4,5], Inés G. Viana[4], Zulema Varela[1], Carlos Real[6], Rubén Villares[6], Jesús R. Aboal[1]

1. CRETUS Centre, Department of Functional Biology, Ecology Unit, Universidade de Santiago de Compostela, Santiago de Compostela, 15782, Spain
2. CIQUS Centre, Department of Physical Chemistry, Universidade de Santiago de Compostela, Santiago de Compostela, 15782, Spain
3. Department of Statistics, Mathematical Analysis and Optimization, Universidade de Santiago de Compostela, Santiago de Compostela, 15782, Spain
4. Instituto Español de Oceanografía (IEO-CSIC), Centro Oceanográfico de A Coruña, A Coruña, 15001, Spain
5. Department of Earth Sciences, University of Hawaii at Mānoa, 1680 East-West Road, POST 719B, Honolulu, HI, 96822, United States
6. Department of Functional Biology, Ecology Unit, Universidade de Santiago de Compostela, Escola Politécnica Superior de Enxeñaría Lugo, 27002, Spain

* Corresponding author. Email: mcarme.pacin@usc.es

Number of pages: 36. Number of tables: 7. Number of figures: 20

Supporting Information includes:

- Additional information for Linear Mixed Models (LMM)
- Supplementary tables. Table S1 (Number of sampling sites per year and species), Table S2 (Quality analysis results), Table S3 Median PTE concentrations per year and species, and significant interannual Dunn's test results), Table S4 (Detailed PTE concentrations per sampling site and sampling campaign), Table S5 (Bioconcentration factors and sediment contribution), Table S6 (Summary of key outputs from LMMs), and Table S7 (Percentage of variability explained by each factor in PMF models).
- Supplementary figures. Figs. S1-S9 (Overview of PTEs concentrations on the sampling sites), Figs. S10- S11 (Overview of PTEs concentrations over time), Figs. S12-S19 (Maps of percentage changes in PTES concentrations), S20 (correlation matrix and PCA).

Supporting information_2_TableS4 includes Table S4 which consists in an excel file containing sampling sites information including Coordinates (WGS84), Ría, Species, Year of sampling, and Potentially Toxic Elements (PTEs) concentrations.

Additional information for Linear Mixed Models (LMM)

All data were first explored for outliers, normality, homogeneity of variance and collinearity. Logarithm transformations were applied to obtain a better approximation to a normal distribution.

The statistical significance of interannual trends in elements was assessed, with species and year of sampling as fixed factors, and ría as random factor, fitting several models:

Model 1. Element concentration ~ Year

Model 2. Element concentration ~ Year + (1 | ría)

Model 3. Element concentration ~ Year + (Year | ría)

Model 4. Element concentration ~ Year + Species + (1| ría)

Model 5. Element concentration ~ Year + Species + (Year| ría)

The different models were compared using the Bayesian Information Criterion (BIC) and the Akaike Information Criterion (AIC). From each model, we obtained fitted values, residuals, R^2, p values for F-statistics and goodness of fit by an analysis of variance (ANOVA). Standard residual validation techniques (q–q plot, residual histograms and scatterplots of predictors vs. residuals) were applied to validate the final model. Main outputs of the selected models can be found in Table S4, with p-values corrected using the Benjamini-Hochberg (BH) method

Supplementary Tables

Table S1. Number of sampling sites per year and species.

	1990	2001	2003	2005	2007	2021
Fucus ceranoides	79	14	14	14	14	58
Fucus vesicuosus - F. spiralis	48	25	34	35	35	76

Table S2. Quality analysis results in terms of limit of quantification (LOQ) expressed in μg l^{-1} for all elements except Hg (ng g^{-1}), sample size, Relative Percent Differences (RPD, %), and recovery from reference materials (%). The recovery is shown only for elements with certified concentrations in the reference material.

	Sample size	LOQ	RPD	Recovery
Al	16	29.13	5.3	-
Cr	16	0.97	8.9	-
Fe	16	17.72	3.1	-
Ni	16	0.49	3.3	-
Cu	16	3.11	4.1	89
Zn	16	7.31	3.3	96
As	16	1.48	2.5	109
Cd	16	0.55	3.4	99
Hg	31	3.59	2.7	97

Table S3. Median concentrations of Al, Cr, Fe, Ni, Cu, Zn, As, and Cd (μg g^{-1}, dry weight), and Hg (ng g^{-1}, dry weight) in *Fucus* spp. collected from NW Spain (1990-2021). 'Year' indicates sampling year, and 'All' combines all years. *F.v-F.s* refers to *F. vesiculosus* and *F. spiralis*, *F.c* to *F. ceranoides,* and *Fucus* spp. represents these species combined. COD (coefficient of dispersion) represents the median absolute deviation divided by the median (%). The 'Dunn-test' column identified significant interannual variations through Dunn's post-hoc tests with Benjamini-Hochberg correction, following significant Kruskal-Wallis results (α = 0.001) across all *Fucus* spp. Significant differences ($p<0.05$) are indicated by distinct lowercase letters.

Element	Year	Median (*F.v-F.s*)	Median (*F.c*)	Median (*Fucus* spp.)	COD (*Fucus* spp.)	Dunn's test (*Fucus* spp.)
Al n=446	1990	80.3	143	124	44.1	a
	2001	134	585	263	66.0	a
	2003	51.3	642	82.3	86.4	a
	2005	52.3	617	147	94.1	a
	2007	45.8	559	75.3	87.8	a
	2021	413	1515	917	80.6	b
	All	90.5	502	180	85.0	
Cr n=446	1990	8.26	10.1	8.64	71.3	a
	2001	3.64	7.34	4.41	48.2	ab
	2003	2.48	9.64	3.15	60.4	b
	2005	3.13	11.1	6.54	60.3	ab
	2007	1.62	8.88	2.30	53.4	b
	2021	0.67	1.62	1.14	78.1	c
	All	2.23	7.10	3.16	82.0	
Fe n=446	1990	204	315	277	32.1	a
	2001	172	499	295	52.3	ab
	2003	111	573	172	58.1	a
	2005	123	650	197	73.4	a
	2007	101	565	131	58.8	a
	2021	257	994	651	70.8	b
	All	164	506	295	65.9	
Ni n=446	1990	9.84	11.0	10.6	41.7	a
	2001	5.66	7.46	5.92	25.9	b
	2003	3.33	7.80	4.31	41.5	b
	2005	3.53	9.55	4.72	42.9	b
	2007	4.03	8.25	4.63	42.6	b
	2021	1.39	2.53	1.65	38.4	c

	All	3.52	7.57	5.00	60.6	
Cu n=446	1990	47.8	47.4	47.4	60.7	a
	2001	11.4	13.7	12.0	54.5	bd
	2003	3.39	6.48	4.89	52.6	c
	2005	8.68	13.5	10.4	50.8	d
	2007	17.9	21.9	18.3	46.7	ab
	2021	2.47	4.75	3.39	52.5	c
	All	7.68	14.9	10.1	75.1	
Zn n=446	1990	45.8	55.1	50.4	39.0	a
	2001	46.2	71.3	53.2	29.5	a
	2003	39.1	49.9	44.3	24.3	ab
	2005	38.5	52.5	40.6	19.4	ab
	2007	38.1	77.8	41.3	30.3	b
	2021	31.7	45.8	37.4	36.2	b
	All	38.9	52.8	43.4	33.3	
As n=446	1990	40.7	35.2	37.6	25.8	a
	2001	36.8	30.0	34.1	16.4	a
	2003	33.7	23.7	31.7	22.0	ab
	2005	28.5	23.0	27.9	13.1	cb
	2007	28.3	19.5	25.3	14.6	c
	2021	61.8	46.4	55.8	29.1	d
	All	37.7	34.9	36.0	28.7	
Cd n=446	1990	0.84	0.85	0.8	30.4	a
	2001	0.58	0.86	0.7	25.8	ab
	2003	0.66	0.66	0.7	34.1	bc
	2005	0.79	0.56	0.7	24.3	ab
	2007	0.65	0.66	0.6	25.5	cb
	2021	0.50	0.51	0.5	26.1	c
	All	0.64	0.68	0.66	32.7	
Hg n=425	1990	60.8	69.2	64.6	39.0	a
	2001	24.4	20.4	24.1	25.1	b
	2003	17.4	19.5	18.1	24.9	b
	2005	16.1	21.7	17.1	29.8	b
	2007	16.4	22.5	18.2	30.4	b
	2021	16.4	18.1	17.5	26.3	b
	All	20.3	29.7	22.5	41.3	

Table S4. Excel file (provided in Supplementary material 2) containing sampling sites information including Coordinates (WGS84), Ría, Species, Year of sampling, and Potential Toxic Elements (PTEs) concentrations for each sample of Fucus collected in NW Spain from 1990 to 2021. Element concentrations are expressed in μg g-1, except for Hg in ng g -1. Additionally, the Relative Standard Deviation (RSD, expressed as a percentage) is included.

Table S5. Analysis of: (1) bioconcentration factors (BCF) for Potentially Toxic Elements (PTEs) in *Fucus* spp. (2021 data) relative to seawater (2023 data), and (2) sediment-derived contributions (%) to algal PTE concentrations (year-matched samples). Calculations follow Equations (1) and (2) (Material and Methods section).

	Year	Al	Cr	Cu	Fe	Ni	Zn	Cd	Hg
BCF seawater	2021/ 2023	39.1	10.4	6.26	64.5	2.48	0.047	20.3	-
Sediment contrib.	1990		0.43	0.095	11.4	0.25	0.37	-	
	2001		-	-	112	11.5	4.36	-	
	2003		-	-	99.1	6.06	3.52	-	
	2005		7.54	4.56	83.4	6.06	5.41	0.67	17.2
	2007		6.24	1.96	60.4	4.26	2.28	0.61	8.16
	All		2.18	0.23	54.0	3.54	1.33	0.66	15.0

Table S6. Summary of key outputs from linear mixed models assessing temporal trends of Potential Toxic Elements (PTEs). The "Model" column indicates the selected model (see combinations tested in Additional information for Linear Mixed Models (LMM) at this file). "R^2 marg" and "R^2 cond" represent marginal and conditional R^2, respectively. Columns include estimates for "Year" and "Species", residual variance, and p-values corrected using the Benjamini-Hochberg method for both "Year" and "Species".

PTE	Model	Estimate (Year)	Estimate (Species)	Residual Variance	R^2 marg	R^2 cond	p-value year	p-value species
Al	Model 4	0.063	-1.532	1.212	0.395	0.513	4.515E-37	1.085E-35
Cr	Model 5	-0.073	-0.681	0.922	0.416	0.601	1.735E-06	2.238E-11
Fe	Model 4	0.024	-1.101	0.649	0.305	0.411	1.068E-12	4.309E-35
Ni	Model 5	-0.051	-0.371	0.342	0.469	0.635	4.135E-09	1.762E-09
Cu	Model 5	-0.085	-0.557	0.974	0.480	0.609	9.823E-08	4.356E-08
Zn	Model 5	-0.011	-0.402	0.210	0.138	0.550	9.866E-04	2.947E-16
As	Model 5	0.012	0.129	0.204	0.103	0.212	1.837E-03	4.486E-03
Cd	Model 2	-0.015	-	0.250	0.093	0.320	4.788E-13	-
Hg	Model 5	-0.037	-0.267	0.314	0.299	0.574	2.540E-07	6.998E-06

Table S7. Percentage of variability explained by each factor in the Positive matrix factorization models applied separately for the sampling dates 1990, 2001-2007, and 2021.

	Factor 1	Factor 2	Factor 3	Factor 4
1990	24.88	37.48	25.96	11.68
2001-2007	30.61	35.16	18.64	15.59
2021	38.34	25.16	19.66	16.84

Supplementary Figures

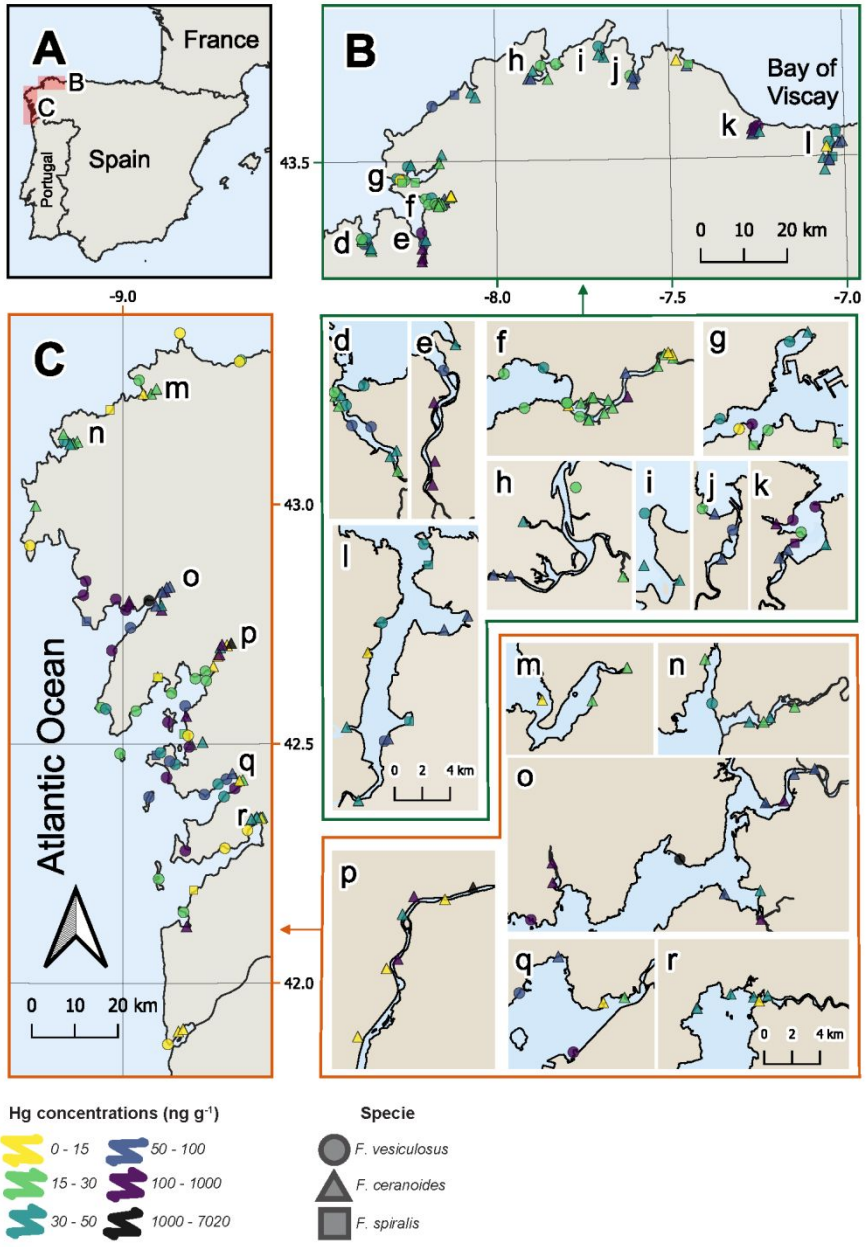

Fig. S1. Overview of Hg median concentrations (ng g $^{-1}$) in the sampling sites. Panels A-C display an overview of the region, with B and C showing the sampling sites. Panels d-l and m-r present detailed maps of sites that are densely clustered and difficult to distinguish in B and C, respectively. Different symbols represent the species sampled (*Fucus ceranoides, F. spiralis* and *F. vesiculosus*).

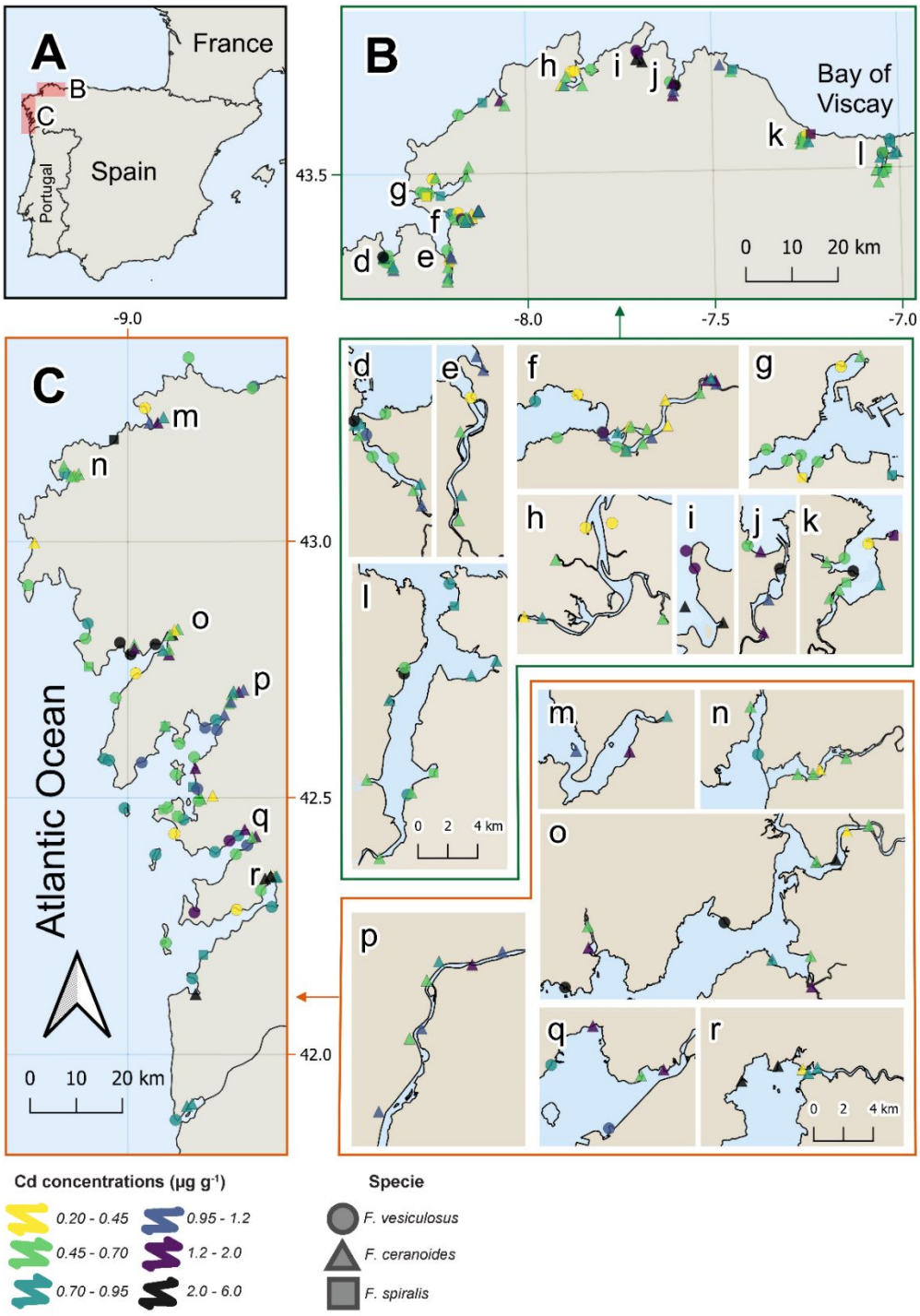

Fig. S2. Overview of Cd median concentrations (µg g^{-1}) in the sampling sites. Panels A-C display an overview of the region, with B and C showing the sampling sites. Panels d-l and m-r present detailed maps of sites that are densely clustered and difficult to distinguish in B and C, respectively. Different symbols represent the species sampled (*Fucus ceranoides, F. spiralis* and *F. vesiculosus*).

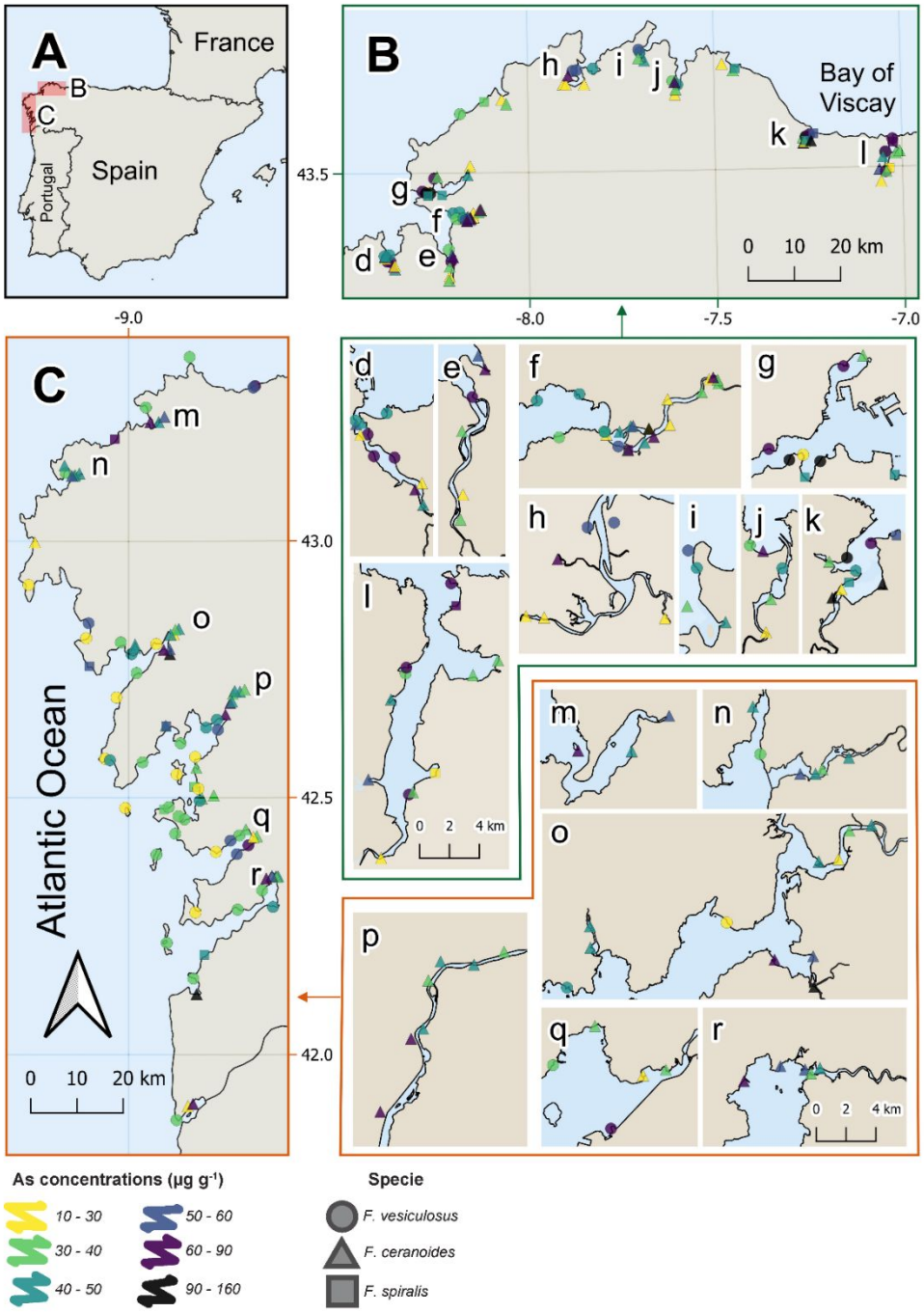

Fig. S3. Overview of As median concentrations (µg g $^{-1}$) in the sampling sites. Panels A-C display an overview of the region, with B and C showing the sampling sites. Panels d-l and m-r present detailed maps of sites that are densely clustered and difficult to distinguish in B and C, respectively. Different symbols represent the species sampled (*Fucus ceranoides, F. spiralis* and *F. vesiculosus*).

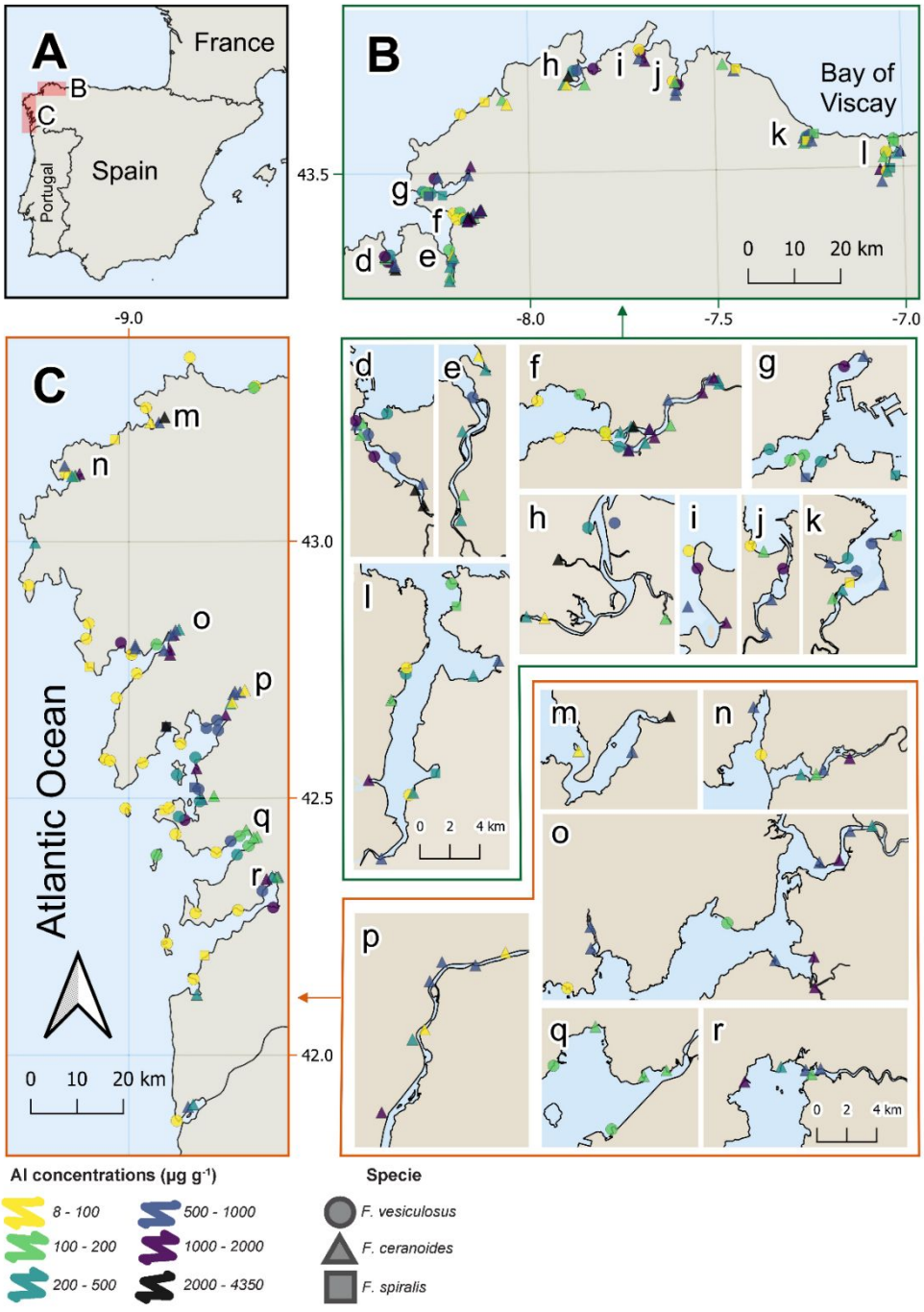

Fig. S4. Overview of Al median concentrations (µg g $^{-1}$) in the sampling sites. Panels A-C display an overview of the region, with B and C showing the sampling sites. Panels d-l and m-r present detailed maps of sites that are densely clustered and difficult to distinguish in B and C, respectively. Different symbols represent the species sampled (*Fucus ceranoides, F. spiralis* and *F. vesiculosus*).

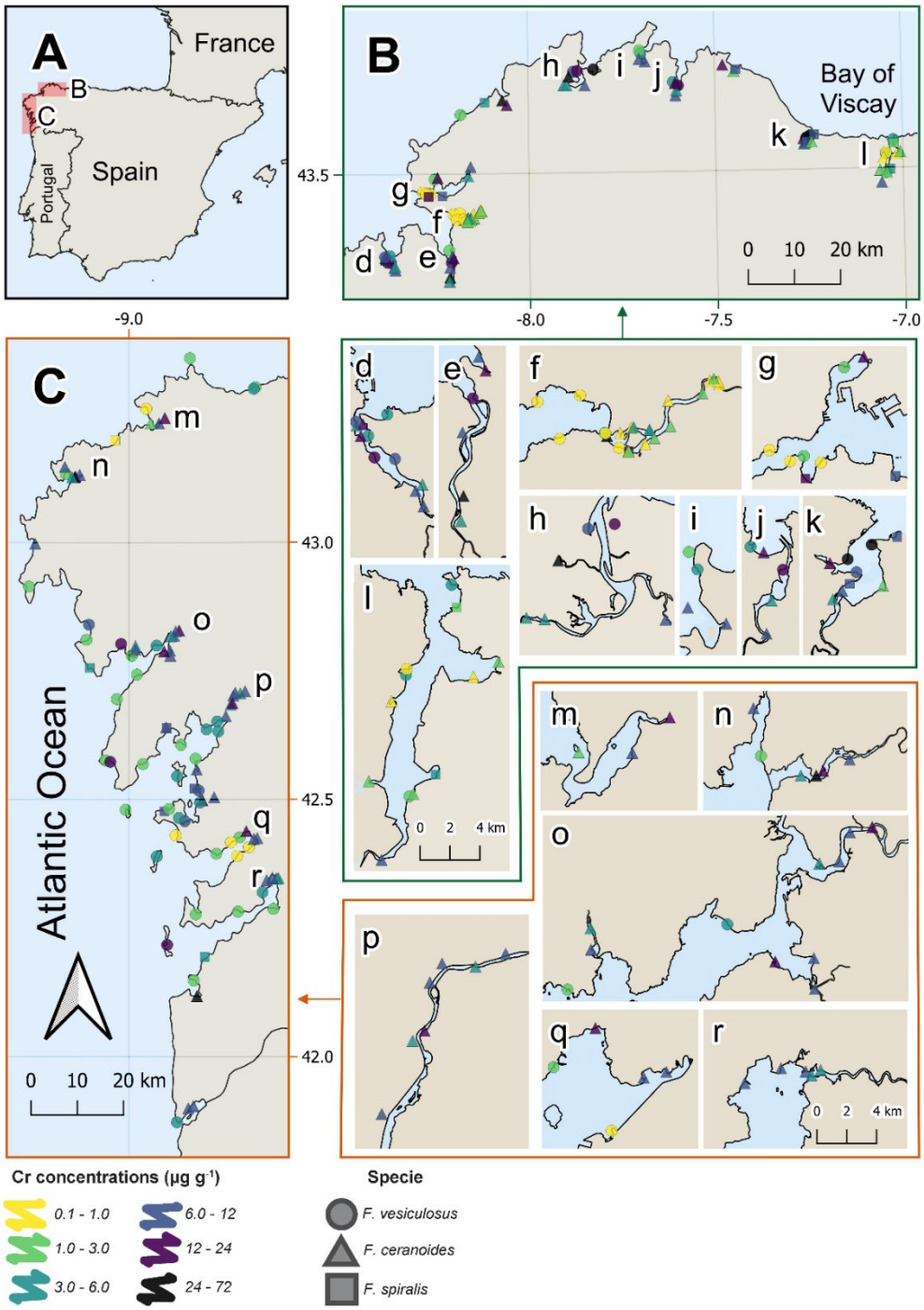

Fig. S5. Overview of Cr median concentrations (µg g $^{-1}$) in the sampling sites. Panels A-C display an overview of the region, with B and C showing the sampling sites. Panels d-l and m-r present detailed maps of sites that are densely clustered and difficult to distinguish in B and C, respectively. Different symbols represent the species sampled (*Fucus ceranoides, F. spiralis* and *F. vesiculosus*).

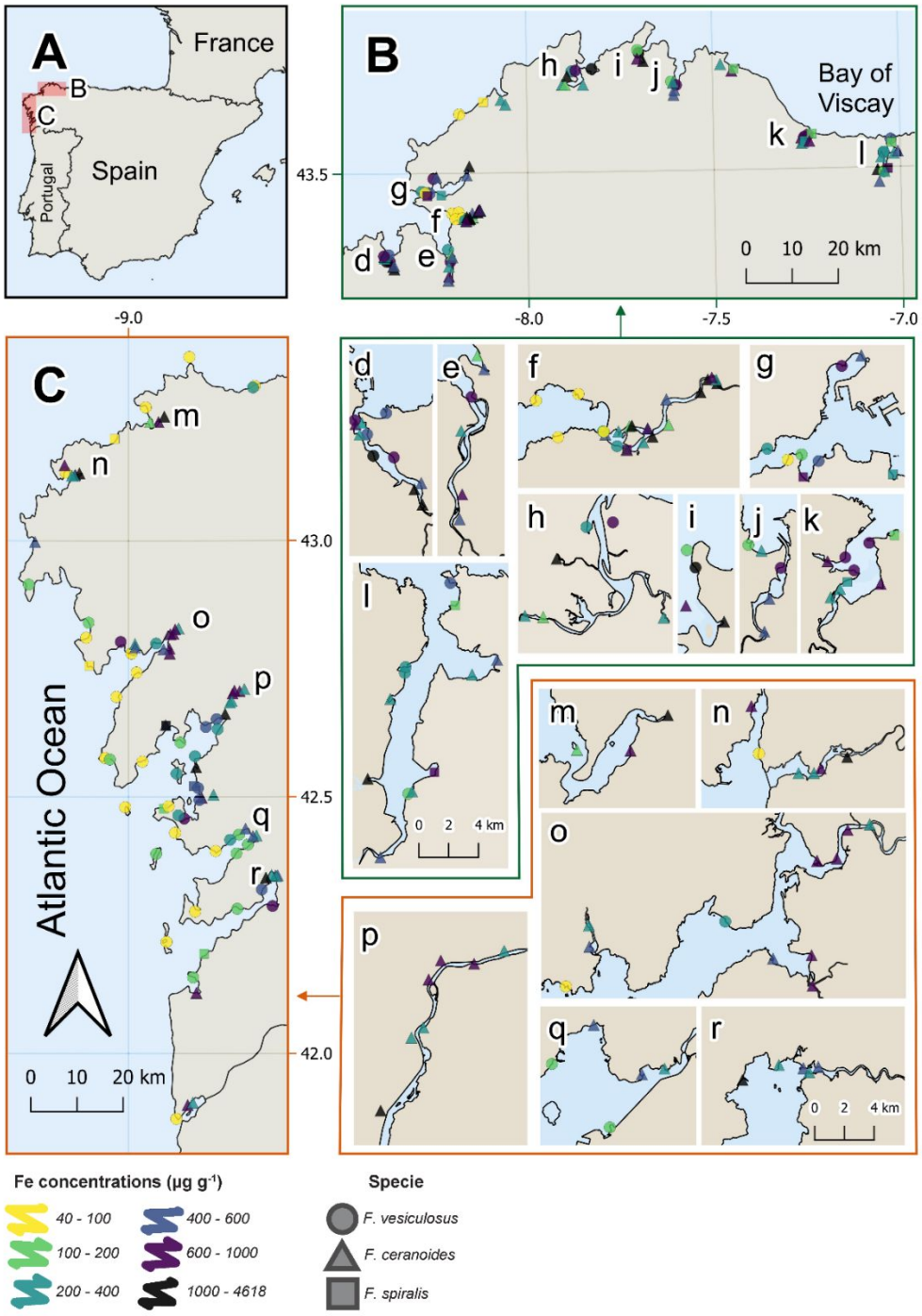

Fig. S6. Overview of Fe median concentrations (µg g $^{-1}$) in the sampling sites. Panels A-C display an overview of the region, with B and C showing the sampling sites. Panels d-l and m-r present detailed maps of sites that are densely clustered and difficult to distinguish in B and C, respectively. Different symbols represent the species sampled (*Fucus ceranoides, F. spiralis* and *F. vesiculosus*).

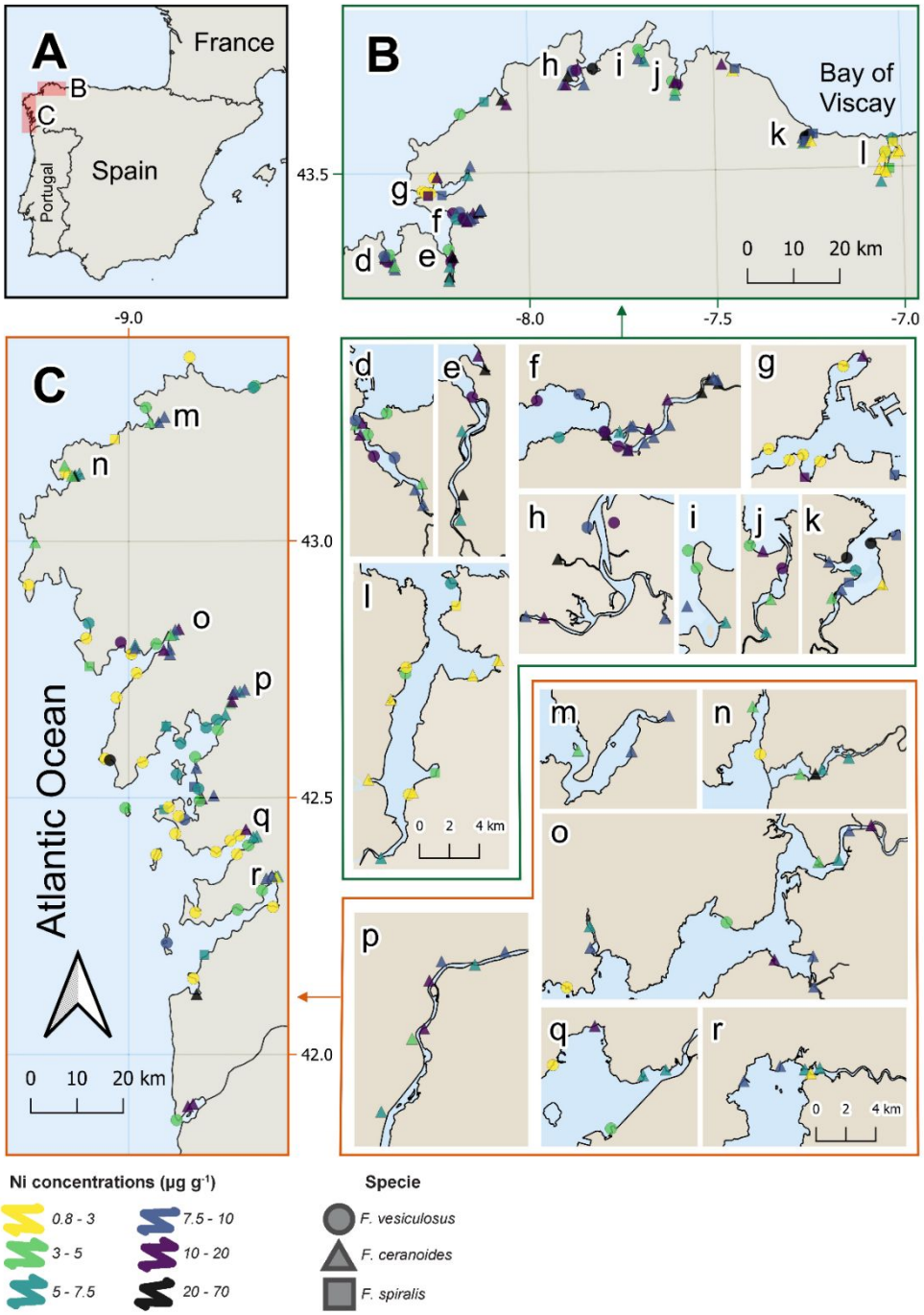

Fig. S7. Overview of Ni median concentrations (µg g $^{-1}$) in the sampling sites. Panels A-C display an overview of the region, with B and C showing the sampling sites. Panels d-l and m-r present detailed maps of sites that are densely clustered and difficult to distinguish in B and C, respectively. Different symbols represent the species sampled (*Fucus ceranoides, F. spiralis* and *F. vesiculosus*).

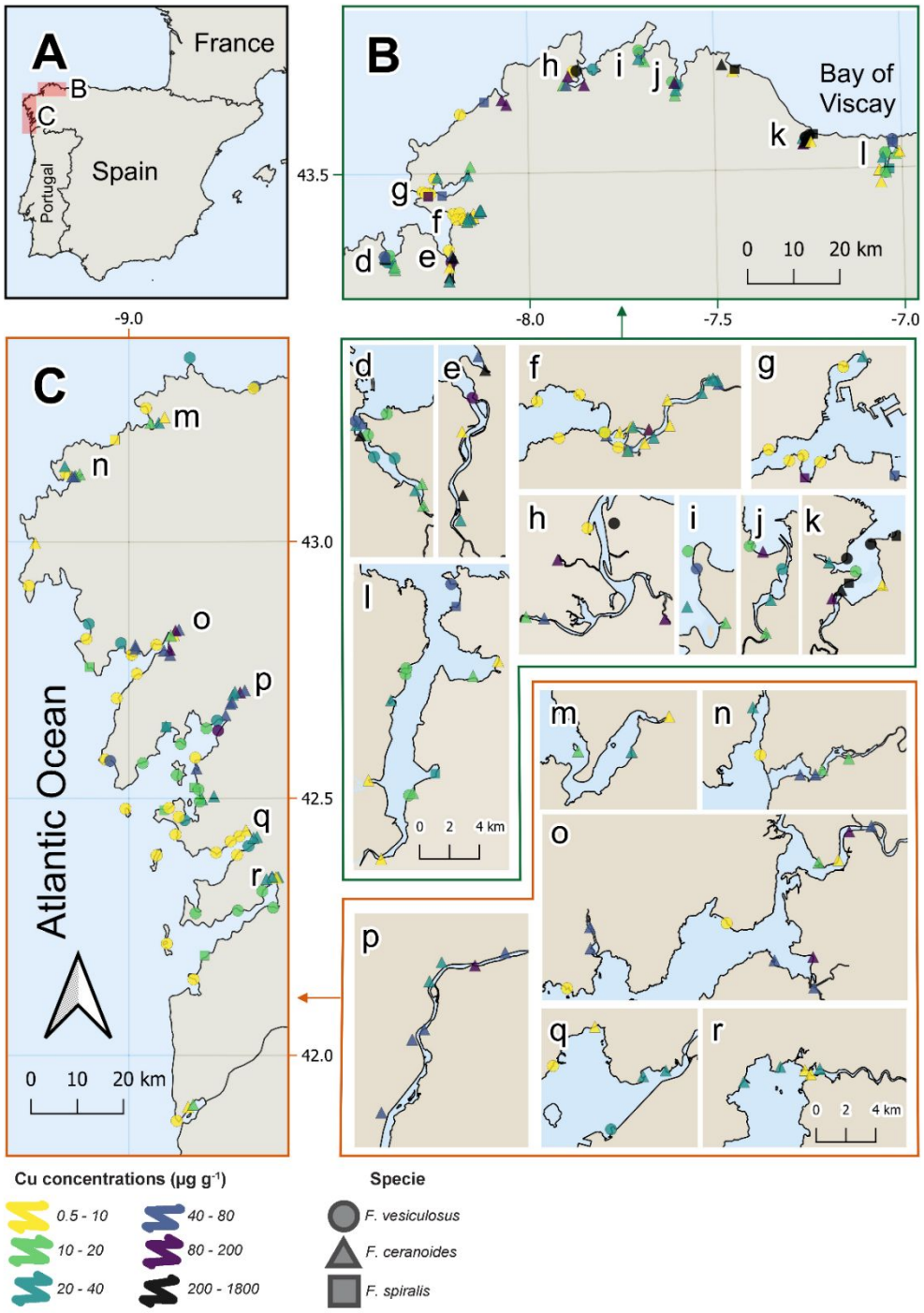

Fig. S8. Overview of Cu median concentrations (µg g $^{-1}$) in the sampling sites. Panels A-C display an overview of the region, with B and C showing the sampling sites. Panels d-l and m-r present detailed maps of sites that are densely clustered and difficult to distinguish in B and C, respectively. Different symbols represent the species sampled (*Fucus ceranoides, F. spiralis* and *F. vesiculosus*).

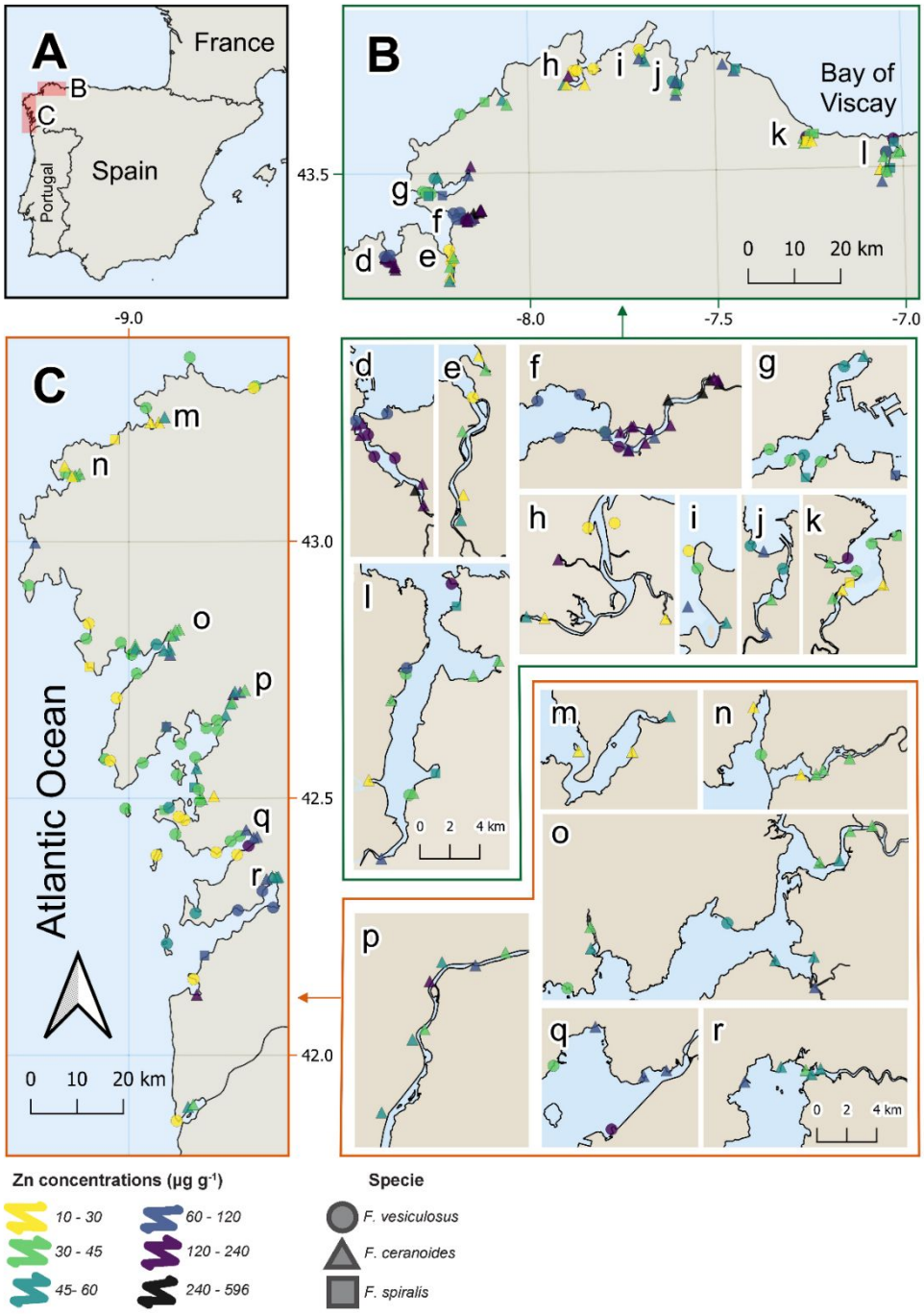

Fig. S9. Overview of Zn median concentrations (µg g $^{-1}$) in the sampling sites. Panels A-C display an overview of the region, with B and C showing the sampling sites. Panels d-l and m-r present detailed maps of sites that are densely clustered and difficult to distinguish in B and C, respectively. Different symbols represent the species sampled (*Fucus ceranoides, F. spiralis* and *F. vesiculosus*).

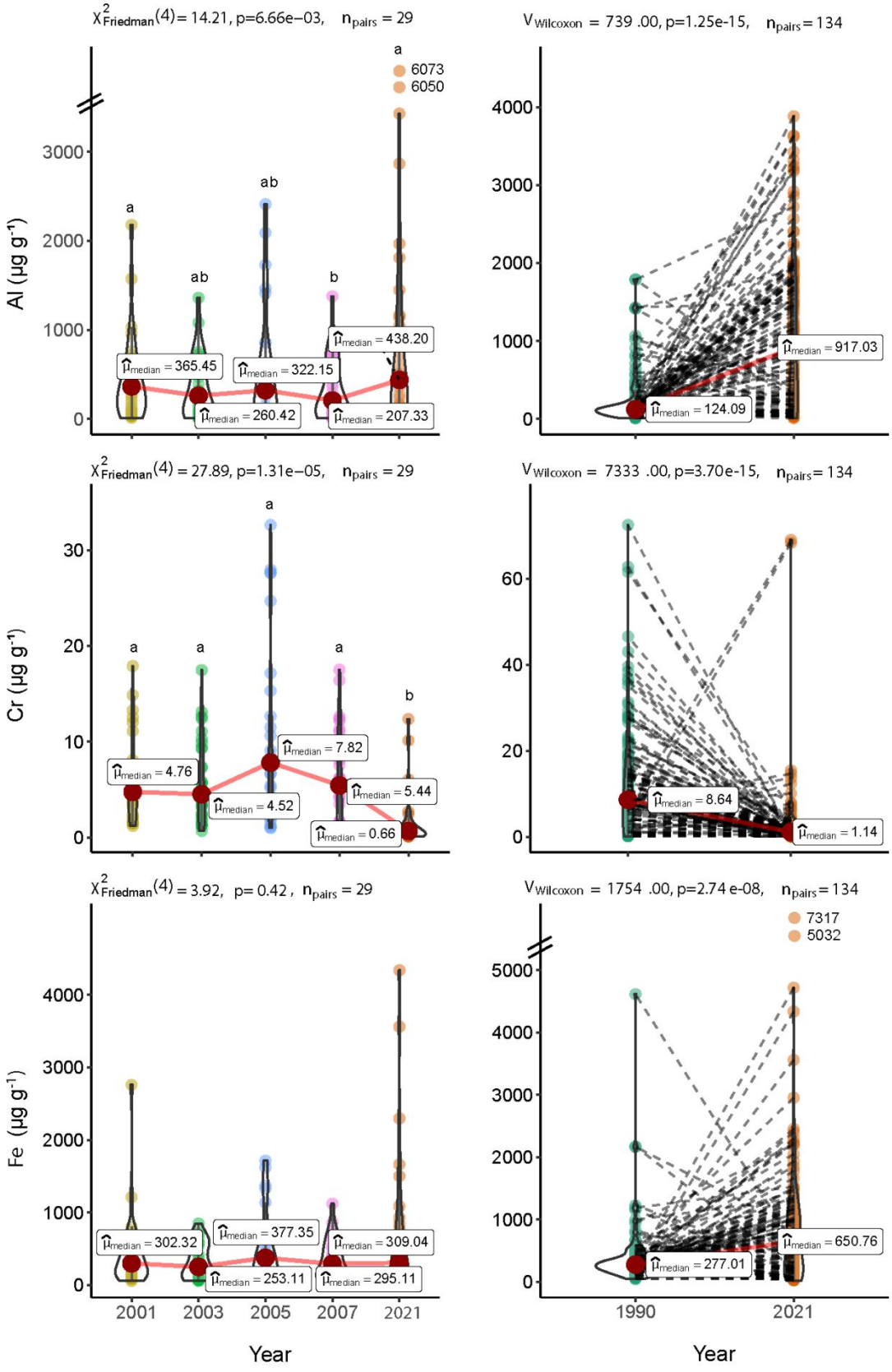

Fig. S10. Temporal trends of Al (µg g⁻¹), Cr (µg g⁻¹), and Fe (µg g⁻¹) concentrations in *Fucus* spp. Left panel: Repeated measures (2001-2021) analyzed by Friedman test with

Durbin-Conover post-hoc comparisons. Right panel: Paired 1990 vs 2021 comparisons (Wilcoxon test). Distinct lowercase letters indicate significant differences between years ($p<0.05$, no shared letters = significant).

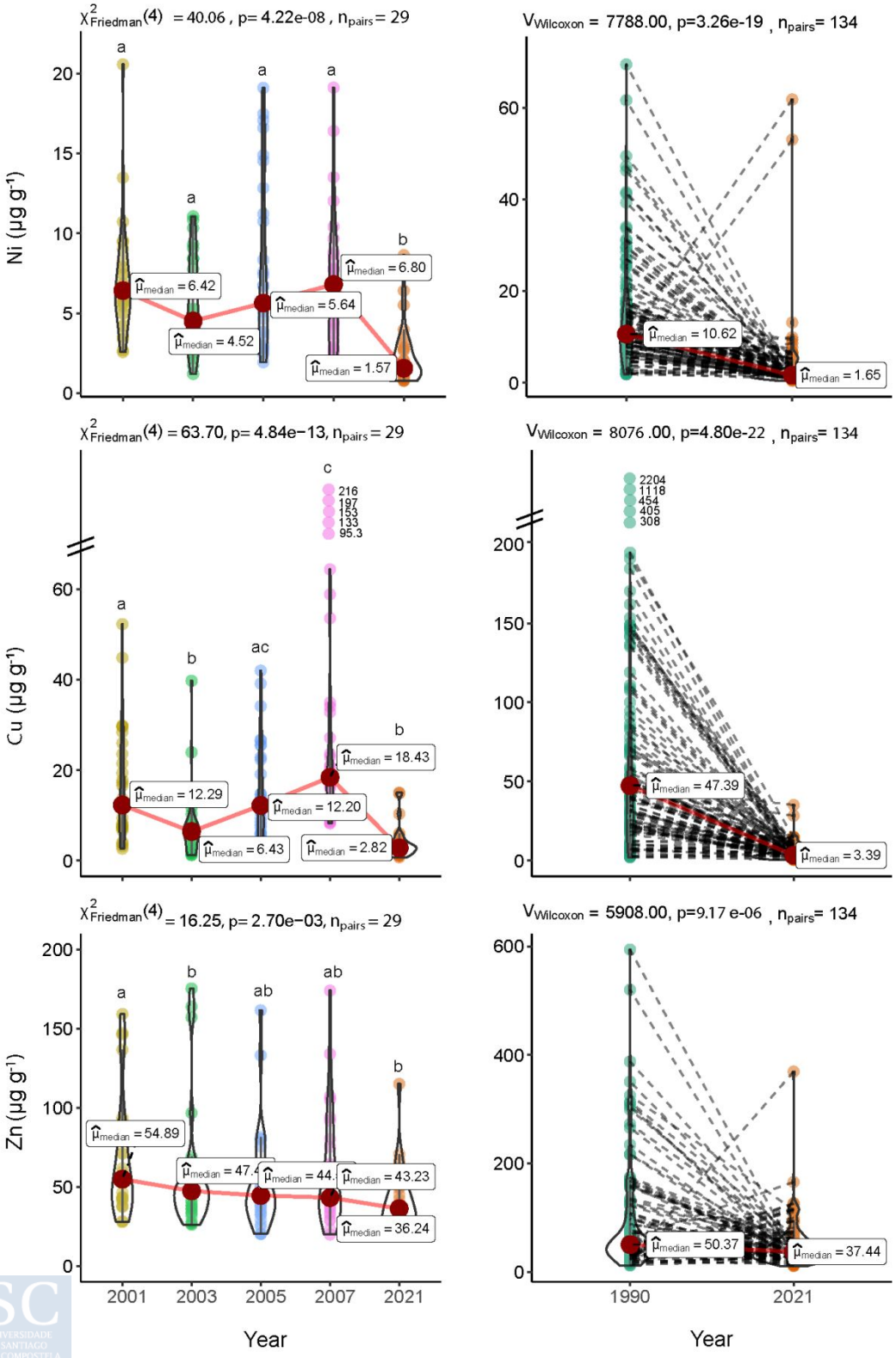

Fig. S11. Temporal trends of Ni (µg g^{-1}), Cu (µg g^{-1}), and Zn (µg g^{-1}) concentrations in *Fucus* spp. Left panel: Repeated measures (2001-2021) analyzed by Friedman test with Durbin-Conover post-hoc comparisons. Right panel: Paired 1990 vs 2021 comparisons (Wilcoxon test). Distinct lowercase letters indicate significant differences between years ($p<0.05$, no shared letters = significant).

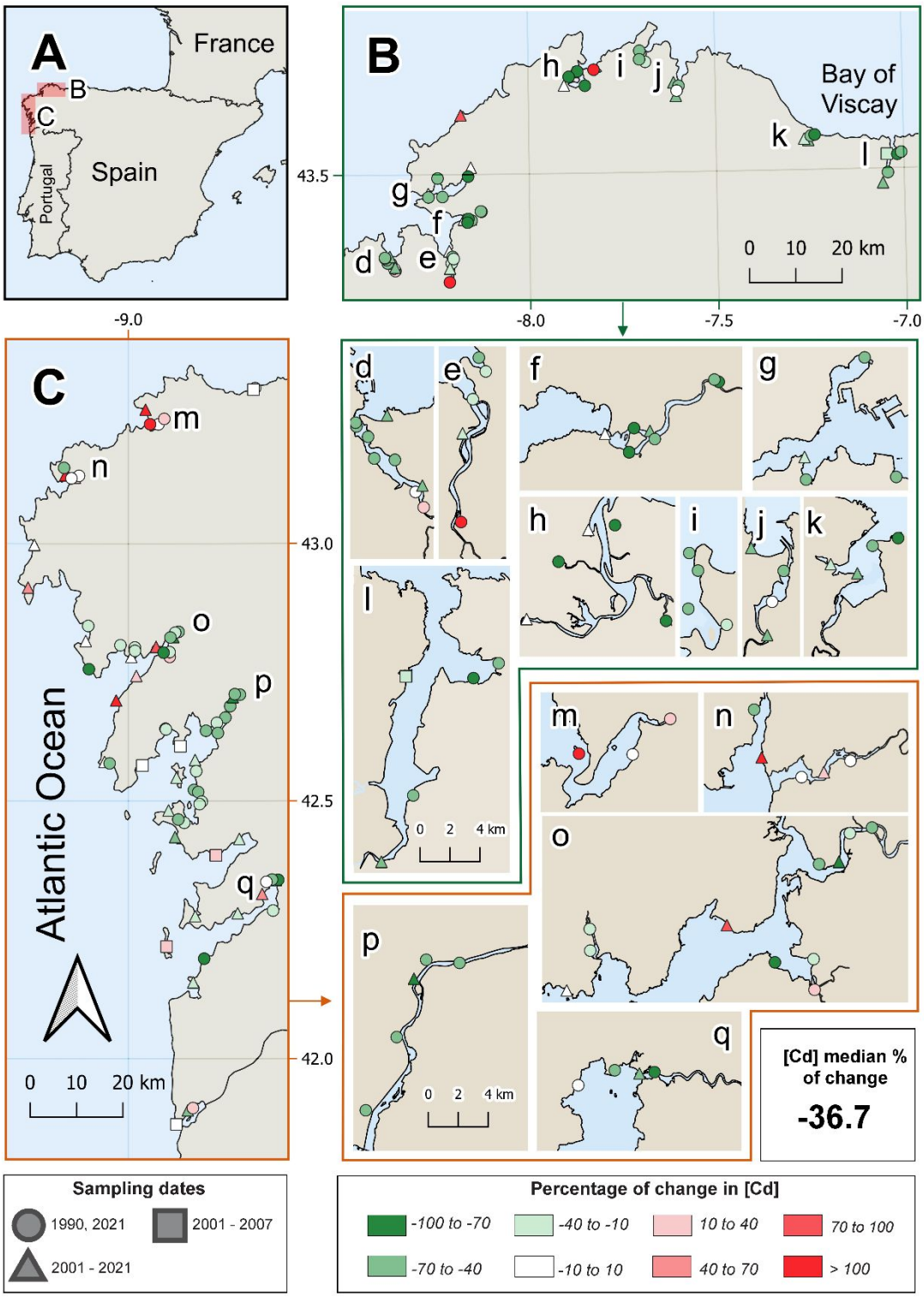

Fig. S12. Map of percentage changes in Cd concentrations over time. Panels A-C provide a regional overview, with B and C showing the differences between the final and initial

Cd concentrations (in %) at each sampling station. Panels d-l and m-q offer detailed views of sampling sites that are densely clustered and hard to distinguish in B and C, respectively. Different colors represent the percentage changes in Cd concentrations, while distinct symbols indicate the sampling dates: 1990 and 2021, 2001-2021, and 2001-2007. The total median percentage change, calculated as the median of the percentage changes across all sampling sites, is displayed below.

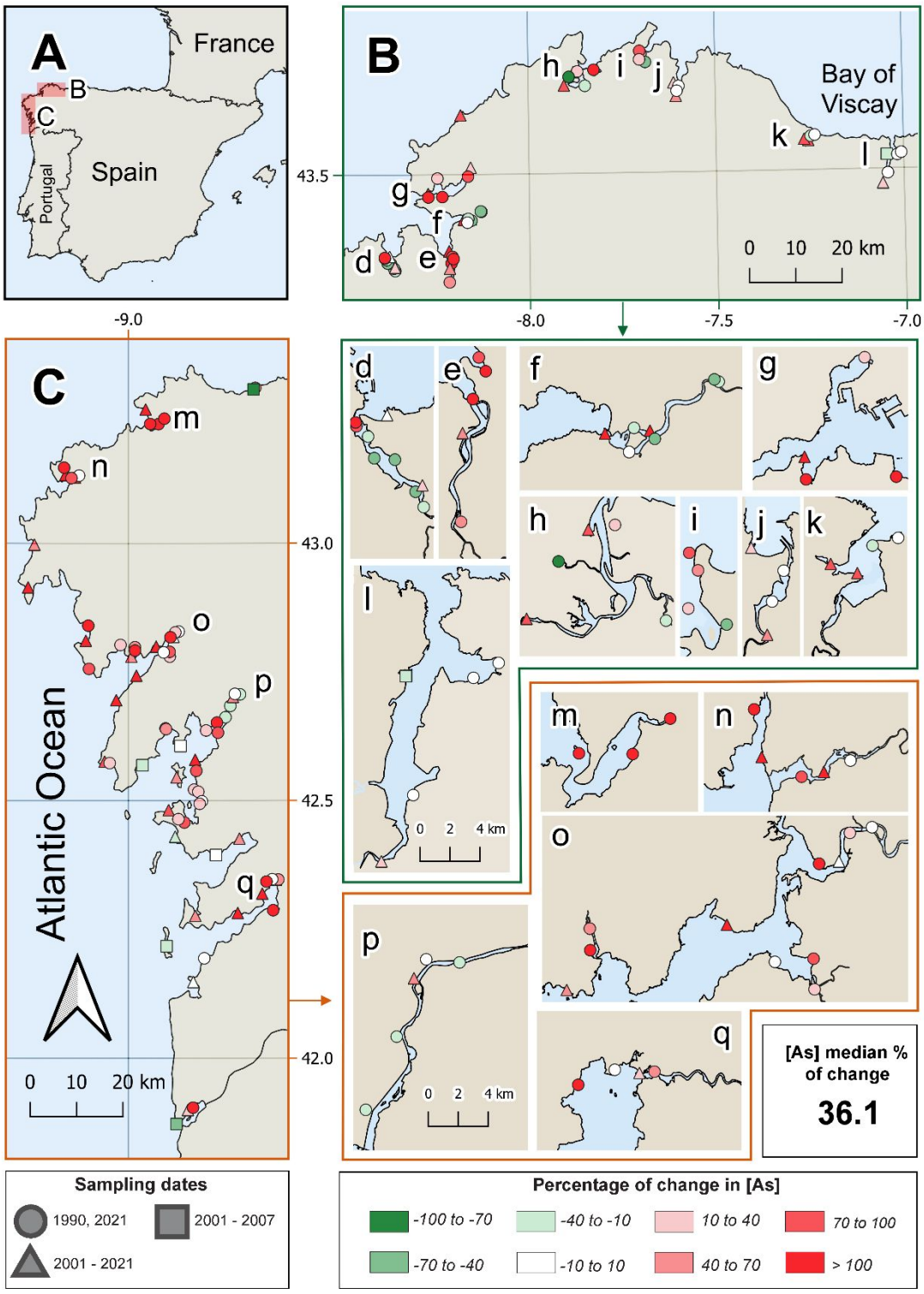

Fig. S13. Map of percentage changes in As concentrations over time. Panels A-C provide a regional overview, with B and C showing the differences between the final and initial As concentrations (in %) at each sampling station. Panels d-l and m-q offer detailed views

of sampling sites that are densely clustered and hard to distinguish in B and C, respectively. Different colors represent the percentage changes in As concentrations, while distinct symbols indicate the sampling dates: 1990 and 2021, 2001-2021, and 2001-2007. The total median percentage change, calculated as the median of the percentage changes across all sampling sites, is displayed below.

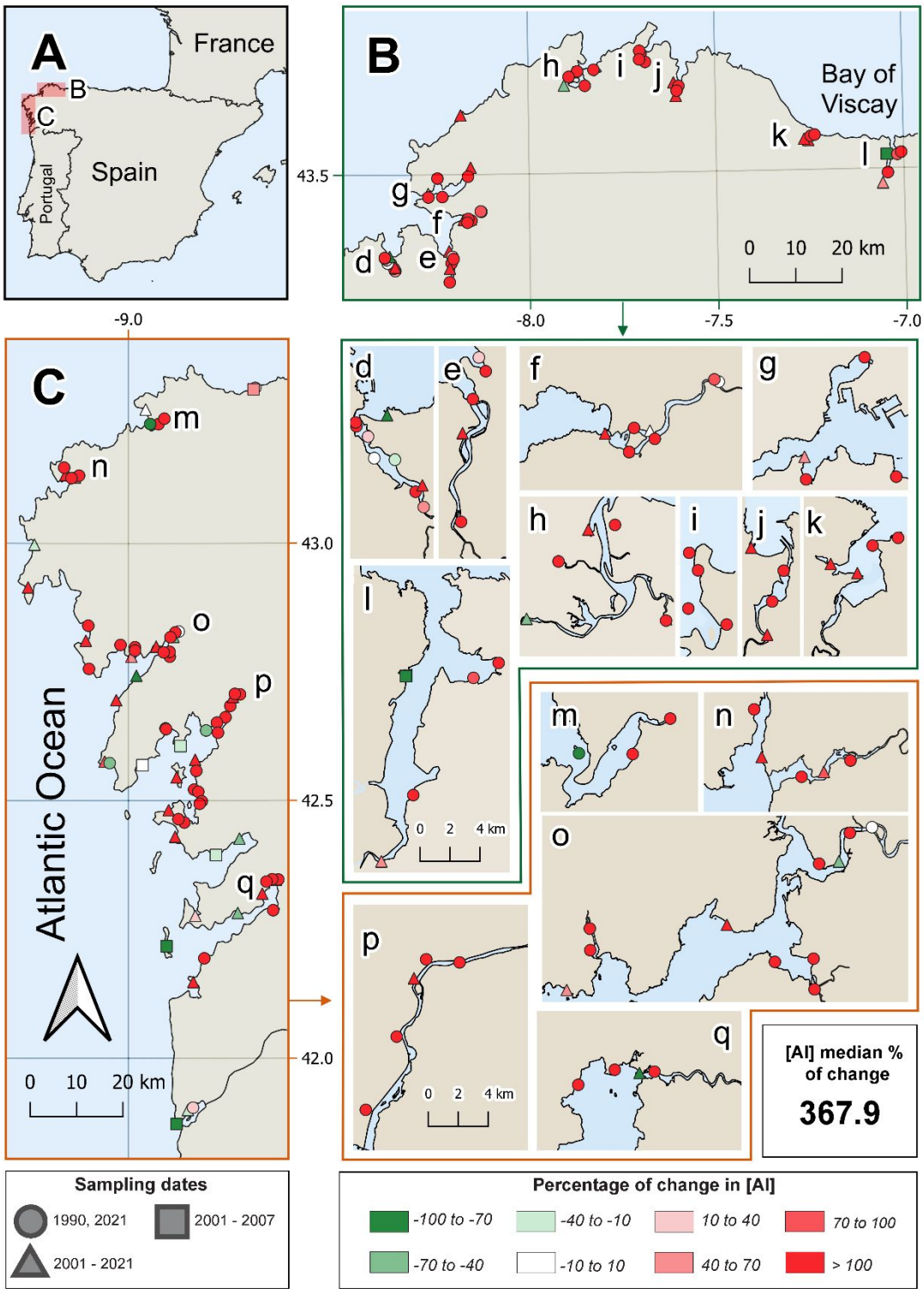

Fig. S14. Map of percentage changes in Al concentrations over time. Panels A-C provide a regional overview, with B and C showing the differences between the final and initial Al concentrations (in %) at each sampling site. Panels d-l and m-q offer detailed views

of stations that are densely clustered and hard to distinguish in B and C, respectively. Different colors represent the percentage changes in Al concentrations, while distinct symbols indicate the sampling dates: 1990 and 2021, 2001-2021, and 2001-2007. The total median percentage change, calculated as the median of the percentage changes across all stations, is displayed below.

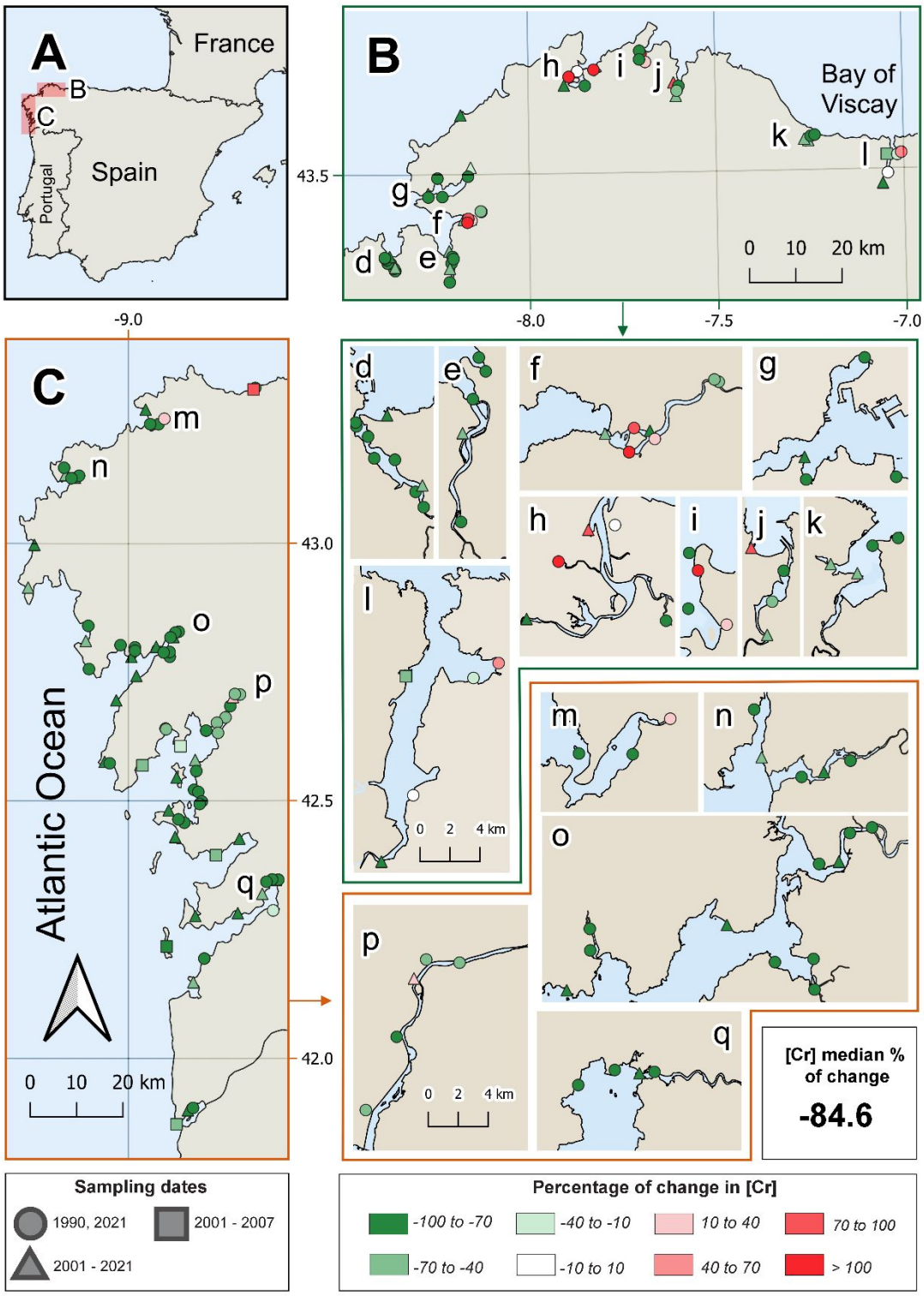

Fig. S15. Map of percentage changes in Cr concentrations over time. Panels A-C provide a regional overview, with B and C showing the differences between the final and initial Cr concentrations (in %) at each sampling site. Panels d-l and m-q offer detailed views

of stations that are densely clustered and hard to distinguish in B and C, respectively. Different colors represent the percentage changes in Cr concentrations, while distinct symbols indicate the sampling dates: 1990 and 2021, 2001-2021, and 2001-2007. The total median percentage change, calculated as the median of the percentage changes across all stations, is displayed below.

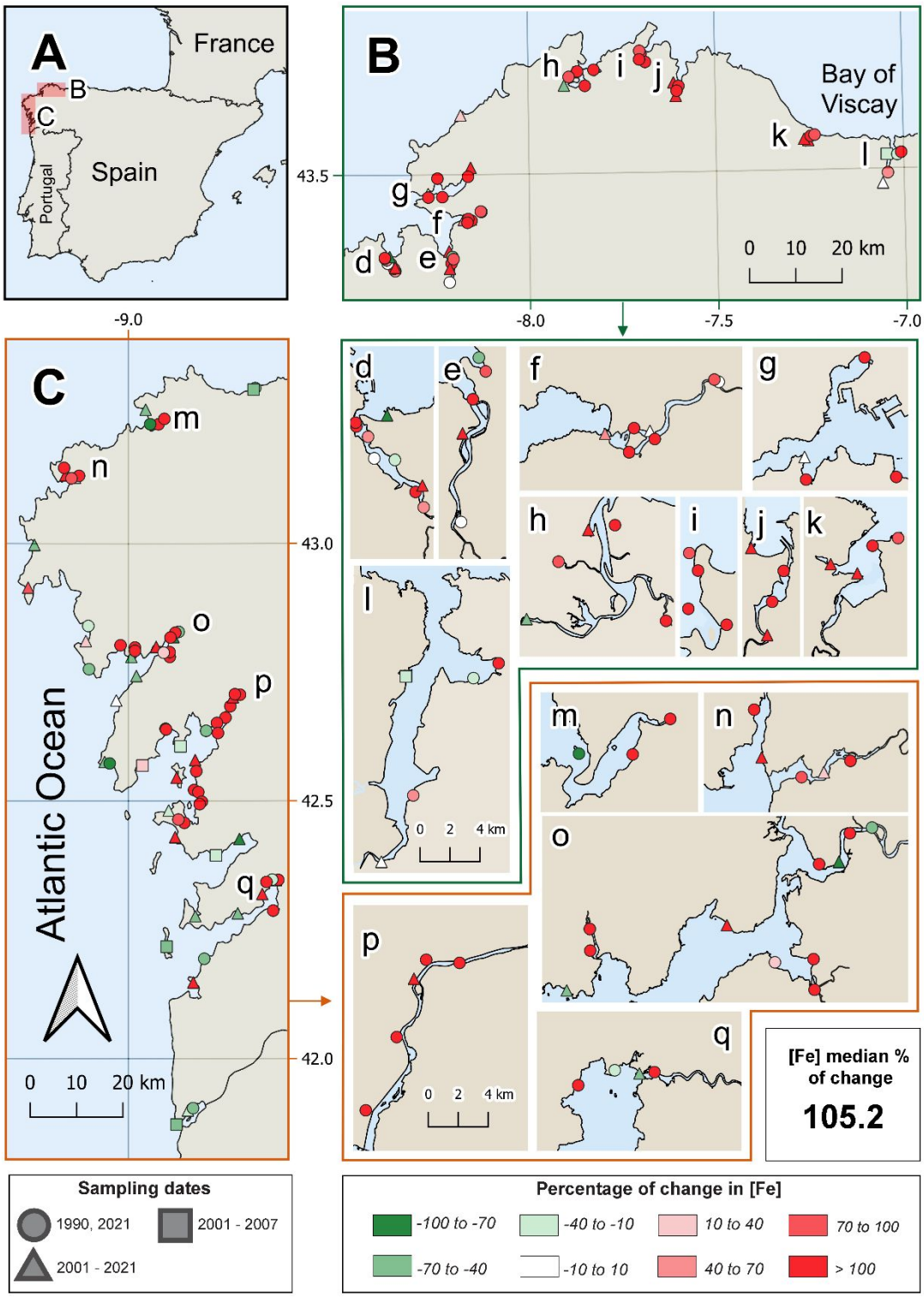

Fig. S16. Map of percentage changes in Fe concentrations over time. Panels A-C provide a regional overview, with B and C showing the differences between the final and initial Fe concentrations (in %) at each sampling site. Panels d-l and m-q offer detailed views

of stations that are densely clustered and hard to distinguish in B and C, respectively. Different colors represent the percentage changes in Fe concentrations, while distinct symbols indicate the sampling dates: 1990 and 2021, 2001-2021, and 2001-2007. The total median percentage change, calculated as the median of the percentage changes across all stations, is displayed below.

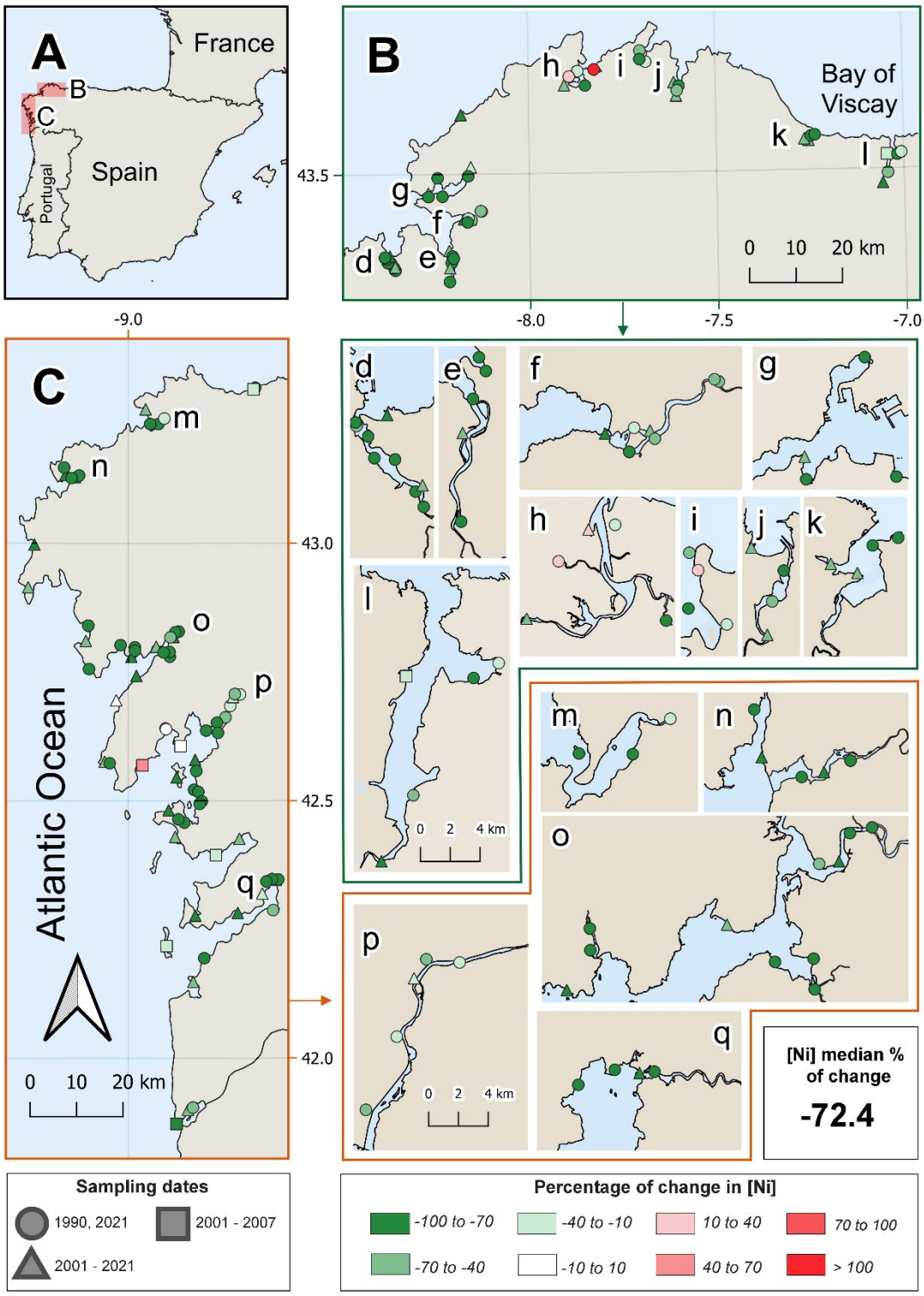

Fig. S17. Map of percentage changes in Ni concentrations over time. Panels A-C provide a regional overview, with B and C showing the differences between the final and initial Ni concentrations (in %) at each sampling site. Panels d-l and m-q offer detailed views

of stations that are densely clustered and hard to distinguish in B and C, respectively. Different colors represent the percentage changes in Ni concentrations, while distinct symbols indicate the sampling dates: 1990 and 2021, 2001-2021, and 2001-2007. The total median percentage change, calculated as the median of the percentage changes across all stations, is displayed below.

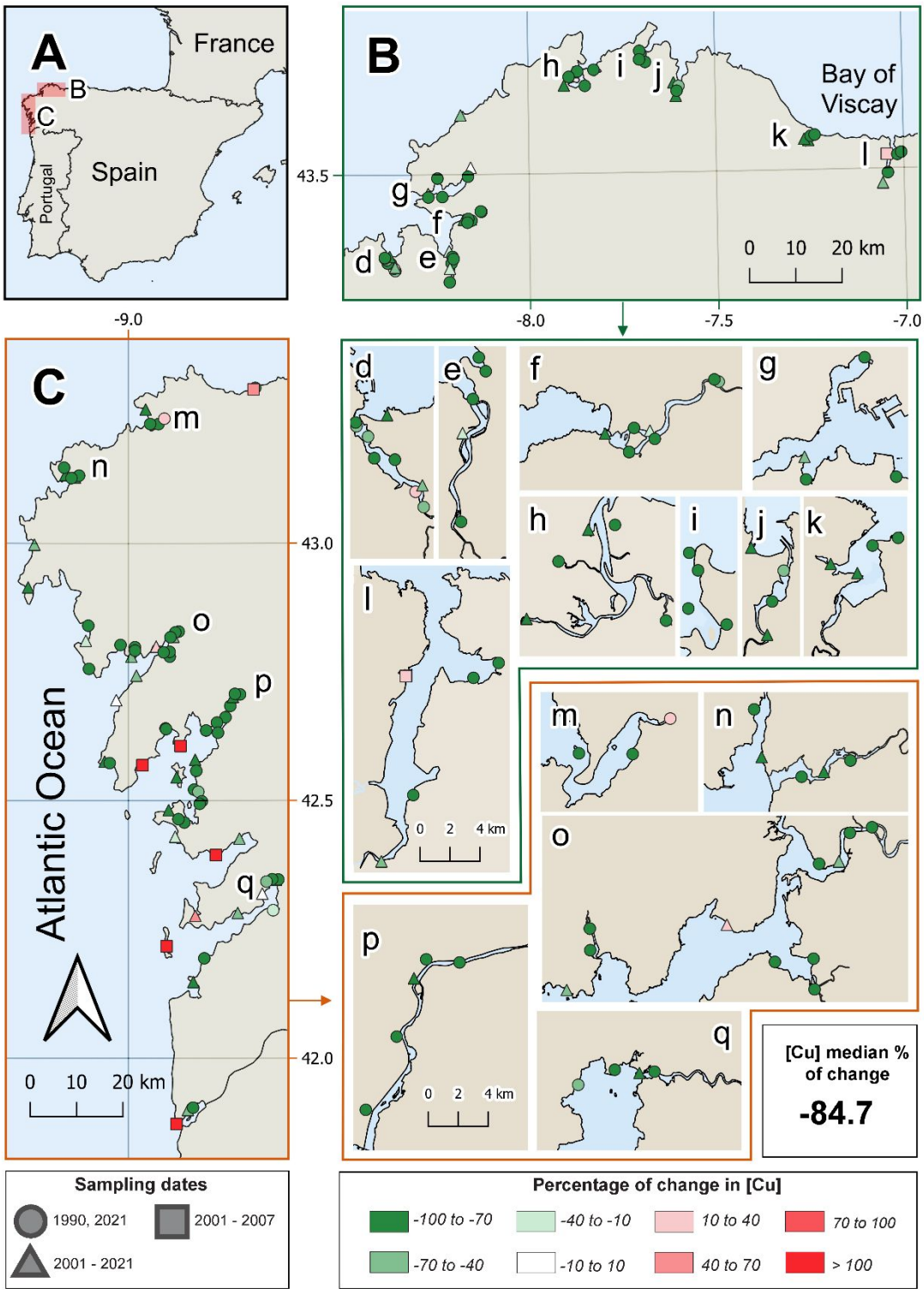

Fig. S18. Map of percentage changes in Cu concentrations over time. Panels A-C provide a regional overview, with B and C showing the differences between the final and initial Ni concentrations (in %) at each sampling site. Panels d-l and m-q offer detailed views

of stations that are densely clustered and hard to distinguish in B and C, respectively. Different colors represent the percentage changes in Ni concentrations, while distinct symbols indicate the sampling dates: 1990 and 2021, 2001-2021, and 2001-2007. The total median percentage change, calculated as the median of the percentage changes across all stations, is displayed below.

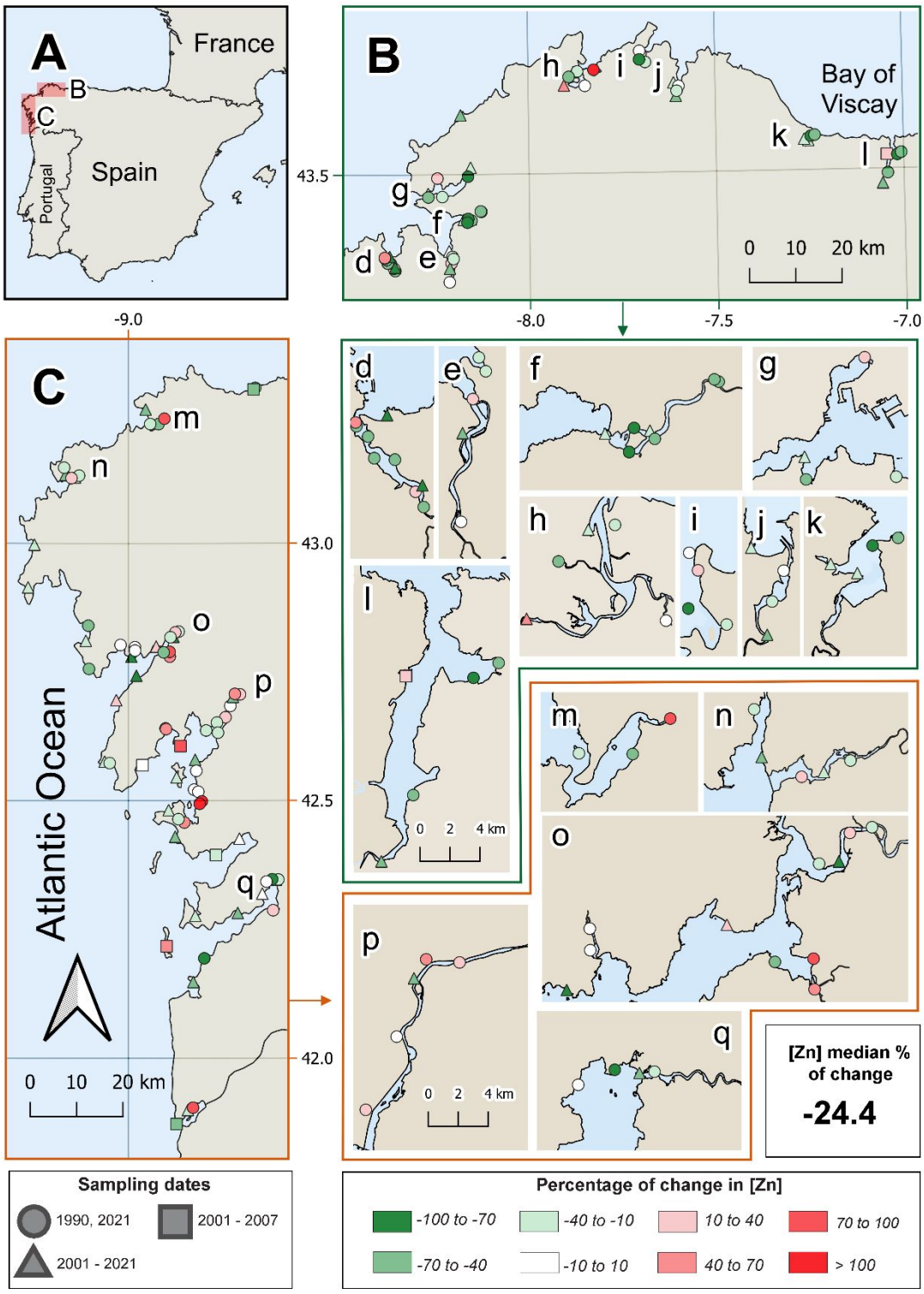

Fig. S19. Map of percentage changes in Zn concentrations over time. Panels A-C provide a regional overview, with B and C showing the differences between the final and initial Zn concentrations (in %) at each sampling site. Panels d-l and m-q offer detailed views

of stations that are densely clustered and hard to distinguish in B and C, respectively. Different colors represent the percentage changes in Zn concentrations, while distinct symbols indicate the sampling dates: 1990 and 2021, 2001-2021, and 2001-2007. The total median percentage change, calculated as the median of the percentage changes across all stations, is displayed below.

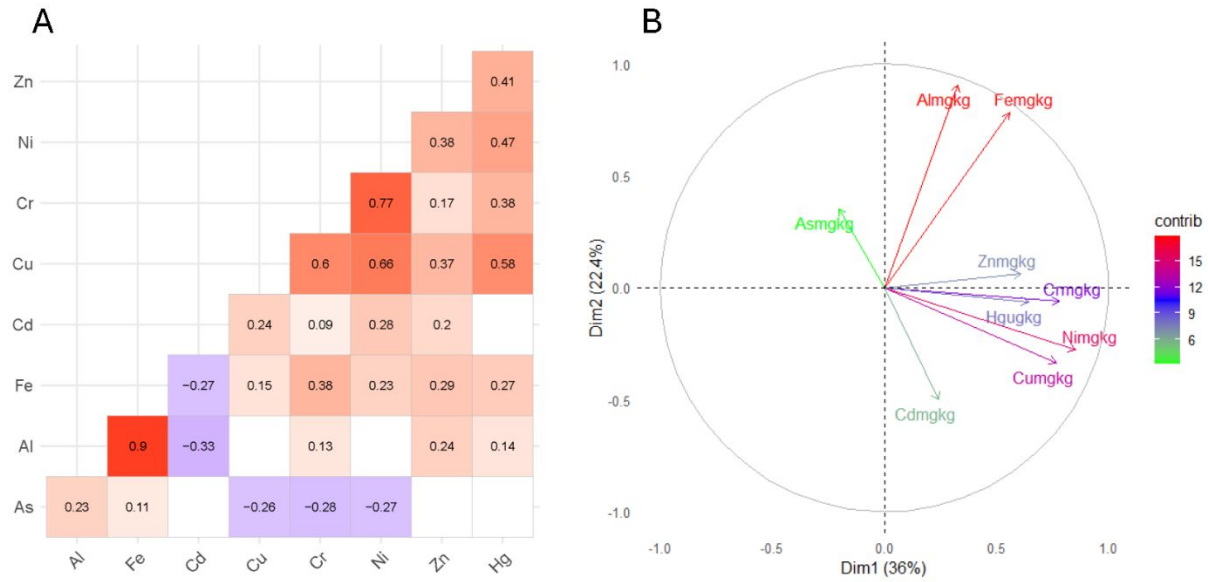

Fig. S20. Correlation matrix (A) and PCA (B) in PTEs concentrations in *Fucus* spp. A) Significant Spearman correlations ($p<0.005$, p-values adjusted using the Benjamini-Hochberg method) are indicated by displaying the correlation value. B) contribution loads of each PTE to the Dimension 1 and 2 are represented by color-coding.

4.3. Capítulo 3. The Return of Natural Lead to the Northeast Atlantic Ocean Captured by Brown Algae

Referencia:

Pacín, C.*; Aboal, J. R.1; Fernández, J.A.1; Vázquez-Arias, A.1; Šípková, A.3; Komárek, M.3; Chrastný, V. The Return of Natural Lead to the Northeast Atlantic Ocean Captured by Brown Algae. J Hazard Mater 2025, 496, 139289.
https://doi.org/10.1016/j.jhazmat.2025.139289

**corresponding author.*

Autoría e filiación:

Carme Pacín[1,2]; Jesús R. Aboal[1], J. Ángel Fernández[1]; Antón Vázquez-Arias[1]; Adéla Šípková[3]; Michael Komárek[3], Vladislav Chrastný[3]

[1]CRETUS, Ecology Area, Department of Functional Biology, Faculty of Biology, Universidade de Santiago de Compostela, Santiago de Compostela, 15782, Spain

[2]CIQUS Centre, Department of Physical Chemistry, Universidade de Santiago de Compostela, Santiago de Compostela 15782, Spain

[3]Department of Environmental Geosciences, Faculty of Environmental Sciences, Czech University of Life Sciences Prague, Kamýcká 129, 165 00, Prague-Suchdol, Czech Republic

Datos da publicación:

Ano: 2025

DOI: https://doi.org/10.1016/j.jhazmat.2025.139289

Información da revista:

Nome: Journal of Hazardous Materials ISSN: 1873-3336

Índice de impacto: 11.3 (2024)

Posición na área: 5/83 (Engineering, Environmental), 19/374 (Environmental Sciences)

Contribución da doutoranda:

Recollida de mostras para o ano 2021, determinación analítica de concentracións de Pb e de isótopos, análise estatística, visualización, e escritura do artigo.

Autorización da revista:

Journal of Hazardous Material forma parte da editorial Elsevier, que permite que as autoras empreguen os artigos en teses de doutoramento, como se pode ver no anexo 1.

Material suplementario:

Anexado ao final do artigo, excepto a Táboa S2, que se pode descargar en: https://doi.org/10.1016/j.jhazmat.2025.139289

Journal of Hazardous Materials 496 (2025) 139289

Contents lists available at ScienceDirect

Journal of Hazardous Materials

journal homepage: www.elsevier.com/locate/jhazmat

The return of natural lead to the Northeast Atlantic Ocean captured by brown algae

Carme Pacín [a,b,*], Jesús R. Aboal [a], J. Ángel Fernández [a], Antón Vázquez-Arias [a], Adéla Šípková [c], Michael Komárek [c], Vladislav Chrastný [c]

[a] CRETUS Center, Department of Functional Biology, Ecology Unit, Universidade de Santiago de Compostela, Santiago de Compostela 15782, Spain
[b] CIQUS Center, Department of Physical Chemistry, Universidade de Santiago de Compostela, Santiago de Compostela 15782, Spain
[c] Department of Environmental Geosciences, Faculty of Environmental Sciences, Czech University of Life Sciences Prague, Kamýcká 129, Prague-Suchdol 16500, Czech Republic

HIGHLIGHTS

- Long-term Pb isotope data reveal 30-year pollution trends in brown algae.
- Isotopic shifts show declining anthropogenic Pb contamination since 1990.
- Pb concentrations in *Fucus* spp. remained stable despite regulatory actions.
- Stable Pb levels likely reflect increased bioavailability and sediment influence.
- This study establishes a robust isotopic baseline for a region with scarce data.

GRAPHICAL ABSTRACT

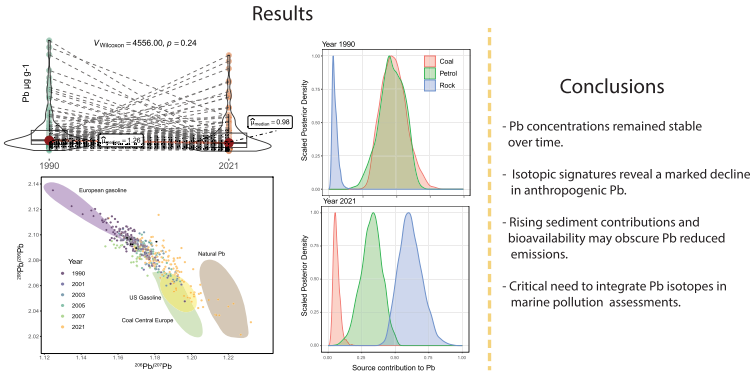

ARTICLE INFO

Keywords:
Stable isotopes
Heavy metal
Potentially Toxic Elements
Temporal trend
Pollution
Biomonitoring
Seaweed

ABSTRACT

Lead (Pb) is a highly toxic pollutant with serious ecological implications. This study investigates 30-year trends (1990–2021) in Pb concentrations and isotopic signatures ($^{206}Pb/^{207}Pb$ and $^{208}Pb/^{206}Pb$) in the brown algae *Fucus* spp. from the Northeast Atlantic Ocean (n = 446). Pb concentrations showed only modest, non-significant 21.9 % decline. In contrast, isotopic data revealed a clear shift from anthropogenic to natural sources. Bayesian mixing models (MixSIAR) supported this trend, indicating an increase in natural contributions, rising from 4.7 % in 1990 to 61.5 % in 2021, mirroring reductions in coal combustion (from 48.4 % to 6.3 %) and petrol-related sources (from 46.9 % to 32.2 %). This divergence between concentrations and isotopic trends likely reflects a substantial increase in sediment-derived Pb (189.3 % in 2021 compared to 13–49 % during 1990–2007), as well as enhanced bioavailability driven by environmental changes such as ocean acidification. Elevated Pb levels were found in inner estuarine zones dominated by *Fucus ceranoides*, but no latitudinal pattern or isotopic differences among species were observed. Overall, the findings highlight the complex dynamics of Pb in coastal ecosystems and the limitations of relying solely on concentration data to assess pollution trends. Isotope analyses have

* Corresponding author at: CRETUS Center, Department of Functional Biology, Ecology Unit, Universidade de Santiago de Compostela, Santiago de Compostela 15782, Spain.
E-mail address: mcarme.pacin@usc.es (C. Pacín).

https://doi.org/10.1016/j.jhazmat.2025.139289
Received 10 March 2025; Received in revised form 9 July 2025; Accepted 15 July 2025
Available online 17 July 2025

proven essential for source attribution, revealing a progressive shift toward natural Pb sources and supporting the effectiveness of regulatory measures such as the global phase-out of leaded gasoline. However, the study underscores that increased Pb bioavailability, driven by acidification and other global environmental changes, may offset the benefits of reduced emissions. Finally, this work provides a valuable isotopic baseline for a region where such data remain scarce, supporting future environmental monitoring and source-tracing efforts.

1. Introduction

Lead is one of the most toxic elements, with no known metabolic function in organisms and adverse effects even at trace levels [1,2]. While the natural weathering of Earth's crust can contribute to environmental Pb levels [3], its widespread prevalence in the environment today is largely a consequence of anthropogenic activities, including mining, industrial processes, and the historical use of leaded gasoline [4,5]. Emissions peaked in the 20th century but declined after the phase-out of leaded gasoline from the 1990s onwards [6]. However, certain sources persist, such as cement production, battery manufacturing, ceramics, mining, and residual Pb in fuels [7–9].

Coastal ecosystems are particularly vulnerable to Pb pollution as they act as sinks for terrestrial sources of contamination due to their proximity to land-based inputs [10–12]. In these environments, Pb can be found in sediment particles, dissolved in the water, or concentrated by the biota, including intertidal seaweeds of the genus *Fucus*. These foundational species are vital in North Atlantic coastal ecosystems as habitat engineers and primary producers in dynamic intertidal zones [13,14]. However, their ability to accumulate Pb and other potentially toxic elements [15–17] raises ecological concerns.

Beyond their environmental impact, the capacity of brown algae to bioconcentrate contaminants also enables their use as biomonitors of coastal pollution. This characteristic has led to their widespread application in monitoring pollutants such as Pb. Traditional assessments of Pb pollution that rely on measuring total Pb concentrations, while informative, do not identify pollution sources. In contrast, the Pb isotopic ratios $^{206}Pb/^{207}Pb$ and $^{208}Pb/^{206}Pb$, act as unique chemical signatures [18], enabling the identification and tracking of contamination sources [19–22]. Unlike for other elements (e.g. N, C, Hg, etc.) [23], metabolic and biogeochemical processes display no isotopic discrimination for Pb, so these dynamics do not affect Pb isotopic ratios. Therefore, analyzing the isotopic signature of Pb accumulated on seaweeds can provide valuable information on marine pollution sources, informing on contamination pathways and ecological impacts. However, research on marine organisms, particularly seaweeds, remains scarce [24–26]. Moreover, because environmental fractionation does not occur for Pb, the use of a temporal series of samples can provide information on the evolution of pollution sources over time, helping us understand the effectiveness of environmental regulations. However, to date only a few studies have evaluated temporal trends of Pb isotopic ratios in marine biota, all with a limited sample size [27–31], highlighting the need to better understand how contamination sources and environmental responses evolve over time in marine environments.

This study addresses the scarcity of temporal data in marine organisms by making use of a high-resolution, multi-decadal dataset with broad spatial coverage and a robust number of samples. Specifically, we analyzed samples from the Galician Environmental Specimens Bank, which contains over three decades of coastal monitoring data. The dataset comprises 446 samples of *Fucus ceranoides*, *F. spiralis*, and *F. vesiculosus* collected between 1989 and 2021 from 173 stations along the NW Spanish coast. This region represents a microcosm of broader environmental challenges in the Northern Hemisphere, characterized by a densely populated coastline, intense industrial activity, high maritime traffic, and strict environmental regulations like other European nations. By analyzing total Pb concentrations and isotopic compositions, this study aims to: (1) assess temporal trends in Pb pollution; (2) identify the origin of Pb contamination impacting *Fucus* spp. and their ecosystem over the past 30 years; and (3) evaluate spatial and species-specific patterns in Pb accumulation and isotopic ratios. The hypothesis to be tested is that Pb concentrations and isotopic ratios in *Fucus* spp. have remained stable over time, with no significant spatial, or species-specific variation.

2. Material and methods

2.1. Survey area

The study was conducted in the northwest of Spain (Galicia region). This region boasts a 1498 km coastline along the Atlantic Ocean and the Bay of Biscay (approximately 25 % of the Iberian Peninsula), characterized by unique coastal inlets known as rias, formed by the submergence of river valleys due to land subsidence (see Fig. 1). Galicia's oceanic climate is mild, with abundant precipitation [32]. In addition, the geological diversity of the region includes mainly granite, but also schists, slates, basic and ultrabasic rocks, limestone, and quartzites, each with variable Pb content [33].

In the last decades, Galicia's coastline has supported major industries such as automotive manufacturing, shipbuilding, energy production, wood industry, ferrous and non-ferrous metallurgy, and dense human populations [34]. As in most European countries, Spain banned leaded gasoline in 2001 [6].

2.2. Sample collection

Sampling campaigns were conducted during low tide in July of 1989–1990 (hereafter referred to as 1990), 2001, 2003, 2005, 2007, and 2021. A total of 173 sites were sampled leading to the collection of 446 samples of the brown algae *Fucus ceranoides, F. vesiculosus,* and *F. spiralis* (Fig. 1). At each site, a composite sample (n = 30 thalli), was obtained to account for intra-site variability along a 50-meter transect in a zigzag pattern. The algae were cleaned on-site with seawater, in order to remove sediment particles and epiphytes, according to the most recent recommendations [35], and transported to the laboratory in a cooler. Detailed protocols for sampling, washing, and processing can be consulted in the Supporting Information [35].

With few exceptions, samples collected in 1990 were also taken from the same sites in 2021. Similarly, samples gathered in 2001 were collected again at the same sites in 2003, 2005, 2007, and 2021. Sampling sites were distributed along the entire coastline of the study area, covering open sea zones, estuaries, areas impacted by anthropogenic activities (e.g., industries, urban developments), and regions without known pollution sources. The selection included both protected areas, such as national parks and sites within the Natura 2000 network, and historically impacted areas, such as the ria O Burgo (ria d in Fig. 1), once considered the most contaminated estuary in Europe. This comprehensive site selection allows for an accurate representation of the overall regional pattern of coastal pollution.

Fucus ceranoides is restricted to brackish inner rias, while *F. spiralis* and *F. vesiculosus* are found in more exposed, ocean-influenced areas, where they often coexist and hybridize [36]. Although *F. vesiculosus* is generally distinguished by air bladders, these structures are not always present, which complicates field identification. Recent studies have further introduced taxonomic uncertainty by dividing *F. spiralis* into *F. spiralis* and *F. macroguiryi* [37]. To address these taxonomic uncertainties and identification challenges, *F. spiralis* and *F. vesiculosus*

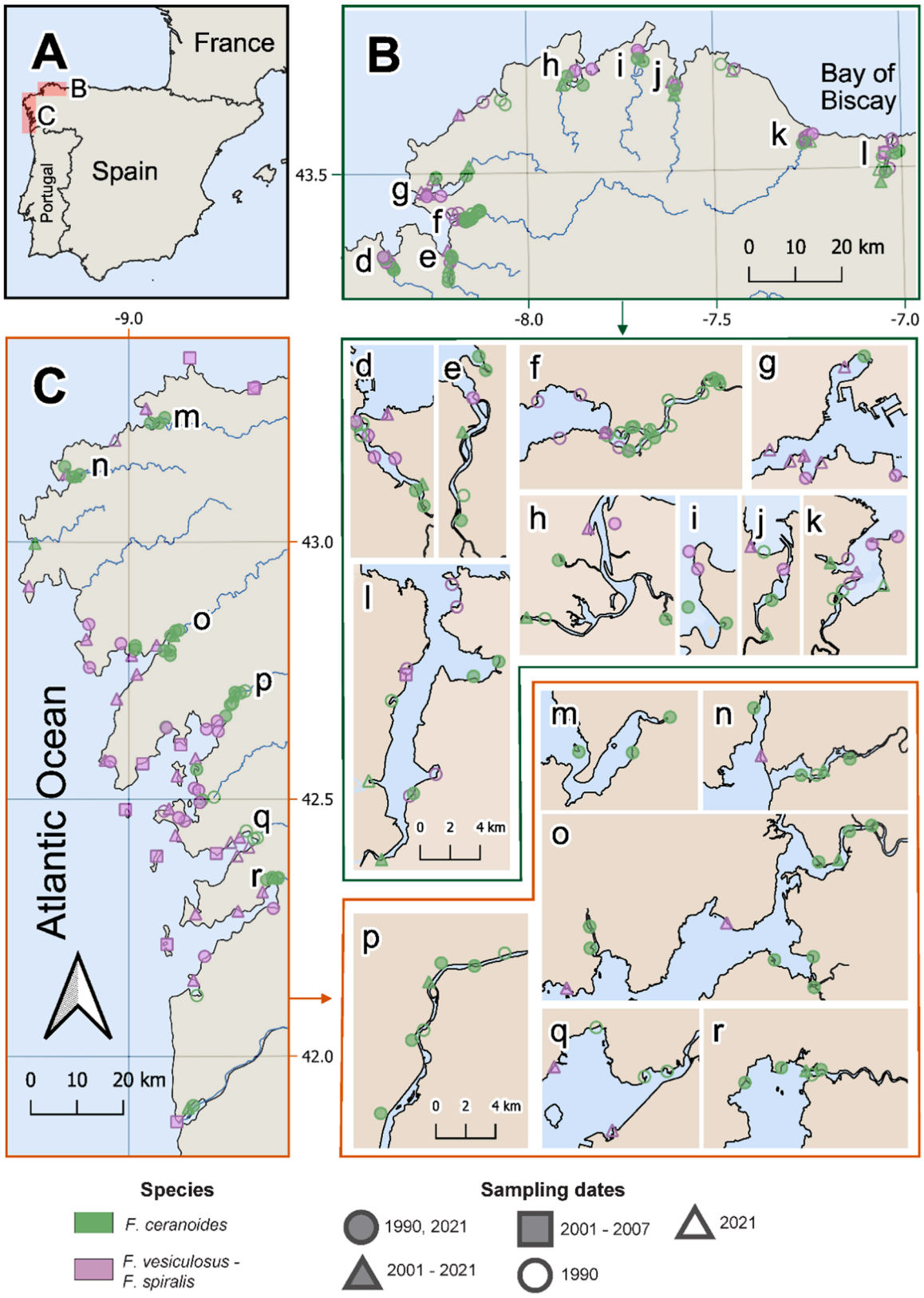

Fig. 1. Map of the study area. Panels A-C display an overview of the region, with B and C showing the sampling sites (sites). Panels d-l and m-r present detailed maps of sites that are densely clustered and difficult to distinguish in B and C, respectively. Different colors represent the species sampled (*F. ceranoides* and *F. vesiculosus–F. spiralis*) while distinct symbols indicate the sampling periods: 1990–2021, 2001–2021, and 2001–2007, or those sampled exclusively in 1990 or 2021. To reduce clutter, incomplete samplings from 2001, 2003, 2005, and 2007 are grouped under the 2001–2007 symbol.

Table 1
Isotopic signatures of reference materials from this study and compiled from the literature. Reported values correspond to $^{206}Pb/^{207}Pb$ and $^{208}Pb/^{206}Pb$ ratios. Sources selected for the MixSIAR model (coal, unleaded petrol and diesel, leaded petrol, and rock) are indicated with "(MixSIAR)" in parentheses. Pb concentrations of the sediments analyzed in this study are provided in Table S2.

		$^{206}Pb/^{207}Pb$	$^{208}Pb/^{206}Pb$	Reference
Coal	**La Jagua (Columbia)**	1.219	2.077	Farmer et al., 1999 [53]
(MixSIAR)	**Study area (As Pontes)**	1.130	2.017	Díaz-Somoano et al., 2007 [54]
	Study area (Meirama)	1.183	2.019	Díaz-Somoano et al., 2007 [54]
	Median European Coal	1.185	2.079	Díaz-Somoano et al., 2009 [55]
	Indonesia	1.184	2.093	Díaz-Somoano et al., 2009 [55]
	Powder River Basin (US)	1.224	2.032	Whang et al., 2019 [56]
	Tarragona (Spain)	1.185	2.075	Plasencia et al., 2025 [57,58]
	Mean	1.187	2.056	-
	sd	0.031	0.032	-
Unleaded Petrol	**Gasoline Study Area**	1.160	2.104	This study
(MixSIAR)	**Diesel Study Area**	1.166	2.095	This study
	France	1.131	2.128	Cloquet et al., 2006 [57]
	Gasoline Greenland	1.160	2.060	Astray et al., 2024 [19]
	Gasoline Norway	1.148	2.124	Chrastný et al., 2018 [9]
	Diesel Norway	1.153	2.129	Chrastný et al., 2018 [9]
	Diesel Tarragona (Spain)	1.132	2.134	Plasencia et al., 2025 [58]
	Gasoline Tarragona (Spain)	1.161	2.104	Plasencia et al., 2025 [58]
	Mean	1.151	2.110	
	sd	0.013	0.025	
Leaded Petrol	**Gasoline France**	1.083	-	Véron et al., 1999 [59]
(MixSIAR)	**Gasoline France**	1.084		Monna et al., 1997 [60]
	Gasoline Switzerland	1.113	2.144	Chiaradia & Cupelin, 2000 [61]
	Gasoline Czech Republic	1.040	2.221	Novak et al., 2003 [62]
	Mean	1.086	2.182	
	sd	0.029	0.038	
Rocks (Study area, MixSIAR)	**calc-alkaline granite Viveiro**	1.228	1.990	This study
	calc-alkaline granite O Pindo	1.211	2.030	This study
	two-micas alkaline granite Vilarseco	1.305	1.865	This study
	Peridotite (Dunite) Ortigueira	1.219	2.076	This study
	Pizarra Viveiro	1.209	2.070	This study
	Schist Ordes	1.243	2.022	This study
	Mean	1.236	2.009	
	sd	0.036	0.077	
Sediments	**S1, 1990**	1.227	2.036	This study
(Study área)	**S2, 1990**	1.170	2.094	This study
	S3, 2007	1.181	2.095	This study
	S4, 2001	1.170	2.090	This study
	S5, 2005	1.168	2.093	This study
	S6, 2007	1.194	2.072	This study
	S7, 2001	1.165	2.098	This study
	S8, 2005	1.167	2.093	This study
	S9, 2003	1.175	2.089	This study
	S10, 1990	1.167	2.097	This study
	S11, 1990	1.169	2.101	This study
	S12, 2021	1.189	2.074	This study
	S13, 2021	1.175	2.092	This study
	S14, 2021	1.188	2.070	This study
	S15, 2021	1.181	2.098	This study
	S16, 2021	1.170	2.095	This study
	S17, 2021	1.166	2.102	This study
	S18, 2021	1.175	2.089	This study
	S19, 2021	1.171	2.097	This study
	S20, 2021	1.175	2.091	This study
Upper continental crust		1.205	2.06	Kylander et al., 2005 [63]
Ores	**Study Area**	1.146	2.125	Tornos & Arias, 1993 [64]
	Study Area	1.144	2.127	Tornos et al., 1996 [65]
	Study Area	1.147	2.123	Arias, 1989 [66]
	North Portugal	1.169	2.097	Neiva et al., 2008 [67]
	Study area	1.165	2.103	Millos et al., 2014 [68]
Ceramic industry	**Arcade (Study area)**	1.189	2.073	This study
Waste incineration	**Switzerland**	1.151	2.108	Hansmann & Köppel., 2000 [69]
	France	1.154	2.107	Carignan et al., 2005 [70]
	Tarragona (Spain)	1.162	2.101	Plasencia et al., 2025 [58]
	France	1.149	-	Monna et al., 1997 [60]
E-waste	**México**	1.190	2.053	Río-Salas et al., 2025 [71]
	East Antartica	1.150	2.117	Townsend et al., 2009 [72]
	Shantou (China)	1.152	2.109	Jiang et al., 2019 [73]
Aerosols	**Prepollution (Study area)**	1.255	-	Kylander et al., 2005 [74]
	Sahara dust	1.209	2.062	Schleicher et al., 2020 [75]
	Spain aerosol	1.109	2.149	Bollhöfer & Rosman, 2001 [76]
	Morocco and Senegal	1.159	2.104	Zhang et al., 2024 [77]

(*continued on next page*)

Table 1 (*continued*)

		$^{206}Pb/^{207}Pb$	$^{208}Pb/^{206}Pb$	Reference
Seawater	**NE Atlantic Ocean**	1.1815	2.059	Véron et al., 1994 [78]
	NE Atlantic Ocean	1.173	2.082	Pinedo-González et al., 2018 [79]
	NE Atlantic Ocean	1.184	2. 069	Zurbrick et al., 2018 [80]
Mussel	**France**	1.167	2.0887	Couture et al., 2010[30]
	France	~1.170	~2.095	Barreira et al., 2025 [31]
Seaweed	***Fucus* spp., Greenland**	1.138	2.120	Søndergaard et al., 2010[27]
	***Iridaea cordata*, East Antartica**	1.086	2.170	Runcie et al., 2009 [25]

were combined for analysis in this study, so we refer to them as *F. vesiculosus – F. spiralis*, while *F. ceranoides* was examined separately.

2.3. Sample preparation and analysis

The apical parts of each thallus corresponding to the three apical dichotomies and representing the last growth period [35] were selected. Samples with reproductive structures, apparent damage, or epiphytes were excluded. Selected thalli were dried in a forced-air oven at 40ºC until constant weight and then homogenized using a tangential mixer mill with zirconium oxide grinding vessels (Retsch MM400). Homogenized samples were stored in hermetically sealed glass containers, at room temperature, protected from light in the Galician Environmental Specimen Bank [38] until chemical analysis.

Before analysis, 0.3 g of the samples were re-dried at 100°C and digested with 69 % (w/w) HNO_3 in a Milestone Ultrawave. Pb isotopic compositions were determined using a Thermo Scientific™ iCAP™ Q ICP-MS (Inductively Coupled Plasma Mass Spectrometer) at the Czech University of Life Sciences, Prague. Pb concentrations were determined with an Agilent 7700x ICP-MS at the Research Support Services Unit of the Universidade de Santiago de Compostela.

2.4. Representative materials

Representative materials were selected to represent potential sources of Pb contamination and characterize the range of Pb isotopic signatures in the study area (Table 1). Sediment samples from 1990, 2001, 2003, 2005, 2007 and 2021 were collected concurrently with the algal samples in their immediate vicinity using a spatula, taking the top 5 mm of the sediment layer to capture recent deposition. Following collection, samples were sieved through a 200 nm mesh and dried prior to chemical analysis. Other representative materials, collected in 2023, included representative geological materials (calc-alkaline granite, two-mica alkaline granite, peridotite, slate, and schist), local ceramics with high Pb content, and gasoline and diesel from a local refinery. Isotopic compositions and Pb concentrations for the reference materials were determined following the same protocols applied to the algal samples.

2.5. Quality control

Quality control measures for Pb concentration analysis included analytical blanks, sample replicates, and certified reference material (*Fucus vesiculosus* ERM-CD200) analyzed at a frequency of one per 30 samples. The Percent Relative Difference was 3.7 %, with a recovery rate of 93.2 %.

The procedural blanks exhibited Pb concentrations ranging between 0.035 and 0.138 μg L^{-1}, with a limit of quantification (LOQ) of 0.73 μg L^{-1}, corresponding to approximately 0.12 μg g^{-1} in the solid samples. This LOQ was exceeded in all samples except one. For isotopic ratios, each sample was analyzed in 10 replicate scans, with an integration time of 60 ms per isotope (^{206}Pb, ^{207}Pb, and ^{208}Pb). Lead concentrations in solution ranged between 0.2–2 μg L^{-1}. The relative standard deviation (RSD) for isotope ratios was below 0.2 % for individual sample runs; otherwise, the instrument was recalibrated before proceeding. The replicates showed Percent Relative Difference of 0.42 % for $^{206/207}Pb$ and 0.50 % for $^{208}Pb/^{206}Pb$. Importantly, these replicate values correspond to the same sample analyzed across different analytical sessions (i.e., on different days). NIST SRM 981 was analyzed as an isotopic standard every two samples, with each sample corrected using the most recent standard measurement (sample-standard bracketing approach). Raw isotope ratios were corrected using empirically derived normalization factors (1.0933 for $^{206}Pb/^{207}Pb$ and 2.168 for $^{208}Pb/^{206}Pb$) that account for the instrument's mass bias characteristics. The measured ratios of NIST SRM 981 showed excellent agreement with reference values, with median deviations of + 0.28 % for $^{206}Pb/^{207}Pb$ (median measured: 1.0964 vs reference: 1.0933) and −0.64 % for $^{208}Pb/^{206}Pb$ (median measured: 2.1542 vs reference: 2.168). The high recovery rates (100.28 % and 99.36 %, respectively) and low median relative standard deviations (RSD < 0.33 % for both ratios) demonstrate both the accuracy and precision of our measurements [39].

Isotopic ratios were verified against NIST SRM 1573a (tomato leaves), NIST SRM 1515 (apple leaves), and IAEA-336 (epiphytic lichen). Measured values closely matched reported values (Table S1) [40–42].

Finally, to evaluate whether matrix components could limit the accuracy of isotopic measurements, we conducted additional tests using standard anion exchange chromatography on three thalli and three sediment samples. An aliquot of each sample was evaporated to dryness and re-dissolved in 0.5 M HNO_3 - 0.2 M HBr. The separation was carried out using a column containing 2 mL of AG1-X8 resin (100–200 mesh), which was first cleaned with demineralized water and equilibrated with 0.5 M HNO_3 - 0.2 M HBr. The sample was then loaded onto the column, and the matrix components were eluted. Lead was collected using 0.45 M HNO_3 - 0.03 M HBr, evaporated to dryness, re-dissolved in 2 % HNO_3, and subsequently analyzed by ICP-MS. The isotopic ratios obtained from the purified samples were then compared to those from the same samples analyzed without prior separation. Differences were minimal: 0.1 % for $^{206}Pb/^{207}Pb$ and −0.01 % for $^{208}Pb/^{206}Pb$. These results indicate that matrix effects were negligible under our analytical conditions, and incomplete purification did not significantly affect the accuracy of isotopic measurements. Therefore, full separation was not applied systematically to all samples.

2.6. Data analysis

All statistical analyses were performed in R v4.4.1 [43] using the car, ggstatsplot, ggplot2, and MixSIAR packages [44–47]. Descriptive statistics and Shapiro-Wilk test were used to assess normality of Pb concentrations and isotopic ratios ($^{206}Pb/^{207}Pb$ and $^{208}Pb/^{206}Pb$). Due to significant deviations from normality, non-parametric methods were applied throughout. Differences in Pb and isotopic ratios between species and sampling years (n = 446) were tested using Kruskal-Wallis and Dunn's post hoc tests. Later, the dataset was restricted to only those sites that were resampled in different campaigns: the Wilcoxon signed-rank test compared concentrations in sites sampled in 1990 and 2021, and Friedman and Durbin-Conover post-hoc tests compared sites sampled in 2001 and revisited in 2003, 2005, 2007 and 2021. For years with co-occurring species at a given site, comparisons were made between each species across time. Pb/Fe ratios were also evaluated using the same approach. Spearman's rank correlations were used to examine relationships between Pb and Fe concentrations in algae, isotopic ratios in algae vs. sediments ($^{206}Pb/^{207}Pb$ and $^{208}Pb/^{206}Pb$), and between

$^{206}Pb/^{207}Pb$ and the inverse of Pb concentrations.

Spatial patterns were visualized using QGIS 3.36.3 [48], and Pb concentrations and isotopic ratio changes for each site across the study period were determined by comparing the earliest with the most recent available data points.

To estimate the proportional contributions of different Pb sources, a Bayesian isotopic mixing model was run using MixSIAR [47]. Source categories included Petrol (combined leaded/unleaded petrol and diesel), Coal, and Natural rock background. The initially disaggregated fuel sources exhibited strong posterior correlations in MixSIAR outputs (pairwise source correlation < –0.9), which indicated poor isotopic discrimination, justifying their aggregation into a single "Petrol-related sources" category. Different rock types representative of the study area's lithology (e.g., slates, schists, granites) were grouped into a single "natural source" end-member, as their Pb isotopic signatures showed substantial overlap. Sources such as e-waste or municipal waste incineration were excluded due to highly variable isotopic signatures and the lack of region-specific data. Coal isotope data from Colombia, Indonesia, and the U.S. were included to reflect the shift of the study area power plants toward imported coal in the early 2000s, ensuring realistic representation of the sources. Samples from 2001 to 2007 were grouped into a single temporal category after verifying consistent source contributions. The model was run with 3 chains of 300 000 iterations (burn-in = 150 000; thinning = 100) and showed excellent convergence (Gelman-Rubin < 1.05 for all parameters). Source signatures are detailed in Table 1.

To assess changes in Pb speciation over time, we used thermodynamic modeling with Visual MINTEQ [49] under representative seawater conditions for the study region. Regional acidification has been estimated at –0.0012 pH units per year, with surface seawater pH decreasing from approximately 8.10 to 8.06 between 1990 and 2021 [50]. Based on available data, we used a median Pb^{2+} concentration of 0.65 µg/L [51,52], and representative seawater temperatures of 15.36 °C for 1990 and 15.80 °C for 2021. We therefore modelled two scenarios: one representing baseline conditions (pH 8.10, 15.36 °C) and another representing 2021 conditions (pH 8.06, 15.80 °C). These simulations allowed us to estimate potential changes in Pb^{2+} speciation associated with ocean acidification and warming.

Sediment contributions to Pb concentrations were estimated using Fe as a geological tracer [81], with Pb and Fe ratios calculated from published sediment data for 1990, 2003, 2005, and 2007 [38,82], and supplemented by nine newly analyzed sediment samples from 2021. For each sampling site, sediment contributions were determined by pairing algal Pb concentrations with corresponding sediment data from the same year and site, using the following equation:

$$\text{sediment contribution} = \frac{\frac{[Pb]_{sediment}}{[Pb]_{algae}}}{\frac{[Fe]_{sediment}}{[Fe]_{algae}}} \quad (1)$$

The median sediment contribution was calculated for each year. Additionally, a Spearman correlation between Fe and Pb concentrations in algae was performed to further explore the potential sedimentary origin of Pb in the biota.

3. Results

Detailed Pb and Fe concentrations, isotopic ratios, site coordinates, and ria classifications for each site and Year of sampling for *Fucus* spp. and sediment samples are provided in Table S2.

3.1. Pb concentrations and temporal trends

Pb concentrations in *Fucus* ranged from 0.079 to 53.181 µg g^{-1} (dry weight), with a median of 1.1 µg g^{-1}. *F. ceranoides* showed significantly higher values (1.51 µg g^{-1}) than *F. vesiculosus–F. spiralis* (0.91 µg g^{-1}, $p = 4.46 \times 10^{-12}$), consistent with elevated levels where it predominantly occurs (Fig. 1, Fig. S1). No clear spatial gradient was detected, but localized hotspots, such as Ria do Burgo and Ria de Vigo (labeled d and r in Fig. S1, respectively), exhibited high concentrations.

Pb levels remained fairly stable over time, with slight recent declines. Kruskal-Wallis ($p = 3.45 \times 10^{-4}$) and post-hoc Dunn tests revealed differences between 1990–2003 ($p = 1.56 \times 10^{-3}$) and 2003–2007 ($p = 3.78 \times 10^{-3}$), but no consistent downward trend was detected. Site-specific analyses using Friedman ($p = 0.03$), Durbin-Conover, and Wilcoxon tests ($p = 0.24$) showed no significant variations among 2001, 2003, 2005, 2007, and 2021, and between 1990 and 2021, though 2021 consistently showed the lowest values (Fig. 2). At the individual site level, temporal patterns were mixed, with both increases and decreases and no consistent spatial trend. Median percent change across sites indicated a moderate decline of –21.87 % (Fig. S2). A similar pattern of stability was observed among the 50 samples showing the highest Pb concentrations. Lead and Fe concentrations in algae were strongly correlated (rho = 0.58, $p < 2.2 \times 10^{-16}$), suggesting the influence of the sediment. Additionally, using Fe as a lithogenic tracer [82], estimated sediment contributions to algal Pb were 43.5 % (1990), 46.3 % (2003), 49.3 % (2005), 13.0 % (2007), and 189.3 % (2021). The notably high value in 2021 (> 100 %) indicates a lower Pb concentration than expected based on sediment composition alone, while the opposite occurred for the rest of the years, and particularly for 2007. Accordingly, the Pb/Fe ratio in algae showed significant decreases over time, with 2021 values being notably lower than those of all other years ($p < 0.05$). Despite differences in sediment exposure, with *Fucus ceranoides* being more exposed than *F. vesiculosus–F. spiralis* due to its position within the rias, both groups exhibited similar temporal trends in Pb concentrations and Pb/Fe ratios. Sediment Pb concentrations were highest in 1990 and 2021, with lower values recorded in the intervening years. However, due to the limited sample sizes available for the intermediate years (n = 14 for each of 2001, 2003, 2005, and 2007) and for 2021 (n = 9), these temporal comparisons should be interpreted with caution. Finally, simulations incorporating acidification and increased sea surface temperature (SST) over the study period showed a 5.9 % increase in the concentration of bioavailable Pb^{2+}, rising from 1.41 × 10^{-7} mol L^{-1} in 1990 to1.49 × 10^{-7} mol L^{-1} in 2021.

3.2. Isotopic ratios and temporal trends

The $^{206}Pb/^{207}Pb$ ratios ranged from 1.125 to 1.233 (median = 1.175), and $^{208}Pb/^{206}Pb$ from 2.021 to 2.136 (median = 2.088). Samples from northern rias generally exhibited lower $^{206}Pb/^{207}Pb$ ratios compared to those from southern sites, whereas $^{208}Pb/^{206}Pb$ were higher. No clear inner-to-outer rias pattern was observed, and accordingly, no significant differences between species were detected. Samples from rias known for their higher industrial and anthropogenic influence (e.g., rias d, e, f, q, and r) exhibited lower $^{206}Pb/^{207}Pb$ and higher $^{208}Pb/^{206}Pb$ ratios compared to others. No consistent inner–outer gradient or interspecific differences were observed (Figs. S3, S4).

Both ratios shifted significantly over time, with $^{206}Pb/^{207}Pb$ increasing and $^{208}Pb/^{206}Pb$ decreasing. These trends were consistent across site-level analyses (Wilcoxon and Friedman tests) and full-dataset comparisons (Kruskal–Wallis test), with $p << 0.001$ for all tests except Friedman for $^{208}Pb/^{206}Pb$ ($p = 3.7 \times 10^{-3}$; Fig. 3). The strongest changes occurred between 1990 and 2021 ($p << 0.001$), though 1990 also differed from 2001–2007 (except 2007 for $^{206}Pb/^{207}Pb$). Years 2001–2007 showed similar $^{208}Pb/^{206}Pb$ ratios, while $^{206}Pb/^{207}Pb$ in 2007 was significantly lower than in 2001–2005 ($p < 0.005$). In 2021, values differed from 2001–2007, with minor exceptions (2003 in Friedman tests, and 2001–2003 in Kruskal–Wallis for $^{208}Pb/^{206}Pb$). At the sampling site level, trends were consistent with an overall rise in $^{206}Pb/^{207}Pb$ and decline in $^{208}Pb/^{206}Pb$, without a clear spatial pattern (Figs. S5, S6). A similar pattern in isotopic ratios was observed among the 50 samples showing the highest Pb concentrations.

Isotopic ratios of reference materials are shown in Table 1. Rocks had

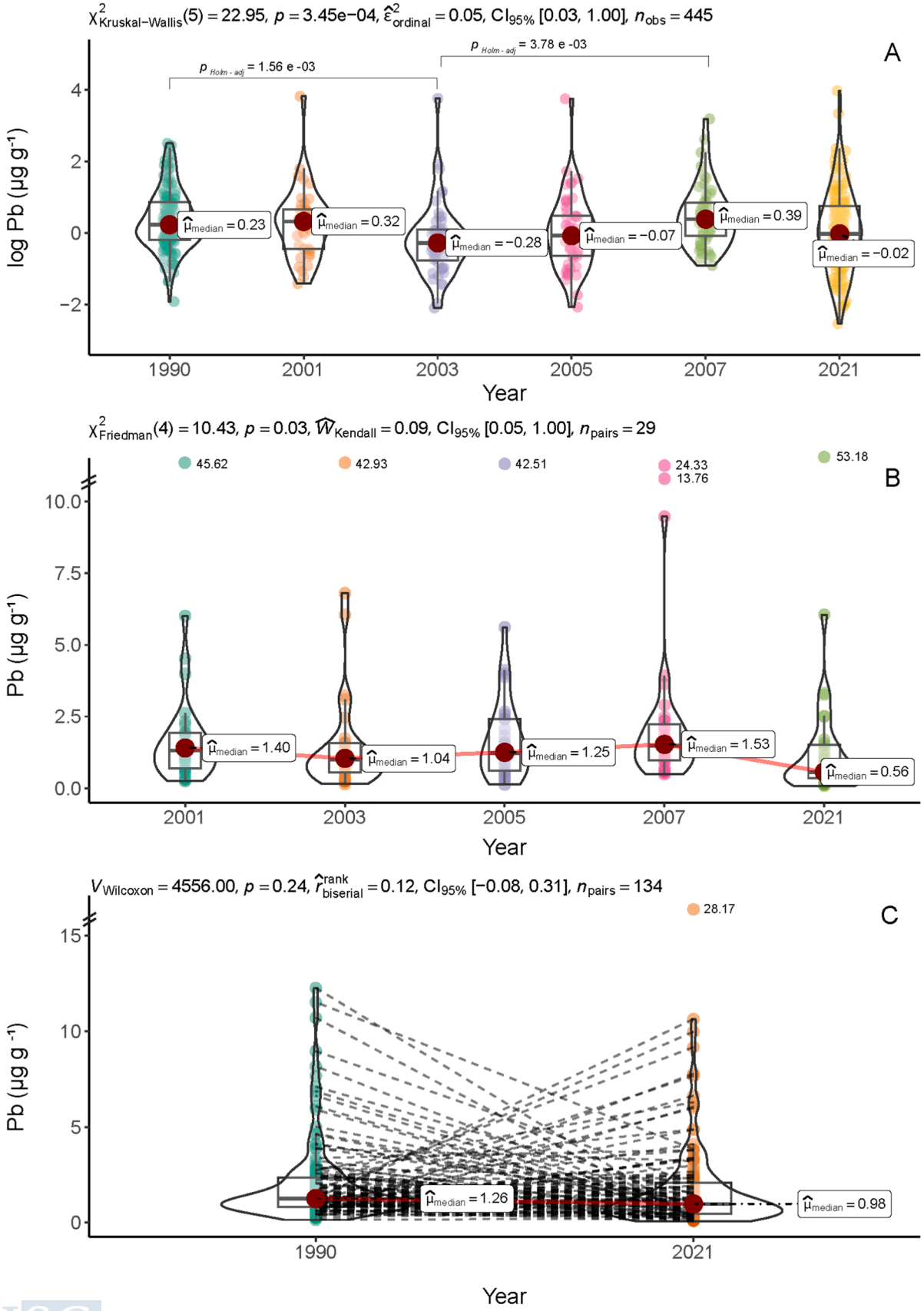

Fig. 2. Pb concentrations over time. Overview of Pb concentrations (µg g $^{-1}$ dry weight) temporal trends: (A) Boxplots (logarithmic scale) with statistical summaries, with significance assessed using the Kruskal-Wallis test followed by Dunn's post-hoc analysis (B) repeated samples from 2001, 2003, 2005, 2007, and 2021 analyzed by Friedman test and Durbin Conover post-hoc analysis, and C) paired samples from 1990 and 2021 analyzed by Wilcoxon paired test. P-values showed only significant pairwise comparisons ($p < 0.05$).

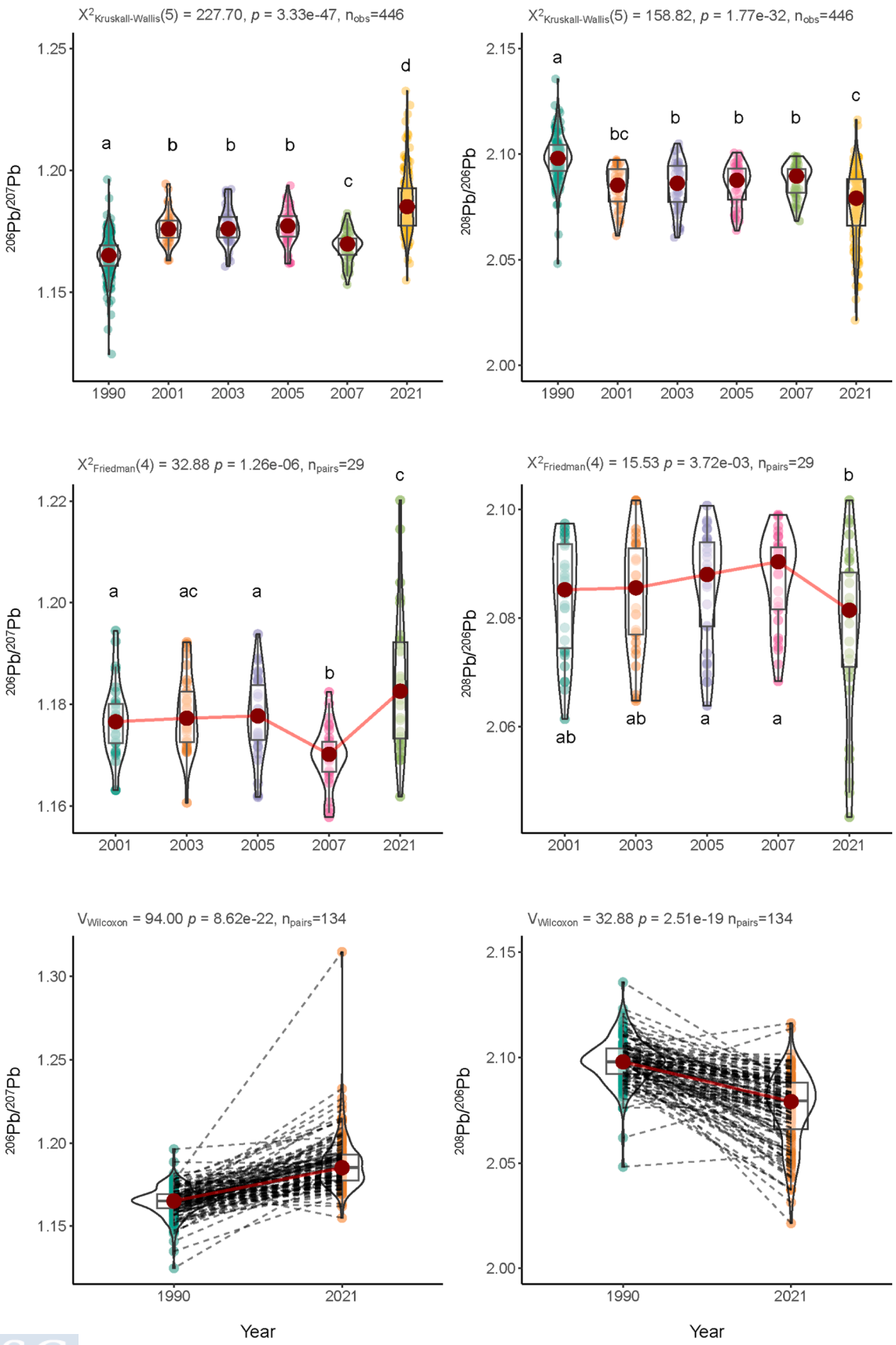

Fig. 3. $^{206}Pb/^{207}Pb$ and $^{208}Pb/^{206}Pb$ over time. Overview of $^{206}Pb/^{207}Pb$ and $^{208}Pb/^{206}Pb$ temporal trends: (A) Boxplots with statistical summaries, with significance assessed using the Kruskal-Wallis test followed by Dunn's post-hoc analysis; (B) Repeated measures from 2001, 2003, 2005, 2007 and 2021 analyzed by Friedman test and Durbin Conover post-hoc analysis; (C) Paired samples from 1990 and 2021 analyzed by Wilcoxon paired test. Distinct lowercase letters indicate significant differences between years (no shared letters = significant, $p < 0.05$).

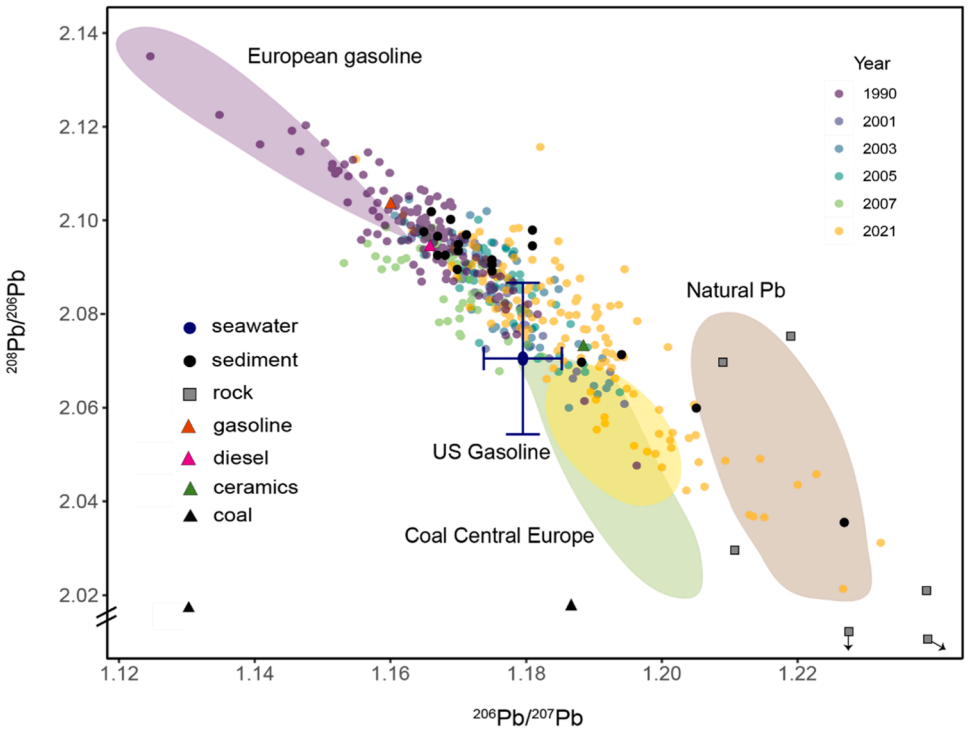

Fig. 4. Three-isotope plot of $^{206}Pb/^{207}Pb$ and $^{208}Pb/^{206}Pb$ ratios for samples of *Fucus vesiculosus* collected in 1990, 2001, 2003, 2005, 2007, and 2021. Samples are color-coded by the year of collection. Shaded areas represent isotopic contributions from different worldwide sources as reviewed by Komárek et al# (2008). Reference values for seawater [78–80] and coal from the study area [54] were obtained from the literature. Other reference materials from the study area are also plotted and listed in the legend.

higher $^{206}Pb/^{207}Pb$ (1.236 ± 0.036) and lower $^{208}Pb/^{206}Pb$ (2.009 ± 0.077) than sediments (1.177 ± 0.014 and 2.088 ± 0.015, respectively). Gasoline and diesel showed similar ratios between them. Ceramics plotted in an intermediate position, without a clearly distinctive isotopic signature. Sediment and algal samples from the same site were significantly correlated (rho = 0.49, $p = 0.03$ for $^{206}Pb/^{207}Pb$; rho = 0.64, $p = 0.003$ for $^{208}Pb/^{206}Pb$).

3.3. Pb sources

The three-isotope plot (Fig. 4) showed a strong correlation between $^{206}Pb/^{207}Pb$ and $^{208}Pb/^{206}Pb$ (rho = −0.84, $p < 2.2 \times 10^{-16}$), but no significant relationship was found between $^{206}Pb/^{207}Pb$ and the inverse of Pb concentrations (rho = 0.11, p = 0.078), indicating that isotopic variation is independent of total Pb levels. When grouping samples by whether Pb concentrations increased or decreased between 1990 and 2021, we observed that shifts in $^{206}Pb/^{207}Pb$ were slightly greater in samples where Pb levels declined; however, this difference was not statistically significant (Wilcoxon test, $p = 0.079$, Fig. S7). Spatial and temporal patterns further support these trends: samples from 1990 clustered near European leaded petrol signatures, while those from 2001 to 2007 occupied intermediate positions reflecting mixed contributions from unleaded petrol, diesel, ceramics, and other anthropogenic Pb sources reported in the literature (Table 1). By 2021, samples aligned more closely with natural sources, such as Galician rock formations (Fig. 4).

MixSIAR results confirmed this temporal shift: in 1990, Pb inputs were dominated by petrol (46.9 %) and coal (48.4 %), with 4.7 % from geological sources. By 2001–2007, petrol (38.9 %) and coal (40.1 %) decreased. In 2021, natural sources dominated (61.5 %), with reduced petrol (32.2 %) and coal (6.3 %) inputs, pointing to a long-term decline in anthropogenic Pb sources (Fig. S8).

4. Discussion

4.1. Trends in Pb concentrations

Lead pollution has driven one of the most transformative environmental regulations in history: the global phase-out of leaded gasoline [83]. This regulatory measure, along with reductions in industrial emissions and improved waste management [84], has significantly lowered environmental Pb inputs in recent decades [85]. Consequently, widespread declines in Pb levels have been reported in seawater [79], sediments [86], and marine biota [31]. Global meta-analyses on *Fucus* spp. indicate sustained reductions since the 1970s, though the rate of decrease has slowed since the early 2000s [87].

In contrast, our study shows only modest decreases in Pb concentrations in *Fucus* spp. from the Northeast Atlantic Ocean over the past 30 years. Specifically, we observed a 21.9 % median reduction across sampling stations (Fig. S2), with slight, non-significant downward trends from 1990 to 2021 (Fig. 2). This is consistent with previous regional studies reporting no significant changes between 2015 and 2019 in *F. vesiculous* [88], and even an increased Pb pollution probability in mosses from 2014 relative to 2000 [89]. In addition, these limited changes contrast with the pronounced declines observed for other Potentially Toxic Elements (e.g., Hg, Cd, Cr) in the same sites and period [90].

Despite the limited temporal decline, the median Pb concentration in our dataset (1.02 μg g^{-1} dry weight) is notably lower than the world median for *Fucus* spp. (2.87 μg g^{-1}) [87], suggesting limited Pb pollution impact for these populations. Most samples fall below the EU safety limit for edible seaweeds (3.0 μg g^{-1}) [91], though 60 samples exceeded this threshold, identifying areas of concern. The highest Pb concentrations were consistently recorded in the Ria do Burgo and Ria de Vigo (rias d and r, respectively, in Fig. S1), both of which have a history of intense industrial activity [92,93]. In these highly impacted sites, Pb concentrations remain elevated and stable over time.

Species-specific differences were observed: *F. ceranoides*, found in inner estuarine areas, exhibited higher Pb concentrations than *F. vesiculosus–F. spiralis,* which dominate more open, marine-influenced zones [94,95]. However, temporal trends were similar across species, suggesting that environmental factors rather than intrinsic physiological differences primarily drive the observed patterns, which is consistent with studies showing no significant interspecific differences under similar environmental conditions [81,82].

4.2. Changes in Pb isotopic composition and source apportionment

Over the 30-year study period, isotopic ratios ($^{206}Pb/^{207}Pb$ and $^{208}Pb/^{206}Pb$) showed clear temporal shifts from signatures characteristic of anthropogenic sources, such as regional ores, European leaded and unleaded gasoline, ceramics, waste incineration, and industrial aerosols, towards more natural (geogenic) values (Fig. 4, Table 1) [18,93]. These trends are consistent with previous sediment-based isotopic studies in the region [93].

MixSIAR source apportionment models reinforce this transition, showing a marked decline in anthropogenic contributions over time. Coal-related Pb inputs decreased sharply from 48.4 % in 1990 to 6.3 % in 2021, in line with the 2020 shutdown or downsizing of the region's main coal power plants (As Pontes, 1468.5 MW; and Cerceda-Meirama, 580 MW) [96]. Similarly, petrol-related inputs declined from 46.9 % to 32.2 %, indicating that traffic remains a diffuse, albeit diminished, source of Pb pollution [9]. Conversely, natural contributions increased from 4.7 % to 61.5 %.

These results suggest the effectiveness of environmental regulations over recent decades, including the ban on leaded fuel [6], and the implementation of the Urban Waste Water Treatment Directive [97], the Water Framework Directive [98], and the Marine Strategy Framework Directive [99]. These measures have contributed to improved wastewater treatment and reduced industrial emissions to coastal waters [84,90]. While major changes in isotopic signatures were expected around the 1990s–2000s due to the leaded petrol phase-out, continued shifts over time suggest that multiple regulatory interventions have played a role.

Median isotopic ratios fall within the range reported for North Atlantic seawater, mussels, and other seaweeds (Table 1, Fig. S9) while still showing sufficient variability to differentiate Pb sources. No significant isotopic differences were detected between *Fucus* species or between inner and outer ria zones, indicating no species-specific fractionation and suggesting spatially homogeneous Pb sources across habitats.

Spatial isotopic patterns further reflect anthropogenic influence: rias with long-standing industrial activity and urban population, such as Pontevedra (paper industry), Vigo (ceramics, automotive), Ferrol (metallurgy, shipyards), and O Burgo (fertilizers, chemicals) [34], exhibited lower $^{206}Pb/^{207}Pb$ ratios and higher $^{208}Pb/^{206}Pb$ ratios (Fig. S3, S4).

Interestingly, except for some heavily industrialized and populated rias, southern rias tended to exhibit higher $^{206}Pb/^{207}Pb$ and lower $^{208}Pb/^{206}Pb$ ratios than northern ones. This may be partly explained by regional geology: the southern rias are predominantly composed of alkaline and calc-alkaline granites, which have naturally higher $^{206}Pb/^{207}Pb$ and lower $^{208}Pb/^{206}Pb$ signatures compared to the slates and peridotites common in the north (Table 1) [33].

Finally, isotopic ratios in algae moderately correlated with those in sediments (rho = 0.49, $p = 0.03$ for $^{206}Pb/^{207}Pb$; rho = 0.64, $p = 0.003$ for $^{208}Pb/^{206}Pb$), likely reflecting differences in integration timescales. While algae reflect Pb exposure over days to weeks [100], the 5-mm sediment layers analyzed here reflect contamination over months to years [101,102]. This highlights the value of algal isotopic signatures for detecting recent shifts in Pb sources with greater temporal resolution than sediment analyses.

4.3. Factors explaining observed trends

As previously discussed, Pb concentrations in *Fucus* spp. did not show a significant decline over time, despite a clear shift in isotopic ratios ($^{206}Pb/^{207}Pb$ and $^{208}Pb/^{206}Pb$) toward more natural signatures. This decoupling suggests complex environmental dynamics. Notably, although not statistically significant ($p = 0.079$, Fig. S7), changes in $^{206}Pb/^{207}Pb$ between 1990 and 2021 tended to be slightly larger in those sites where Pb concentrations declined, suggesting that reductions in Pb load may be accompanied by more pronounced source shifts.

On one hand, this pattern may reflect the persistence of Pb inputs despite regulatory advances. Emerging sources, like batteries, electronic waste, or other modern materials, have intensified in recent years [103,104], and long-range atmospheric transport from other regions may also contribute [105]. However, these sources do not typically exhibit natural-like isotopic signatures, weakening this hypothesis. Similarly, the remobilization of legacy Pb from sediments [106] is an unlikely explanation, as such Pb usually retains anthropogenic isotopic fingerprints, contrary to the observed natural trend.

Alternatively, environmental Pb levels may indeed have declined, but this reduction may not be reflected in algae due to increased sediment contribution in 2021 (189 % compared to 13–49 % between 1990–2007). As sediments often carry high Pb loads, their accumulation on algal surfaces may elevate measured concentrations, masking a true decline in dissolved Pb. Previous studies report substantial sediment contributions to algal Pb ranging from 28–112 % [107–109]. Thus, although the same sampling washing protocol [110] was followed in 2021, persistent sediment particles were visually detected after rinsing. This, combined with strong Fe–Pb correlations and the observed decline in Pb/Fe ratios in algae in 2021 –indicating a real decrease in Pb when normalized to sediment-associated Fe– support this interpretation. Variability in sediment adhesion may arise from environmental factors such as enhanced terrestrial runoff due to storms or heavy rainfall, reduced water movement that limits natural cleaning of the thallus, or shifts in salinity and circulation patterns affecting particle deposition. Sediment contamination remains a well-known limitation in biomonitoring, and no method has proven fully effective at removing all particles without compromising tissue integrity.

In parallel, increased Pb bioavailability under changing environmental conditions may help explain stable concentrations despite lower inputs. This interpretation is supported by speciation simulations using Visual MINTEQ, which indicate a 5.9 % increase in free Pb^{2+} concentrations between 1990 and 2021. These results align with other studies [111,112].

Additionally, factors like intense rainfall [113] and rising temperature [114] may also promote Pb uptake. Despite differing concentrations especially elevated in *F. ceranoides*, no isotopic differences were observed among species, suggesting that the difference in metal uptake is driven by bioavailability, not source heterogeneity. Similarly, the most polluted sites exhibited stable concentrations but isotopic shifts toward natural values, indicating changes in source contribution rather than total load. Weak correlations between algal and seawater Pb concentrations [115] further support the idea that algae primarily reflect the bioavailable Pb fraction. However, the lack of high-resolution, long-term physicochemical data limits a proper evaluation of environmental drivers on Pb bioavailability.

Biological processes may also play a role. Elevated pCO_2 can induce oxidative stress and alter metal binding mechanisms [116,117]. Since Pb is mainly bound to cell walls (Vázquez-Arias et al., submitted), increased cell wall polysaccharide production under stress [118] could enhance Pb retention. Genetic or epigenetic adaptations may further influence Pb accumulation [119].

In addition, natural biological variability could itself explain the absence of clear temporal trends in some cases, especially when concentrations fall within the range of background fluctuation. However, in sites with historically high Pb pollution, algae consistently reflected the

contaminated status over time. For instance, samples from the inner parts of the Ría de Vigo and the Ría do Burgo remained highly enriched in Pb and showed isotopic signatures characteristic of intense anthropogenic sources. This suggests that while subtle changes may be obscured by biological noise, algae remain effective qualitative indicators of severe contamination.

Taken together, the results suggest that increased sediment contribution and enhanced bioavailability, both shaped by evolving environmental conditions, are key drivers of the observed stability in algal Pb concentrations, despite declining anthropogenic inputs. This interpretation is supported by isotopic data and MixSIAR modelling (Fig. S8), which consistently indicate a growing dominance of natural Pb sources in recent years, and consistent with emission trends [120] and regulatory milestones [90]. Yet the sustained Pb levels in biota remain a cause for concern, potentially offsetting the benefits achieved through emission reductions.

4.4. Limitations and future research

This study has several limitations that should be considered when interpreting the results. A key constraint is the limited availability of Pb isotopic data for the region. While MixSIAR provides useful insights, the lack of isotopic signatures for regional industrial sources and the uncertainty regarding the origin and composition of historically used coal hinder a complete reconstruction of source contributions. By generating new baselines across sites, materials, and years, this study begins to fill those gaps.

Another major limitation is the variable influence of sediment over time. The high estimated sediment contribution, especially in 2021, suggests that sediment-bound Pb can significantly elevate total tissue concentrations, potentially masking trends in dissolved or bioavailable Pb. This effect is difficult to correct for, as no washing protocol can remove attached sediment particles entirely without damaging the algal tissue, further complicating the interpretation of temporal patterns. Additionally, changes in environmental conditions, such as ocean acidification, ionic competition, and increased organic matter, may enhance Pb bioavailability, but the absence of long-term, high-resolution physicochemical data in the study area limits our capacity to assess these effects.

Biological variability and the complexities of field sampling introduce uncertainty but also represent a key strength: biomonitors provide organism-level insight that sediment or water analyses alone cannot capture. Given the often weak correlations among environmental compartments, separate assessments remain essential. Expanding this approach to other ecologically important species and increasing the temporal resolution through more frequent sampling would improve the detection of subtle trends in Pb concentrations and source dynamics.

Finally, the use of quadrupole ICP-MS, rather than more precise methods like MC-ICP-MS with resin purification, may introduce analytical bias. To assess the potential impact of matrix effects, six samples were subjected to anion-exchange purification and compared with their untreated counterparts, yielding negligible differences. We acknowledge that this limited comparison may not fully capture all potential inaccuracies, particularly in samples with low Pb concentrations, and that such uncertainties could influence the input data used in the MixSIAR model. Nevertheless, our rigorous quality control procedures, including the use of certified reference materials and analytical replicated, helped minimize this risk.

In light of these limitations, future research should focus on expanding regional isotopic datasets for key sources, incorporating long-term physicochemical monitoring to better understand the drivers of Pb bioavailability, and applying isotopic tools to a broader range of ecologically relevant species. These efforts will enhance the resolution and interpretation of metal pollution trends in coastal ecosystems and strengthen the role of biomonitors in environmental assessment.

5. Conclusions

This study provides one of the most comprehensive long-term datasets to date on Pb concentrations and isotopic signatures in marine organisms, specifically *Fucus* spp., from a coastal region where such information is extremely scarce.

Despite decades of regulatory action, including the global phase-out of leaded gasoline, our results reveal only modest declines in Pb concentrations in *Fucus* spp. from the Northeast Atlantic over the past 30 years. In contrast, Pb isotopic signatures show a clear and consistent shift from anthropogenic to more natural sources between 1990 and 2021, as confirmed by MixSIAR modelling.

These findings highlight the limitations of relying solely on concentration data and underscore the value of Pb isotopes in disentangling changes in pollution sources. However, in highly contaminated areas, *Fucus* spp. continues to serve as a reliable biomonitor, reflecting elevated Pb concentrations. By using marine organisms, the study goes beyond measuring environmental levels, capturing instead the fraction of Pb that is biologically available and potentially bioaccumulative.

The results also emphasize the importance of long-term monitoring: shifts in source contributions and environmental processes are only evident over multi-decadal timescales. By integrating isotopic and biological data across 30 years, this study captures subtle but meaningful trends that would remain undetected in short-term assessments.

Overall, our results point to a long-term reduction in anthropogenic Pb inputs but also expose the complex biogeochemical behavior of Pb in marine environments, shaped by sediment interaction, redox dynamics, and ocean chemistry. The new isotopic baseline data presented here fills a critical gap for the Northeast Atlantic and offers a valuable reference for future source apportionment and environmental assessments. Continued monitoring and sustained regulatory action remain necessary to further reduce Pb pollution and safeguard coastal ecosystems.

Environmental implication

While isotopic data support the effective reduction of anthropogenic Pb inputs to the Northeast Atlantic, stable concentrations in *Fucus* spp. suggest an increasing influence of sediment-derived Pb and bioavailability driven by acidification. This shift highlights critical gaps in concentration-based monitoring, demanding the integration of isotope fingerprinting into regulatory frameworks to identify Pb sources, especially in estuaries, where sediment disturbance and climate change may maintain elevated Pb uptake by organisms despite declines in anthropogenic Pb sources.

CRediT authorship contribution statement

Adéla Šípková: Writing – review & editing. **Michael Komárek:** Writing – review & editing, Conceptualization. **Vladislav Chrastný:** Writing – review & editing. **Pacin Carme:** Writing – review & editing, Writing – original draft, Formal analysis. **Jesús R. Aboal:** Writing – review & editing, Funding acquisition, Conceptualization. **J. Ángel Fernández:** Writing – review & editing, Funding acquisition, Conceptualization. **Antón Vázquez-Arias:** Writing – review & editing.

Declaration of Generative AI and AI-assisted technologies in the writing process

During the preparation of this work the authors used chat GPT in order to improve readability and language. After using this tool, the authors reviewed and edited the content as needed and take full responsibility for the content of the publication.

Declaration of Competing Interest

The authors declare that they have no known competing financial

interests or personal relationships that could have appeared to influence the work reported in this paper.

Acknowledgments

C. Pacín was supported by a predoctoral grant from Xunta de Galicia (ED481A 2022/374) and a research stay grant from CRETUS, which enabled isotope measurements during her stay in the Czech Republic. We sincerely thank Dr. Teresa Taboada for her assistance in selecting representative rock formations from the study area. We also thank Julia Bairstow for her careful revision of the English language. Finally, we thank the anonymous reviewers for their constructive comments, which significantly improved the quality of the manuscript.

Appendix A. Supporting information

Supplementary data associated with this article can be found in the online version at doi:10.1016/j.jhazmat.2025.139289.

Data availability

Data will be made available on request.

References

[1] Singh, N., Kumar, A., Gupta, V.K., Sharma, B., 2018. Biochemical and molecular bases of lead-induced toxicity in mammalian systems and possible mitigations. Chem Res Toxicol 31 (10), 1009–1021. https://doi.org/10.1021/ACS.CHEMRESTOX.8B00193/ASSET/IMAGES/MEDIUM/TX-2018-00193E_0007.GIF.

[2] Rahman, Z., Singh, V.P., 2019. The relative impact of toxic heavy metals (THMs) (Arsenic (As), Cadmium (Cd), Chromium (Cr)(VI), Mercury (Hg), and Lead (Pb)) on the total environment: an overview. Environ Monit Assess 191 (7), 1–21. https://doi.org/10.1007/S10661-019-7528-7/TABLES/3.

[3] Garrett, R.G., 2000. Natural sources of metals to the environment. Hum Ecol Risk Assess 6 (6), 945–963. https://doi.org/10.1080/10807030091124383.

[4] Obeng-Gyasi, E., 2019. Sources of lead exposure in various countries. Rev Environ Health 34 (1), 25–34. https://doi.org/10.1515/REVEH-2018-0037/MACHINEREADABLECITATION/RIS.

[5] Raj, K., Das, A.P., 2023. Lead pollution: impact on environment and human health and approach for a sustainable solution. Environ Chem Ecotoxicol 5, 79–85. https://doi.org/10.1016/J.ENCECO.2023.02.001.

[6] Ritchie, Hanna, 2022. How the World eliminated lead from gasoline. Our World data. ⟨https://ourworldindata.org/leaded-gasoline-phase-out⟩ (accessed 2024-11-29).

[7] Chavez-Garcia, J.A., Noriega-León, A., Alcocer-Zuñiga, J.A., Robles, J., Cruz-Jiménez, G., Juárez-Pérez, C.A., Martinez-Alfaro, M., 2022. Association between lead source exposure and blood lead levels in some lead manufacturing countries: a systematic review and meta-analysis. J Trace Elem Med Biol 71, 126948. https://doi.org/10.1016/J.JTEMB.2022.126948.

[8] Arfala, Y., Douch, J., Assabbane, A., Kaaouachi, K., Tian, H., Hamdani, M., 2018. Assessment of heavy metals released into the air from the cement kilns Co-burning waste: case of Oujda cement manufacturing (Northeast Morocco). Sustain Environ Res 28 (6), 363–373. https://doi.org/10.1016/J.SERJ.2018.07.005.

[9] Chrastný, V., Šillerová, H., Vítková, M., Francová, A., Jehlička, J., Kocourková, J., Aspholm, P.E., Nilsson, L.O., Berglen, T.F., Jensen, H.K.B., Komárek, M., 2018. Unleaded gasoline as a significant source of Pb emissions in the subarctic. Chemosphere 193, 230–236. https://doi.org/10.1016/j.chemosphere.2017.11.031.

[10] Zhou, Q., Wang, S., Liu, J., Hu, X., Liu, Y., He, Y., He, X., Wu, X., 2022. Geological evolution of offshore pollution and its long-term potential impacts on marine ecosystems. Geosci Front 13 (5), 101427. https://doi.org/10.1016/J.GSF.2022.101427.

[11] Sharifi, Z., Hossaini, S.M.T., Renella, G., 2016. Risk assessment for sediment and stream water polluted by heavy metals released by a municipal solid waste composting plant. J Geochem Explor 169, 202–210. https://doi.org/10.1016/j.gexplo.2016.08.001.

[12] Boyle, E.A., Lee, J.M., Echegoyen, Y., Noble, A., Moos, S., Carrasco, G., Zhao, N., Kayser, R., Zhang, J., Gamo, T., Obata, H., Norisuye, K., 2014. Anthropogenic lead emissions in the ocean: the evolving global experiment. Oceanography 27 (1), 69–75. https://doi.org/10.5670/OCEANOG.2014.10.

[13] Buck-Wiese, H., Andskog, M.A., Nguyen, N.P., Bligh, M., Asmala, E., Vidal-Melgosa, S., Liebeke, M., Gustafsson, C., Hehemann, J.H., 2023. Fucoid brown algae inject fucoidan carbon into the ocean. Proc Natl Acad Sci USA 120 (1), e2210561119. https://doi.org/10.1073/PNAS.2210561119/SUPPL_FILE/PNAS.2210561119.SAPP.PDF.

[14] Thomsen, M., South, P., Staehr, P., 2024. Fabulous but forgotten fucoid forests. Ecol Evol 14, e70491. https://doi.org/10.1002/ece3.70491.

[15] Pawlik-Skowrońska, B., Pirszel, J., Brown, M.T., 2007. Concentrations of phytochelatins and glutathione found in natural assemblages of seaweeds depend on species and metal concentrations of the habitat. Aquat Toxicol 83 (3), 190–199. https://doi.org/10.1016/J.AQUATOX.2007.04.003.

[16] Ramesh, K., Berry, S., Brown, M.T., 2015. Accumulation of silver by fucus Spp. (Phaeophyceae) and its toxicity to fucus ceranoides under different salinity regimes. Ecotoxicology 24 (6), 1250–1258. https://doi.org/10.1007/S10646-015-1495-8/TABLES/2.

[17] Sundhar, S., Arisekar, U., Shakila, R.J., Shalini, R., Al-Ansari, M.M., Al-Dahmash, N.D., Mythili, R., Kim, W., Sivaraman, B., Jenishma, J.S., Karthy, A., 2024. Potentially toxic metals in seawater, sediment and seaweeds: bioaccumulation, ecological and human health risk assessment. Environ Geochem Health 46 (2), 1–21. https://doi.org/10.1007/S10653-023-01789-0/TABLES/1.

[18] Komárek, M., Ettler, V., Chrastný, V., Mihaljevič, M., 2008. Lead isotopes in environmental sciences: a review. Environ Int 34 (4), 562–577. https://doi.org/10.1016/J.ENVINT.2007.10.005.

[19] Astray, B., Šípková, A., Baragaño, D., Pechar, J., Krejci, R., Komárek, M., Chrastný, V., 2024. Measuring Pb isotope ratios in fresh snow filtrate refines the apportioning of contaminant sources in the arctic. Environ Pollut 345, 123457. https://doi.org/10.1016/J.ENVPOL.2024.123457.

[20] Bohdalkova, L., Novak, M., Stepanova, M., Fottova, D., Chrastny, V., Mikova, J., Kubena, A.A., 2014. The fate of atmospherically derived Pb in central european catchments: insights from spatial and temporal pollution gradients and Pb isotope ratios. Environ Sci Technol 48 (8), 4336–4343. https://doi.org/10.1021/ES500393Z/SUPPL_FILE/ES500393Z_SI_007.PDF.

[21] Peng, B., Juhasz, A., Fang, X., Jiang, C., Wu, S., Li, X., Xie, S., Dai, Y., 2022. Lead isotopic fingerprinting as a tracer to identify the sources of heavy metals in sediments from the four rivers' inlets to Dongting Lake, China. Catena (Amst) 219, 106594. https://doi.org/10.1016/J.CATENA.2022.106594.

[22] Distribution of Pb Isotopes in Different Chemical Fractions in Bed Sediments from Lower Reaches of the Xiangjiang River, Hunan Province of China. *Science of The Total Environment* 2022, *829*, 154394. https://doi.org/10.1016/J.SCITOTENV.2022.154394.

[23] Le Croizier, G., Point, D., Renedo, M., Munaron, J.-M., Espinoza, P., Amezcua-Martinez, F., Lanco Bertrand, S., Lorrain, A., 2022. Mercury concentrations, biomagnification and isotopic discrimination factors in two seabird species from the humboldt current ecosystem. Mar Pollut Bull 177, 113481. https://doi.org/10.1016/j.marpolbul.2022.113481.

[24] Søndergaard, J., Mosbech, A., 2022. Mining pollution in greenland - the lesson learned: a review of 50 years of environmental studies and monitoring. Sci Total Environ 812, 152373. https://doi.org/10.1016/j.scitotenv.2021.152373.

[25] Runcie, J.W., Townsend, A.T., Seen, A.J., 2009. The application of lead isotope ratios in the antarctic macroalga iridaea cordata as a contaminant monitoring tool. Mar Pollut Bull 58 (7), 961–966. https://doi.org/10.1016/j.marpolbul.2009.03.010.

[26] Soto-Jiménez, M.F., Páez-Osuna, F., Scelfo, G., Hibdon, S., Franks, R., Aggarawl, J., Flegal, A.R., 2008. Lead pollution in subtropical ecosystems on the SE Gulf of California coast: a study of concentrations and isotopic composition. Mar Environ Res 66 (4), 451–458. https://doi.org/10.1016/J.MARENVRES.2008.07.009.

[27] Søndergaard, J., Asmund, G., Johansen, P., Elberling, B., 2010. Pb isotopes as tracers of mining-related pb in lichens, seaweed and mussels near a former Pb-Zn mine in West Greenland. Environ Pollut 158 (5), 1319–1326. https://doi.org/10.1016/j.envpol.2010.01.006.

[28] Outridge, P.M., Evans, R.D., Wagemann, R., Stewart, R.E.A., 1997. Historical trends of heavy metals and stable lead isotopes in beluga (Delphinapterus leucas) and Walrus (Odobenus rosmarus Rosmarus) in the Canadian Arctic. Sci Total Environ 203 (3), 209–219. https://doi.org/10.1016/S0048-9697(97)00142-3.

[29] Kelly, A.E., Reuer, M.K., Goodkin, N.F., Boyle, E.A., 2009. Lead concentrations and isotopes in corals and water near Bermuda, 1780–2000. Earth Planet Sci Lett 283 (1–4), 93–100. https://doi.org/10.1016/J.EPSL.2009.03.045.

[30] Couture, R.M., Chiffoleau, J.F., Auger, D., Claisse, D., Gobeil, C., Cossa, D., 2010. Seasonal and decadal variations in lead sources to eastern North Atlantic mussels. Environ Sci Technol 44 (4), 1211–1216. https://doi.org/10.1021/ES902352Z/SUPPL_FILE/ES902352Z_SI_001.PDF.

[31] Barreira, J., Araújo, D.F., Knoery, J., Briant, N., Machado, W., Grouhel-Pellouin, A., 2024. The french mussel watch program reveals the attenuation of coastal lead contamination over four decades. Mar Pollut Bull 199, 115975. https://doi.org/10.1016/J.MARPOLBUL.2023.115975.

[32] Mapas Climáticos de España y ETo - Agencia Estatal de Meteorología - AEMET. Gobierno de España.

[33] Xunta de Galicia. *Atlas Geoquímico de Galicia*; 1992.

[34] PRTR España. *Registro Estatal de Emisiones y Fuentes Contaminantes*.

[35] García-Seoane, R., Fernández, J.A., Villares, R., Aboal, J.R., 2018. Use of macroalgae to biomonitor pollutants in coastal waters: optimization of the methodology. Ecol Indic 84, 710–726. https://doi.org/10.1016/j.ecolind.2017.09.015.

[36] Wallace, A.L., Klein, A.S., Mathieson, A.C., 2004. Determining the affinities of salt marsh fucoids using microsatellite markers: evidence of hybridization and introgression between two species of fucus (Phaeophyta) in a maine estuary. J Phycol 40 (6), 1013–1027. https://doi.org/10.1111/j.1529-8817.2004.04085.x.

[37] Almeida, S.C., Neiva, J., Sousa, F., Martins, N., Cox, C.J., Melo-Ferreira, J., Guiry, M.D., Serrão, E.A., Pearson, G.A., 2022. A low-latitude species pump: peripheral isolation, parapatric speciation and mating-system evolution converge

in a marine radiation. Mol Ecol 31 (18), 4797–4817. https://doi.org/10.1111/MEC.16623.
[38] Viana, I.G., Aboal, J.R., Fernández, J.A., Real, C., Villares, R., Carballeira, A., 2010. Use of macroalgae stored in an environmental specimen bank for application of some european framework directives. Water Res 44 (6), 1713–1724. https://doi.org/10.1016/J.WATRES.2009.11.036.
[39] National Institute of Standards and Technology. *Standard Reference Material 3328 Lead (Pb) Isotopic Standard Solution CERTIFICATE OF ANALYSIS*; 2023.
[40] Judd, C.D., Swami, K., 2010. ICP-MS determination of lead isotope ratios in legal and counterfeit cigarette tobacco samples. Isot Environ Health Stud 46 (4), 484–494. https://doi.org/10.1080/10256016.2010.528839.
[41] Ďurišová, J., Ackerman, L., Strnad, L., Chrastný, V., Borovička, J., 2015. Lead isotopic composition in biogenic certified reference materials determined by different ICP-based mass spectrometric techniques. Geostand Geoanal Res 39 (2), 209–220. https://doi.org/10.1111/J.1751-908X.2014.00280.X.
[42] *GeoReM: Geological and Enviornmental Reference Materials*. Max Planck Gesellschaft. https://doi.org/10.1111/GGR.12460.
[43] R Core Team. R: A Language and Environment for Statistical Computing, Version 4.4.1. R Foundation for Statistical. 2024.
[44] Fox J.; Weisberg S. *An R Companion to Applied Regression.*, Third.; Sage: Thousand Oaks CA., 2019; Vol. Third edition.
[45] Wickham, H., 2016. Ggplot2: Elegant Graphics for Data Analysis. Springer-Verlag, New York.
[46] Patil, I., 2021. Visualizations with statistical details: the "ggstatsplot" approach. J Open Source Softw 6 (61), 3167. https://doi.org/10.21105/joss.03167.
[47] Stock, B.C., Jackson, A.L., Ward, E.J., Parnell, A.C., Phillips, D.L., Semmens, B.X., 2018. Analyzing mixing systems using a new generation of Bayesian tracer mixing models. PeerJ 6, e5096. https://doi.org/10.7717/peerj.5096.
[48] QGIS Development Team, 2024. QGIS Geographic Information System, Version 3.36.3. 2024.
[49] Gustafsson, J.P. Visual MINTEQ Version 3.1. KTH Royal Institute of Technology, Department of Land and Water Resources Engineering, Stockholm, Sweden. 2013.
[50] Padin, X.A., Velo, A., Pérez, F.F., 2020. ARIOS: a database for ocean acidification assessment in the iberian upwelling system (1976-2018). Earth Syst Sci Data 12 (4), 2647–2663. https://doi.org/10.5194/ESSD-12-2647-2020.
[51] Zhang, X., Zhang, Y., Ding, D., Zhao, J., Liu, J., Yang, W., Qu, K., 2016. On-site determination of Pb2 + and Cd2 + in seawater by double stripping voltammetry with bismuth-modified working electrodes. Microchem J 126, 280–286. https://doi.org/10.1016/J.MICROC.2015.12.010.
[52] Zhang, X., Ma, S., Cui, Z., Chen, J., Cui, Y., Zhao, J., Feng, X., 2011. Sensitive determination of trace Pb2+ in seawater using columnar glassy carbon electrode. J Chin Chem Soc 58 (5), 681–687. https://doi.org/10.1002/JCCS.201190106.
[53] Sugden, C.L., Farmer, J.G., MacKenzie, A.B., 1993. Isotopic ratios of lead in contemporary environmental material from Scotland. Environ Geochem Health 15 (2), 59–65. https://doi.org/10.1007/BF02627823.
[54] Díaz-Somoano, M., Suárez-Ruiz, I., Alonso, J.I.G., Ruiz Encinar, J., López-Antón, M.A., Martínez-Tarazona, M.R., 2007. Lead isotope ratios in Spanish coals of different characteristics and origin. Int J Coal Geol 71 (1), 28–36. https://doi.org/10.1016/j.coal.2006.05.006.
[55] Díaz-Somoano, M., Kylander, M.E., López-Antón, M.A., Suárez - Ruiz, I., Martínez-Tarazona, M.R., Ferrat, M., Kober, B., Weiss, D.J., 2009. Stable lead isotope compositions in selected coals from around the world and implications for present day aerosol source tracing. Environ Sci Technol 43 (4), 1078–1085. https://doi.org/10.1021/ES801818R/SUPPL_FILE/ES801818R_SI_001.PDF.
[56] Wang, Z., Dwyer, G.S., Coleman, D.S., Vengosh, A., 2019. Lead isotopes as a new tracer for detecting coal fly ash in the environment. Environ Sci Technol Lett 6 (12), 714–719. https://doi.org/10.1021/ACS.ESTLETT.9B00512/SUPPL_FILE/EZ9B00512_SI_001.PDF.
[57] Cloquet, C., Carignan, J., Libourel, G., 2006. Atmospheric pollutant dispersion around an urban area using trace metal concentrations and pb isotopic compositions in epiphytic lichens. Atmos Environ 40 (3), 574–587. https://doi.org/10.1016/J.ATMOSENV.2005.09.073.
[58] Plasencia Sánchez, E., Rosell, M., Torrentó, C., Sánchez-Soberón, F., Rovira, J., Sierra, J., Schuhmacher, M., Soler, A., Widory, D., 2025. Improving air pollution source apportionment in size-segregated PM using Pb isotope-based bayesian mixing models in tarragona (Spain). Atmos Res 316, 107939. https://doi.org/10.1016/J.ATMOSRES.2025.107939.
[59] Véron, A., Flament, P., Bertho, M.L., Alleman, L., Flegal, R., Hamelin, B., 1999. Isotopic evidence of pollutant lead sources in Northwestern France. Atmos Environ 33 (20), 3377–3388. https://doi.org/10.1016/S1352-2310(98)00376-8.
[60] Monna, F., Lancelot, J., Croudace, I.W., Cundy, A.B., Lewis, J.T., 1997. Pb isotopic composition of airborne particulate material from France and the Southern United Kingdom: implications for Pb pollution sources in urban areas. Environ Sci Technol 31, 2277–2286. https://doi.org/10.1021/ES960870.
[61] Chiaradia, M., Cupelin, F., 2000. Behaviour of airborne lead and temporal variations of its source effects in Geneva (Switzerland): comparison of anthropogenic versus natural processes. Atmos Environ 34 (6), 959–971. https://doi.org/10.1016/S1352-2310(99)00213-7.
[62] Novák, M., Emmanuel, S., Vile, M.A., Erel, Y., Véron, A., Pačes, T., Wieder, R.K., Vaněček, M., Štěpánová, M., Břízová, E., Hovorka, J., 2003. Origin of lead in Eight central European peat bogs determined from isotope ratios, strengths, and operation times of regional pollution sources. Environ Sci Technol 37 (3), 437–445. https://doi.org/10.1021/ES0200387;SUBPAGE:STRING:ABSTRACT;JOURNAL:JOURNAL:ESTHAG;REQUESTEDJOURNAL:JOURNAL:ESTHAG;WGROUP:STRING:ACHS.
[63] Kylander, M.E., Klaminder, J., Bindler, R., Weiss, D.J., 2010. Natural lead isotope variations in the atmosphere. Earth Planet Sci Lett 290 (1–2), 44–53. https://doi.org/10.1016/J.EPSL.2009.11.055.
[64] Tornos, F., Arias, D., 1993. Sulphur and lead isotope geochemistry of the rubiales Zn-Pb Ore deposit (NW Spain). Eur J Mineral 5 (4), 763–774. https://doi.org/10.1127/EJM/5/4/0763.
[65] Tornos, F., Ribera, F., Shepherd, T.J., Spiro, B., 1996. The geological and metallogenic setting of stratabound carbonate-hosted Zn-Pb mineralizations in the West Asturian Leonese Zone, NW Spain. Min Depos 31 (1–2), 27–40. https://doi.org/10.1007/BF00225393/METRICS.
[66] Arias Prieto, D. El Yacimiento de Pb-Zn de Rubiales (Lugo, España): Hipótesis Genética. 1989..
[67] Neiva, A.M.R., Andráš, P., Ramos, J.M.F., 2008. Antimony Quartz and antimony–gold Quartz veins from Northern Portugal. Ore Geol Rev 34 (4), 533–546. https://doi.org/10.1016/J.OREGEOREV.2008.03.004.
[68] Jorge Millos; Paula Álvarez; Beatriz Comendador. Provenance of the Prehistoric Silver Set of Antas de Ulla, North-Western Iberia, Using Lead Stable Isotope Ratios.
[69] Hansmann, W., Köppel, V., 2000. Lead-isotopes as tracers of pollutants in soils. Chem Geol 171 (1–2), 123–144. https://doi.org/10.1016/S0009-2541(00)00230-8.
[70] Carignan, J., Libourel, G., Cloquet, C., Le Forestier, L., 2005. Lead isotopic composition of fly ash and flue gas residues from municipal solid waste combustors in France: implications for atmospheric lead source tracing. Environ Sci Technol 39 (7), 2018–2024. https://doi.org/10.1021/ES048693X.
[71] Del Rio-Salas, R., Moreno-Rodríguez, V., Loredo-Portales, R., Salgado-Souto, S., Rader, S., Valencia-Moreno, M., Romo-Morales, D., Aguirre-Noyola, J.L., Ramos-Pérez, D., 2025. Do efflorescent salts from worn lead-acid automotive batteries represent potential non-exhaust emissions to urban pollution? A Pb isotope perspective. J Hazard Mater 488, 137366. https://doi.org/10.1016/J.JHAZMAT.2025.137366.
[72] Townsend, A.T., Snape, I., Palmer, A.S., Seen, A.J., 2009. Lead isotopic signatures in antarctic marine sediment cores: a comparison between 1 M HCl partial extraction and HF total digestion pre-treatments for discerning anthropogenic inputs. Sci Total Environ 408 (2), 382–389. https://doi.org/10.1016/J.SCITOTENV.2009.10.014.
[73] Jiang, S., Luo, J., Ye, Y., Yang, G., Pi, W., He, W., 2019. Using Pb isotope to quantify the effect of various sources on multi-metal polluted soil in Guiyu. Bull Environ Contam Toxicol 102 (3), 413–418. https://doi.org/10.1007/S00128-018-02534-5/FIGURES/3.
[74] Kylander, M.E., Weiss, D.J., Martínez Cortízas, A., Spiro, B., Garcia-Sanchez, R., Coles, B.J., 2005. Refining the pre-industrial atmospheric Pb isotope evolution curve in europe using an 8000 year old peat core from NW Spain. Earth Planet Sci Lett 240 (2), 467–485. https://doi.org/10.1016/J.EPSL.2005.09.024.
[75] Schleicher, N.J., Dong, S., Packman, H., Little, S.H., Ochoa Gonzalez, R., Najorka, J., Sun, Y., Weiss, D.J., 2020. A global assessment of copper, zinc, and lead isotopes in mineral dust sources and aerosols. Front Earth Sci 8, 492950. https://doi.org/10.3389/FEART.2020.00167/XML/NLM.
[76] Bollhöfer, A., Rosman, K.J.R., 2001. Isotopic source signatures for atmospheric lead: the Northern hemisphere. Geochim Cosmochim Acta 65 (11), 1727–1740. https://doi.org/10.1016/S0016-7037(00)00630-X.
[77] Zhang, X., Lemaitre, N., Rickli, J.D., Suhrhoff, T.J., Shelley, R., Benhra, A., Faye, S., Jeyid, M.A., Vance, D., 2024. Tracing anthropogenic aerosol trace metal sources in the North Atlantic ocean using Pb, Zn and Ni isotopes. Mar Chem 258, 104347. https://doi.org/10.1016/J.MARCHEM.2023.104347.
[78] Véron, A.J., church, T.M., Patterson, C.C., Flegal, A.R., 1994. Use of stable lead isotopes to characterize the sources of anthropogenic lead in North Atlantic surface waters. Geochim Cosmochim Acta 58 (15), 3199–3206. https://doi.org/10.1016/0016-7037(94)90047-7.
[79] Pinedo-González, P., West, A.J., Tovar-Sanchez, A., Duarte, C.M., Sañudo-Wilhelmy, S.A., 2018. Concentration and isotopic composition of dissolved Pb in surface waters of the modern global ocean. Geochim Cosmochim Acta 235, 41–54. https://doi.org/10.1016/J.GCA.2018.05.005.
[80] Zurbrick, C.M., Boyle, E.A., Kayser, R.J., Reuer, M.K., Wu, J., Planquette, H., Shelley, R., Boutorh, J., Cheize, M., Contreira, L., Barraqueta, J.L.M., Lacan, F., Sarthou, G., 2018. Dissolved Pb and Pb isotopes in the North Atlantic from the GEOVIDE Transect (GEOTRACES GA-01) and their decadal evolution. Biogeosciences 15 (16), 4995–5014. https://doi.org/10.5194/BG-15-4995-2018.
[81] Barreiro, R., Picado, L., Real, C., 2002. Biomonitoring heavy metals in estuaries: a field comparison of two brown algae species inhabiting upper estuarine reaches. Environ Monit Assess 2002 752 75 (2), 121–134. https://doi.org/10.1023/A:1014479612811.
[82] Carballeira, A., Carral, E., Puente, X., Villares, R., 2000. Regional-scale monitoring of coastal contamination. Nutrients and heavy metals in estuarine sediments and organisms on the coast of galicia (Northwest Spain). Int J Environ Pollut 13 (1/2/3/4/5/6), 534. https://doi.org/10.1504/IJEP.2000.002333.
[83] Von Storch, H., Costa-Cabral, M., Hagner, C., Feser, F., Pacyna, J., Pacyna, E., Kolb, S., 2003. Four decades of gasoline lead emissions and control policies in Europe: a retrospective assessment. Sci Total Environ 311 (1), 151–176. https://doi.org/10.1016/S0048-9697(03)00051-2.
[84] *Censo Nacional de Vertidos (CNV)*. ⟨https://www.miteco.gob.es/es/cartografia-y-sig/ide/descargas/agua/censo-nacional-vertidos.html⟩.
[85] *Heavy metal emissions in Europe (Indicator) | European zero pollution dashboards*. ⟨https://www.eea.europa.eu/en/european-zero-pollution-dashboards/indicators/heavy-metal-emissions-in-europe-indicator⟩ (accessed 2025-05-21).

[86] Logemann, A., Reininghaus, M., Schmidt, M., Ebeling, A., Zimmermann, T., Wolschke, H., Friedrich, J., Brockmeyer, B., Pröfrock, D., Witt, G., 2022. Assessing the chemical anthropocene – development of the legacy pollution fingerprint in the North Sea during the last century. Environ Pollut 302, 119040. https://doi.org/10.1016/J.ENVPOL.2022.119040.
[87] Aboal, J.R., Pacín, C., García-Seoane, R., Varela, Z., González, A.G., Fernández, J. A., 2023. Global decrease in heavy metal concentrations in brown algae in the last 90 years. J Hazard Mater 445, 130511. https://doi.org/10.1016/J.JHAZMAT.2022.130511.
[88] García-Seoane, R., Fernández, J.A., Boquete, M.T., Aboal, J.R., 2021. Analysis of intra-Thallus and temporal variability of trace elements and nitrogen in fucus vesiculosus: sampling protocol optimization for biomonitoring. J Hazard Mater 412, 125268. https://doi.org/10.1016/J.JHAZMAT.2021.125268.
[89] Giráldez, P., Crujeiras, R.M., Fernández, J.Á., Aboal, J.R., 2022. Establishment of background pollution levels and spatial analysis of moss data on a regional scale. Sci Total Environ 839, 156182. https://doi.org/10.1016/J.SCITOTENV.2022.156182.
[90] Pacín, C., Fernández, J.Á., Conde-Amboage, M., Lazzari, M., García-Seoane, R., G. Viana, I., Varela, Z., Real, C., Villares, R., Aboal, J.R., 2025. Three decades of change in potentially toxic elements in brown algae in the Northeast Atlantic Ocean. Environ Sci Technol. https://doi.org/10.1021/acs.est.4c14013.
[91] Lähteenmäki-Uutela, A., Rahikainen, M., Camarena-Gómez, M.T., Piiparinen, J., Spilling, K., Yang, B., 2021. European union legislation on macroalgae products. Aquac Int 29 (2), 487–509. https://doi.org/10.1007/S10499-020-00633-X/TABLES/1.
[92] Beiras, R., Fernández, N., Bellas, J., Besada, V., González-Quijano, A., Nunes, T., 2003. Integrative assessment of marine pollution in galician estuaries using sediment chemistry, mussel bioaccumulation, and embryo-larval toxicity bioassays. Chemosphere 52 (7), 1209–1224. https://doi.org/10.1016/S0045-6535(03)00364-3.
[93] Álvarez-Iglesias, P., Rubio, B., Millos, J., 2012. Isotopic identification of natural vs. Anthropogenic lead sources in marine sediments from the inner Ría de Vigo (NW Spain). Sci Total Environ 437, 22–35. https://doi.org/10.1016/J.SCITOTENV.2012.07.063.
[94] Billard, E., Daguin, C., Pearson, G., Serrão, E., Engel, C., Valero, M., 2005. Genetic isolation between three closely related taxa: fucus vesiculosus, F. Spiralis, and F. ceranoides (Phaophyceae). J Phycol 41 (4), 900–905. https://doi.org/10.1111/j.0022-3646.2005.04221.x.
[95] Neiva, J., Pearson, G.A., Valero, M., Serrão, E.A., 2012. Fine-scale genetic breaks driven by historical range dynamics and ongoing density-barrier effects in the Estuarine seaweed fucus ceranoides L. BMC Evol Biol 12 (1), 1–16. https://doi.org/10.1186/1471-2148-12-78/FIGURES/5.
[96] Garha, N.S., 2022. From decarbonization to depopulation: an emerging challenge for the carbon-intensive regions under the energy transition in Spain. Sustainability 14 (22), 14786. https://doi.org/10.3390/SU142214786.
[97] Council Directive. *Urban Wastewater Treatment Directive* (*91/271/EEC*); 1991.
[98] European Parliament and Council. *Directive 2000/60/EC Water Framework Directive*; 2000. ⟨https://eur-lex.europa.eu/eli/dir/2000/60/oj⟩ (accessed 2024-10-06).
[99] European Environment Agency. *Marine Strategy Framework Directive 2008/56/EC*; 2008. ⟨https://www.eea.europa.eu/policy-documents/2008-56-ec⟩.
[100] Vázquez-Arias, A., Pacín, C., Ares, Á., Fernández, J.Á., Aboal, J.R., 2023. Do we know the cellular location of heavy metals in seaweed? An up-to-date review of the techniques. Sci Total Environ 856 (September 2022). https://doi.org/10.1016/j.scitotenv.2022.159215.
[101] Bonachea, J., Remondo, J., Rivas, V., 2024. Estuaries in Northern Spain: an analysis of their sedimentation rates. Sustainability 16 (16), 6856. https://doi.org/10.3390/SU16166856.
[102] Perez-Arlucea, M., Mendez, G., Clemente, F., Nombela, M., Rubio, B., Filgueira, M., 2005. Hydrology, sediment yield, erosion and sedimentation rates in the estuarine environment of the Ria de Vigo, Galicia, Spain. J Mar Syst 54 (1–4), 209–226. https://doi.org/10.1016/J.JMARSYS.2004.07.013.
[103] Nathaniel, S.P., 2021. Ecological footprint and human well-being nexus: accounting for broad-based financial development, globalization, and natural resources in the Next-11 countries. Future Bus J 7 (1), 1–18. https://doi.org/10.1186/S43093-021-00071-Y.
[104] *Electronic waste (e-waste)*. ⟨https://www.who.int/news-room/fact-sheets/detail/electronic-waste-%28e-waste%29?utm_source=chatgpt.com⟩ (accessed 2025-01-14).
[105] Brooks, H.L., Miner, K.R., Kreutz, K.J., Winski, D.A., 2025. A global review of long-range transported lead concentration and isotopic ratio records in snow and ice. Environ Sci Process Impacts 27 (4), 878–891. https://doi.org/10.1039/D4EM00526K.
[106] Rusiecka, D., Gledhill, M., Milne, A., Achterberg, E.P., Annett, A.L., Atkinson, S., Birchill, A., Karstensen, J., Lohan, M., Mariez, C., Middag, R., Rolison, J.M., Tanhua, T., Ussher, S., Connelly, D., 2018. Anthropogenic signatures of lead in the Northeast Atlantic. Geophys Res Lett 45 (6), 2734–2743. https://doi.org/10.1002/2017GL076825.
[107] Bryan, G., Langston, W., Hummerstone, L.G., Burt, G.R., 1985. A guide to the assessment of heavy metal contamination in estuaries using biological indicators. Mar Biol Assoc 4, 92.
[108] Bryan, G.W., 1983. Brown seaweed, fucus vesiculosus, and the gastropod, littorina littoralis, as indicators of trace-metal availability in estuaries. Sci Total Environ 28 (1–3), 91–104. https://doi.org/10.1016/S0048-9697(83)80010-2.
[109] Barnett, B.E., Ashcroft, C.R., 1985. Heavy metals in fucus vesiculosus in the humber estuary. Environ Pollut Ser B Chem Phys 9 (3), 193–213. https://doi.org/10.1016/0143-148X(85)90033-3.
[110] García-Seoane, R., Fernández, J.A., Varela, Z., Real, C., Boquete, M.T., Aboal, J. R., 2019. Sampling optimization for biomonitoring metal contamination with marine macroalgae. Environ Pollut 255, 113349. https://doi.org/10.1016/j.envpol.2019.113349.
[111] Caldeira, K., Wickett, M.E., 2003. Anthropogenic carbon and ocean PH, 365–365 Nature 425 (6956). https://doi.org/10.1038/425365a.
[112] Millero, F.J., Woosley, R., Ditrolio, B., Waters, J., 2009. Effect of ocean acidification on the speciation of metals in seawater. Oceanography 22 (4), 72–85. https://doi.org/10.5670/OCEANOG.2009.98.
[113] Vignier, J., Champeau, O., Atalah, J., South, P., McDougall, D., Jeffs, A., Blackwell, D., Tremblay, L.A., Rolton, A., 2025. Land-derived metals impact the survival and settlement of larval mussels. Environ Pollut 367, 125675. https://doi.org/10.1016/J.ENVPOL.2025.125675.
[114] Lan, W.R., Huang, X.G., Lin, L. xiu, Li, S.X., Liu, F.J., 2020. Thermal discharge influences the bioaccumulation and bioavailability of metals in oysters: implications of ocean warming. Environ Pollut 259, 113821. https://doi.org/10.1016/J.ENVPOL.2019.113821.
[115] Vázquez-Arias, A., Boquete, M.T., Fernández, J.Á., Aboal, J.R., 2025. Assessing the effectiveness of seaweed transplants in reflecting seawater pollution levels. Environ Pollut 377, 126456. https://doi.org/10.1016/j.envpol.2025.126456.
[116] Schultz, J., Berry Gobler, D.L., Young, C.S., Perez, A., Doall, M.H., Gobler, C.J., 2024. Ocean acidification significantly alters the trace element content of the Kelp, Saccharina Latissima. Mar Pollut Bull 202, 116289. https://doi.org/10.1016/J.MARPOLBUL.2024.116289.
[117] Maharana, D., Jena, K., Pise, N.M., Jagtap, T.G., 2010. Assessment of oxidative stress indices in a marine macro brown alga padina tetrastromatica (hauck) from comparable polluted coastal regions of the Arabian Sea, West Coast of India. J Environ Sci 22 (9), 1413–1417. https://doi.org/10.1016/S1001-0742(09)60268-0.
[118] Andrade, L.R., Leal, R.N., Noseda, M., Duarte, M.E.R., Pereira, M.S., Mourão, P.A. S., Farina, M., Amado Filho, G.M., 2010. Brown algae overproduce cell wall polysaccharides as a protection mechanism against the heavy metal toxicity. Mar Pollut Bull 60 (9), 1482–1488. https://doi.org/10.1016/j.marpolbul.2010.05.004.
[119] García-Seoane, R.; Richards, C.L.; Aboal, J.R.; Fernández, J.Á.; Schmid, M.W.; Boquete, M.T. A Field Study of the Molecular Response of Brown Macroalgae to Heavy Metal Exposure: An (Epi)Genetic Approach. https://doi.org/10.2139/SSRN.4896934.
[120] European Environment Agency. *Heavy metal emissions in Europe*. ⟨https://www.eea.europa.eu/data-and-maps/indicators/eea32-heavy-metal-hm-emissions-2/assessment⟩. croalgae to Heavy Metal Exposure: An (Epi)Genetic Approach. https://doi.org/10.2139/SSRN.4896934.

Supporting information

The Return of Natural Lead to the North Atlantic Captured by Brown Algae

Carme Pacín[1,2*], Jesús R. Aboal[1], J. Ángel Fernández[1], Antón Vázquez-Arias[1], Adéla Šípková[3], Michael Komárek[3], Vladislav Chrastný[3]

1. CRETUS Center, Department of Functional Biology, Ecology Unit, Universidade de Santiago de Compostela, Santiago de Compostela, 15782, Spain

2. CIQUS Center, Department of Physical Chemistry, Universidade de Santiago de Compostela, Santiago de Compostela, 15782, Spain

3. Department of Environmental Geosciences, Faculty of Environmental Sciences, Czech University of Life Sciences Prague, Kamýcká 129, 165 00, Prague-Suchdol, Czech Republic

* corresponding author: Email: mcarme.pacin@usc.es

Supporting Information includes:

- Additional sampling details for methodological clarity.
- Supplementary Figures (Figs. S1-S7):
    - Figs. S1-S6: Maps illustrating Pb concentrations and isotopic ratios across sampling sites, along with percentage changes.
    - Fig. S7: Variation in 206Pb/207Pb by trend in Pb concentrations (1990–2021).
    - Fig. S8: Estimated Pb source contributions to Fucus spp. over time based on MixSIAR.
    - Fig. S9: Compilation of Pb isotopic ratios in seaweed from published literature).
- Supplementary tables:
    - Table S1: Measured vs. reported isotopic ratios for reference materials
    - Table S2: Selected Pb end-members with isotopic ratios and Pb concentrations.

Additional sampling details

Sample collection

As elemental concentrations in intertidal seaweeds vary depending on their depth in the intertidal strip, samplings were designed to cover the whole area. To this end, samplings were carried out during low tide, and seaweeds were collected following a transect of at least 50 m following a zig-zag pattern. To account for the interindividual variability, 30 subsamples were collected in each sampling site, each subsample representing a single thallus or a set of thalli attached to substrate at the same point.

Sample processing

Once collected, sample cleaning was done by rinsing the thalli in seawater after collection, as using other cleaning agents risks damaging the cell membranes by osmotic shock. After this, samples were placed in polyethylene bags and placed in a cooler with icepacks in order to ensure their integrity during transport to the laboratory.

Elemental concentrations vary along the length of the thalli depending on the age of the section. So, in order to standardize the age of the material analyzed, the three most apical dichotomies of healthy thalli without reproductive structures were selected. To prevent contamination, the selected sections were cut using glassware, which was also used to remove epiphytes.

Reference:

García-Seoane, R.; Fernández, J. A.; Villares, R.; Aboal, J. R. Use of Macroalgae to Biomonitor Pollutants in Coastal Waters: Optimization of the Methodology. Ecological Indicators. 2018, pp 710–726. https://doi.org/10.1016/j.ecolind.2017.09.015.

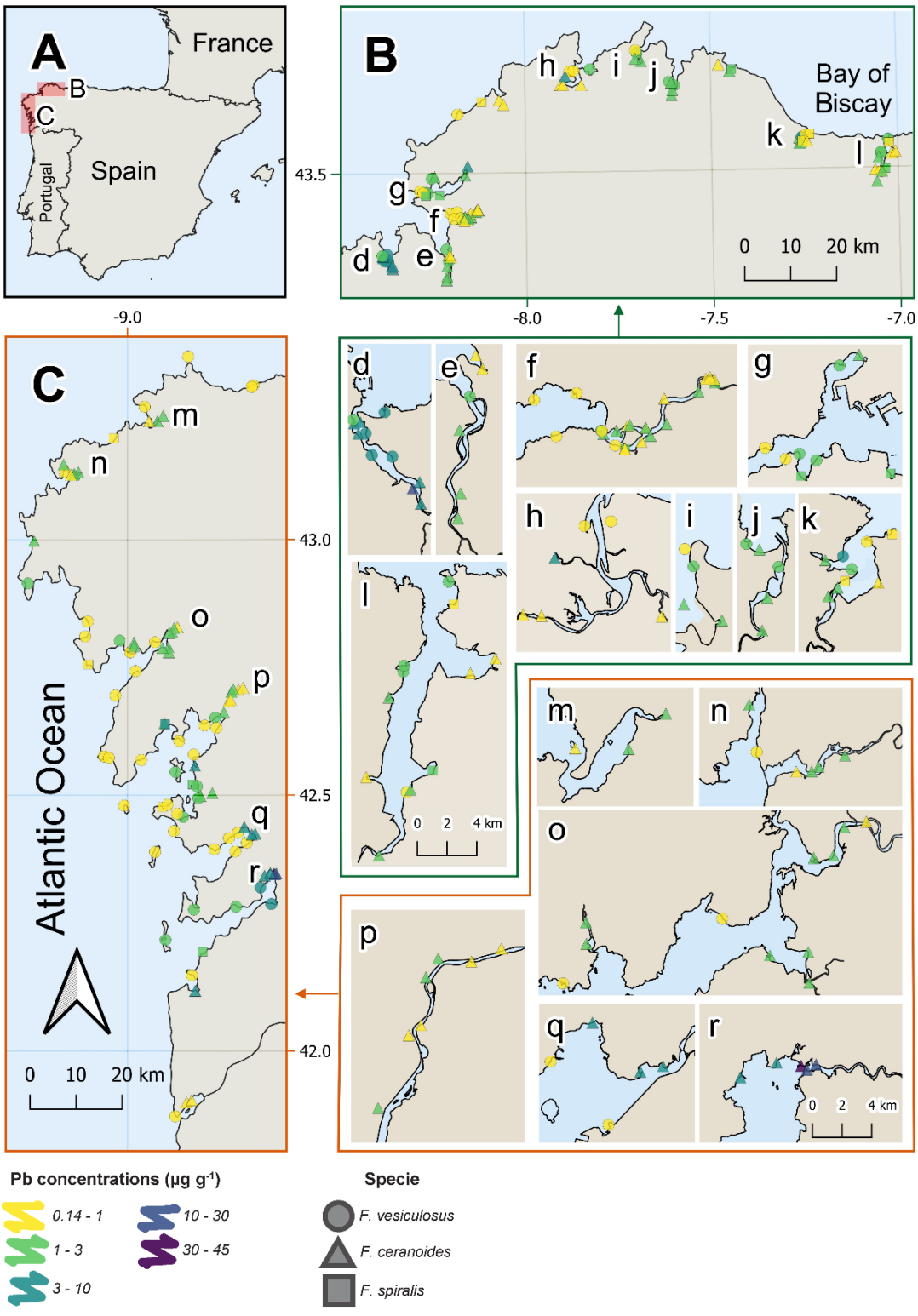

Fig. S1. Overview of Pb median concentrations (µg g $^{-1}$) in the sampling sites. Panels A-C display an overview of the region, with B and C showing the sampling sites. Panels d-l and m-r present detailed maps of sites that are densely clustered and difficult to distinguish

in B and C, respectively. Different symbols represent the species sampled (*Fucus ceranoides and F. vesiculosus – F. spiralis*).

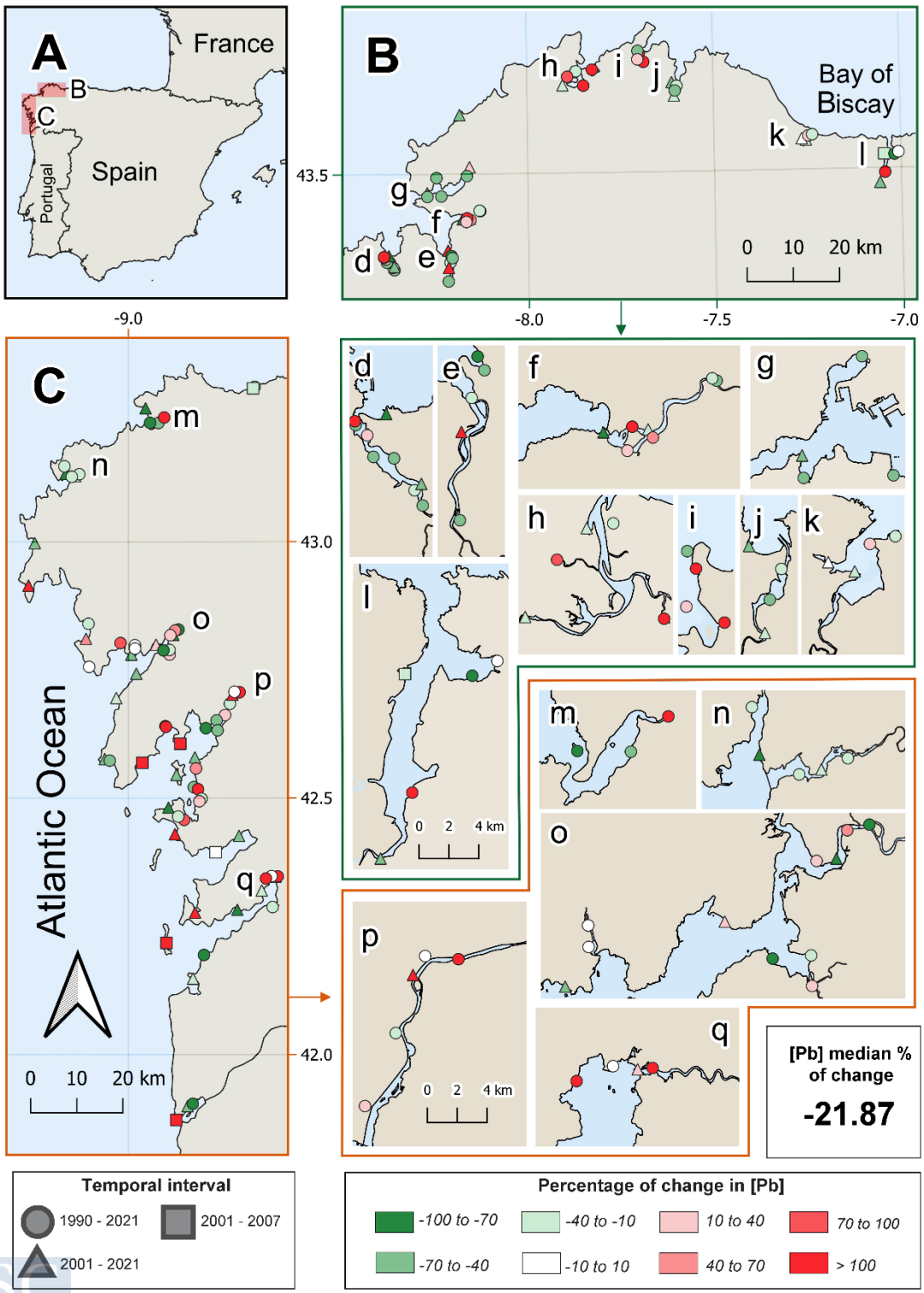

Fig. S2. Map of percentage changes in Pb concentrations over time. Panels A-C provide a regional overview, with B and C showing the differences between the final and initial Hg concentrations (in %) at each sampling station. Panels d-l and m-q offer detailed views of sampling sites that are densely clustered and hard to distinguish in B and C, respectively. Different colours represent the percentage changes in Pb concentrations, while distinct symbols indicate the sampling periods: 1990-2021, 2001-2021, and 2001-2007. The total median percentage change, calculated as the median of the percentage changes across all sampling sites, is displayed below.

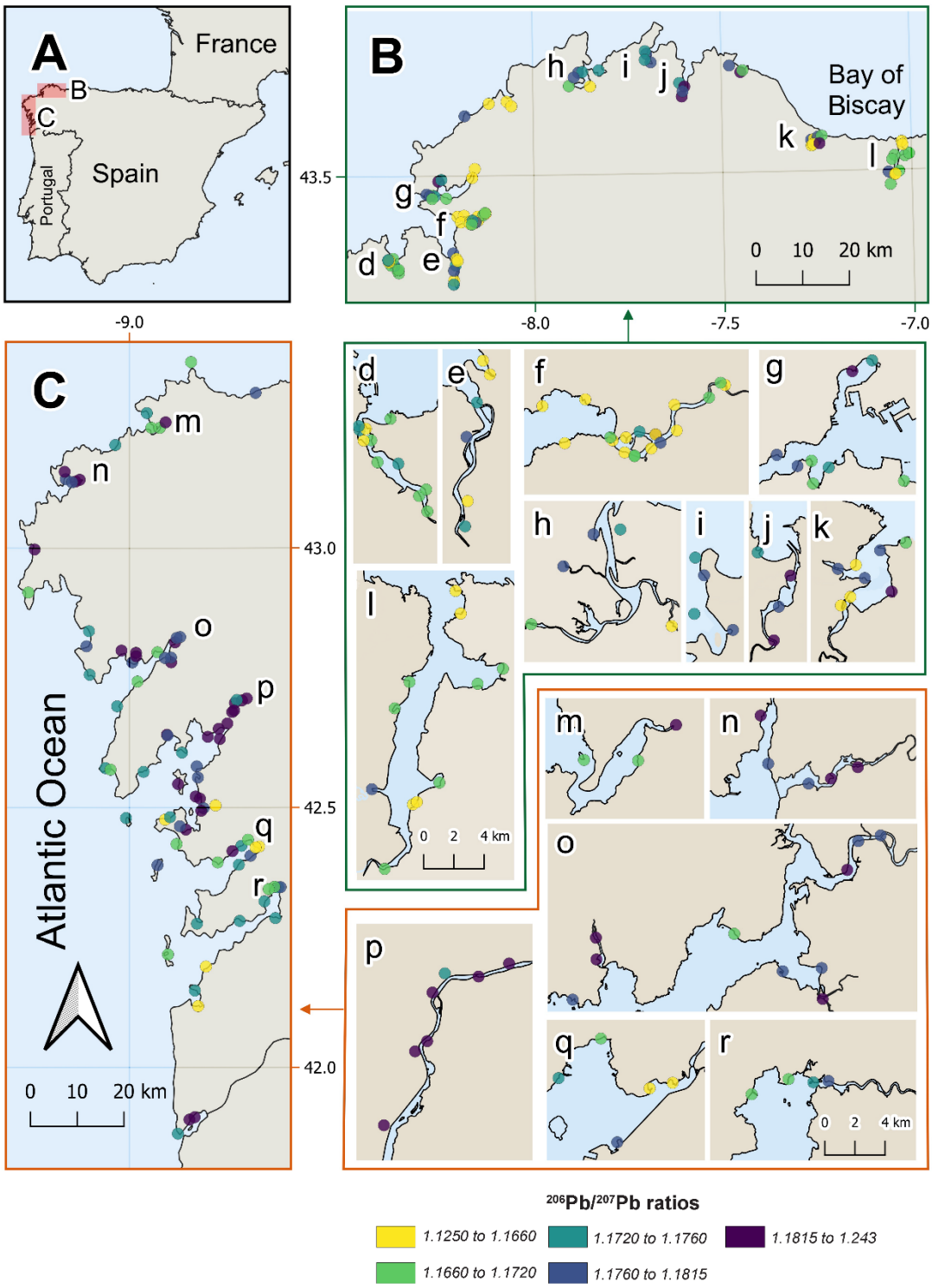

Fig. S3. Overview of $^{206}Pb/^{207}Pb$ median ratios in the sampling sites. Panels A-C display an overview of the region, with B and C showing the sampling sites. Panels d-l and m-r present detailed maps of sites that are densely clustered and difficult to distinguish in B and

C, respectively. Different symbols represent the species sampled (*Fucus ceranoides and F. vesiculosus – F. spiralis*).

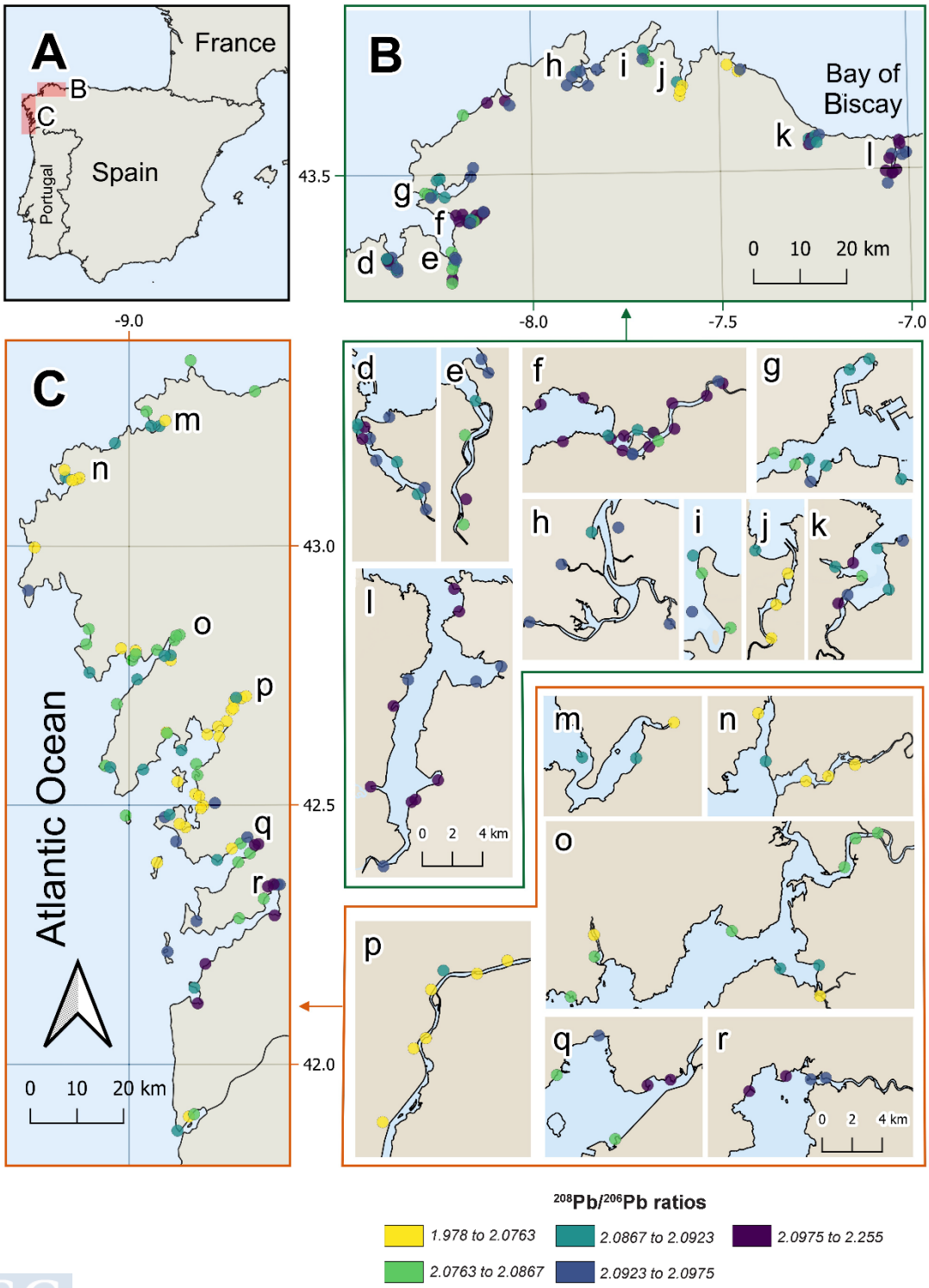

Fig. S4. Overview of $^{208}Pb/^{206}Pb$ median ratios in the sampling sites. Panels A-C display an overview of the region, with B and C showing the sampling sites. Panels d-l and m-r present detailed maps of sites that are densely clustered and difficult to distinguish in B and C, respectively. Different symbols represent the species sampled (*Fucus ceranoides and F. vesiculosus – F. spiralis*).

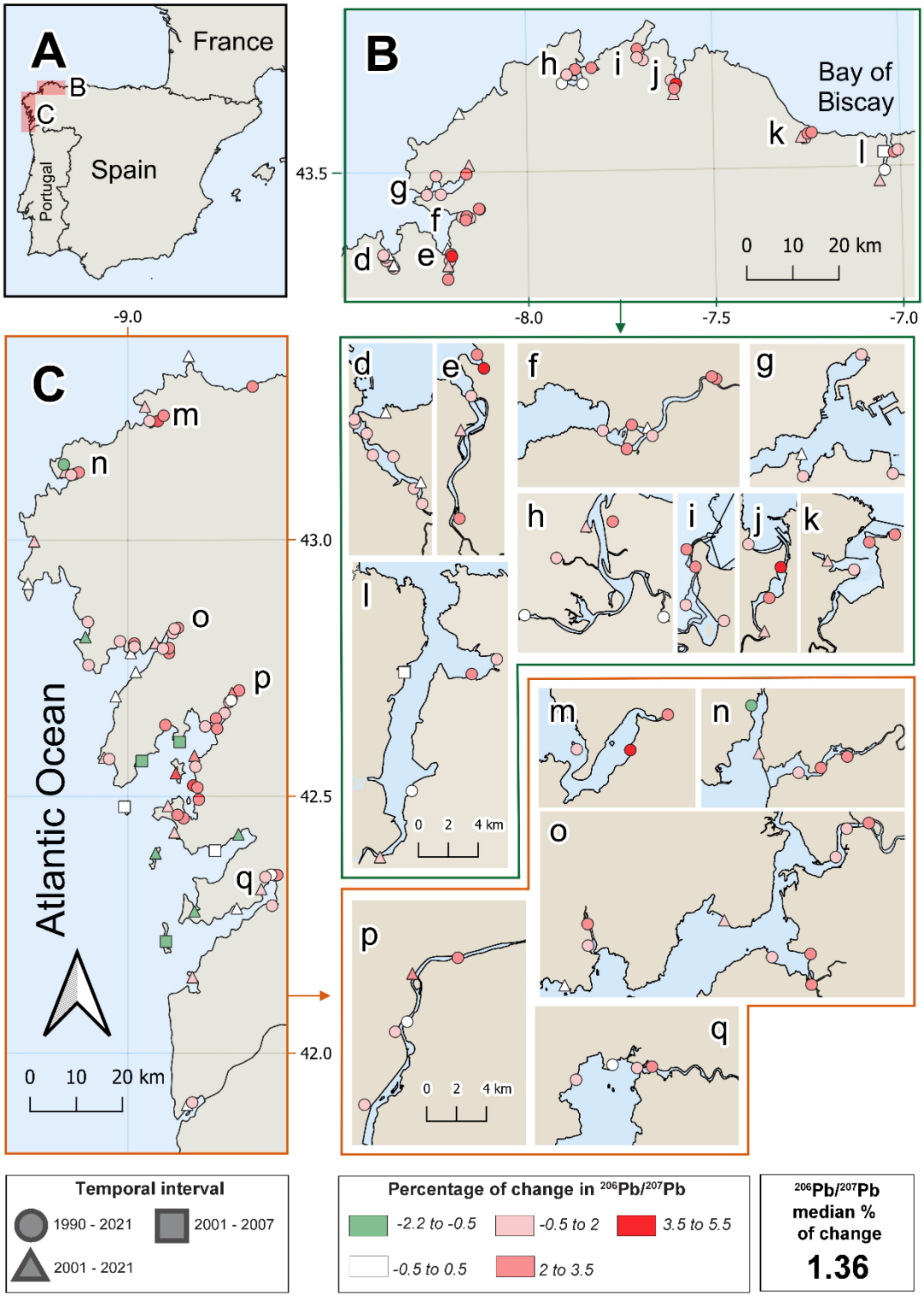

Fig. S5. Map of percentage changes in $^{206}Pb/^{207}Pb$ ratios over time. Panels A-C provide a regional overview, with B and C showing the differences between the final and initial $^{206}Pb/^{207}Pb$ ratios at each sampling station. Panels d-l and m-q offer detailed views of

sampling sites that are densely clustered and hard to distinguish in B and C, respectively. Different colours represent the percentage changes in $^{206}Pb/^{207}Pb$ ratios, while distinct symbols indicate the sampling periods: 1990-2021, 2001-2021, and 2001-2007. The total median percentage change, calculated as the median of the percentage changes across all sampling sites, is displayed below.

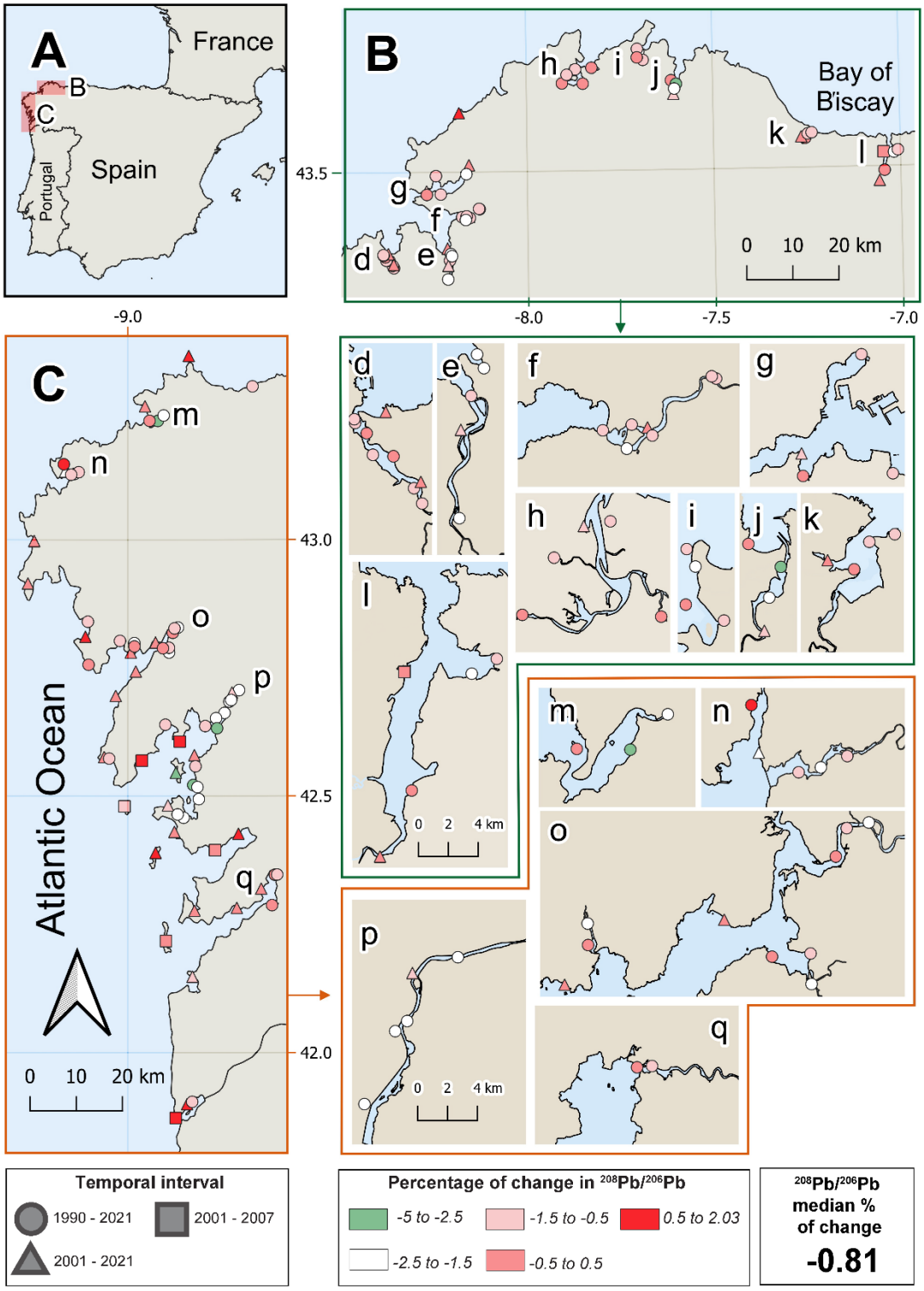

Fig. S6. Map of percentage changes in $^{208}Pb/^{206}Pb$ ratios over time. Panels A-C provide a regional overview, with B and C showing the differences between the final and initial $^{208}Pb/^{206}Pb$ ratios (in %) at each sampling station. Panels d-l and m-q offer detailed views of

sampling sites that are densely clustered and hard to distinguish in B and C, respectively. Different colours represent the percentage changes in $^{208}Pb/^{206}Pb$ ratios, while distinct symbols indicate the sampling periods: 1990-2021, 2001-2021, and 2001-2007. The total median percentage change, calculated as the median of the percentage changes across all sampling sites, is displayed below.

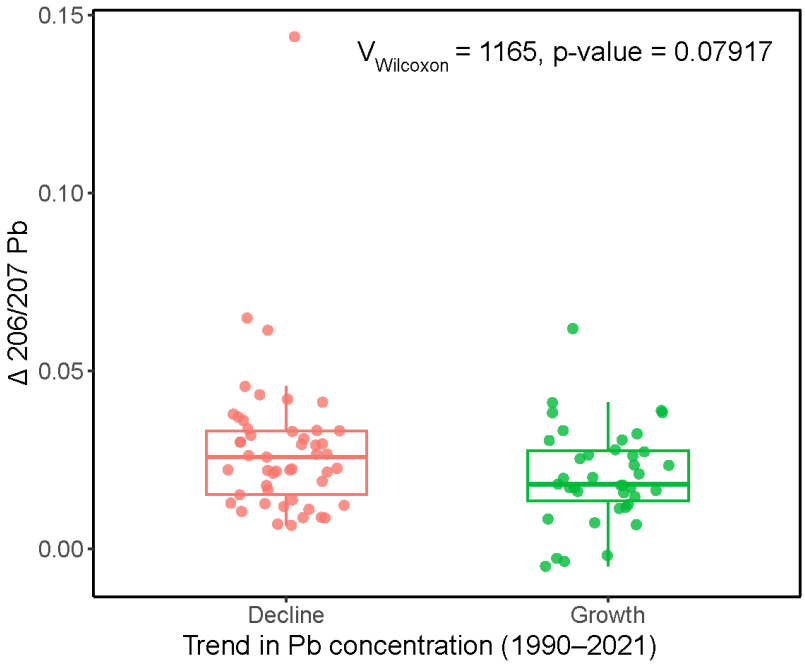

Fig. S7. Boxplot showing the variation in $^{206}Pb/^{207}Pb$ ratios between 1990 and 2021, grouped by Pb concentration trend (Decline vs. Growth). Each point represents the change in isotopic ratio for a given sampling site ($\Delta^{206}Pb/^{207}Pb$). Although sites with declining Pb concentrations tended to show slightly larger isotopic shifts, this difference was not statistically significant.

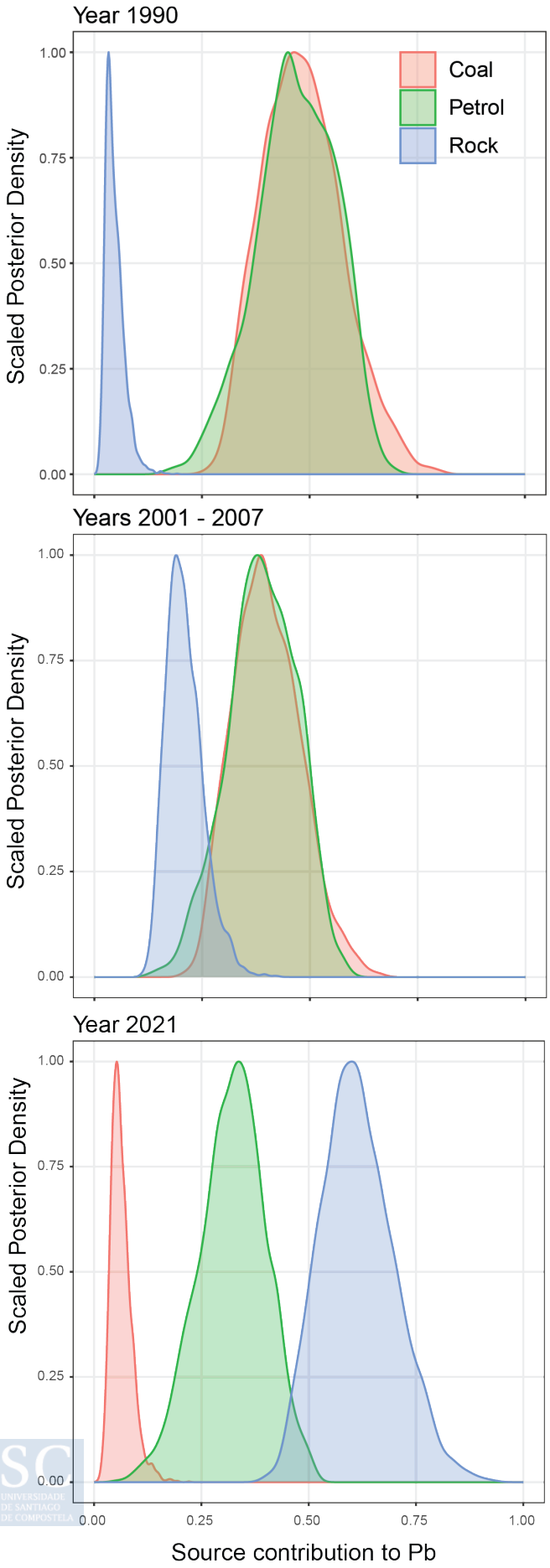

Fig. S8. Estimated contribution of different Pb sources to *Fucus* spp. based on MixSIAR outputs, shown for 1990, 2001–2007, and 2021. Each panel displays the posterior distribution of the proportion of Pb originating from coal combustion, petrol-related sources (including diesel), and natural geological background (rocks), inferred from $^{206}Pb/^{207}Pb$ and $^{208}Pb/^{206}Pb$ (Table 1). The x-axis represents the estimated proportion of Pb from each source, while the y-axis shows the scaled posterior density.

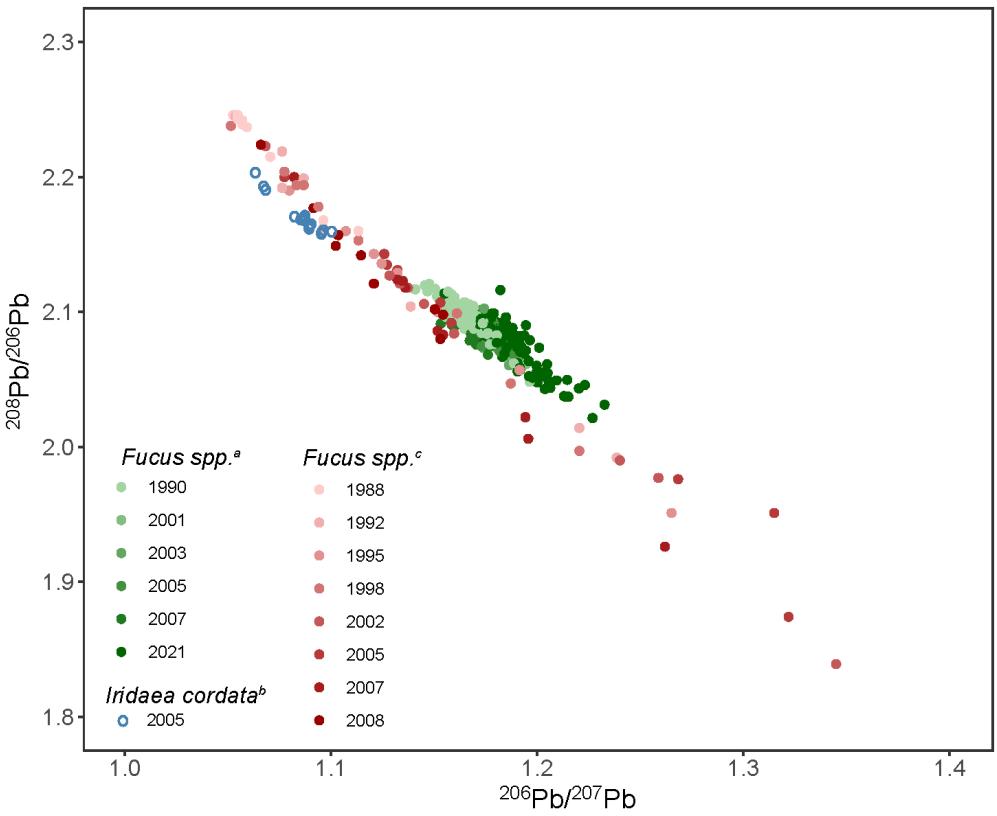

Fig. S9. Three-isotope plot of lead isotopic ratios ($^{206}Pb/^{207}Pb$ and $^{208}Pb/^{206}Pb$) in macroalgae. Data points are color-coded by study: (a) the current study, (b) the Antartica study with *Iridaea cordata*, and (c) the Greenland study with *Fucus* spp. Within studies (a) and (c), variations in shading represent different sampling years, while study (b) has a single color as sampling was conducted in a single year.

Table S1. Comparison of isotopic ratios for reference materials, including NIST SRM 1573a (tomato leaves), NIST SRM 1515 (apple leaves), and IAEA-336 (epiphytic lichen). Reported isotopic ratios from the literature are presented alongside the measured values obtained in this study.

	^{206}Pb / ^{207}Pb		^{208}Pb / ^{206}Pb	
	Reported	**Obtained**	**Reported**	**Obtained**
N1573a	1.2099-1.2209	1.2163	2.020-2.030	2.0294
N1515	1.2028-1.2036	1.1992	2.0411-2.0468	2.0441
IAEA336	1.1450	1.1430	2.1150	2.1178

Table S2. Excel file (provided in Supplementary material 2) containing sampling sites information including Coordinates (WGS84), Ría, Species, Year of sampling, Pb and Fe, and $^{206}Pb/^{207}Pb$ and $^{208}Pb/^{206}Pb$ concentrations for each sample of Fucus collected in NW Spain from 1990 to 2021, and for sediments. Element concentrations are expressed in $\mu g\ g^{-1}$.

5. CAPÍTULOS SEN PUBLICAR

5.1. Long-Term Silver Contamination in the Ocean: Insights from Brown Algae on Dissolved Ag and Nanoparticles

Carme Pacín[1*], Massimo Lazzari[1], J. Ángel Fernández[2], Jesús R. Aboal[2]

1. CIQUS Center, Department of Physical Chemistry, Universidade de Santiago de Compostela, Santiago de Compostela, 15782, Spain

2. CRETUS Center, Department of Functional Biology, Ecology Unit, Universidade de Santiago de Compostela, Santiago de Compostela, 15782, Spain

*corresponding author.

Under review.

Abstract

Silver nanoparticles (AgNPs) are increasingly released into the environment, yet their presence and behavior in marine biota remain poorly understood. Brown algae, known for their high metal accumulation capacity, have never been directly analyzed for AgNPs under natural conditions. Moreover, total silver (Ag) data in marine organisms are scarce, despite Ag's high toxicity and potential for biomagnification.

In this study, we analyzed *Fucus* spp. samples collected from 173 sites along the Galician coast (NW Iberian Peninsula) between 1990 and 2021 to assess long-term trends in total Ag and AgNP concentrations. A total of 446 samples were analyzed for Ag, and 30 samples from 10 representative sites (1990, 2005–2007, 2021) were assessed for AgNPs. We also conducted a global review of Ag concentrations in brown algae worldwide.

Total Ag concentrations in *Fucus* declined significantly over the past three decades (−58.1%), in line with the global downward trend observed in brown algae since the 1980s. AgNP concentrations also decreased over time and showed a positive correlation with total Ag levels, despite the increasing release of engineered AgNPs. These results suggest that AgNPs found in algal tissues are not directly accumulated from external sources but rather formed *in situ* via algal-mediated reduction of dissolved Ag.

Our findings indicate that brown algae serve not only as sentinels of Ag pollution but also as active agents in AgNP formation. Although AgNPs accounted for less than 5% of total Ag, their persistence and potential for biomagnification highlight the need for continued monitoring. By integrating long-term data, nanoparticle detection, and a global perspective, this study provides new insights into the behavior and fate of silver in marine ecosystems.

Keywords

Biomonitoring; marine pollution; hazardous elements; temporal trends; coastal ecosystems; seaweed

1. Introduction

Silver (Ag) is a trace metal naturally occurring in the marine environment at extremely low concentrations, typically in the picomolar range (Barriada et al., 2007; Ranville et al., 2005). Although its use dates back centuries, with historical mining activities releasing Ag into the environment, modern industrial applications —including electronics, photography, catalysis, medical instruments, and wastewater discharge (Flegal et al., 2007; Sañudo-Wllhelmy and Flegalf, 1992; Squire et al., 2002)— have led to substantial Ag inputs into marine ecosystems.

Silver ranks among the most toxic trace metals, with its free ionic form (Ag^+) second only to Hg in toxicity (Bryan, 1971). However, its toxicity depends on its chemical speciation, which is strongly influenced by environmental factors such as salinity, organic matter, and redox conditions. In seawater, Ag primarily forms stable, insoluble complexes with chloride, iodide and bromide (Luo et al., 2013; Miller and Bruland, 1995; Tappin et al., 2010), which significantly reduce its bioavailability and toxicity. Nevertheless, under changing environmental conditions, these complexes can release Ag^+ (Rong et al., 2018; Valverde et al., 2008), maintaining their ecological relevance. In estuarine environments, where salinity is lower, Ag is more likely to associate with organic matter or form AgHS, which are less stable and more prone to releasing Ag^+ under fluctuating salinity, redox conditions, and pH, making estuaries particularly vulnerable to Ag toxicity (Tappin et al., 2010).

In recent years, silver nanoparticles (AgNPs) have emerged as an additional and rapidly growing source of Ag pollution, with global annual production estimated at 185-500 tons and further increasing in the next years ("The Global Market for Nanomaterials 2010-2030 - Advanced and Emerging Technology Market Research," n.d.). Their nanoscale size, high

surface-area-to-volume ratio, and potent antibacterial activity have driven widespread use in consumer products (e.g., textiles, cosmetics) (Behera et al., 2024; Vance et al., 2015). AgNP toxicity is attributed to direct membrane interactions, oxidative stress, and Ag^+ release via dissolution (Banu et al., 2021; Dobias and Bernier-Latmani, 2013). In seawater the salinity enhances AgNP dissolution, increasing Ag^+ release, while organic matter may stabilize nanoparticles, prolonging their persistence (Miao et al., 2009; Zhang et al., 2016).

The toxic effects of Ag and AgNPs have been documented in a wide range of marine organisms, including invertebrates, fish, and macroalgae (Gambardella et al., 2015; García-Alonso et al., 2014; Ramesh et al., 2015; Turner et al., 2012). Brown algae, in particular, can bioconcentrate Ag (Johnstone et al., 2016; Peng et al., 2022), leading to potential Ag transfer through marine food webs. Notably, they are also capable of producing AgNPs via the isolation of specific bioactive compounds (Princy and Gopinath, 2021; Savitri et al., 2024). In addition to their role in metal transformation, brown algae (e.g., *Fucus* spp.) have been widely used as biomonitors, offering insights into metal contamination patterns in coastal ecosystems (Aboal et al., 2023). As key primary producers and foundational species in coastal ecosystems, brown algae are ecologically significant (Thomsen et al., 2024). This combination of ecological and biomonitor roles underscores the importance of monitoring Ag and AgNPs in brown algae to better understand their environmental fate, bioavailability, and potential risks.

Tracking long-term trends in Ag contamination is particularly relevant due to the significant shifts in Ag inputs over recent decades. Regulatory measures (e.g. wastewater treatment improvements, reductions in industrial discharges, etc.) and technological shifts (i.e. digital photography replacing film) have reduced Ag inputs from traditional sources (Beck et al., 2009; Gunther et al., 1999; Ohanian and Phillips, 2013). Conversely, the increasing use of AgNPs has introduced a new and growing source of Ag into the environment, making Ag a "re-emerging" contaminant (Courtois et al., 2019). These dynamics are further complicated by global change, with shifts in ocean salinity, pH, and redox conditions influencing the behavior, bioavailability, and toxicity of Ag and AgNPs (Courtois et al., 2019; Deycard et al., 2017; Ramesh et al., 2015).

Despite the importance for assessing the effectiveness of regulatory measures, identifying emerging threats, and predicting their ecological impacts, studies evaluating long-term temporal trends of Ag contamination across abiotic (water, sediment) and biotic compartments remain scarce (Beck et al., 2009; Li et al., 2025; Lu et al., 2020; Rainbow et al., 2011).

Moreover, Ag in marine organisms, including brown algae, is often overlooked or grouped with other metals, with limited discussion of its specific behavior and impacts. Additionally, to the best of our knowledge, only one study has quantified AgNP concentrations in natural marine organisms (Xu et al., 2020). Research to date has been thus restricted to ecotoxicological assays (Gambardella et al., 2015), and temporal trends of AgNPs in marine ecosystems remain entirely unexplored.

This study addresses these gaps by analyzing Ag contamination in *Fucus* spp. samples systematically collected between 1990 and 2021 and archived in the Galician Environmental Specimen Bank, with the aim of assessing the temporal evolution of Ag pollution in Northeast Atlantic coastal ecosystems. As a novel approach, we also analyzed samples from ten sites collected in three time points (1990, 2005/2007, and 2021) to investigate, for the first time, the presence, concentrations, and size distribution of AgNPs in natural populations of marine organisms. Finally, we conducted a global review of Ag concentrations in brown algae, compiling data from 275 sites from studies worldwide. We hypothesize that (i) Ag concentrations in *Fucus* spp. from the Northeast Atlantic have remained stable over time and space; (ii) AgNP concentrations and size distributions in these algae have shown no significant temporal or spatial variation; and (iii) there are no consistent global trends in Ag contamination in brown algae.

2. Material and methods

2.1. Study area

The experimental part of the research took place in Galicia, a region in the northwest of Spain with a 1498 km coastline along the Atlantic Ocean. This coastline is distinguished by the presence of distinctive coastal inlets known as rias (Fig. 1). Galicia experiences an oceanic climate, with mild temperatures and abundant rainfall (Agencia Estatal de Meteorología, n.d.). The geological composition is predominantly composed of granite (Romaní, 2023).

Galicia's coastal zone has experienced significant industrialization since the mid-20th century, driven by the growth of key economic sectors such as automotive manufacturing, shipbuilding, energy production, papermill, and metallurgical industries (both ferrous and non-ferrous) (PRTR España, n.d.). This development, coupled with rapid urban expansion along the coastline, has resulted in sustained wastewater discharges into the rias since the 1950s.

2.2. Sample collection

Sampling campaigns were carried out during low tide in July of 1989-1990 (hereafter referred to as 1990), 2001, 2003, 2005, 2007 and 2021. Over these years, a total of 173 sampling sites were sampled resulting in the collection of 446 samples of *Fucus ceranoides*, *F. spiralis* and *F. vesiculosus* (Fig. 1). With few exceptions, sites sampled in 1990 were revisited in 2021, and those surveyed in 2001 were subsequently resampled in 2003, 2005, 2007 and 2021. In addition, eight samples collected in 2017 were also analyzed; however, due to their low representativeness, they were not included in the main analyses, although they were considered in the global review of Ag concentrations (Section 2.5).

The species *Fucus ceranoides* is restricted to brackish inner rias, while *F. spiralis* and *F. vesiculosus* are typically found in more exposed, oceanic-influenced areas, where they often coexist and hybridize (Fig. 1). Due to the difficulty in distinguishing between these two species in the field, and their high degree of hybridization (Wallace et al., 2004), samples identified as *F. vesiculosus* or *F. spiralis* were grouped under *F. vesiculosus – F. spiralis*, whereas *F. ceranoides* was examined separately.

At each sampling site, a composite sample was obtained by collecting at least 30 thalli along a 50-meter transect using a zig-zag pattern. The thalli were rinsed with seawater on-site and transported to the laboratory in coolers. In the laboratory, only the apical portions of each thallus, corresponding to the last three dichotomies and representing the most recent growth period, were selected. Samples containing reproductive structures, visible damage, or epiphytes were excluded. Detailed protocols can be consulted (García-Seoane et al., 2018). The selected thalli were dried in a forced-air oven at 40°C until reaching a constant weight and subsequently homogenized using a tangential mixer mill equipped with zirconium oxide grinding vessels (Retsch MM400). Homogenized samples were stored in hermetically sealed glass containers, at room temperature protected from light in the Galician Environmental Specimen Bank (Universidade de Santiago de Compostela) until chemical analysis.

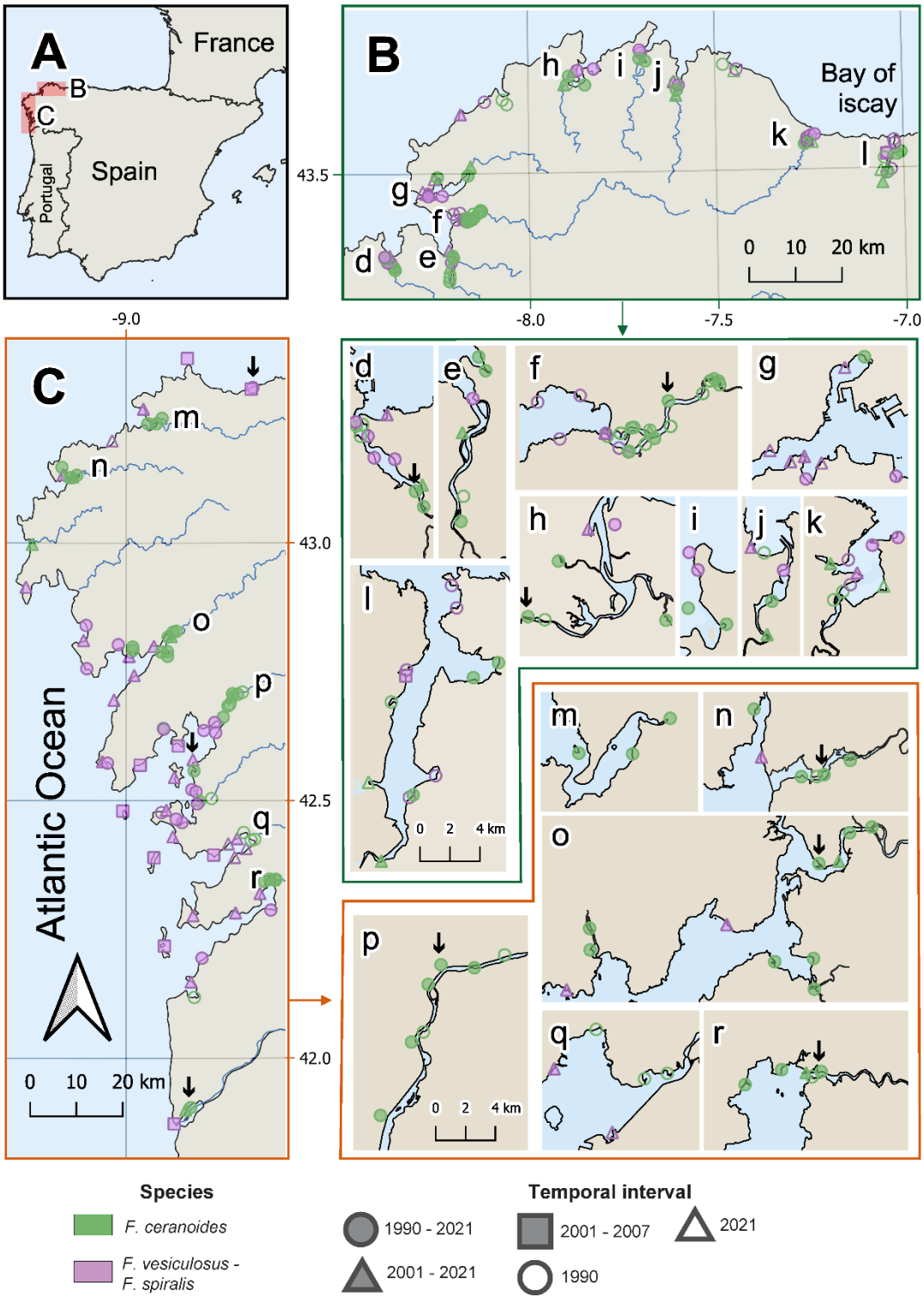

Fig. 1. Map of the study area. Panels A-C display an overview of the region, with B and C showing the sampling sites (sites). Panels d-l and m-r present detailed maps of sites that are densely clustered and difficult to distinguish in B and C, respectively. Different colors represent the species sampled (F. ceranoides and F. vesiculosus - F. spiralis), while distinct symbols indicate the sampling periods: 1990-2021, 2001-2021, and 2001-2007, or those sampled exclusively in 1990 or 2021. To reduce clutter, incomplete samplings from 2001, 2003,

2005, and 2007 are grouped under the 2001-2007 symbol. Black arrows in panels C (n=3), d, f, h, n, o, p, and r indicate the locations of samples analyzed for Ag nanoparticles.

2.3. Ag concentrations

Ag concentrations were analyzed in all available samples (n = 446). Before analysis, all the samples were re-dried at 100°C and digested with HNO_3 (69% w/w) in a Milestone Ultrawave. Ag concentrations were measured with an Agilent 7700x ICP-MS at the Research Support Services Unit of the Universidade de Santiago de Compostela. Quality control measures for Ag concentration analysis included analytical blanks and sample replicates, analyzed at a frequency of one per 30 samples. The overall analytical error was 4.7%, with a limit of quantification (LOQ) of 2.80 ng g-1, which was exceeded in all samples.

2.4. AgNP analysis

Ten sampling sites across different areas of Galicia were selected to represent a range of Ag concentration levels (Fig. 1). In each site, samples from 1990, 2005 (2007 on one occasion), and 2021 were analyzed for AgNPs (n = 30). For each dry sample, a 25 mg was placed into a 10 mL polyethylene tube containing 7 mL of a 2 mM citric acid/2 mM trisodium citrate buffer (pH = 4.5). The mixture was sonicated in an ice bath for 2.5 minutes using 1.0-second pulses (total time: 5 minutes) with the ultrasound probe operating at 20% amplitude. Following sonication, 2.0 mL of a 25 g/L Macerozyme R-10® solution was added. The extract was then incubated in a Boxcult temperature-controlled chamber at 37°C and 150 rpm for 6 hours. After incubation, the extracts were filtered using 5.0 μm cellulose syringe filters and subsequently diluted with 1.0% (v/v) glycerol prior to analysis by SP-ICP-MS.

Enzymatic extracts were further diluted by at least 100 times with 1.0% (v/v) glycerol and subjected to bath-sonication for 1 minute before SP-ICP-MS analysis. The Syngistix™ Nano Application Software was used to perform multiple measurements to determine the transport efficiency (TE) of nanoparticles to the nebulizer.

Finally, the concentration and size distributions of AgNPs in the diluted extracts were directly obtained from the software following analysis. Each sample underwent three separate extractions, with each extraction analyzed between 3 and 5 times to ensure precision and reliability. The full protocol is available in López-Mayán et al., 2022.

The limit of quantification (LOQ) was 3.22×10^6 AgNPs g^{-1}, with 5 out of 30 samples falling below this threshold. The average coefficient of variation (CV) was 36%.

2.5. Global review

A comprehensive search was conducted using the SCOPUS database, Google Scholar and reference lists from selected articles to identify studies on Ag contamination in brown algae (Phaeophyceae). The following search query was used in both databases:

(Ag OR silver) AND (macroalgae OR "brown algae" OR seaweed OR Fucus OR Fucaceae OR Laminariaceae OR Dictyotaceae or Sargassaceae) AND (biomonitoring OR content OR composition OR monitoring OR accumulation OR bioaccumulation).

This search yielded 118 articles in SCOPUS and 444 in Google Scholar. All retrieved articles were manually screened, selecting only those that reported at least the genus of the algae, sampling coordinates or identifiable places of sampling through a map or a name, and Ag concentrations in dry weight. The year of sampling was also recorded whenever available; if missing, the publication year of the paper was used instead.

After applying these criteria, 37 papers were included in the final review. Theses, annual reports, and similar literature sources were excluded.

In addition to the review of literature data, a second analysis was performed in which these data were combined with the Ag concentrations measured in the present study, allowing for a more robust temporal evaluation of trends

2.6. Statistical analysis

Basic descriptive statistics, including medians, ranges, and Shapiro-Wilk normality tests, were conducted in R v. 4.4.1 (R Core Team, 2024). Data visualization and statistical analyses were performed using the ggplot2 and ggstatsplot packages (H. Wickham., 2016; Patil, 2021).

Comparisons of Ag concentrations between species in the regional study were performed using the Wilcoxon rank-sum test. Temporal trends across all surveys (1990 - 2021) and samples were evaluated with the Kruskal-Wallis and Dunn's tests. For sites sampled in both 1990 and 2021, differences were tested using the Wilcoxon signed-rank test. Sites revisited in 2001, 2003, 2005, 2007, and 2021 were analyzed using the Friedman test followed by Durbin-Conover pairwise comparisons.

We evaluated spatial patterns by mapping site-specific median Ag concentrations and their temporal changes (expressed as percentage differences between earliest and most recent measurements) using QGIS 3.36.3 (QGIS Development Team, 2024). The median percentage change across all sites was calculated to summarize overall temporal trends.

Finally, recognizing the lithogenic influence on Ag distribution, we examined relationships between regional Ag concentrations and potential geochemical tracers (Fe and Al) using Spearman's rank correlation.

Temporal trends in silver nanoparticle counts (AgNPs g^{-1}) were assessed using repeated measures ANOVA and pairwise t-tests, following confirmation of normality for yearly count distributions. Relationships between Ag concentrations and AgNP counts were evaluated using linear models (LMs) and Pearson correlation coefficients. To evaluate temporal changes in particle diameter, we fitted a generalized linear mixed model (GLMM) with a Gamma distribution using the glmmTMB package in R (McGillycuddy et al., 2025).

Additionally, the proportion of ionic and nanoparticulate silver (Ag) was calculated for each sample by estimating the mass of silver nanoparticles. The mass of AgNPs was determined using the volume of a spherical nanoparticle, which was calculated from the median diameter of the particles, and the known density of silver (10.49 g cm^{-3}). This allowed the calculation of the nanoparticulate fraction, with the remaining Ag mass considered ionic.

To investigate global trends in algal pollution, Generalized Additive Models (GAMs) were applied to the logarithmic concentrations of Ag reported in the literature across different algal families over time (n = 275). Additionally, we compared Ag concentrations between the two most extensively documented families (Fucaceae and Sargassaceae), using the Wilcoxon rank-sum test.

3. Results

3.1. Regional Ag concentrations

The distribution of Ag concentrations was non-normal and right skewed, with values ranging from 0.011 to 1.27 µg g^{-1} and a median of 0.090 µg g^{-1}. No significant interspecific variation was observed between *F. ceranoides* and *F. vesiculosus – F. spiralis*. Additionally, no spatial patterns were detected based on the inner-outer distribution of the rias, nor were any north-south pattern observed (Fig. 2). However, certain rias (e.g., rias e, j, and q) exhibited notably

high concentrations. Weak-to-moderate negative correlations emerged with lithogenic elements, showing stronger Ag-Fe association ($\rho = -0.108$, $p = 4.2 \times 10^{-6}$) than Ag-Al ($\rho = -0.21$, $p = 0.021$).

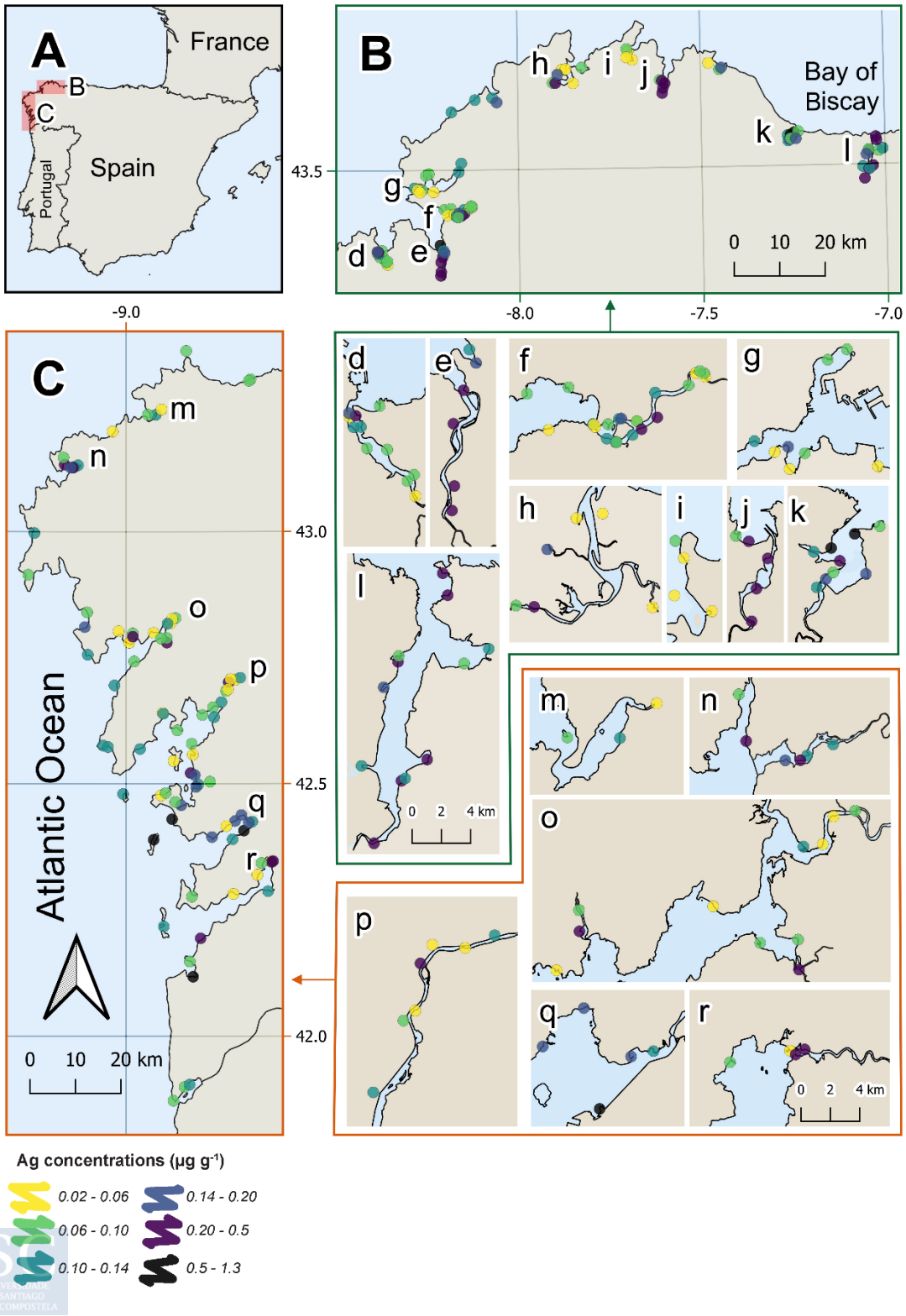

Fig. 2. Overview of Ag median concentrations (µg g^{-1}) in the sampling sites. Panels A-C display an overview of the region, with B and C showing the sampling sites. Panels d-l and m-r present detailed maps of sites that are densely clustered and difficult to distinguish in B and C, respectively.

Long-term trends in regional Ag concentrations were assessed using three complementary statistical approaches (Fig. 3): a) The Kruskal-Wallis non-parametric test, followed by Dunn's post-hoc analysis, was used to compare concentrations across sampling years (1990–2021). This approach did not account for spatial variability, as sampling sites differed annually. Results indicated significantly lower concentrations in 2021 compared to 1990, 2001, 2003, 2005, and 2007 ($p << 0.001$). Additionally, concentrations in 2007 were significantly reduced relative to 1990 ($p = 9.24 \times 10^{-6}$; Fig. 3A); b) For sites consistently sampled across 2001, 2003, 2005, 2007, and 2021, the Friedman test with Durbin-Conover post-hoc tests was applied. Accordingly with the previous analyses, this within-site analysis revealed significant decreases in 2021 compared to 2001, 2003, and 2005 ($p < 0.05$; Fig. 3B); c) The Wilcoxon signed-rank test was used to evaluate paired samples from sites surveyed in both 1990 and 2021. This confirmed significant reductions in Ag concentrations over the three-decade period ($p < 4.42 \times 10^{-17}$; Fig. 3C).

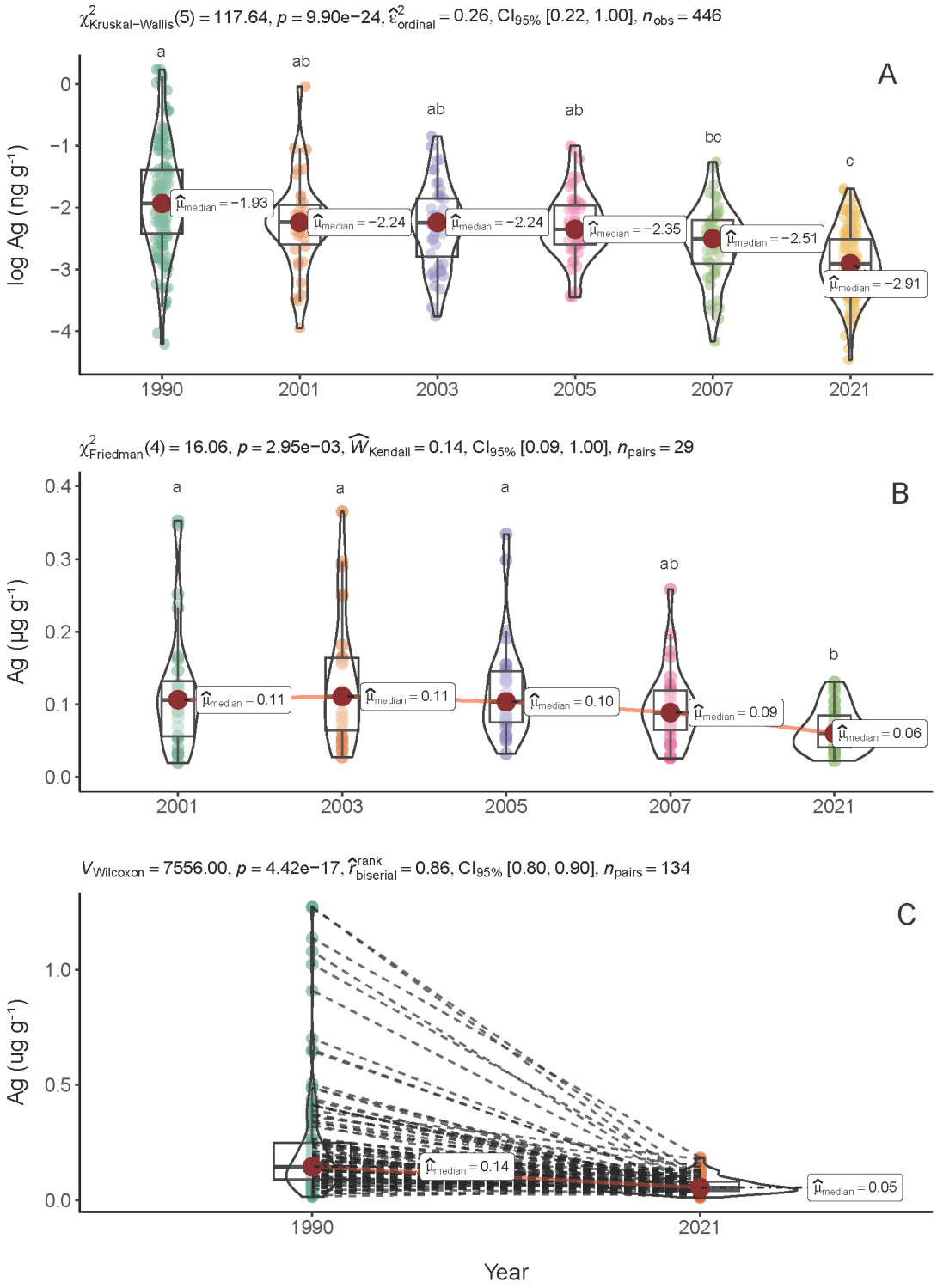

Fig. 3. Ag concentrations over time. Overview of Ag median concentrations (µg g -1) temporal trends: (A) Boxplots (logarithmic scale) with statistical summaries, with significance assessed using the Kruskal-Wallis test followed by Dunn's post-hoc analysis (B) Samples collected in the same site in 2001, 2003, 2005, 2007 and 2021 analysed by Friedman test and Durbin Conover post-hoc analysis, and C) paired samples from 1990 and 2021 analyzed by Wilcoxon paired test. Distinct lowercase letters indicate significant differences between years (no shared letters = significant).

Spatial mapping of percentage changes from the first to the last survey revealed widespread decreases in Ag concentration, with increases and stabilizations observed only at specific sites, primarily in the outer parts of the rias (Fig. 4). No consistent latitudinal pattern was observed. The overall percentage variation, calculated as the median of changes across all sites, showed a decrease of -58.1%.

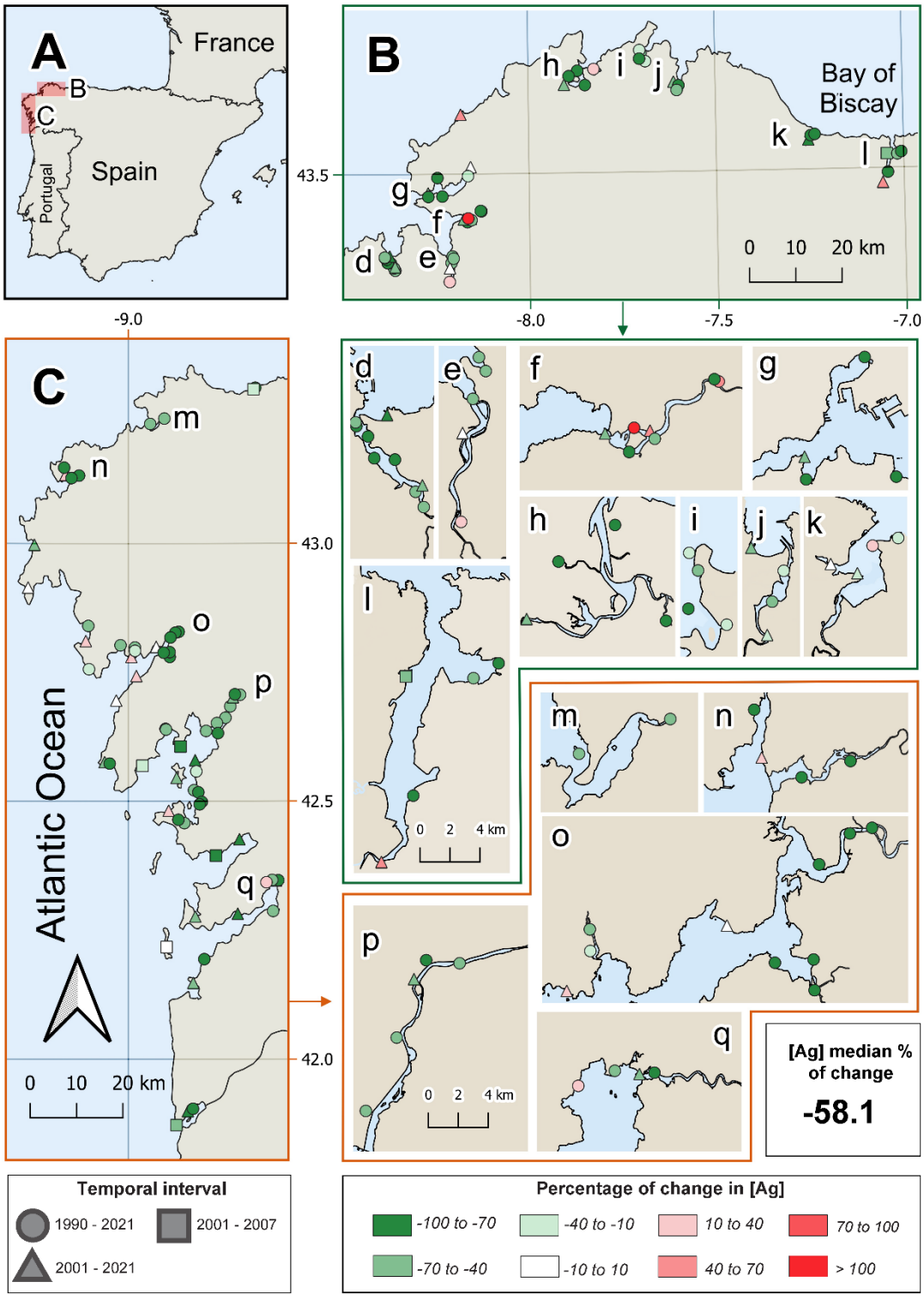

Fig. 4. Map of percentage changes in Ag concentrations over time. Panels A-C provide a regional overview, with B and C showing the differences between the final and initial Hg concentrations (in %) at each sampling station. Panels d-l and m-q offer detailed views of sampling sites that are densely clustered and hard to distinguish in B and C, respectively. Different colors represent the percentage changes in Ag concentrations, while distinct symbols indicate the sampling periods: 1990-2021, 2001-2021, and 2001-2007. The total median

percentage change, calculated as the median of the percentage changes across all sampling sites, is displayed below.

3.2. Ag nanoparticles

Median number of Ag nanoparticles was 3.07 x 10^7 g^{-1}, ranging from 1.75 x 10^6 to 1.81 x 10^8. Temporal evolution at each sampling site is shown in Fig. 5, with median nanoparticles g^{-1} of 7.89 x 10^7 in 1990, 1.98 x 10^7 in 2005, and 2.70 x 10^7 in 2021. ANOVA for repeated measures and pairwise t-tests confirmed significant decreases from 1990 to 2005 ($p = 0.009$) and from 1990 to 2021 ($p = 0.015$), while no significant differences were detected between 2005 and 2021, despite a slight increase can be observed. A significant positive correlation between Ag nanoparticles and Ag concentration was found ($p < 0.05$), with a Pearson correlation coefficient of 0.4017. The ionic form of Ag accounted for 75.7% to 98.8% of the total Ag mass, with a median of 95.1%, leaving only a small fraction attributable to Ag nanoparticles. The mean concentration of AgNPs was 6.28 ng g^{-1}, underscoring their relatively minor contribution to total Ag levels. Regarding AgNP sizes, the median diameter was 25 nm, with a non-normal distribution ranging from 12 to 204 nm. Although the model detected a statistically significant increase in diameter in 2021 compared to 1990, median values remained highly similar across years (25 and 26 nm in 1990 and 2021, respectively), suggesting that the observed difference is not ecologically meaningful (Fig. 6).

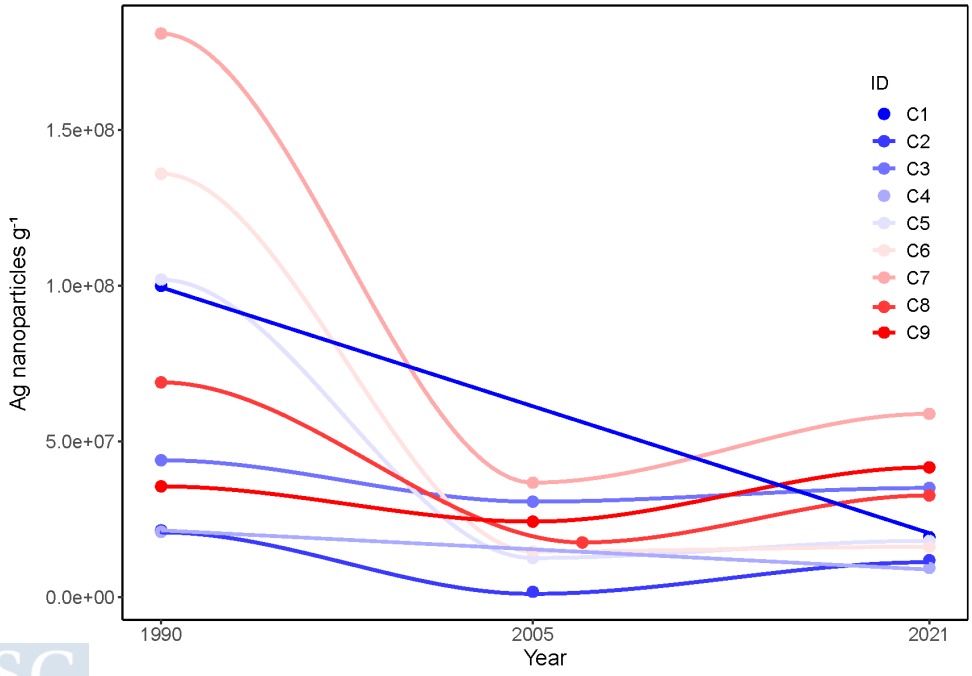

Fig. 5. Temporal evolution of Ag nanoparticle (AgNP) concentrations in *Fucus* spp. across sampling sites. The plot displays the number of AgNPs per gram (particles g^{-1}) for each site by year, with individual data points and LOESS smoothing lines colored by site ID. Colors follow a blue-to-red gradient based on the latitudinal position of each site, with more northern locations shown in deep blue tones and more southern locations in vivid red. Significant decreases in AgNP concentrations were observed between 1990 and both 2005 and 2021.

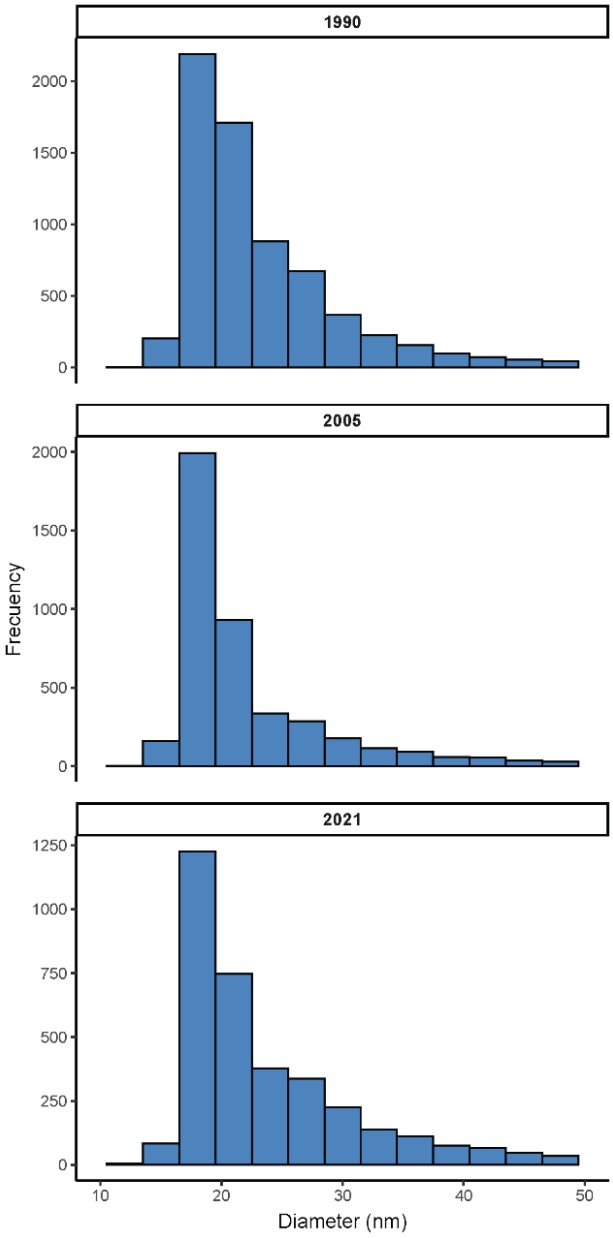

Fig. 6. Size distribution histograms of silver nanoparticles (AgNPs) for each sampling year (1990, 2005, and 2021). Each panel shows the frequency of AgNPs across diameter classes, highlighting temporal changes in particle size. Frequencies were weighted to account for differences in the number of replicates per sample.

3.3. Global Ag concentrations

The median global concentration of Ag in brown algae reported in the literature was 0.17 μg g^{-1} (dry weight), with values ranging from 0.01 to 190 μg g^{-1}. Although some extreme concentrations were observed, 97.5% of non-zero Ag values fall within a narrower range of 0.01 to 3.94 μg g^{-1}. No significant temporal trends were detected over the full period from 1952 to 2023 when considering all available data. However, by excluding two outlier studies reporting Ag concentrations between 20 and 190 μg g^{-1}, a significant decreasing trend emerged, beginning around the early 1980s (Fig. 7A). This pattern was also obtained when combining the literature data with the Ag concentrations measured in this study, revealing a serpentine but overall decreasing trend that started before 1980 and became especially pronounced from the 1990s onward (Fig. 7B).

Among the studied families, Fucaceae (n = 131) and Sargassaceae (n = 92) were the most extensively documented in the literature, with Fucaceae exhibiting significantly higher Ag concentrations ($p < 0.001$). However, when including the data generated in this study, this difference was no longer statistically significant, suggesting that the initial pattern may have been influenced by sampling bias or limited geographic or temporal coverage in previous studies.

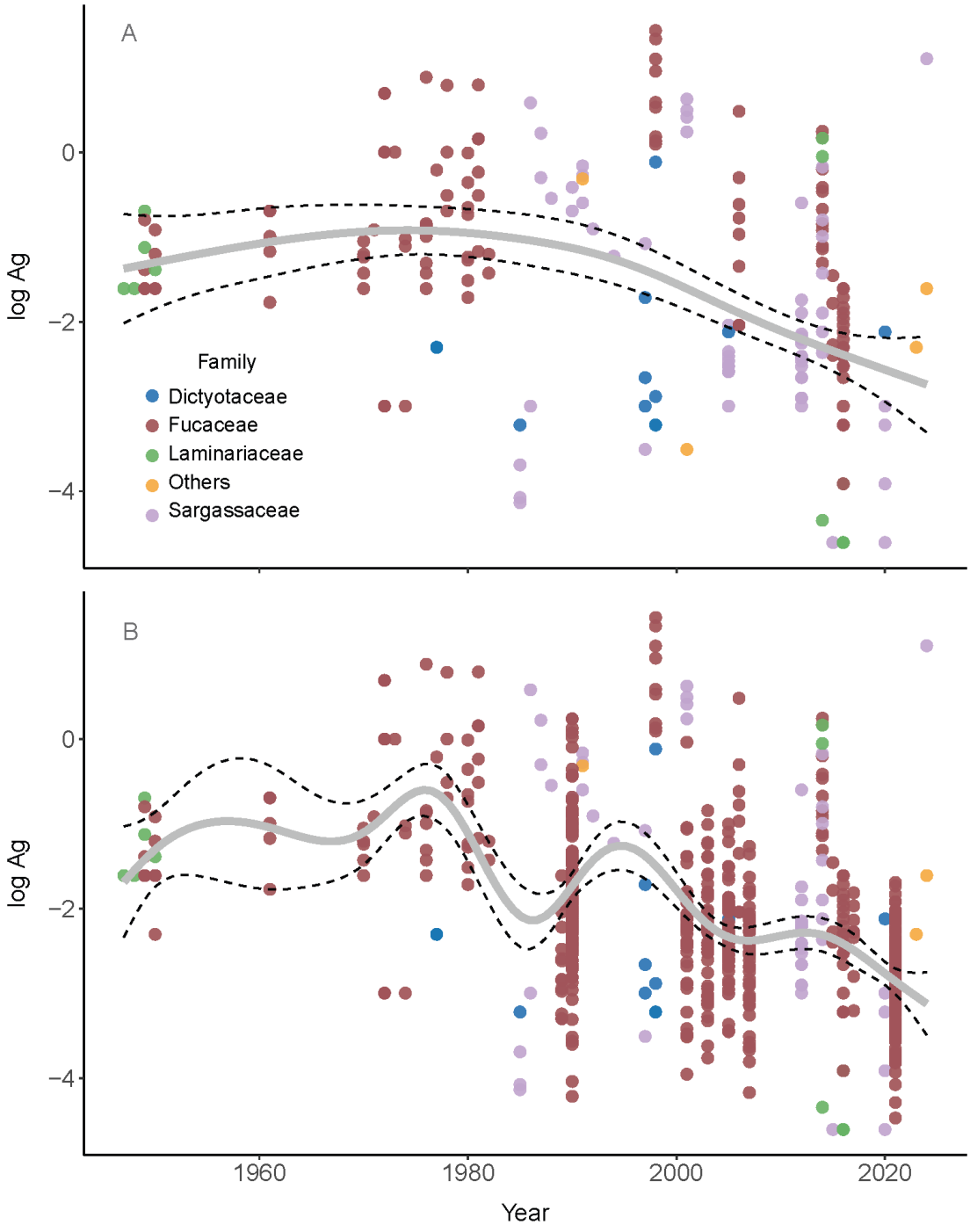

Fig. 7. Worldwide temporal trends in log-transformed Ag concentrations (µg g^{-1} DW) across different families of brown algae. The solid grey line represents the Generalized Additive Model (GAM) fit, while the dashed black lines indicate the 95% confidence interval limits. Data points are colored by family. Panel (a) shows the literature-based dataset excluding two outlier studies, while panel (b) includes the same filtered literature data combined with the Ag concentrations generated in the present study.

4. Discussion

4.2. Total Ag concentrations

Regional Ag concentrations in brown algae (median: 0.090 μg g^{-1}; range: 0.011–1.27 μg g^{-1}) were substantially lower than the global median (0.17 μg g^{-1}). Similarly, these concentrations were generally lower than those reported for other marine organisms such as mussels, crustaceans, corals, and bivalves (Asante et al., 2008; Lu et al., 2019, 2017), as well as for other algae and seagrasses (Ryabushko et al., 2024). This suggests that brown algae may either possess a lower capacity for silver accumulation or more effective mechanisms for metal regulation and excretion. No clear spatial trends were observed in relation to inner vs. outer ria zones or along a north–south gradient, implying that large-scale environmental drivers are not the main determinants of Ag distribution. Nevertheless, certain localized hotspots—specifically in rias e, j, and q in Fig. 2—showed consistently elevated Ag levels, likely due to localized point-source contamination, such as industrial discharges, urban runoff, or maritime activities in port areas. Importantly, even the highest concentrations recorded in these hotspots remain low in comparison to those found in brown algae from more heavily impacted coastal areas (Table 1SM) or in other marine organisms (Deheyn et al., 2005; Denton et al., 2006), reinforcing the conclusion that silver contamination in the study area is generally limited.

The absence of significant differences in Ag concentrations between outer ria species (*Fucus vesiculosus* - *F. spiralis*) and the inner ria species *F. ceranoides* contrasts with the clear spatial patterns observed for other Potentially Toxic Elements (PTEs) (Pacín et al., 2025). For example, metals such as Pb and Hg were consistently higher in *F. ceranoides*, likely due to greater sediment influence rather than intrinsic differences in bioaccumulation capacity among species (Barreiro et al., 2002; Carballeira et al., 2000). This discrepancy suggests that Ag may follow distinct biogeochemical pathways, with a comparatively weaker dependence on sedimentary inputs. Supporting this, weak to moderate negative correlations were observed between Ag and lithogenic tracers (Fe: $\rho = -0.108$, $p = 4.2 \times 10^{-6}$; Al: $\rho = -0.21$, $p = 0.021$), reinforcing the hypothesis that Ag is not primarily associated with particulate-bound phases. Instead, these relationships may indicate competitive interactions at algal binding sites or preferential assimilation of dissolved Ag species, such as free Ag^+ ions or small organic complexes, directly from the water column (Cleveland et al., 2012; Ramesh et al., 2015). This is consistent with the known geochemistry of Ag, which readily forms insoluble compounds (e.g., Ag_2S or Ag-organic complexes) in sediments, limiting its bioavailability unless redox conditions shift. In contrast, more bioavailable species like Ag^+ and $AgCl^-$ dominate in seawater (Barriada et al.,

2007; Cleveland et al., 2012; Ramesh et al., 2015; Tappin et al., 2010). Thus, even though the inner rias may receive higher Ag inputs from anthropogenic activities (Álvarez-Vázquez et al., 2020; Belzune-Segarra et al., 2008), this may be counterbalanced by lower Ag bioavailability due to complexation and precipitation processes.

Ag concentrations in brown macroalgae vary widely at the global scale (0.01–190 $\mu g\ g^{-1}$), though this range is largely driven by a few extreme outliers, with most values falling within a moderate interval (0.01 – 3.94 $\mu g\ g^{-1}$). In the literature-based dataset, Fucaceae showed significantly higher Ag concentrations than Sargassaceae ($p < 0.001$). However, this difference was not maintained when the dataset was expanded to include the Ag concentrations measured in this study, suggesting that the initially observed pattern may have been influenced by uneven sampling effort, limited spatial or temporal coverage, or other confounding factors. Nonetheless, biological explanations remain plausible, including the contrasting distribution of both families. Fucaceae are widespread in temperate Atlantic ecosystems and typically occupy intertidal zones (Bringloe et al., 2020; Neiva et al., 2016), where frequent exposure to air and water exchange increases contact with anthropogenic inputs. In contrast, Sargassaceae are more common in tropical and subtropical regions and usually inhabit subtidal areas (Bringloe et al., 2020; Yip et al., 2020). In addition, differences in alginate composition—particularly the higher density of carboxyl groups in Fucaceae—may enhance Ag binding and contribute to interspecific variability under certain conditions (McHugh., 2003; Haug et al., 1974; Rehm, 2009).

Silver uptake in brown algae appears to involve both passive adsorption to cell wall polysaccharides, such as fucoidans and alginates, and active or facilitated transport mechanisms (Ratte, 1999; Torres et al., 2005). Ag^{+} may mimic essential cations such as Cu^{+}, allowing it to enter cells via non-specific metal transporters (Clemens, 2006; Wu et al., 2009). While it is known that some elements, such as Pb, tend to remain adsorbed to the cell wall, and others, such as Co and Ni, are often internalized into the cytoplasm or organelles, elements like Cu and Zn have been reported in both compartments (Vázquez-Arias et al., 2024). The precise subcellular localization of Ag, however, remains unclear. Current techniques such as NanoSIMS and synchrotron-based X-ray fluorescence (XRF) do not yet allow for confident intracellular mapping of Ag in algal tissues, because of its low concentration in the tissues. Based on its chemical properties, such as its ionic radius and covalent index, Ag may behave similarly to Cu, exhibiting both surface retention and potential cytoplasmic translocation,

possibly accumulating in physodes or other cellular compartments (Catarino et al., 2018), although this remains to be confirmed.

4.2. Temporal trends in Ag concentrations

The regional dataset revealed a consistent long-term decline in Ag concentrations, with a median reduction of 58.1%. Statistical analyses employing three complementary approaches provided robust evidence for a significant decrease in Ag levels over the past three decades (Fig. 3). These findings are consistent with trends reported in both abiotic (Li et al., 2025; Squire et al., 2002) and biotic (Gunther et al., 1999; Lanceleur et al., 2011; Rainbow et al., 2011; Ramesh et al., 2015) environmental compartments.

This decline likely reflects broader environmental improvements, particularly the upgrade of wastewater treatment infrastructure (Araújo et al., 2019; Deycard et al., 2017; Flegal et al., 2007; Vane et al., 2020). The implementation of advanced treatment technologies between 1990 and 2010, including the construction of 21 WWTPs from 1990–2000 and an additional 34 facilities from 2000–2010 in the study area ("Censo Nacional de Vertidos (CNV)," n.d.; Pacín et al., 2025), could significantly enhanced Ag removal efficiencies, that have been reported to be higher than 80% (Deycard et al., 2017; Liu et al., 2022; Shafer et al., 1998). Concomitantly, the phase-out of Ag-based photographic processing and the introduction of stricter industrial discharge regulations may have contributed to reduced environmental Ag inputs (Council Directive, 1991; European Commission, 2000; European Environment Agency, 2008; European Parliament and the Council, 2006; Juncos et al., 2017).

At the global scale, our literature-based review also revealed a marked decrease in Ag concentrations beginning around 1980 (Fig. 7), which persisted through subsequent decades. This broader pattern is consistent with regional trends, indicating that the regional improvements observed in this study may be part of a broader, global pattern driven by enhanced Ag management practices.

Spatial mapping of temporal trends supports these interpretations, with most sites exhibiting declining Ag concentrations (Fig. 3). Notably, sites that presented the highest Ag concentrations experienced pronounced decreases (see rías e, j and q in Fig. 2 and Fig. 4), reinforcing the overall pattern of environmental recovery. In contrast, a few sites showed stabilization or slight

increases, primarily in outer ria areas. These localized anomalies may reflect specific point-source inputs or hydrodynamic conditions that favor contaminant accumulation.

4.3. AgNPs

The median concentration of AgNPs in brown algae (3.07×10^7 g^{-1}; 6.28 ng g^{-1}) lacks well-established baselines for marine biota, with only a few data reporting environmental AgNPs in marine organisms (Xu et al., 2020). Most available data derive from controlled exposure experiments, making field-based comparisons difficult (Scown et al., 2010; Sendra et al., 2017; Zuykov et al., 2011). Nonetheless, the values reported here fall within the range observed in marine sediments (Gottschalk et al., 2015; Zhao et al., 2021), exceed those typically found in seawater samples (Peters et al., 2018; Xu et al., 2020), and are comparable to the few values reported for other marine organisms such as mollusks (Xu et al., 2020).

The significant positive correlation between AgNP and total Ag concentrations ($r = 0.40$, $p < 0.05$), along with the observed temporal decline in AgNP levels from 1990 to both 2005 and 2021 (Fig. 5) mirroring the overall decrease in total Ag concentrations (Fig. 3), strongly suggest that AgNPs are primarily formed *in vivo* through algal-mediated reduction of ionic Ag^+, rather than through direct uptake of engineered nanoparticles from the environment. This interpretation is supported by the known redox activity of brown algal polyphenols, which when extracted and isolated, have been shown to reduce Ag^+ to elemental silver (Ag^0), enabling nanoparticle formation (Princy and Gopinath, 2021; Savitri et al., 2024). Furthermore, the rapid dissolution of engineered AgNPs in seawater, often within 24 hours (Mbanga et al., 2022; Sikder et al., 2018; Wimmer et al., 2020), makes it unlikely that the particles detected in algal tissues originate from persistent environmental sources.

The median diameter of AgNPs (25 nm) closely matches values reported for AgNPs synthesized using seaweed-derived compounds (El Shehawy et al., 2023; Fernandes et al., 2023; Princy and Gopinath, 2021), with the exception of one study in F. vesiculosus that found a larger average size (113.3 nm) (Savitri et al., 2024). While the size range overlaps with that of commercial AgNPs, which vary widely depending on formulation and use (Khorrami et al., 2018; Mostafa et al., 2022; Prabhu and Poulose, 2012), the relatively broad distribution observed here (12–204 nm) contrasts with the narrow size profiles typically reported for engineered nanoparticles. This variability, coupled with the absence of significant size shifts over time, further supports

the hypothesis of de novo formation within the algal matrix, rather than fluctuating inputs from external sources.

Altogether, these findings point to the ability of brown algae to act as active mediators in the transformation of dissolved Ag into nanoparticulate forms through physiologically and chemically controlled pathways. While previous studies have relied on algal extracts to synthesize AgNPs under laboratory conditions (Eka et al., 2024; Shanmuganathan et al., 2023), this is, to our knowledge, the first study providing direct evidence of *in situ* AgNP formation within brown algal tissues in the natural environment.

The observed temporal decline in AgNP concentrations is likely attributable to improved wastewater treatment infrastructure and stricter emission regulations implemented in recent decades (Kaegi et al., 2011; Vilela et al., 2018). However, a slight, non-significant rebound in AgNPs was observed in 2021 (Fig. 5), potentially reflecting increased use of AgNP-containing consumer products (Courtois et al., 2019; Sati et al., 2025). Although AgNPs accounted for less than 5% of total Ag content in *Fucus*, suggesting a potentially limited immediate ecological relevance, their potential for biomagnification (Babaei et al., 2022) warrants continued monitoring.

4.4. Limitations and future research

This study faced several key limitations that should be considered in future research. One of the main constraints is the lack of standardized protocols for detecting and quantifying AgNPs in marine compartments. Existing studies employ divergent methods, ranging from digestion protocols to detection limits and analytical techniques, hindering meaningful cross-study comparisons and the development of consistent monitoring frameworks (Le Viet et al., 2025; López-Mayán et al., 2022; Xu et al., 2020). In addition, the absence of certified reference materials for Ag or AgNPs in *Fucus* or similar marine organisms limits method validation and reduces confidence in absolute concentration values.

The quantification of AgNPs in the present study also presented considerable variability (coefficient of variation > 30%), reflecting both the inherent analytical challenges of detecting particulate forms and the limitations of current methods. This is further complicated by the assumption of spherical particle shape for estimation purposes. This simplification, while common, overlooks the fact that nanoparticle morphology can vary considerably and influence

both reactivity and toxicity (Carnovale et al., 2019; Kinnear et al., 2017). Although we were able to quantify both total Ag and its nanoparticulate fraction, we lacked detailed speciation data, such as the presence of organo-complexed or sulfurized forms, which are crucial for understanding Ag's bioavailability and ecological behavior.

Another important limitation is the absence of direct ultrastructural or chemical evidence, such as transmission electron microscopy (TEM), to confirm the formation of AgNPs within algal tissues. While the biochemical context strongly suggests *in vivo* formation, future studies employing these advanced techniques will be essential to conclusively determine the origin of AgNPs in seaweeds. Moreover, the potential effects of global change should not be overlooked: warming, acidification, and altered nutrient regimes may affect algal physiology and Ag bioavailability, with unknown consequences for AgNP formation and toxicity (Fabrega et al., 2011; Rainbow et al., 2011; Yang et al., 2024).

Additionally, a significant challenge in assessing AgNP impact is the scarcity of comparable and representative data, particularly for marine ecosystems. Most available measurements are derived from freshwater systems or controlled laboratory studies, with little to no field data on AgNP concentrations in marine organisms. As a result, there are no established baseline levels for AgNPs in marine biota, making it difficult to determine whether observed values are typical, elevated, or anomalous. This data gap is especially problematic for regulation: while benchmarks exist for freshwater and drinking water (e.g., U.S. EPA guideline of 0.1 $\mu g\ L^{-1}$ for Ag), there are no marine-specific standards, hindering both ecological risk interpretation and the development of effective management and mitigation strategies (McGillicuddy et al., 2017).

5. Conclusions

This study provides the first comprehensive, multi-decadal assessment of Ag and Ag nanoparticle (AgNP) concentrations in *Fucus* spp. In parallel, it offers a global review of Ag concentrations in brown algae and establishes a field-based baseline for AgNP levels in seaweeds. The global review provides broad geographic coverage, albeit with lower analytical resolution and methodological heterogeneity. In contrast, the regional dataset combines a large number of well-characterized samples with standardized Ag analyses, offering high resolution over a more limited geographic area. Together, these complementary approaches provide a robust framework for understanding both global patterns and local dynamics of Ag pollution in marine ecosystems. Notably, this is also the first study to detect AgNPs directly in brown algal

tissues collected from the environment and to present evidence that their formation may occur naturally rather than solely through the action of isolated algal extracts, as shown in previous laboratory-based studies.

Despite interspecific and geographic variability, both the regional dataset and the global literature review revealed a consistent temporal decline in total Ag concentrations. AgNP concentrations similarly decreased over time and showed a significant positive correlation with total Ag, supporting the hypothesis that AgNPs are primarily formed *in situ* through algal-mediated reduction of ionic Ag, rather than through direct uptake of engineered nanoparticles from the environment. Although AgNPs represented less than 5% of total Ag content, suggesting limited ecological relevance in this system, their potential for biomagnification, combined with increasing commercial use and the lack of regulatory baselines in marine environments, underscores the need for caution. Given current knowledge gaps, especially regarding AgNP behavior and occurrence in the environment, it is premature to dismiss their environmental impact.

To address these uncertainties, long-term monitoring efforts will be essential. Such efforts will provide critical data to detect emerging trends and support the development of evidence-based strategies for managing nanomaterial pollution in marine ecosystems.

References

Aboal, J.R., Pacín, C., García-Seoane, R., Varela, Z., González, A.G., Fernández, J.A., 2023. Global decrease in heavy metal concentrations in brown algae in the last 90 years. J Hazard Mater 445, 130511. https://doi.org/10.1016/J.JHAZMAT.2022.130511

Agencia Estatal de Meteorología, n.d. Mapas climáticos de España y ETo. https://www.aemet.es/gl/conocermas/recursos_en_linea/publicaciones_y_estudios/publicaciones/detalles/MapasclimaticosdeEspana (accessed 5.22.25).

Álvarez-Vázquez, M.A., Álvarez-Iglesias, P., De Uña-Álvarez, E., Quintana, B., Caetano, M., Prego, R., 2020. Industrial supply of trace elements during the “Anthropocene”: A record in estuarine sediments from the Ria of Ferrol (NW Iberian Peninsula). Mar Chem 223, 103825. https://doi.org/10.1016/J.MARCHEM.2020.103825

Araújo, D.F., Ponzevera, E., Briant, N., Knoery, J., Sireau, T., Mojtahid, M., Metzger, E., Brach-Papa, C., 2019. Assessment of the metal contamination evolution in the Loire estuary using Cu

and Zn stable isotopes and geochemical data in sediments. Mar Pollut Bull 143, 12–23. https://doi.org/10.1016/J.MARPOLBUL.2019.04.034

Asante, K.A., Agusa, T., Mochizuki, H., Ramu, K., Inoue, S., Kubodera, T., Takahashi, S., Subramanian, A., Tanabe, S., 2008. Trace elements and stable isotopes (δ13C and δ15N) in shallow and deep-water organisms from the East China Sea. Environmental Pollution 156, 862–873. https://doi.org/10.1016/J.ENVPOL.2008.05.020

Babaei, M., Tayemeh, M.B., Jo, M.S., Yu, I.J., Johari, S.A., 2022. Trophic transfer and toxicity of silver nanoparticles along a phytoplankton-zooplankton-fish food chain. Science of The Total Environment 842, 156807. https://doi.org/10.1016/J.SCITOTENV.2022.156807

Banu, A.N., Kudesia, N., Raut, A.M., Pakrudheen, I., Wahengbam, J., 2021. Toxicity, bioaccumulation, and transformation of silver nanoparticles in aqua biota: a review. Environmental Chemistry Letters 2021 19:6 19, 4275–4296. https://doi.org/10.1007/S10311-021-01304-W

Barreiro, R., Picado, L., Real, C., 2002. Biomonitoring Heavy Metals in Estuaries: A Field Comparison of Two Brown Algae Species Inhabiting Upper Estuarine Reaches. Environmental Monitoring and Assessment 2002 75:2 75, 121–134. https://doi.org/10.1023/A:1014479612811

Barriada, J.L., Tappin, A.D., Evans, E.H., Achterberg, E.P., 2007. Dissolved silver measurements in seawater. TrAC Trends in Analytical Chemistry 26, 809–817. https://doi.org/10.1016/J.TRAC.2007.06.004

Beck, A.J., Cochran, J.K., Sañudo-Wilhelmy, S.A., 2009. Temporal trends of dissolved trace metals in jamaica bay, ny: Importance of wastewater input and submarine groundwater discharge in an urban estuary. Estuaries and Coasts 32, 535–550. https://doi.org/10.1007/S12237-009-9140-5/TABLES/2

Behera, M., Behera, P.R., Sethi, G., Pradhan, B., Adarsh, V., Alkilayh, O.A., Samantaray, D.P., Singh, L., 2024. Cyanobacterial Silver Nanoparticles and Their Potential Utility—Recent Progress and Prospects: A Review. J Basic Microbiol 64, e2400256. https://doi.org/10.1002/JOBM.202400256

Belzunce, M.J., Prego, R., Wilson, M.J., Bacon, J., Santos-Echeandía, J., 2008. Metal speciation in surface sediments of the Vigo Ria (NW Iberian Peninsula). Sci. mar. 72(1), 119-26.

Bringloe, T.T., Starko, S., Wade, R.M., Vieira, C., Kawai, H., De Clerck, O., Cock, J.M., Coelho, S.M., Destombe, C., Valero, M., Neiva, J., Pearson, G.A., Faugeron, S., Serrão, E.A., Verbruggen, H., 2020. Phylogeny and Evolution of the Brown Algae. CRC Crit Rev Plant Sci 39, 281–321. https://doi.org/10.1080/07352689.2020.1787679

Bryan, G.W., 1971. The effects of heavy metals (other than mercury) on marine and estuarine organisms. Proc R Soc Lond B Biol Sci 177, 389–410. https://doi.org/10.1098/rspb.1971.0037

Carballeira, A., Carral, E., Puente, X., Villares, R., 2000. Regional-scale monitoring of coastal contamination. Nutrients and heavy metals in estuarine sediments and organisms on the coast of Galicia (northwest Spain). Int J Environ Pollut 13, 534. https://doi.org/10.1504/IJEP.2000.002333

Carnovale, C., Bryant, G., Shukla, R., Bansal, V., 2019. Identifying Trends in Gold Nanoparticle Toxicity and Uptake: Size, Shape, Capping Ligand, and Biological Corona. ACS Omega 4, 242–256. https://doi.org/10.1021/ACSOMEGA.8B03227

Catarino, M.D., Silva, A.M.S., Cardoso, S.M., 2018. Phycochemical Constituents and Biological Activities of Fucus spp. Marine Drugs 2018, Vol. 16, Page 249 16, 249. https://doi.org/10.3390/MD16080249

Censo Nacional de Vertidos (CNV). https://www.miteco.gob.es/es/cartografia-y-sig/ide/descargas/agua/censo-nacional-vertidos.html

Clemens, S., 2006. Toxic metal accumulation, responses to exposure and mechanisms of tolerance in plants. Biochimie 88, 1707–1719. https://doi.org/10.1016/J.BIOCHI.2006.07.003

Cleveland, D., Long, S.E., Pennington, P.L., Cooper, E., Fulton, M.H., Scott, G.I., Brewer, T., Davis, J., Petersen, E.J., Wood, L., 2012. Pilot estuarine mesocosm study on the environmental fate of Silver nanomaterials leached from consumer products. Science of The Total Environment 421–422, 267–272. https://doi.org/10.1016/J.SCITOTENV.2012.01.025

Council Directive, 1991. Urban Wastewater Treatment Directive (91/271/EEC).

Courtois, P., Rorat, A., Lemiere, S., Guyoneaud, R., Attard, E., Levard, C., Vandenbulcke, F., 2019. Ecotoxicology of silver nanoparticles and their derivatives introduced in soil with or without sewage sludge: A review of effects on microorganisms, plants and animals. Environmental Pollution 253, 578–598. https://doi.org/10.1016/J.ENVPOL.2019.07.053

Deheyn, D.D., Gendreau, P., Baldwin, R.J., Latz, M.I., 2005. Evidence for enhanced bioavailability of trace elements in the marine ecosystem of Deception Island, a volcano in Antarctica. Mar Environ Res 60, 1–33. https://doi.org/10.1016/J.MARENVRES.2004.08.001

Denton, G.R.W., Concepcion, L.P., Wood, H.R., Morrison, R.J., 2006. Trace metals in marine organisms from four harbours in Guam. Mar Pollut Bull 52, 1784–1804. https://doi.org/10.1016/J.MARPOLBUL.2006.09.010

Deycard, V.N., Schäfer, J., Petit, J.C.J., Coynel, A., Lanceleur, L., Dutruch, L., Bossy, C., Ventura, A., Blanc, G., 2017. Inputs, dynamics and potential impacts of silver (Ag) from urban wastewater to a highly turbid estuary (SW France). Chemosphere 167, 501–511. https://doi.org/10.1016/J.CHEMOSPHERE.2016.09.154

Dobias, J., Bernier-Latmani, R., 2013. Silver release from silver nanoparticles in natural waters. Environ Sci Technol 47, 4140–4146. https://doi.org/10.1021/ES304023P/

Eka, E., Willian, N., Fitriani, R., 2024. Silver nanoparticles (NPAg) using padina australis seaweed. BIO Web Conf 134, 01009. https://doi.org/10.1051/BIOCONF/202413401009

El Shehawy, A.S., Elsayed, A., El-Shehaby, O.A., Ali, E.M., 2023. Potentiality of the green synthesized silver nanoparticles for heavy metal removal using Laurencia papillosa seaweed. Egypt J Aquat Res 49, 513–519. https://doi.org/10.1016/J.EJAR.2023.10.001

European Commission, 2000. Water Framework Directive (2000/60/EC).

European Environment Agency, 2008. Marine Strategy Framework Directive 2008/56/EC.

European Parliament and the Council, 2006. Directive on pollution caused by certain dangerous substances discharged into the aquatic environment of the Community - 2006/11.

Fabrega, J., Luoma, S.N., Tyler, C.R., Galloway, T.S., Lead, J.R., 2011. Silver nanoparticles: Behaviour and effects in the aquatic environment. Environ Int 37, 517–531. https://doi.org/10.1016/J.ENVINT.2010.10.012

Fernandes, M., González-Ballesteros, N., da Costa, A., Machado, R., Gomes, A.C., Rodríguez-Argüelles, M.C., 2023. Antimicrobial and anti-biofilm activity of silver nanoparticles biosynthesized with Cystoseira algae extracts. Journal of Biological Inorganic Chemistry 28, 439–450. https://doi.org/10.1007/S00775-023-01999-Y

Flegal, A.R., Brown, C.L., Squire, S., Ross, J.R.M., Scelfo, G.M., Hibdon, S., 2007. Spatial and temporal variations in silver contamination and toxicity in San Francisco Bay. Environ Res 105, 34–52. https://doi.org/10.1016/J.ENVRES.2007.05.006

Gambardella, C., Costa, E., Piazza, V., Fabbrocini, A., Magi, E., Faimali, M., Garaventa, F., 2015. Effect of silver nanoparticles on marine organisms belonging to different trophic levels. Mar Environ Res 111, 41–49. https://doi.org/10.1016/J.MARENVRES.2015.06.001

García-Alonso, J., Rodriguez-Sanchez, N., Misra, S.K., Valsami-Jones, E., Croteau, M.N., Luoma, S.N., Rainbow, P.S., 2014. Toxicity and accumulation of silver nanoparticles during development of the marine polychaete Platynereis dumerilii. Science of The Total Environment 476–477, 688–695. https://doi.org/10.1016/J.SCITOTENV.2014.01.039

García-Seoane, R., Fernández, J.A., Villares, R., Aboal, J.R., 2018. Use of macroalgae to biomonitor pollutants in coastal waters: Optimization of the methodology. Ecol Indic. https://doi.org/10.1016/j.ecolind.2017.09.015

Gottschalk, F., Lassen, C., Kjoelholt, J., Christensen, F., Nowack, B., 2015. Modeling Flows and Concentrations of Nine Engineered Nanomaterials in the Danish Environment. International Journal of Environmental Research and Public Health 2015, Vol. 12, Pages 5581-5602 12, 5581–5602. https://doi.org/10.3390/IJERPH120505581

Gunther, A.J., Davis, J.A., Hardin, D.D., Gold, J., Bell, D., Crick, J.R., Scelfo, G.M., Sericano, J., Stephenson, M., 1999. Long-term Bioaccumulation Monitoring with Transplanted Bivalves in the San Francisco Estuary. Mar Pollut Bull 38, 170–181. https://doi.org/10.1016/S0025-326X(98)00185-4

H. Wickham., 2016. ggplot2: Elegant Graphics for Data Analysis. Springer-Verlag, New York.

Haug, A., Larsen, B., Smidsrød, O., 1974. Uronic acid sequence in alginate from different sources. Carbohydr Res 32, 217–225. https://doi.org/10.1016/S0008-6215(00)82100-X

Johnstone, K.M., Rainbow, P.S., Clark, P.F., Smith, B.D., Morritt, D., 2016. Trace metal bioavailabilities in the Thames estuary: continuing decline in the 21st century. Journal of the Marine Biological Association of the United Kingdom 96, 205–216. https://doi.org/10.1017/S0025315415001952

Juncos, R., Campbell, L., Arcagni, M., Daga, R., Rizzo, A., Arribére, M., Ribeiro Guevara, S., 2017. Variations in anthropogenic silver in a large Patagonian lake correlate with global shifts in photographic processing technology. Environmental Pollution 223, 685–694. https://doi.org/10.1016/J.ENVPOL.2017.02.003

Kaegi, R., Voegelin, A., Sinnet, B., Zuleeg, S., Hagendorfer, H., Burkhardt, M., Siegrist, H., 2011. Behavior of metallic silver nanoparticles in a pilot wastewater treatment plant. Environ Sci Technol 45, 3902–3908. https://doi.org/10.1021/ES1041892

Khorrami, S., Zarrabi, A., Khaleghi, M., Danaei, M., Mozafari, M.R., 2018. Selective cytotoxicity of green synthesized silver nanoparticles against the MCF-7 tumor cell line and their enhanced antioxidant and antimicrobial properties. Int J Nanomedicine 13, 8013–8024. https://doi.org/10.2147/IJN.S189295

Kinnear, C., Moore, T.L., Rodriguez-Lorenzo, L., Rothen-Rutishauser, B., Petri-Fink, A., 2017. Form Follows Function: Nanoparticle Shape and Its Implications for Nanomedicine. Chem Rev 117, 11476–11521. https://doi.org/10.1021/ACS.CHEMREV.7B00194

Lanceleur, L., Schäfer, J., Chiffoleau, J.F., Blanc, G., Auger, D., Renault, S., Baudrimont, M., Audry, S., 2011. Long-term records of cadmium and silver contamination in sediments and oysters from the Gironde fluvial–estuarine continuum – Evidence of changing silver sources. Chemosphere 85, 1299–1305. https://doi.org/10.1016/J.CHEMOSPHERE.2011.07.036

Le Viet, H., Miyamaru, H., Nguyen Quang, H., 2025. The use of low-energy particle-induced X-ray emission for evaluation of colloidal silver nanoparticles in aqueous solution. Radiation Physics and Chemistry 234, 112797. https://doi.org/10.1016/J.RADPHYSCHEM.2025.112797

Li, A., Boardwine, A.J., Hoang, T.C., 2025. Metals in sediment of the lower Great Lakes and region-wide discoveries. J Hazard Mater 487, 137099. https://doi.org/10.1016/J.JHAZMAT.2025.137099

Liu, Y., Li, F., Li, H., Tong, Y., Li, W., Xiong, J., You, J., 2022. Bioassay-based identification and removal of target and suspect toxicants in municipal wastewater: Impacts of chemical properties and transformation. J Hazard Mater 437, 129426. https://doi.org/10.1016/J.JHAZMAT.2022.129426

López-Mayán, J.J., Álvarez-Fernández, B., Peña-Vázquez, E., Barciela-Alonso, M.C., Moreda-Piñeiro, A., Bermejo-Barrera, P., 2022. Ultrasonication followed by enzymatic hydrolysis as a sample pre-treatment for the determination of Ag nanoparticles in edible seaweed by SP-ICP-MS. Talanta 247, 123556. https://doi.org/10.1016/J.TALANTA.2022.123556

Lu, G., Pan, K., Zhu, A., Dong, Y., Wang, W.X., 2020. Spatial-temporal variations and trends predication of trace metals in oysters from the Pearl River Estuary of China during 2011–2018. Environmental Pollution 264, 114812. https://doi.org/10.1016/J.ENVPOL.2020.114812

Lu, G., Zhu, A., Fang, H., Dong, Y., Wang, W.X., 2019. Establishing baseline trace metals in marine bivalves in China and worldwide: Meta-analysis and modeling approach. Science of The Total Environment 669, 746–753. https://doi.org/10.1016/J.SCITOTENV.2019.03.164

Lu, G.Y., Ke, C.H., Zhu, A., Wang, W.X., 2017. Oyster-based national mapping of trace metals pollution in the Chinese coastal waters. Environmental Pollution 224, 658–669. https://doi.org/10.1016/J.ENVPOL.2017.02.049

Luo, M., Hou, X., He, C., Liu, Q., Fan, Y., 2013. Speciation analysis of 129I in seawater by carrier-free AgI-AgCl coprecipitation and accelerator mass spectrometric measurement. Anal Chem 85, 3715–3722. https://doi.org/10.1021/AC400060Q

Mbanga, O., Cukrowska, E., Gulumian, M., 2022. Dissolution kinetics of silver nanoparticles: Behaviour in simulated biological fluids and synthetic environmental media. Toxicol Rep 9, 788–796. https://doi.org/10.1016/J.TOXREP.2022.03.044

McGillicuddy, E., Murray, I., Kavanagh, S., Morrison, L., Fogarty, A., Cormican, M., Dockery, P., Prendergast, M., Rowan, N., Morris, D., 2017. Silver nanoparticles in the environment: Sources, detection and ecotoxicology. Science of The Total Environment 575, 231–246. https://doi.org/10.1016/J.SCITOTENV.2016.10.041

MchHugh, D.J., 2003. A guide to the seaweed industry**.** FOOD AND AGRICULTURE ORGANIZATION OF THE UNITED NATIONS. https://www.fao.org/4/y4765e/y4765e00.htm

McGillycuddy, M., Warton, D.I., Popovic, G., Bolker, B.M., 2025. Parsimoniously Fitting Large Multivariate Random Effects in glmmTMB. J Stat Softw 112. https://doi.org/10.18637/jss.v112.i01

Miao, A.J., Schwehr, K.A., Xu, C., Zhang, S.J., Luo, Z., Quigg, A., Santschi, P.H., 2009. The algal toxicity of silver engineered nanoparticles and detoxification by exopolymeric substances. Environmental Pollution 157, 3034–3041. https://doi.org/10.1016/J.ENVPOL.2009.05.047

Miller, L.A., Bruland, K.W., 1995. Organic Speciation of Silver in Marine Waters. Environ Sci Technol 29, 2616–2621. https://doi.org/10.1021/ES00010A024/

Mostafa, M., Kandile, N.G., Mahmoud, M.K., Ibrahim, H.M., 2022. Synthesis and characterization of polystyrene with embedded silver nanoparticle nanofibers to utilize as antibacterial and wound healing biomaterial. Heliyon 8, e08772. https://doi.org/10.1016/J.HELIYON.2022.E08772

Neiva, J., Serrão, E.A., Assis, J., Pearson, G.A., Coyer, J.A., Olsen, J.L., Hoarau, G., Valero, M., 2016. Climate Oscillations, Range Shifts and Phylogeographic Patterns of North Atlantic Fucaceae. Seaweed Phylogeography: Adaptation and Evolution of Seaweeds under Environmental Change 279–308. https://doi.org/10.1007/978-94-017-7534-2_11

Ohanian, T., Phillips, N., 2013. Digital filmmaking: The changing art and craft of making motion pictures, Second edition. Digital Filmmaking: The Changing Art and Craft of Making Motion Pictures 1–308. https://doi.org/10.4324/9780080504407

Pacín, C., Fernández, J.A., Conde-Amboage, M., Lazzari, M., García-Seoane, R., Viana, I.G., Varela, Z., Real, C., Villares, R., Aboal, J.R., 2025. Three Decades of Change in Potentially Toxic Elements in Brown Algae in the Northeast Atlantic Ocean. Environ Sci Technol. https://doi.org/10.1021/acs.est.4c14013

Patil, I., 2021. Visualizations with statistical details: The "ggstatsplot" approach. J Open Source Softw 6, 3167. https://doi.org/10.21105/joss.03167

Peng, Z., Guo, Z., Wang, Z., Zhang, R., Wu, Q., Gao, H., Wang, Y., Shen, Z., Lek, S., Xiao, J., 2022. Species-specific bioaccumulation and health risk assessment of heavy metal in seaweeds in tropic coasts of South China Sea. Science of The Total Environment 832, 155031. https://doi.org/10.1016/J.SCITOTENV.2022.155031

Peters, R.J.B., van Bemmel, G., Milani, N.B.L., den Hertog, G.C.T., Undas, A.K., van der Lee, M., Bouwmeester, H., 2018. Detection of nanoparticles in Dutch surface waters. Science of The Total Environment 621, 210–218. https://doi.org/10.1016/J.SCITOTENV.2017.11.238

Prabhu, S., Poulose, E.K., 2012. Silver nanoparticles: mechanism of antimicrobial action, synthesis, medical applications, and toxicity effects. International Nano Letters 2012 2:1 2, 1–10. https://doi.org/10.1186/2228-5326-2-32

Princy, K.F., Gopinath, A., 2021. Green synthesis of silver nanoparticles using polar seaweed Fucus gardeneri and its catalytic efficacy in the reduction of nitrophenol. Polar Sci 30, 100692. https://doi.org/10.1016/J.POLAR.2021.100692

PRTR España, n.d. Registro Estatal de Emisiones y Fuentes Contaminantes [WWW Document].

QGIS Development Team, 2024., 2024. QGIS Geographic Information System, Version 3.36.3.

R Core Team, 2024. R: A language and environment for statistical computing, Version 4.4.1. R Foundation for Statistical.

Rainbow, P.S., Kriefman, S., Smith, B.D., Luoma, S.N., 2011. Have the bioavailabilities of trace metals to a suite of biomonitors changed over three decades in SW England estuaries historically affected by mining? Science of The Total Environment 409, 1589–1602. https://doi.org/10.1016/J.SCITOTENV.2011.01.012

Ramesh, K., Berry, S., Brown, M.T., 2015. Accumulation of silver by Fucus spp. (Phaeophyceae) and its toxicity to Fucus ceranoides under different salinity regimes. Ecotoxicology 24, 1250–1258. https://doi.org/10.1007/S10646-015-1495-8/

Ranville, Mara A, Flegal, A Russell, Ranville, M A, Flegal, A R, 2005. Silver in the North Pacific Ocean. Geochemistry, Geophysics, Geosystems 6, 3–4. https://doi.org/10.1029/2004GC000770

Ratte, H.T., 1999. Bioaccumulation and toxicity of silver compounds: A review. Environ Toxicol Chem 18, 89–108. https://doi.org/10.1002/ETC.5620180112

Rehm, B.H.A. (Ed.), 2009. Alginates: Biology and Applications. Microbiology Monographs 13. https://doi.org/10.1007/978-3-540-92679-5

Romaní, J.R.V., 2023. Introduction to the Geology of Galicia. The Environment in Galicia: A Book of Images: Galician Environment Through Images 21–35. https://doi.org/10.1007/978-3-031-33114-5_3

Rong, H., Garg, S., Waite, T.D., 2018. Transformation of AgCl Particles under Conditions Typical of Natural Waters: Implications for Oxidant Generation. Environ Sci Technol 52, 11621–11631. https://doi.org/10.1021/ACS.EST.8B02902

Ryabushko, V.I., Gureeva, E. V., Kapranov, S. V., Prazukin, A. V., Toichkin, A.M., Simokon, M. V., Bobko, N.I., 2024. Element composition of several marine macrophytes (Crimea, Black Sea) and correlations with the element abundances in sediments and seawater. Environ Res 257, 119380. https://doi.org/10.1016/J.ENVRES.2024.119380

Sañudo-Wllhelmy, S.A., Flegalf, R., 1992. Anthropogenic Silver in The Southern California Bight: A New Tracer of Sewage in Coastal Waters. Environ Sci Technol 26, 2147–2151. https://doi.org/10.1021/ES00035A012/

Sati, A., Ranade, T.N., Mali, S.N., Ahmad Yasin, H.K., Pratap, A., 2025. Silver Nanoparticles (AgNPs): Comprehensive Insights into Bio/Synthesis, Key Influencing Factors, Multifaceted Applications, and Toxicity─A 2024 Update. ACS Omega. https://doi.org/10.1021/ACSOMEGA.4C11045/

Savitri, E.S., Rahmawaty, A.E., Minarno, E.B., 2024. Antioxidant, anti-collagenase, and antibacterial activities of Fucus vesiculosus silver nanoparticles. Narra J 4, e882–e882. https://doi.org/10.52225/NARRA.V4I3.882

Scown, T.M., Santos, E.M., Johnston, B.D., Gaiser, B., Baalousha, M., Mitov, S., Lead, J.R., Stone, V., Fernandes, T.F., Jepson, M., van Aerle, R., Tyler, C.R., 2010. Effects of Aqueous Exposure to Silver Nanoparticles of Different Sizes in Rainbow Trout. Toxicological Sciences 115, 521–534. https://doi.org/10.1093/TOXSCI/KFQ076

Secondary Drinking Water Standards: Guidance for Nuisance Chemicals. US EPA, 2025. URL https://www.epa.gov/sdwa/secondary-drinking-water-standards-guidance-nuisance-chemicals (accessed 6.12.25).

Sendra, M., Yeste, M.P., Gatica, J.M., Moreno-Garrido, I., Blasco, J., 2017. Direct and indirect effects of silver nanoparticles on freshwater and marine microalgae (Chlamydomonas reinhardtii and Phaeodactylum tricornutum). Chemosphere 179, 279–289. https://doi.org/10.1016/J.CHEMOSPHERE.2017.03.123

Shafer, M.M., Overdier, J.T., Armstong, D.E., 1998. Removal, partitioning, and fate of silver and other metals in wastewater treatment plants and effluent-receiving streams. Environ Toxicol Chem 17, 630–641. https://doi.org/10.1897/1551-5028(1998)017

Shanmuganathan, R., Brindhadevi, K., Al-Ansari, M.M., Al-Humaid, L., Barathi, S., Lee, J., 2023. In vitro investigation of silver nanoparticles synthesized using Gracilaria veruccosa – A seaweed against multidrug resistant Staphylococcusaureus. Environ Res 227, 115782. https://doi.org/10.1016/J.ENVRES.2023.115782

Sikder, M., Lead, J.R., Chandler, G.T., Baalousha, M., 2018. A rapid approach for measuring silver nanoparticle concentration and dissolution in seawater by UV–Vis. Science of The Total Environment 618, 597–607. https://doi.org/10.1016/J.SCITOTENV.2017.04.055

Squire, S., Scelfo, G.M., Revenaugh, J., Flegal, A.R., 2002. Decadal trends of silver and lead contamination in San Francisco Bay surface waters. Environ Sci Technol 36, 2379–2386. https://doi.org/10.1021/ES015746R

Tappin, A.D., Barriada, J.L., Braungardt, C.B., Evans, E.H., Patey, M.D., Achterberg, E.P., 2010. Dissolved silver in European estuarine and coastal waters. Water Res 44, 4204–4216. https://doi.org/10.1016/J.WATRES.2010.05.022

The Global Market for Nanomaterials 2010-2030 - Advanced and Emerging Technology Market Research, n.d. URL https://www.futuremarketsinc.com/the-global-market-for-nanomaterials-2010-2030/ (accessed 6.18.25).

Thomsen, M., South, P., Staehr, P., 2024. Fabulous but Forgotten Fucoid Forests. Ecol Evol 14, e70491. https://doi.org/10.1002/ece3.70491

Torres, E., Mata, Y.N., Blázquezy, M.L., Muñoz, J.A., González, F., Ballester, A., 2005. Gold and silver uptake and nanoprecipitation on calcium alginate beads. Langmuir 21, 7951–7958. https://doi.org/10.1021/LA046852K

Turner, A., Brice, D., Brown, M.T., 2012. Interactions of silver nanoparticles with the marine macroalga, Ulva lactuca. Ecotoxicology 21, 148–154. https://doi.org/10.1007/S10646-011-0774-2/

Valverde, F., Costas, M., Pena, F., Lavilla, I., Bendicho, C., 2008. Determination of total silver and silver species in coastal seawater by inductively-coupled plasma mass spectrometry after

batch sorption experiments with Chelex-100 resin. Chemical Speciation and Bioavailability 20, 217–226. https://doi.org/10.3184/095422908X381306

Vance, M.E., Kuiken, T., Vejerano, E.P., McGinnis, S.P., Hochella, M.F., Hull, D.R., 2015. Nanotechnology in the real world: Redeveloping the nanomaterial consumer products inventory. Beilstein Journal of Nanotechnology 6:181 6, 1769–1780. https://doi.org/10.3762/BJNANO.6.181

Vane, C.H., Turner, G.H., Chenery, S.R., Richardson, M., Cave, M.C., Terrington, R., Gowing, C.J.B., Moss-Hayes, V., 2020. Trends in heavy metals, polychlorinated biphenyls and toxicity from sediment cores of the inner River Thames estuary, London, UK. Environ Sci Process Impacts 22, 364–380. https://doi.org/10.1039/C9EM00430K

Vázquez-Arias, A., Boquete, M.T., Martín-Jouve, B., Tucoulou, R., Rodríguez-Prieto, C., Fernández, J.Á., Aboal, J.R., 2024. Nanoscale distribution of potentially toxic elements in seaweeds revealed by synchrotron X-ray fluorescence. J Hazard Mater 480, 136454. https://doi.org/10.1016/j.jhazmat.2024.136454

Vázquez-Arias, A., Rodríguez-Prieto, C., Yamada, Y., Ito, M., Fernández, J.Á., Aboal, J.R., n.d. Deciphering uptake mechanisms of potentially toxic elements in seaweeds using high resolution imaging analysis. under review.

Vilela, P., Liu, H., Lee, S.C., Hwangbo, S., Nam, K.J., Yoo, C.K., 2018. A systematic approach of removal mechanisms, control and optimization of silver nanoparticle in wastewater treatment plants. Science of The Total Environment 633, 989–998. https://doi.org/10.1016/J.SCITOTENV.2018.03.247

Wallace, A.L., Klein, A.S., Mathieson, A.C., 2004. Determining the affinities of salt marsh fucoids using microsatellite markers: Evidence of hybridization and introgression between two species of Fucus (Phaeophyta) in a Maine estuary. J Phycol 40, 1013–1027. https://doi.org/10.1111/J.1529-8817.2004.04085.X

Wimmer, A., Urstoeger, A., Funck, N.C., Adler, F.P., Lenz, L., Doeblinger, M., Schuster, M., 2020. What happens to silver-based nanoparticles if they meet seawater? Water Res 171, 115399. https://doi.org/10.1016/J.WATRES.2019.115399

Wu, X., Sinani, D., Kim, H., Lee, J., 2009. Copper Transport Activity of Yeast Ctr1 Is Down-regulated via Its C Terminus in Response to Excess Copper. Department of Biochemistry: Faculty Publications. https://doi.org/10.1074/jbc.M807909200

Xu, L., Wang, Z., Zhao, J., Lin, M., Xing, B., 2020. Accumulation of metal-based nanoparticles in marine bivalve mollusks from offshore aquaculture as detected by single particle ICP-MS. Environmental Pollution 260, 114043. https://doi.org/10.1016/J.ENVPOL.2020.114043

Yang, Y., Wang, K., Liu, X., Xu, C., You, Q., Zhang, Y., Zhu, L., 2024. Environmental behavior of silver nanomaterials in aquatic environments: An updated review. Science of The Total Environment 907, 167861. https://doi.org/10.1016/J.SCITOTENV.2023.167861

Yip, Z.T., Quek, R.Z.B., Huang, D., 2020. Historical biogeography of the widespread macroalga Sargassum (Fucales, Phaeophyceae). J Phycol 56, 300–309. https://doi.org/10.1111/JPY.12945

Zhang, L., Li, J., Yang, K., Liu, J., Lin, D., 2016. Physicochemical transformation and algal toxicity of engineered nanoparticles in surface water samples. Environmental Pollution 211, 132–140. https://doi.org/10.1016/J.ENVPOL.2015.12.041

Zhao, J., Wang, X., Hoang, S.A., Bolan, N.S., Kirkham, M.B., Liu, J., Xia, X., Li, Y., 2021. Silver nanoparticles in aquatic sediments: Occurrence, chemical transformations, toxicity, and analytical methods. J Hazard Mater 418, 126368. https://doi.org/10.1016/J.JHAZMAT.2021.126368

Zuykov, M., Pelletier, E., Demers, S., 2011. Colloidal complexed silver and silver nanoparticles in extrapallial fluid of Mytilus edulis. Mar Environ Res 71, 17–21. https://doi.org/10.1016/J.MARENVRES.2010.09.004

Declaration of generative AI and AI-assisted technologies in the writing process.

During the preparation of this work the authors used chat GPT in order to improve readability and language. After using this tool, the authors reviewed and edited the content as needed and take full responsibility for the content of the publication.

Acknowledgments

C. Pacín was supported by a predoctoral grant from Xunta de Galicia (ED481A 2022/374).

Author contributions

Carme Pacín: Formal analysis, Writing - Original Draft, Writing - Review & Editing; Massimo Lazzari: Writing - Review & Editing, J. Ángel Fernández: Funding acquisition, Conceptualization, Writing - Review & Editing; Jesús R. Aboal: Funding acquisition, Conceptualization, Writing - Review & Editing

5.2. Tracing Pollution in Brown Algae: A Compositional Analysis of Potentially Toxic Element Profiles

Carme Pacín[1*], J. Ángel Fernández[2], Jesús R. Aboal[2]

1. CIQUS Center, Department of Physical Chemistry, Universidade de Santiago de Compostela, Santiago de Compostela, 15782, Spain
2. CRETUS Center, Department of Functional Biology, Ecology Unit, Universidade de Santiago de Compostela, Santiago de Compostela, 15782, Spain

*corresponding author

Under review.

Abstract

Brown macroalgae are widely used as biomonitors of marine pollution, but their Potentially Toxic Element (PTE) composition has never been assessed trough compositional data analysis (CoDA). This study presents the first comprehensive application of CoDA to characterize PTE patterns in brown algae worldwide. Across more than 1600 samples, Zn consistently dominated tissue profiles (median = 80%), followed by Cu and Ni, while Pb and Cd contributed modestly and showed higher variability. Multivariate analyses revealed well-structured gradients in elemental composition, with taxonomic identity—particularly species—emerging as the strongest predictor of PTE profiles (R^2 = 33.5%). Extended profiling of *Fucus* spp. revealed a pattern dominated by Fe (42%) and Al (40%), with Zn (9%) and As (7%) as secondary contributors, and trace levels of Cu, Ni, Cr, Cd, Pb, and Hg. Significant shifts in *Fucus* spp. compositional profiles were detected over three decades (1990-2021), with recent samples showing increased Al, Fe, and As, and declines in Cu, Ni, and Cd, suggesting changes in particulate deposition and metal availability. Compositional analysis proved effective in identifying outlier samples from contaminated sites, where Pb became the dominant element, replacing the typical Zn-rich profile. Altogether, our results demonstrate that PTE profiles in brown algae are not random but taxonomically structured, reflecting species-specific physiological capacities for metal regulation. Combining absolute and compositional approaches improves the sensitivity, robustness, and ecological relevance of biomonitoring and bioremediation assessments.

Keywords

CoDA; Marine pollution; Metals; Biomonitoring; Coastal ecosystems; Seaweed

1. Introduction

Pollution is a persistent and widespread threat to the integrity of marine ecosystems. Among the most concerning pollutants are potentially toxic elements (PTEs). PTEs can be harmful across a range of concentrations, depending on the specific element and the sensitivity of the exposed organism (Khan et al., 2019; Zheng et al., 2018). PTEs enter marine environments through various pathways, including riverine discharge, atmospheric deposition, urban and industrial effluents, aquaculture, and maritime traffic (e.g. Förstner & Wittmann, 1981; Islam & Tanaka, 2004).

Coastal ecosystems, located at the land–sea interface, act as natural sinks for PTE pollution (Sharifi et al., 2016; Zhou et al., 2022). Moreover, their semi-enclosed hydrodynamics, combined with intense anthropogenic activity and limited water exchange in areas such as estuaries and bays, further promote the retention and accumulation of contaminants. This makes coastal ecosystems disproportionately affected by PTE pollution compared to other marine systems (Lu et al., 2018).

Coastal ecosystems also host complex and productive habitats, including seagrass meadows, kelp forests, salt marshes, and intertidal algal beds, which provide essential ecosystem services and support high biodiversity (Castro et al., 2023; Lanceman et al., 2025; Unsworth & Cullen-Unsworth, 2014). Chronic exposure to PTEs in these areas may impair physiological functions in marine organisms, alter community structure, and lead to bioaccumulation through food webs, ultimately compromising ecosystem health and resilience (e.g. Johnston & Roberts, 2009; Wang, 2002). Furthermore, changes in environmental conditions, such as acidification, warming or eutrophication, can influence PTEs speciation and bioavailability, potentially enhancing their toxicity and mobility (Stockdale et al., 2016; Takolander et al., 2017; Xie et al., 2024). Understanding the sources, distribution, and biological impact of PTEs is therefore essential for the sustainable management of coastal areas.

Brown algae are ecosystem engineers of coastal environments and are well known for their high capacity to bioconcentrate distinct contaminants from the surrounding water and from particulate matter (e.g. Aboal et al., 2023; Contreras-Porcia et al., 2017), primarily through

passive diffusion and surface adsorption mechanisms (Vázquez-Arias et al., 2024). This ability to integrate contaminant exposure over time, together with their widespread distribution and sessile nature, have made them valuable for biomonitoring programs aimed to assess coastal environmental quality (e.g. Pacín et al., 2025). In addition, brown algae have notable economic relevance, being consumed directly by humans but also widely used in cosmetic and pharmaceutical products (Ferdouse et al., 2018). This has prompted the establishment of safety thresholds for PTE concentrations in edible seaweeds and algae-derived products (e.g. European Union, 2024). As a result, substantial data exist on total concentrations of PTEs in brown algal tissues.

However, PTE uptake in brown algae is a complex process, influenced by multiple interacting factors, including environmental conditions (e.g. salinity, temperature, hydrodynamics), and tissue-specific characteristics (Syaifudin et al., 2025; Vázquez-Arias et al., 2024; Vijayaraghavan et al., 2021). Brown algae also comprise a taxonomically and functionally diverse group, with different taxa displaying markedly different PTE bioconcentration capacities due to differences in morphology, physiology, and metabolic regulation (e.g. Tuzen et al., 2009). In addition to these intrinsic traits, they inhabit a wide range of environments—from upper intertidal to subtidal zones—under varying levels of PTE bioavailability and environmental pressures (Lobban & Harrison, 1994). Although biokinetic models have revealed some interspecific variability (Davis et al., 2003; Holan & Volesky, 1994), many aspects of PTEs uptake, regulation, and storage in brown algae remain poorly understood, and species-specific responses to environmental stressors are still largely unexplored. As a result, PTE concentrations in algal tissues can vary widely across space, time, and taxa, making it difficult to identify consistent contamination patterns or define reliable baselines.

To address these limitations and obtain a more stable, biologically meaningful measure of contamination, an alternative to relying solely on total concentrations is the application of compositional data analysis (CoDA) (Aitchison & Egozcue, 2005; Zhang et al., 2024). By focusing on element ratios and the interdependence among elements rather than absolute values, CoDA minimizes statistical bias and enhances the detection of meaningful trends in PTE profiles, reducing the influence of confounding factors such as tissue hydration, growth stage, or seasonal variation. CoDA also allows for the definition of taxa-specific compositional "fingerprints", or reference profiles that reflect the typical elemental balance in tissues (Lewis et al., 2010). Deviations from these expected profiles can signal abnormal exposure, help detect

contamination events and provide insights into potential pollution sources. This approach has already proven effective in environmental studies involving complex contaminant mixtures such as dioxins, furans, PAHs (Real et al., 2011). However, to the best of our knowledge, CoDA has only been applied once to PTEs in sediments (Somma et al., 2021), and never to brown algae or other marine organisms, despite their widespread use as biomonitors.

Building on this framework, the present study applies CoDA to investigate PTE profiles in brown algae across taxonomic gradients, using decades of published data and globally distributed records. We focused on a core suite of ecologically relevant PTEs—Cd, Cu, Ni, Pb, and Zn—due to their prevalence, toxicity, and broad coverage across studies and taxa. For *Fucus* spp., the brown algae most widely used in biomonitoring (Aboal et al., 2023; García-Seoane et al., 2018), a more comprehensive elemental profile was assessed by additionally including Al, Cr, Fe, As, and Hg, taking advantage of higher data availability. By deriving taxa-specific compositional profiles, we aimed to establish robust and interpretable baselines to support spatial and temporal contamination assessment. These profiles will enhance the detection of changes in pollution sources and ecological risk, strengthening the role of brown algae as sentinel organisms in coastal ecosystems and showcasing the potential of CoDA for marine biomonitoring. We tested the following hypotheses: i) No significant differences exist in the relative proportions of PTEs; ii) No consistent covariation patterns are observed among elements; iii) PTE composition does not significantly vary among families, genera, or species; iv) No significant temporal changes occur in *Fucus* spp. PTE composition from 1990 to 2021; and v) The presence of environmental contamination sources does not significantly alter the internal hierarchy or relative structure of PTE composition in brown algae.

2. Material and methods

2.1. Data compilation

We compiled data on PTE concentrations in brown algae (Phaeophyceae) from a comprehensive literature review covering the period 1952–2020. The search was conducted using the Scopus and Google Scholar databases, focusing on peer-reviewed articles in English that included keywords related to PTEs (e.g., cadmium, copper, zinc), pollution and monitoring (e.g., bioaccumulation, contamination), and macroalgae (e.g., brown algae, seaweed). Theses, technical reports, and other non-peer-reviewed sources were excluded. Additional records were identified through cross-referencing the bibliographies of selected publications.

In addition to the literature review covering studies published up to 2020, we also included data from our own work published after that year, based on samples collected in 2013, 2019, 2021, and 2023 (García-Seoane et al., 2019, 2021; Pacín et al., 2025; Vázquez-Arias et al., 2023, 2025).

We retained studies that met selection criteria, which included the availability of elemental concentration data, taxonomic identification, and precise sampling site information (e.g., coordinates, locality names, or mapped locations). For each record, the following information was extracted: sampling year, species identity, geographic location, and concentrations of the target elements.

Only values reported on a dry weight basis and expressed in micrograms per gram (μg g^{-1} DW) were considered. Units were converted where necessary. When studies reported ranges or multiple replicates, mean values were used. If sampling data were pooled across sites, a mean geographic location was assigned. In cases where elemental concentrations were reported for different parts of the algal thallus, values were averaged to obtain a single value per sample. Additionally, we included data from transplant experiments, but only time-zero measurements were used, as they correspond to specimens collected and analyzed in the same manner as native individuals. The detailed data compilation protocol is available in (Aboal et al., 2023).

2.2. Data selection

Compositional data analysis requires complete records for all selected elements. To balance ecological relevance with data availability, we tested various combinations of priority PTEs—initially including Al, Cr, Fe, Ni, Cu, Zn, As, Ag, Cd, Pb, and Hg—to maximize the number of usable records.

From these, we selected a core group of five elements—Ni, Cu, Zn, Cd, and Pb—that provided the largest number of complete records (n = 1611, from 105 studies). These elements are consistently identified as environmentally relevant pollutants due to their toxicity and widespread occurrence. Although Hg and As are toxicologically relevant, their inclusion markedly reduced the number of complete observations (n = 872 and n = 895, respectively). Consequently, both were excluded from the main compositional dataset but retained for targeted analyses where available.

A broader combination including Al, Cr, Fe, Ni, Cu, Zn, As, Cd, Pb, and Hg (excluding Ag due to limited data) was considered for *Fucus* spp. samples (n = 768). These additional elements were included based on both their consistent presence in the literature and their geochemical or biological relevance (e.g., Fe and Al as proxies for lithogenic input), enabling a more complete compositional characterization for this key biomonitoring taxon.

A detailed summary of the dataset, including species names, geographic metadata, and elemental values, is provided in the Supplementary Material (Table S1).

2.3. Data analysis

Compositional profiles of PTEs were generated for all brown algae samples by treating concentrations as compositional data and applying a centered log-ratio (clr) transformation, enabling appropriate statistical and ordination analyses. For each element, geometric medians and interquartile ranges (IQR) were reported to summarize central tendency and variability within the compositional framework.

Principal Component Analysis (PCA) was performed on CLR-transformed data using Ni, Cu, Zn, Cd, and Pb for all samples. As and Hg, available for a smaller subset of samples, were treated as supplementary variables by applying the same CLR transformation and projecting them onto the PCA space without contributing to the PCA axis construction. The influence of taxonomic and environmental factors was assessed using Permutational Multivariate Analysis of Variance (PERMANOVA) based on Euclidean distances of CLR-transformed data, with 9999 permutations. The factors evaluated included taxonomy (species, genus, family), ocean basin, and sampling year. In addition, Redundancy Analysis (RDA) was performed using species as a constraining variable to evaluate its explanatory power.

Pairwise PERMANOVA tests were conducted between taxa of the same taxonomic level to assess significant compositional differences, with p-values adjusted using Bonferroni correction. To ensure statistical robustness, these analyses were restricted to taxa with at least 30 samples. Exceptions were made for *Padina pavonica* (n = 24), *Padina tetrastromatica* (n = 24), and *Laminaria digitata* (n = 17). Although their results were interpreted with caution due to limited sample size, these taxa were retained to provide preliminary insights into less-represented species.

To compare average elemental compositions with samples from highly contaminated environments, four individual samples collected from sites with elevated Cd or Pb concentrations were contrasted with the median compositional profiles of their respective taxa (Abdallah et al., 2005; Chakraborty & Owens, 2014; Pacín et al., 2025). These enriched samples included *Fucus ceranoides* (Cd-rich), *Fucus ceranoides* (Pb-rich), *Hormophysa cuneiformes* (Pb-rich), and *Padina pavonica* (Cd-rich).

Temporal changes in elemental composition were further evaluated using data from *Fucus* spp. reported in Pacín et al., 2025. Analyses were performed both with the full set of elements and after excluding Al and Fe, which showed disproportionately high loadings in exploratory analyses. Pairwise PERMANOVA tests were carried out between major sampling periods (1990, 2001–2007, and 2021). We selected this dataset because it follows a standardized sampling and analytical protocol, ensuring methodological consistency across years and locations. Additionally, it represents approximately 60% of the total available records for *Fucus* spp., making it a robust foundation for compositional analysis and temporal assessment.

All analyses were conducted in R version 4.1 using the compositions (van den Boogaart et al., 2024), vegan (Oksanen et al., 2025), and ggplot2 packages (H. Wickham., 2016).

3. Results

3.1. Global Patterns of PTE Composition in Brown Algae

The geometric median composition of PTEs across all brown algae samples, assessed in compositional space, was dominated by Zn (80.0%, [IQR: 53.6 – 85.1 %]), followed by Cu (9.36%, [IQR: 5.91 – 16.9%]) and Ni (6.78%, [IQR: 3.3 – 13.1%]), with Pb (2.41%, [IQR: 0.83 – 5.83 %]) and Cd (1.41%, [IQR: 0.63 – 2.81 %]) as minor contributors. All elements exhibited notable interquartile ranges, indicating high variability and suggesting that global profile represents an overall tendency rather than a consistent fingerprint across samples (Figure 1).

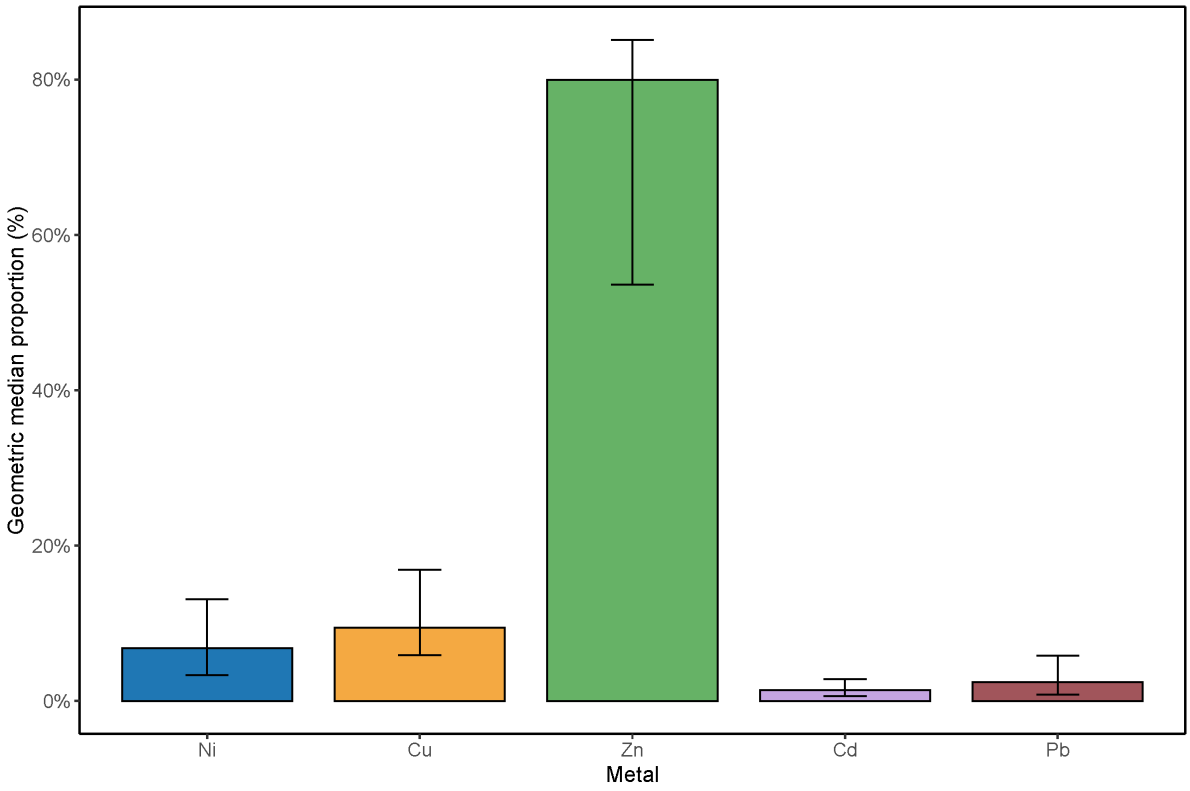

Figure 1. Geometric median proportions of Potentially Toxic Elements (Ni, Cu, Zn, Cd, and Pb) in brown algae across all samples (n = 1611), computed in the compositional space. Error bars indicate the interquartile range (25th–75th percentiles).

Principal component analysis (PCA) of CLR-transformed data identified two main compositional gradients. PC1 (32.9% variance) separated Pb-rich samples from those enriched in Cd and Zn, while PC2 (31.9%) opposed Cu- and Cd-dominated profiles. Although the ordination revealed continuous variation and partial overlap across families and genera, some taxonomic patterns were apparent. Fucaceae, particularly *Fucus* spp., was clustered in the Zn- and Cu-rich quadrant of the ordination space, while Sargassaceae, Laminariaceae, and Dictyotaceae showed more dispersed distributions (Figure 2). Ellipses (80% confidence level) for the three most represented species revealed distinct niches: *Fucus ceranoides* was shifted towards higher Cu (upper PC2), while *Sargassum miyabei* showed a distinct displacement towards higher Cd (lower PC2), with no overlap observed between the two species. *Fucus vesiculosus* occupied an intermediate position along PC2 but leaned right on PC1, indicating higher Cd and Zn and lower Pb. These patterns were accompanied by wide dispersion along PC1 for *S. miyabei* and *F. ceranoides*, indicating heterogeneous Pb contributions within species (Figure 3).

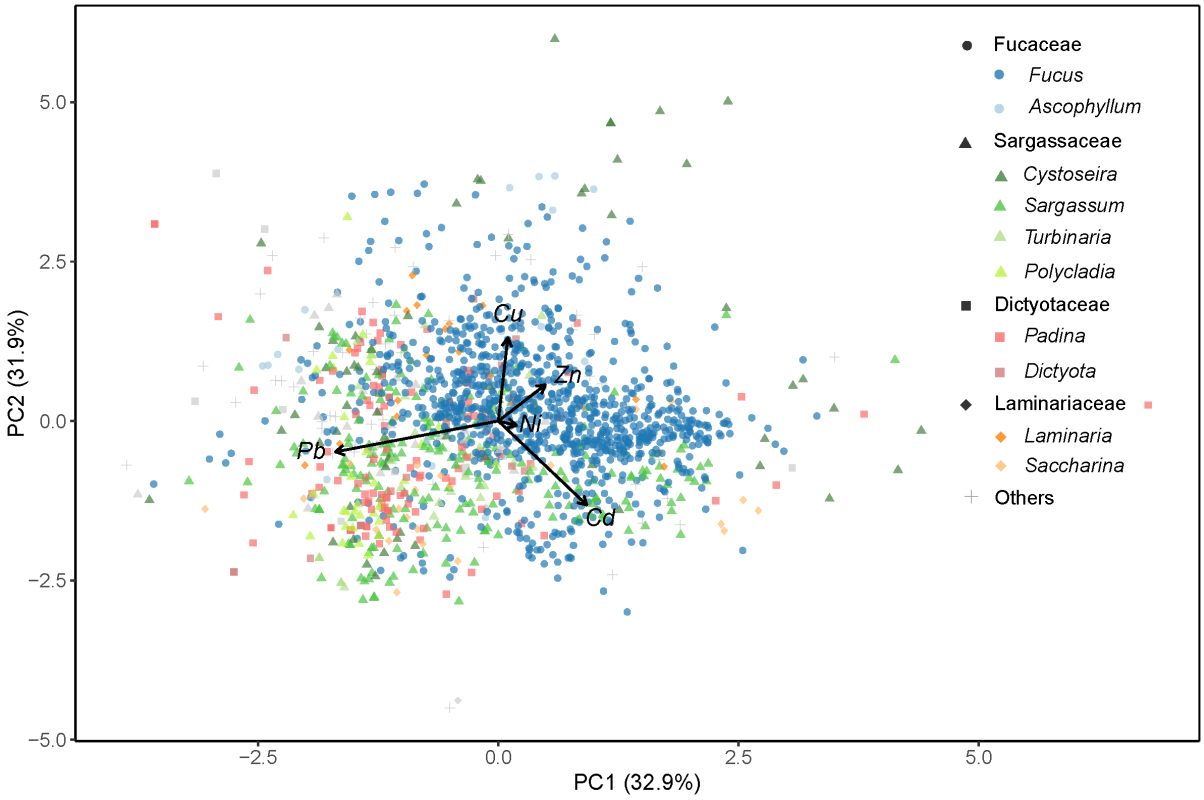

Figure 2. Principal Component Analysis of CLR-transformed Potentially Toxic Element composition in brown algae. Each point represents an individual sample, colored by genus and shaped by family. Grey symbols indicate genera not explicitly represented in the color legend but belonging to the same family.

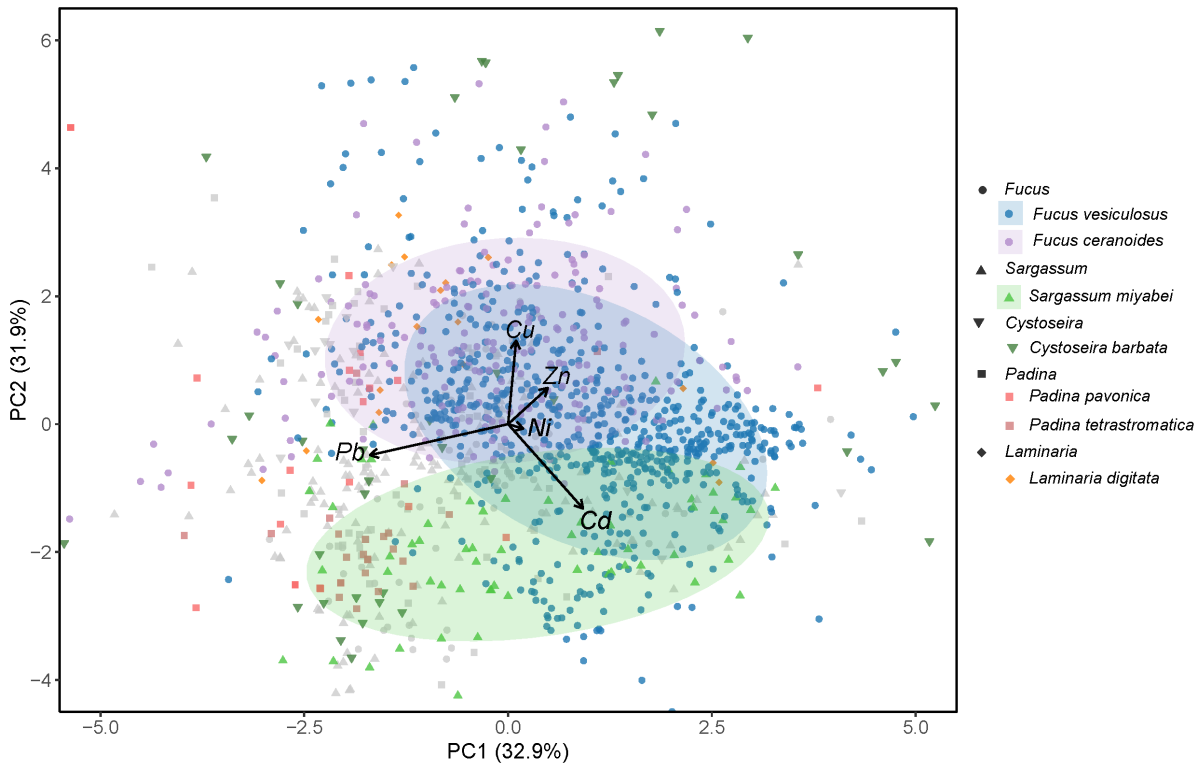

Figure 3. Principal Component Analysis of CLR-transformed Potentially Toxic Element composition in brown algae. Each point represents an individual sample, colored by species and shaped by genus. Grey symbols indicate samples from species not highlighted in the legend but belonging to the same genera. Samples from other genera are not displayed but were included in the data analysis.

Mercury and As, included as supplementary variables due to missing values, had geometric median proportions of 0.027% and 39.3%, respectively. Arsenic was correlated with Zn- and Cd-rich samples, showing a strong alignment with the primary compositional gradient (PC1 loading = 0.44, R^2= 21.7 %, p << 0.001). In contrast, Hg exhibited only a weak association with the overall compositional structure, displaying a slight alignment with Pb-enriched profiles (PC1 loading = –0.11; r^2 = 1.3%; p < 0.01) (Figure S1).

3.2. Drivers of Compositional Variability

PERMANOVA on Euclidean distances of CLR-transformed compositions identified species identity as the strongest predictor of PTE variability (R^2 = 33.5%), followed by genus (20.2%) and family (10.1%), reflecting nested taxonomic effects. Ocean basin also had a significant, but lower and collinear, effect. Sampling year contributed significantly yet marginally (R^2 = 2.0%).

Redundancy analysis (RDA) further confirmed the strong influence of the Species category. The model was highly significant ($F = 7.86$, $p = 0.001$), with the first two constrained axes explaining 14.4% and 11.0% of the total variance (42.8% and 32.8% of the constrained variance, respectively). RDA1 opposed Zn (loading = 2.42) to Pb (–2.03), delineating a compositional gradient from Pb- to Zn-enriched samples. Nickel (–0.70) and Cd (–0.79) also loaded negatively on RDA1. RDA2 was primarily structured by Cd (–2.61), contrasting Cd-rich profiles with those enriched in Pb (1.29), Cu (0.84), and Ni (0.48), and suggesting partial association between Ni and Pb across species (Figure S2).

3.3 Compositional Profiles Across Taxa

When comparing PTE profiles across taxonomic groups, Zn consistently emerged as the dominant element, particularly within Fucaceae and Laminariaceae, where it accounted for over 80% of total PTE content. In contrast, Sargassaceae and Dictyotaceae exhibited higher proportions of Cu, Ni, and Pb. *Cystoseira* spp., within Sargassaceae, showed intermediate profiles (Figure S3, Table 1).

Pairwise PERMANOVA comparisons confirmed significant differences in PTE composition across most taxonomic levels. At the family level, the strongest divergence was observed between Fucaceae and Dictyotaceae ($R^2 = 0.066$, $p < 0.001$), while Dictyotaceae and Sargassaceae showed only marginal separation ($R^2 = 0.006$, $p = 0.019$). Genus-level comparisons revealed distinct profiles for *Fucus*, *Padina*, and *Cystoseira* (e.g., *Padina* vs. *Fucus*: $R^2 = 0.061$, $p < 0.001$), whereas *Padina*/*Turbinaria*/*Polycladia* and *Sargassum*/*Turbinaria* exhibited no significant differences. At the species level, differences were particularly strong between *Laminaria digitata* and *Sargassum miyabei* ($R^2 = 0.36$, $p < 0.001$), while even congeneric species such as *Fucus vesiculosus* and *F. ceranoides* showed significant compositional divergence ($R^2 = 0.069$, $p < 0.001$). *Padina pavonica* and *P. tetrastromatica* did not differ significantly (Table 1, Figure S3). These patterns must be interpreted with caution due to uneven sampling effort.

Table 1. Mean relative composition and interquartile range (in brackets) of Potentially Toxic Elements (Ni, Cu, Zn, Cd, Pb) in brown algae across taxonomic levels. Values are expressed as percentages of total elements content. Significant differences ($p < 0.05$) are indicated by distinct lowercase (Families), uppercase (Genus) or italic-lowercase (Species) letters.

Taxa	Ni	Cu	Zn	Cd	Pb	pairwise

Families						
Fucaceae	5.35	8.37	83.68	1.17	1.42	a
(n= 985)	[2.89–7.74]	[5.32–15.1]	[70.5–86.9]	[0.64–2.17]	[0.67–2.71]	
Sargassaceae	16.22	14.41	58.05	2.73	8.59	b
(n= 376)	[8.60–23.6]	[7.98–18]	[39.5–67.2]	[0.88–5.79]	[2.72–14]	
Dictyotaceae	13.48	15.68	56.07	2.73	12.04	c
(n= 143)	[7.70–20.2]	[7.38–22.8]	[40.7–61.6]	[0.78–4.11]	[4.18–18.1]	
Laminariaceae	3.66	7.06	82.70	2.03	4.55	d
(n= 42)	[1.66–5.01]	[3.82–7.47]	[70.7–89.8]	[0.38–4.39]	[0.67–10.5]	
Genus						
Fucus	5.42	8.39	83.54	1.22	1.43	A
(n= 965)	[2.98–7.82]	[5.32–15.1]	[70.3–86.9]	[0.65–2.2]	[0.67–2.67]	
Sargassum	16.3	13.78	58.09	3.46	8.38	B
(n= 220)	[8.96–24.5]	[8.57- 16.5]	[39.5–61.9]	[1.2–7.29]	[2.45–14.1]	
Cystoseira	11.93	9.71	74.89	0.56	2.91	C
(n= 62)	[5.04–22.4]	[3.51–16]	[56.0–81.5]	[0.05–1.53]	[0.09–9.08]	
Padina	14.44	15.34	55.15	2.66	12.41	D
(n= 115)	[7.79–22.3]	[8.27–23.1]	[40.4–60.3]	[0.8–4.16]	[4.24–17.9]	
Polycladia	14.86	12.44	51.22	3.14	18.34	D
(n= 36)	[10.8–16.7]	[7.87–15.3]	[36.9–68.2]	[0.29–5.13]	[5.79–25.8]	
Turbinaria	20.58	17.63	50.57	3.38	7.84	BD
(n= 32)	[14.2–26.8]	[8.81–21.4]	[39.0–55.4]	[1.26–5.95]	[4.48–13.7]	
Species						
F. vesiculosus	4.83	7.57	84.85	1.53	1.23	*a*
(n= 702)	[2.85–7.24]	[4.93–11.5]	[75.5–87.3]	[0.73–2.42]	[0.59–2.31]	
F. ceranoides	6.97	16.00	74.40	0.79	1.85	*b*
(n= 203)	[3.58–9.98]	[8.40–32.2]	[51.3–81.9]	[0.50–1.04]	[0.91–3.08]	
S. miyabei	14.25	11.50	60.68	7.37	6.21	*c*
(n= 62)	[9.50–20.3]	[8.62–12.3]	[53.8–63.1]	[4.61–9.02]	[1.71–12.4]	
C. barbata	11.20	8.33	77.86	0.64	1.97	*d*
(n= 47)	[4.63–20.2]	[3.20–13.2]	[59.4–81.4]	[0.02–1.75]	[0.07–9.01]	
P. pavonica	13.90	10.13	52.26	2.08	21.63	*e*
(n= 24)	[7.45–20]	[6.24–13.6]	[43.1–66.1]	[0.29–3.65]	[3.57–27.2]	

P.tetrastromatica	15.63	11.67	50.88	4.26	17.56	*e*
(n= 24)	[12.6–19.6]	[7.85–14.5]	[37.2–61.5]	[2.81–5.82]	[12.4–20.5]	
L. digitata	1.72	4.73	91.63	0.22	1.69	*g*
(n= 17)	[1.18–2.69]	[3.77–9.24]	[85.3–92.8]	[0.09–0.57]	[0.68–2.84]	

3.4. Compositional profiles in highly contaminated samples

Distinct compositional profiles were observed between samples collected from sites with elevated Pb or Cd and the average profile of the corresponding species or genus (Figure 4). In Pb-rich samples, Pb became the dominant element, replacing Zn as the main contributor. Specifically, Pb represented 59.1% of the total metal profile in *Fucus ceranoides* (Pb rich) and 62.8% in *Hormophysa cuneiformes* (Pb rich), compared to 1.8% and 8.3% in Fucus *ceranoides* and *Sargassum*, respectively. Similarly, Cd-rich samples showed increased Cd contributions, reaching 2.6% in Fucus ceranoides (Cd rich) and 4.6% in *Padina pavonica* (Cd rich), in contrast to 0.8% and 2.1% in their respective references. The Cd-rich *Fucus ceranoides* sample also exhibited higher proportions of Cu and Ni and lower Pb, whereas the Cd-rich *Padina pavonica* sample showed a higher proportion of Pb but lower contributions from Cu and Ni, with Zn remaining stable. All of these values fell outside IQR of the corresponding species or genus - level distributions (Table 1).

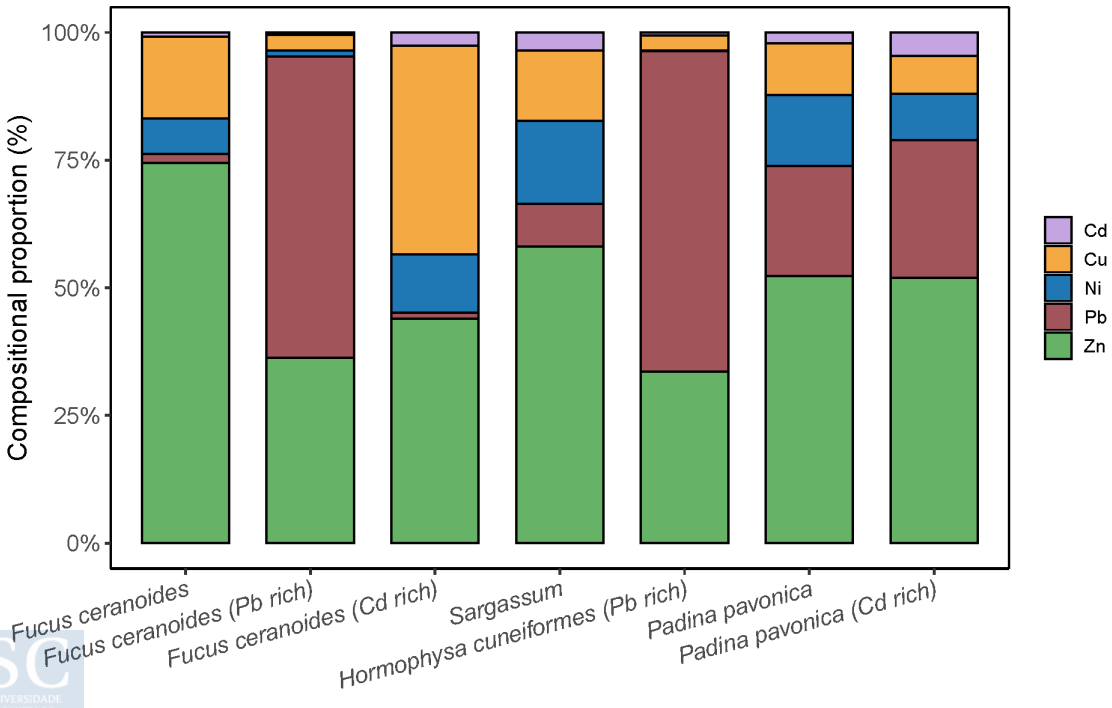

Figure 4. Compositional profiles of Potentially Toxic Elements (Ni, Zn, Cu, Cd, Pb) in brown algae. Bars represent the proportion of each element within the total profile. Median profiles for *Fucus ceranoides*, *Sargassum*, and *Padina pavonica* are based on multiple samples. In contrast, Pb-rich and Cd-rich profiles correspond to individual samples collected from highly contaminated sites.

3.5 Extended Elemental Profile in *Fucus* spp. and Temporal trends

Given its dominance in the dataset, *Fucus* spp. were further analyzed for an extended set of elements, including Al, Fe, As, Cr, and Hg, in addition to core PTEs (Ni, Cu, Zn, Cd, and Pb). The median composition was dominated by Fe (42.4%) and Al (40.2%), followed by Zn (8.57%) and As (6.87%). Cu represented 0.8%, while Ni, Cr, Cd, Pb, and Hg collectively accounted for just 1.15%. Mercury was the least abundant element, with a median contribution of 0.04% (Figure 5, n = 768). Despite this general pattern, high variability was observed across individual samples (IQR > 50% of the median).

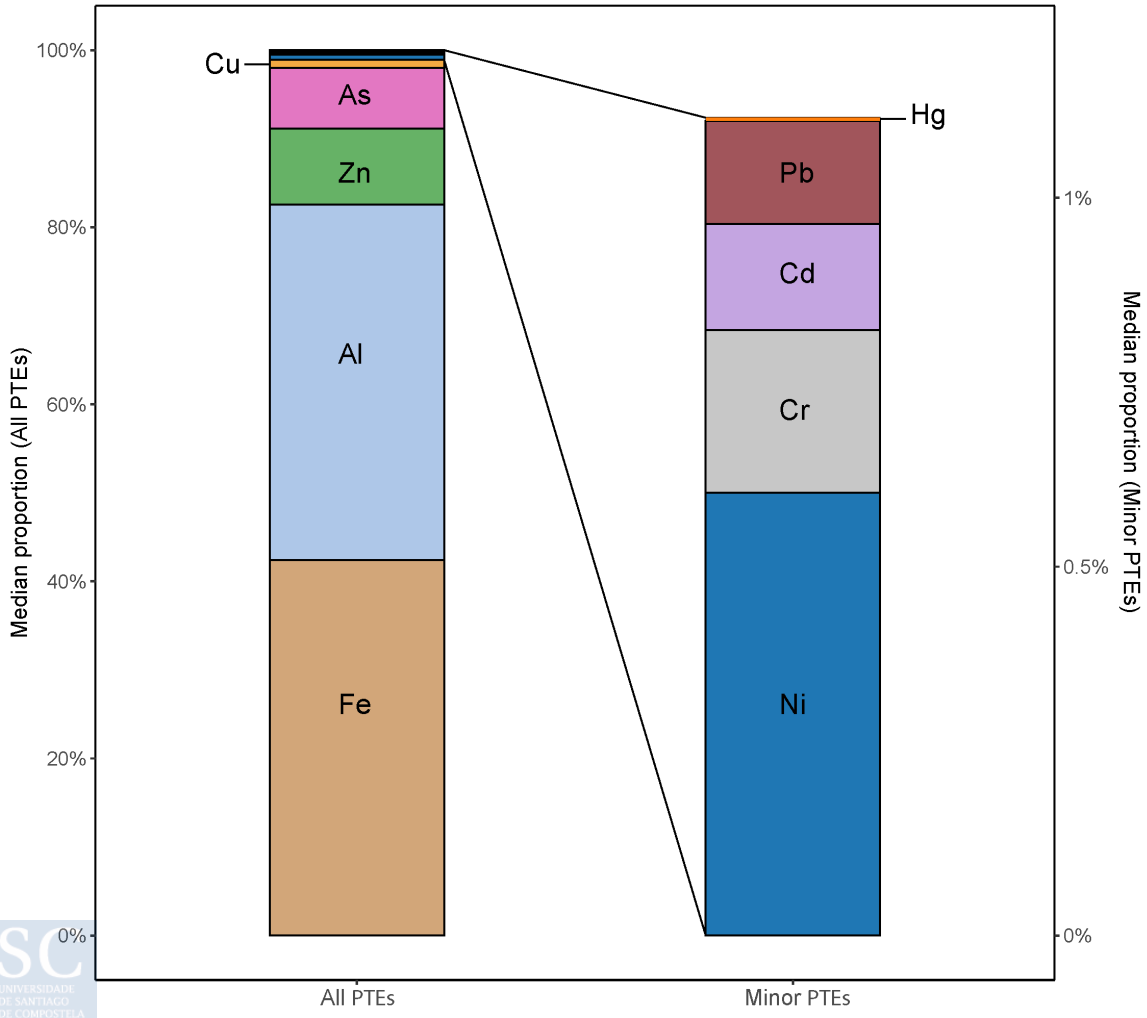

Figure 5. Median compositional profile of Potentially Toxic Elements in brown algae. The left bar represents the average composition across all elements (100%), highlighting the dominance of Fe, Al, Zn, and As. The right bar isolates minor elements (Hg, Pb, Cd, Cr, Ni, and Cu) using a separate y-axis scaled to 1.3%, allowing better visualization of their relative contributions. Color coding is consistent between bars to facilitate comparison.

Significant temporal shifts were detected in the elemental profile of *Fucus* spp. (Figure S4, Figure 6). PERMANOVA revealed that sampling year explained 20.4% of the total variability when all elements were considered ($F = 113.45$, $p < 0.0001$), and 13.9% when Al and Fe were excluded ($F = 71.39$, $p < 0.0001$), confirming a robust temporal structure. Between 1990 and 2001–2007, differences were minor and mainly reflected slightly higher Al and lower Cu. In contrast, 2021 samples exhibited strong increases in Al and Fe, which led to proportional decreases in other elements. When Al and Fe were excluded, As became more dominant in 2021, while Cu, Ni, Cd, and Hg showed slight decreases, and Pb remained relatively stable over time.

Pairwise PERMANOVA confirmed a progressive but non-linear shift. The most pronounced change occurred between 1990 and 2021 ($R^2 = 29.5\%$, $p < 0.0001$), followed by a substantial difference between 2021 and 2001–2007 ($R^2 = 24.5\%$, $p < 0.0001$). The contrast between 1990 and 2001–2007 was smaller but still significant ($R^2 = 4.8\%$, $p < 0.0001$). These patterns remained significant when excluding Al and Fe, with R^2 values of 19.8%, 15.1%, and 5.3%, respectively, indicating long-term, directional shifts in PTE composition, with accelerated changes in recent decades.

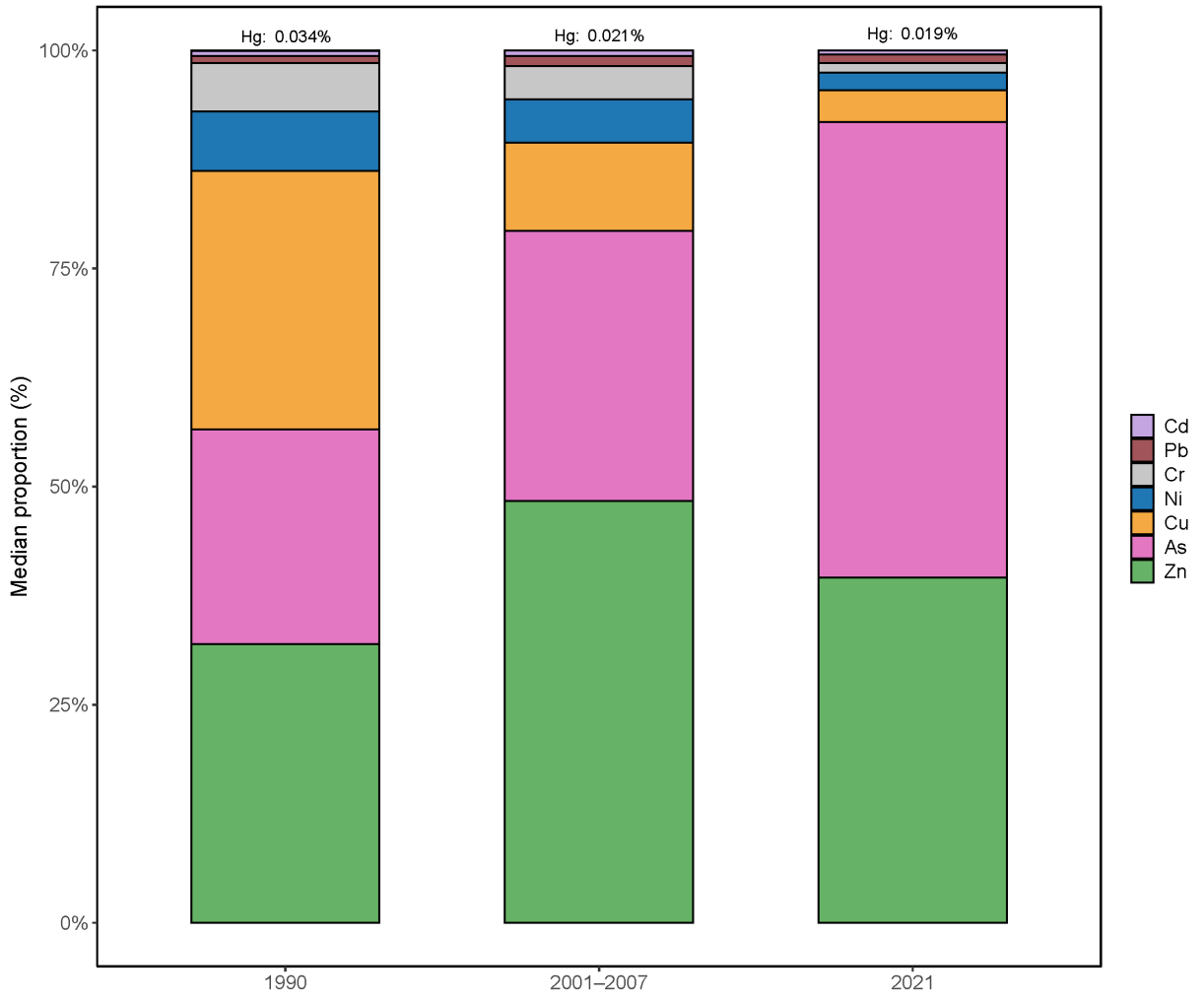

Figure 6. Compositional profiles of potentially toxic elements (PTEs) in *Fucus* spp. across three time periods: 1990, 2001–2007, and 2021 (Pacín et al., 2025). Bars represent centered log-ratio (CLR)-transformed relative contributions of each element to the overall profile. Due to its low contribution, Hg proportions are shown as numeric labels above the corresponding bars rather than as stacked segments.

4. Discussion

4. Global compositions

The elemental composition of brown algae was consistently dominated by Zn, followed at a distance by Cu and Ni, while Pb and Cd contributed more modestly and with greater variability (Figure 1). This general ordering—Zn > Cu ≈ Ni > Pb > Cd—persisted across taxa with minor changes, suggesting underlying physiological and environmental drivers.

Zinc's predominance likely stems from its role as an essential micronutrient and its relatively high bioavailability in seawater (Morel & Price, 2003; Rainbow, 2002). As a cofactor in

multiple metabolic processes, Zn uptake and retention are actively regulated (Andreini et al., 2006; Geddie & Hall, 2019). Additionally, the strong affinity of Zn^{2+} for algal cell wall polysaccharides enhances adsorption from seawater (Brinza et al., 2019; Geddie & Hall, 2019), which is followed by its internalization. Accordingly, Zn has been detected in *F. vesiculosus* in cell wall structures, but predominantly within intracellular physodes (specialized organelles containing phlorotannins) (Vázquez-Arias et al., 2024). Although Zn is not the most abundant trace PTE in seawater and displays considerable variability (EGEOTRACES, n.d.; Park et al., 2020; Vázquez-Arias et al., 2025), its intermediate concentrations, high bioavailable fraction (Zn^{2+}), and active and passive uptake systems explains its dominance in tissue composition across brown algal taxa (Dong et al., 2016; Skipnes et al., 1975).

Copper and Ni contributed intermediate proportions (5–17% and 5–20%, respectively; Table 1). Copper is essential for electron transport and redox regulation and is primarily taken up via specific transporters (Demirevska-Kepova et al., 2004; Thomas et al., 1998). Once internalized, Cu accumulates mainly in physodes, with only a minor fraction associated with cell wall polysaccharides (Vázquez-Arias et al., 2024). In contrast, Ni lacks a known physiological function in brown algae and is likely absorbed passively. Seawater chemistry further influences their relative abundances: only ~10% of total Ni and less than 20% of total Cu are present as bioavailable free ions, compared to > 25% for Zn (Stockdale et al., 2016). The lower tissue levels of Cu and Ni compared to Zn likely reflect both reduced biological demand and lower bioavailable fractions, rather than total concentrations in seawater.

Cadmium and Pb were consistently the least abundant PTEs, with few exceptions for Pb (Figures 1, 4). Their limited contributions align with their low environmental availability and lack of biological function (EGEOTRACES, n.d.; Kahal et al., 2023; Millero et al., 2009). Lead is strongly particle-reactive and poorly bioavailable in dissolved form, while most Cd is complexed in seawater and competes with Zn and Ca for uptake (Chen et al., 2019; Neff, 2002; Noraho & Gaur, 1995; Patterson et al., 1976; Töpperwien et al., 2007). Both elements are likely absorbed via passive adsorption to the surface or non-specific transporters (Mata et al., 2008). Accordingly, Pb has been located in cell walls (Vázquez-Arias et al., n.d.). Altogether, the minimal levels of Cd and Pb reflect the absence of biological demand, low environmental availability, and reliance on non-selective uptake pathways. Moreover, their high variability likely results from sensitivity to pollution sources and the absence of physiological regulation mechanisms.

The extended elemental profile analyzed in *Fucus* spp. revealed that Al and Fe together accounted for over 80% of total PTE content, with Zn (8.6%) and As (6.7%) as secondary components, and Hg occurring only in trace amounts (<0.05%). The high Al and Fe levels likely result from passive accumulation via particle adhesion in estuarine environments, facilitated by strong binding to cell wall polysaccharides (Barreiro et al., 2002; Schropp et al., 1990). The notable As content may result from its phosphate-mimicking behavior, as its structural similarity to phosphate allows it to be taken up via phosphate transporters. However, its extracellular localization suggests possible efflux after uptake (Ender et al., 2019; Garbinski et al., 2019). Mercury scarcity reflects low environmental concentrations and poor bioavailability due to strong complexation with organic matter (Stockdale et al., 2016) and incompatibility with algal transport systems for other divalent cations because of the large ionic radius and high covalent index of Hg^{2+} (Nieboer & Richardson, 1980).

4.2. Multivariate patterns of composition

Beyond individual abundances, PTEs in brown algae exhibited consistent co-variation patterns, revealing distinct compositional gradients across taxa. Principal Component Analysis of CLR-transformed data showed a strong antagonism between Pb and Zn/Cd/Cu along PC1, likely reflecting differences in uptake pathways and environmental behavior (Figure 2, Figure 3). Lead, typically associated with particulates and retained in algal cell walls, contrasted with the more soluble and bioavailable Zn, Cd, and Cu.

Along PC2, Zn and Cu remained tightly clustered, diverging from Cd (Figure 2, Figure 3). Their close alignment is consistent with their essential roles and reliance on active transport and intracellular storage, resulting in relatively stable, coordinated accumulation patterns that are buffered from environmental fluctuations. Cadmium, in contrast, diverged markedly, consistent with passive, non-specific uptake and a lack of physiological regulation. Although Cd may enter cells via Zn transporters due to ionic similarity (Lane et al., 2005; Morel et al., 2020), evidence indicates passive uptake predominates (Jayakumar et al., 2022; Mata et al., 2008), resulting in higher sensitivity to external variation. Lead, while also non-essential, displayed intermediate behavior, likely due to strong adsorption to cell wall polymers such as alginates and fucoidans (Davis et al., 2003). Nickel showed independent variation across both components, supporting passive uptake in the absence of known physiological functions or transporters.

Arsenic, included as a supplementary variable, correlated positively with Zn-, Cu-, and Cd-enriched samples along PC1, and occupied an intermediate position on PC2 (Figure S1). Arsenate may enter cells via phosphate transporters, which are occasionally Zn-regulated (Basit & Hussain, 2024; Meharg & Hartley-Whitaker, 2002), suggesting links between As and Zn/Cu bioconcentration. In contrast, Hg showed minimal alignment with the main compositional gradients (Figure S1). Its weak association with Pb-enriched samples may reflect shared affinity for particles and sediment binding (Xu et al., 2021). However, Hg lacks metabolic analogs and is unlikely to be actively transported. Its interaction with algal tissues appears limited to surface adsorption and passive mechanisms, as strong thiol-binding is unlikely due to the low abundance of cysteine-rich proteins in algal cell walls, and interactions with carboxyl, hydroxyl and sulfate groups from the cell wall polysaccharides are weak (Henriques et al., 2015; Nieboer & Richardson, 1980). Consequently, Hg bioconcentration was low and largely decoupled from both physiological regulation and environmental gradients.

These compositional patterns diverged from those based on absolute concentrations. In *Fucus* spp. (Pacín et al., 2025), absolute data showed co-variation between Cu, Ni, Zn, Cr, and Hg, suggesting shared environmental sources, whereas compositional analysis grouped elements according to physiological processing. For example, As clustered with Zn/Cu/Cd in compositional PCA but showed a negative correlation with Cu in absolute concentrations, likely reflecting different environmental origins. A global nMDS analysis (Aboal et al., 2023) based on absolute concentrations revealed Pb-Cd and Cu-Zn clustering, supporting environmental co-occurrence.

Redundancy Analysis (RDA), constrained by species identity, supported the PCA findings and further clarified PTE relationships. RDA1 revealed a Pb–Ni association contrasting with Zn, underscoring the distinction between actively regulated (Zn-rich) and passively accumulated (Pb-rich) profiles. Along RDA2, the Cd–Cu contrast from the PCA was retained. Overall, ordination analyses suggest that Zn and Cu form a compositional cluster linked to physiological requirements and intracellular regulation, while Pb and Cd represent a separate axis more influenced by environmental exposure. Nickel's alignment with Pb in RDA may indicate shared accumulation in specific taxa or habitats, especially those with low Zn exposure.

4.3. Taxa comparisons

Species identity emerged as the dominant factor shaping PTE compositional profiles in brown algae, accounting for one-third of the total variance, followed by genus (20.2%) and family (10.1%). This strong taxonomic signal, consistent across both unconstrained (PERMANOVA, PCA) and constrained (RDA) analyses, suggests that elemental distributions reflect functional, ecological, and evolutionary adaptations rather than random variation.

All families exhibited significant differences in PTE composition, though divergence was weakest between Dictyotaceae and Sargassaceae (R^2 = 0.6%). Their compositional similarity likely stems from shared subtidal habitats in tropical to subtropical waters, where Zn availability is typically low (GBIF, n.d.; Morel & Price, 2003). Additionally, their flexible thalli, low fucoidan content, and cell walls rich in mannose and uronic acids may facilitate uptake of Ni, Cu, Cd, and Pb (Table 1) (Anjana & Arunkumar, 2024; Ponce & Stortz, 2020).

In contrast, Fucaceae and Laminariaceae, typical of temperate to cold coastal zones, possess thicker thalli and fucoidan-rich cell walls that enhance Zn retention (GBIF, n.d.; Ponce & Stortz, 2020). Despite these similarities, Laminariaceae showed moderately higher proportions of Cd and Pb than Fucaceae, possibly due to differences in environmental exposure (shallow subtidal vs intertidal, respectively).

These trends are also visualized in the PCA (Figure 2): Fucaceae cluster in the Zn-Cu quadrant, while Sargassaceae and Dictyotaceae group in the Cd-Pb quadrant, albeit with variability. Laminariaceae occupy an intermediate position in the Pb-Cu-Zn quadrant, though their distribution is subtler, reflecting a distinct but overlapping PTE profile.

At the genus level, comparable patterns emerged: *Fucus* exhibited high Zn but low Cd and Pb, whereas *Sargassum* accumulated more Cd and Pb and less Zn. The pronounced capacity of *Sargassum* to take up Cd and Pb has been corroborated by previous studies (Hashim & Chu, 2004; Peng et al., 2022). *Cystoseira* diverged notably from the other Sargassaceae genera, with lower Cd and Pb but higher Zn and intermediate Cu and N. These differences are potentially linked to its robust morphology and preference for rocky shores (Pagana et al., 2024). The compositional similarities among *Padina*, *Polycladia*, and *Turbinaria*, as well as between *Sargassum* and *Turbinaria*, underscore the combined influence of phylogenetic relatedness and shared ecological traits on metal profiles (Table 1, Figure 2 and 3).

Species-specific patterns revealed further differentiation: *Fucus ceranoides* was enriched in Cu relative to Cd, *Fucus vesiculosus* in Zn, and *Sargassum miyabei* in Cd (Figure 3). Non-overlapping ellipses for *F. ceranoides* and *S. miyabei* underscored their ecological divergence. Even phylogenetically close species like *F. ceranoides* and *F. vesiculosus* exhibited distinct profiles (PERMANOVA R^2 = 7%), reflecting their divergent estuarine versus coastal habitats (Pacín et al., 2025). The strongest compositional divergence occurred between ecologically *S. miyabei* (high Pb, Cd, Cu, Ni) and *Laminaria digitata* (Zn-dominated, 91.6%; Table 1)—with an R^2 of 36%, highlighting the profound impact of ecological niche on PTE concentration.

4.4. Temporal trends

The low explanatory power of sampling year across the full dataset (R^2 = 2%) contrasts with the significant temporal declines in PTE concentrations previously reported using absolute values (Aboal et al., 2023). This discrepancy likely reflects the different nature of compositional data. Thus, even with decreasing absolute levels, a stable or noisy pattern in the relative distribution of elements may result in weak temporal signals. Additionally, taxonomic heterogeneity in the full dataset, due to species-specific differences in physiology, habitat, and uptake, may further obscure these patterns.

In contrast, the more homogeneous *Fucus* spp. subset revealed pronounced temporal trends, underscoring the importance of taxonomic consistency in compositional analyses. For this genus, the effect of sampling year explained a substantial proportion of variance (20.4%; PERMANOVA $F = 114.45$, $p < 0.0001$), and 14.9% when Al and Fe were excluded.

Between 1990 and 2001–2007, compositional changes were modest (R^2 = 4.8%), mainly involving a slight decline in Cu and a rise in Al. By 2021, however, profiles had shifted markedly, with sharp increases in Al driving a dilution effect on most other elements (R^2 = 29.5% vs. 1990; 24.5% vs. 2001–2007; Figure 6, Figure S4). Arsenic became more dominant, while Cu, Ni, Cd, and Hg declined, and Pb remained comparatively stable. These trends likely reflect increased sedimentation and particulate deposition in the coastal zone, potentially driven by more frequent storms, higher river discharge, or enhanced coastal erosion, which are processes expected to intensify under climate change (Buckley & Dye, 2009; de Santiago et al., 2021). The intertidal habitat of *Fucus* makes it especially vulnerable to such changes, as its tissues are routinely exposed to resuspended particles. Additionally, the observed rise in As may also result from shifts in phosphate uptake dynamics under acidifying conditions, and changes

in temperature salinity and organic matter (Ahmad & Bhattacharya, 2019; Garbinski et al., 2019; Simou et al., 2024; Smedley & Kinniburgh, 2002).

When compared to patterns in absolute concentrations (Pacín et al., 2025), the compositional data—excluding Al and Fe—show broadly consistent temporal declines in Cu, Ni, Cr, and Pb. This convergence supports a general reduction in pollution inputs over time. However, discrepancies also emerge: Zn decreased by 24.4% in absolute terms but increased by 23.7% compositionally, suggesting a decline in total Zn inputs but a relative increase in its share among PTEs, possibly due to stronger declines in other elements. Likewise, As increased by 113% compositionally but only 36.1% in absolute concentration, indicating a disproportionate enrichment in relative terms. Lead showed an apparent increase of 19.2% in the compositional data but decreased by 21.9% in absolute concentration, likely reflecting its stability in relative proportion due to the marked dilution of other elements.

Importantly, despite the magnitude of the changes, the hierarchy of the compositional structure remained broadly conserved, which further reinforces internal regulatory mechanisms that maintain some balances among trace PTEs.

4.5. Applications

The clear divergence in compositional profiles observed in highly contaminated samples underscores the diagnostic power of this approach. In samples with elevated Pb or Cd, the relative abundances of metals shifted dramatically. Lead, for instance, replaced Zn as the dominant contributor, while Cd showed marked increases beyond species-level baselines (Figure 4). These patterns were not subtle fluctuations but substantial compositional reconfigurations that fell well outside the IQR of the reference distributions. This makes compositional analysis particularly useful for identifying pollution hotspots: samples that deviate sharply from expected profiles can be flagged as highly impacted without requiring predefined concentration thresholds. From a practical perspective, this allows for rapid visual screening of polluted sites based on relative element contributions.

Species-specific profiles also revealed that biomonitor selection can substantially affect contamination assessment. PTE patterns diverged strongly between most species, which are not closely related, showed overlapping profiles, indicating that phylogenetic closeness does not

guarantee compositional similarity. Empirical validation is therefore essential in species selection.

Beyond monitoring, the pronounced taxonomic specificity in PTE accumulation has well-documented implications for bioremediation (Ahmady-Asbchin et al., 2009; Davis et al., 2003; Romera et al., 2007). Several brown algae, including *Padina*, *Dictyota*, and members of the Sargassaceae (e.g., Sargassum), displayed high affinity for Pb and Cd. This trait may be advantageous for remediation efforts under varying environmental conditions. In contrast, taxa such as *Fucus* and *Laminaria* showed consistently higher proportions of Zn, suggesting their potential as effective bioconcentrators in Zn-contaminated areas.

4.6. Limitations

This study has several limitations. First, despite the large dataset (n > 1600), taxonomic imbalance, with nearly 60% of samples belonging to *Fucus* spp. from the Northeast Atlantic, underrepresent variability under-sampled genera (e.g. *Sargassum*, *Padina*, *Laminaria*). Second, habitat differences between taxa complicate comparisons. Intertidal species like *Fucus* are regularly exposed to air, sediments, and fluctuating conditions, including atmospheric contamination, which may enhance passive PTE uptake. In contrast, subtidal genera remain submerged and are subject to distinct biogeochemical dynamics. These ecological contrasts introduce additional variability.

Third, methodological inconsistencies, including differences in tissue processing, preservation, and protocols (García-Seoane et al., 2021), may contribute to variability. Moreover, temporal shifts observed even within the same taxon and site (e.g., *Fucus* spp.) point to strong environmental influences on PTE compositional pattern.

In addition, the lack of data on metal speciation limits our ability to fully interpret bioavailability and uptake mechanisms. While compositional data provide valuable insights into relative patterns and reduce certain biases, this approach also has limitations, such as the loss of absolute concentration context and the challenge of interpreting changes when total metal loads vary significantly across samples.

In summary, while species identity is a key structuring factor, PTE profiles in brown algae arise from a complex interplay of biological, ecological, and methodological drivers. To strengthen brown algae knowledge in PTEs content future studies should expand taxonomic and

geographic coverage, standardize sampling and protocols, and integrate critical environmental metadata. Resolving intra-specific variability is essential to distinguish physiological signals from environmental noise and improve the ecological interpretability of compositional data.

Conclusions

This study presents the first global assessment of PTE composition in brown algae using a compositional framework, yielding new insights into species-specific accumulation patterns, temporal dynamics, and potential applications in environmental monitoring and bioremediation. Zinc consistently dominated the elemental profiles, followed by Cu and Ni, while Pb and Cd contributed more modestly and with greater variability. However, PTE composition in brown algae was strongly structured by taxonomy, reflecting a complex interplay between phylogenetic constraints and ecological niche adaptation.

Despite variability in environmental concentrations, the observed patterns suggest that brown algae maintain relatively stable intracellular metal profiles, pointing to biological regulation. However, this regulation is not absolute: local environmental conditions, temporal trends, and physiological plasticity introduce variation. Compositional analysis also proved useful for detecting high contamination loads, with heavily impacted samples showing clear departures from species-level fingerprints.

Compositional data provide a window into the physiological mechanisms governing metal homeostasis in macroalgae. Unlike absolute concentration data, compositional profiles are less affected by transient fluctuations, dilution effects, or sampling inconsistencies, offering a robust and sensitive indicator of pollution. Therefore, we advocate for the joint use of absolute and compositional approaches, as they offer complementary insights. This dual perspective enhances both the diagnostic value of PTE monitoring and our understanding of how macroalgae mediate metal dynamics across marine environments.

References

Abdallah, A., Abdallah, M., & Beltagy, A. (2005). Contents of heavy metals in marine seaweeds from the Egyptian coast of the Red Sea. Chemistry and Ecology, 21(5), 399–411. https://doi.org/10.1080/02757540500290222

Aboal, J. R., Pacín, C., García-Seoane, R., Varela, Z., González, A. G., & Fernández, J. A. (2023). Global decrease in heavy metal concentrations in brown algae in the last 90 years.

Journal of Hazardous Materials, 445, 130511. https://doi.org/10.1016/J.JHAZMAT.2022.130511

Ahmad, A., & Bhattacharya, P. (2019). Environmental arsenic in a changing world. Groundwater for Sustainable Development, 8, 169–171. https://doi.org/10.1016/J.GSD.2018.11.001

Ahmady-Asbchin, S., Andres, Y., Gerente, C., & Cloirec, P. Le. (2009). Natural seaweed waste as sorbent for heavy metal removal from solution. Environmental Technology, 30(7), 755–762. https://doi.org/10.1080/09593330902919401

Aitchison, J., & Egozcue, J. J. (2005). Compositional data analysis: Where are we and where should we be heading? Mathematical Geology, 37(7), 829–850. https://doi.org/10.1007/S11004-005-7383-7/METRICS

Andreini, C., Banci, L., Bertini, I., & Rosato, A. (2006). Zinc through the three domains of life. Journal of Proteome Research, 5(11), 3173–3178. https://doi.org/10.1021/PR0603699

Anjana, K., & Arunkumar, K. (2024). Brown algae biomass for fucoxanthin, fucoidan and alginate; update review on structure, biosynthesis, biological activities and extraction valorisation. International Journal of Biological Macromolecules, 280, 135632. https://doi.org/10.1016/J.IJBIOMAC.2024.135632

Barreiro, R., Picado, L., & Real, C. (2002). Biomonitoring Heavy Metals in Estuaries: A Field Comparison of Two Brown Algae Species Inhabiting Upper Estuarine Reaches. Environmental Monitoring and Assessment 2002 75:2, 75(2), 121–134. https://doi.org/10.1023/A:1014479612811

Basit, A., & Hussain, S. (2024). Soil zinc application decreases arsenic and increases zinc accumulation in grains of zinc-biofortified wheat cultivars. Crop & Pasture Science, 75(4). https://doi.org/10.1071/CP23275

Brinza, L., Geraki, K., Breaban, I. G., & Neamtu, M. (2019). Zn adsorption onto Irish Fucus vesiculosus: Biosorbent uptake capacity and atomistic mechanism insights. Journal of Hazardous Materials, 365, 252–260. https://doi.org/10.1016/J.JHAZMAT.2018.11.009

Buckley, P. J., & Dye, S. R. (2009). Impacts of climate change on the North-East Atlantic ecosystem.

Castro, B. B., Cotas, J., Gomes, L., Pacheco, D., & Pereira, L. (2023). Ecosystem Services Provided by Seaweeds. Hydrobiology, 2(1), 75–96. https://doi.org/10.3390/HYDROBIOLOGY2010006

Chakraborty, S., & Owens, G. (2014). Metal distributions in seawater, sediment and marine benthic macroalgae from the South Australian coastline. International Journal of Environmental Science and Technology, 11(5), 1259–1270. https://doi.org/10.1007/S13762-013-0310-4/

Chen, C. F., Ju, Y. R., Chen, C. W., & Dong, C. Di. (2019). Changes in the total content and speciation patterns of metals in the dredged sediments after ocean dumping: Taiwan continental slope. Ocean & Coastal Management, 181, 104893. https://doi.org/10.1016/J.OCECOAMAN.2019.104893

Commission Regulation (EU) 2023/915 on Maximum Levels for Certain Contaminants in Food and Repealing Regulation (EC) No 1881/2006. (2023). https://eur-lex.europa.eu/eli/reg/2023/915/oj/eng

Contreras-Porcia, L., Meynard, A., López-Cristoffanini, C., Latorre, N., & Kumar, M. (2017). Marine Metal Pollution and Effects on Seaweed Species. Systems Biology of Marine Ecosystems, 35–48. https://doi.org/10.1007/978-3-319-62094-7_3

Davis, T. A., Volesky, B., & Mucci, A. (2003). A review of the biochemistry of heavy metal biosorption by brown algae. Water Research, 37(18), 4311–4330. https://doi.org/10.1016/S0043-1354(03)00293-8

de Santiago, I., Camus, P., González, M., Liria, P., Epelde, I., Chust, G., del Campo, A., & Uriarte, A. (2021). Impact of climate change on beach erosion in the Basque Coast (NE Spain). Coastal Engineering, 167, 103916. https://doi.org/10.1016/J.COASTALENG.2021.103916

Demirevska-Kepova, K., Simova-Stoilova, L., Stoyanova, Z., Hölzer, R., & Feller, U. (2004). Biochemical changes in barley plants after excessive supply of copper and manganese. Environmental and Experimental Botany, 52(3), 253–266. https://doi.org/10.1016/J.ENVEXPBOT.2004.02.004

Dong, Y., Rosenbaum, R. K., & Hauschild, M. Z. (2016). Assessment of Metal Toxicity in Marine Ecosystems: Comparative Toxicity Potentials for Nine Cationic Metals in Coastal

Seawater. Environmental Science and Technology, 50(1), 269–278. https://doi.org/10.1021/ACS.EST.5B01625

eGEOTRACES. (n.d.). Retrieved June 19, 2025, from https://www.egeotraces.org/

Ender, E., Subirana, M. A., Raab, A., Krupp, E. M., Schaumlöffel, D., & Feldmann, J. (2019). Why is NanoSIMS elemental imaging of arsenic in seaweed (Laminaria digitata) important for understanding of arsenic biochemistry in addition to speciation information? Journal of Analytical Atomic Spectrometry, 34(11), 2295–2302. https://doi.org/10.1039/C9JA00187E

Ferdouse, Fatima., Holdt, S. Løvstad., Smith, Rohan., Murúa, Pedro., & Yang, Zhengyong. (2018). The global status of seaweed production, trade and utilization. Globefish Resarch Programme. Food and Agriculture Organization of the United Nations.

Förstner, U., & Wittmann, G. T. W. (1981). Metal Pollution in the Aquatic Environment. Metal Pollution in the Aquatic Environment. https://doi.org/10.1007/978-3-642-69385-4

Garbinski, L. D., Rosen, B. P., & Chen, J. (2019). Pathways of arsenic uptake and efflux. Environment International, 126, 585–597. https://doi.org/10.1016/J.ENVINT.2019.02.058

García-Seoane, R., Fernández, J. A., Boquete, M. T., & Aboal, J. R. (2019). Application of macroalgae analysis to assess the natural variability in selected pollution concentrations (N and Hg), and to detect sources of it in coastal environments. Science of The Total Environment, 650, 1403–1411. https://doi.org/10.1016/J.SCITOTENV.2018.09.156

García-Seoane, R., Fernández, J. A., Boquete, M. T., & Aboal, J. R. (2021). Analysis of intra-thallus and temporal variability of trace elements and nitrogen in Fucus vesiculosus: Sampling protocol optimization for biomonitoring. Journal of Hazardous Materials, 412, 125268. https://doi.org/10.1016/J.JHAZMAT.2021.125268

García-Seoane, R., Fernández, J. A., Villares, R., & Aboal, J. R. (2018). Use of macroalgae to biomonitor pollutants in coastal waters: Optimization of the methodology. Ecological Indicators, 84, 710–726. https://doi.org/10.1016/j.ecolind.2017.09.015

GBIF. (n.d.). Retrieved June 15, 2025, from https://www.gbif.org/es/

Geddie, A. W., & Hall, S. G. (2019). An introduction to copper and zinc pollution in macroalgae: for use in remediation and nutritional applications. Journal of Applied Phycology, 31(1), 691–708. https://doi.org/10.1007/S10811-018-1580-5/

H. Wickham. (2016). ggplot2: Elegant Graphics for Data Analysis. Springer-Verlag.

Hashim, M. A., & Chu, K. H. (2004). Biosorption of cadmium by brown, green, and red seaweeds. Chemical Engineering Journal, 97(2–3), 249–255. https://doi.org/10.1016/S1385-8947(03)00216-X

Henriques, B., Rocha, L. S., Lopes, C. B., Figueira, P., Monteiro, R. J. R., Duarte, A. C., Pardal, M. A., & Pereira, E. (2015). Study on bioaccumulation and biosorption of mercury by living marine macroalgae: Prospecting for a new remediation biotechnology applied to saline waters. Chemical Engineering Journal, 281, 759–770. https://doi.org/10.1016/J.CEJ.2015.07.013

Hoeks, S., Huijbregts, M. A. J., Douziech, M., Hendriks, A. J., & Oldenkamp, R. (2020). Mean Species Abundance as a Measure of Ecotoxicological Risk. Environmental Toxicology and Chemistry, 39(11), 2304–2313. https://doi.org/10.1002/ETC.4850

Holan, Z. R., & Volesky, B. (1994). Biosorption of lead and nickel by biomass of marine algae. Biotechnology and Bioengineering, 43(11), 1001–1009. https://doi.org/10.1002/BIT.260431102

Islam, M. S., & Tanaka, M. (2004). Impacts of pollution on coastal and marine ecosystems including coastal and marine fisheries and approach for management: a review and synthesis. Marine Pollution Bulletin, 48(7–8), 624–649. https://doi.org/10.1016/J.MARPOLBUL.2003.12.004

Jayakumar, V., Govindaradjane, S., Rajamohan, N., & Rajasimman, M. (2022). Biosorption potential of brown algae, Sargassum polycystum, for the removal of toxic metals, cadmium and zinc. Environmental Science and Pollution Research, 29(28), 41909–41922. https://doi.org/10.1007/S11356-021-15185-7

Johnston, E. L., & Roberts, D. A. (2009). Contaminants reduce the richness and evenness of marine communities: A review and meta-analysis. Environmental Pollution, 157(6), 1745–1752. https://doi.org/10.1016/J.ENVPOL.2009.02.017

Kahal, A. Y., El-Sorogy, A. S., Qaysi, S. I., Al-Hashim, M. H., & Al-Dossari, A. (2023). Environmental Risk Assessment and Sources of Potentially Toxic Elements in Seawater of Jazan Coastal Area, Saudi Arabia. Water, 15(18), 3174. https://doi.org/10.3390/W15183174

Khan, M. I., Zahoor, M., Khan, A., Gulfam, N., & Khisroon, M. (2019). Bioaccumulation of Heavy Metals and their Genotoxic Effect on Freshwater Mussel. Bulletin of Environmental Contamination and Toxicology, 102(1), 52–58. https://doi.org/10.1007/S00128-018-2492-4

Lanceman, D., Mayer-Pinto, M., & Glamore, W. (2025). Ecosystem Service Trajectories in Restored Coastal Habitats. Global Change Biology, 31(3), e70151. https://doi.org/10.1111/GCB.70151

Lane, T. W., Saito, M. A., George, G. N., Pickering, I. J., Prince, R. C., & Morell, F. M. M. (2005). Biochemistry: A cadmium enzyme from a marine diatom. Nature, 435(7038), 42. https://doi.org/10.1038/435042A

Lewis, C., Guitart, C., Pook, C., Scarlett, A., Readman, J. W., & Galloway, T. S. (2010). Integrated assessment of oil pollution using biological monitoring and chemical fingerprinting. Environmental Toxicology and Chemistry, 29(6), 1358–1366. https://doi.org/10.1002/ETC.156

Lobban, C. S., & Harrison, P. J. (1994). Seaweed Ecology and Physiology. https://doi.org/10.1017/CBO9780511626210

Lu, Y., Yuan, J., Lu, X., Su, C., Zhang, Y., Wang, C., Cao, X., Li, Q., Su, J., Ittekkot, V., Garbutt, R. A., Bush, S., Fletcher, S., Wagey, T., Kachur, A., & Sweijd, N. (2018). Major threats of pollution and climate change to global coastal ecosystems and enhanced management for sustainability. Environmental Pollution, 239, 670–680. https://doi.org/10.1016/J.ENVPOL.2018.04.016

Mata, Y. N., Blázquez, M. L., Ballester, A., González, F., & Muñoz, J. A. (2008). Characterization of the biosorption of cadmium, lead and copper with the brown alga Fucus vesiculosus. Journal of Hazardous Materials, 158(2–3), 316–323. https://doi.org/10.1016/J.JHAZMAT.2008.01.084

Meharg, A. A., & Hartley-Whitaker, J. (2002). Arsenic uptake and metabolism in arsenic resistant and nonresistant plant species. New Phytologist, 154(1), 29–43. https://doi.org/10.1046/J.1469-8137.2002.00363.X

Millero, F. J., Woosley, R., Ditrolio, B., & Waters, J. (2009). Effect of ocean acidification on the speciation of metals in seawater. Oceanography, 22(4), 72–85. https://doi.org/10.5670/OCEANOG.2009.98

Morel, F. M. M., Lam, P. J., & Saito, M. A. (2020). Trace Metal Substitution in Marine Phytoplankton. Annual Review of Earth and Planetary Sciences, 48, 491–517. https://doi.org/10.1146/ANNUREV-EARTH-053018-060108

Morel, F. M. M., & Price, N. M. (2003). The biogeochemical cycles of trace metals in the oceans. Science, 300(5621), 944–947. https://doi.org/10.1126/SCIENCE.1083545

Neff, J. M. (2002). Cadmium in the Ocean. Bioaccumulation in Marine Organisms, 89–102. https://doi.org/10.1016/B978-008043716-3/50006-3

Nieboer, E., & Richardson, D. H. S. (1980). The replacement of the nondescript term 'heavy metals' by a biologically and chemically significant classification of metal ions. Environmental Pollution Series B, Chemical and Physical, 1(1), 3–26. https://doi.org/10.1016/0143-148X(80)90017-8

Noraho, N., & Gaur, J. P. (1995). Effect of cations, including heavy metals, on cadmium uptake by Lemna polyrhiza L. Biometals, 8(2), 95–98. https://doi.org/10.1007/BF00142006

Oksanen, J., Simpson, G. L., Blanchet, F. G., Kindt, R., Legendre, P., Minchin, P. R., O'Hara, R. B., Solymos, P., Stevens, M. H. H., Szoecs, E., Wagner, H., Barbour, M., Bedward, M., Bolker, B., Borcard, D., Borman, T., Carvalho, G., Chirico, M., De Caceres, M., … Weedon, J. (2025). Community Ecology Package [R package vegan version 2.7-1]. CRAN: Contributed Packages. https://doi.org/10.32614/CRAN.PACKAGE.VEGAN

Pacín, C., Fernández, J. Á., Conde-Amboage, M., Lazzari, M., García-Seoane, R., Viana, I. G., Varela, Z., Real, C., Villares, R., & Aboal, J. R. (2025). Three Decades of Change in Potentially Toxic Elements in Brown Algae in the Northeast Atlantic Ocean. Environmental Science and Technology. https://doi.org/10.1021/ACS.EST.4C14013

Pagana, I., Nava, V., Puglia, G. D., Genovese, C., Emma, G., Salonia, C., Cicero, N., & Alongi, G. (2024). Cystoseira compressa and Ericaria mediterranea: Effective Bioindicators for Heavy- and Semi-Metal Monitoring in Marine Environments with Rocky Substrates. Plants, 13(4), 530. https://doi.org/10.3390/PLANTS13040530

Park, S., Choi, M., Jang, D., Joe, D., & Park, K. (2020). Distribution and Sources of Dissolved and Particulate Heavy Metals (Mn, Co, Ni, Cu, Zn, Cd, Pb) in Masan Bay, Korea. Ocean Science Journal, 55(1), 49–67. https://doi.org/10.1007/S12601-020-0001-2

Patterson, C., Settle, D., & Glover, B. (1976). Analysis of lead in polluted coastal seawater. Marine Chemistry, 4(4), 305–319. https://doi.org/10.1016/0304-4203(76)90017-7

Peng, Z., Guo, Z., Wang, Z., Zhang, R., Wu, Q., Gao, H., Wang, Y., Shen, Z., Lek, S., & Xiao, J. (2022). Species-specific bioaccumulation and health risk assessment of heavy metal in seaweeds in tropic coasts of South China Sea. Science of The Total Environment, 832, 155031. https://doi.org/10.1016/J.SCITOTENV.2022.155031

Ponce, N. M. A., & Stortz, C. A. (2020). A Comprehensive and Comparative Analysis of the Fucoidan Compositional Data Across the Phaeophyceae. Frontiers in Plant Science, 11, 556312. https://doi.org/10.3389/FPLS.2020.556312/

Rainbow, P. S. (2002). Trace metal concentrations in aquatic invertebrates: why and so what? Environmental Pollution, 120(3), 497–507. https://doi.org/10.1016/S0269-7491(02)00238-5

Real, C., Ángel Fernández, J., Aboal, J. R., & Carballeira, A. (2011). Substituting missing data in compositional analysis. Environmental Pollution, 159(10), 2797–2800. https://doi.org/10.1016/J.ENVPOL.2011.05.006

Romera, E., González, F., Ballester, A., Blázquez, M. L., & Muñoz, J. A. (2007). Comparative study of biosorption of heavy metals using different types of algae. Bioresource Technology, 98(17), 3344–3353. https://doi.org/10.1016/J.BIORTECH.2006.09.026

Schropp, S. J., Graham Lewis, F., Windom, H. L., Ryan, J. D., Calder, F. D., & Burney, L. C. (1990). Interpretation of metal concentrations in estuarine sediments of Florida using aluminum as a reference element. Estuaries, 13(3), 227–235. https://doi.org/10.2307/1351913

Sharifi, Z., Hossaini, S. M. T., & Renella, G. (2016). Risk assessment for sediment and stream water polluted by heavy metals released by a municipal solid waste composting plant. Journal of Geochemical Exploration, 169, 202–210. https://doi.org/10.1016/J.GEXPLO.2016.08.001

Simou, A., Mrabet, A., Abdelfattah, B., Bougrine, O., Khaddor, M., & Allali, N. (2024). Distribution, ecological, and health risk assessment of trace elements in the surface seawater

along the littoral of Tangier Bay (Southwestern Mediterranean Sea). Marine Pollution Bulletin, 202, 116362. https://doi.org/10.1016/J.MARPOLBUL.2024.116362

Skipnes, O., Ronald, T., & Haug, A. (1975). Uptake of Zinc and Strontium by Brown Algae. Physiologia Plantarum, 34(4), 314–320. https://doi.org/10.1111/J.1399-3054.1975.TB03845.X

Smedley, P. L., & Kinniburgh, D. G. (2002). A review of the source, behaviour and distribution of arsenic in natural waters. Applied Geochemistry, 17(5), 517–568. https://doi.org/10.1016/S0883-2927(02)00018-5

Somma, R., Ebrahimi, P., Troise, C., De Natale, G., Guarino, A., Cicchella, D., & Albanese, S. (2021). The first application of compositional data analysis (CoDA) in a multivariate perspective for detection of pollution source in sea sediments: The Pozzuoli Bay (Italy) case study. Chemosphere, 274, 129955. https://doi.org/10.1016/J.CHEMOSPHERE.2021.129955

Stockdale, A., Tipping, E., Lofts, S., & Mortimer, R. J. G. (2016). Effect of Ocean Acidification on Organic and Inorganic Speciation of Trace Metals. Environmental Science and Technology, 50(4), 1906–1913. https://doi.org/10.1021/ACS.EST.5B05624

Syaifudin, M., Moussa, M. G., Li, T., & Du, H. (2025). The impact of salinity on heavy metal accumulation in seaweed. Marine Pollution Bulletin, 214, 117819. https://doi.org/10.1016/J.MARPOLBUL.2025.117819

Takolander, A., Leskinen, E., & Cabeza, M. (2017). Synergistic effects of extreme temperature and low salinity on foundational macroalga Fucus vesiculosus in the northern Baltic Sea. Journal of Experimental Marine Biology and Ecology, 495, 110–118. https://doi.org/10.1016/J.JEMBE.2017.07.001

Thomas, J. C., Malick, F. K., Endreszl, C., Davies, E. C., & Murray, K. S. (1998). Distinct responses to copper stress in the halophyte Mesembryanthemum crystallinum. Physiologia Plantarum, 102(3), 360–368. https://doi.org/10.1034/J.1399-3054.1998.1020304.X

Töpperwien, S., Behra, R., & Sigg, L. (2007). Competition among zinc, manganese, and cadmium uptake in the freshwater alga Scenedesmus vacuolatus. Environmental Toxicology and Chemistry, 26(3), 483–490. https://doi.org/10.1897/06-181R.1

Tuzen, M., Verep, B., Ogretmen, A. O., & Soylak, M. (2009). Trace element content in marine algae species from the Black Sea, Turkey. Environmental Monitoring and Assessment, 151(1–4), 363–368. https://doi.org/10.1007/S10661-008-0277-7

Unsworth, R. K. F., & Cullen-Unsworth, L. C. (2014). Biodiversity, ecosystem services, and the conservation of seagrass meadows. Coastal Conservation, 95–130. https://doi.org/10.1017/CBO9781139137089.005

van den Boogaart, K., Tolosana-Delgado R, & Bren M. (2024). compositions: Compositional Data Analysis. https://doi.org/10.32614/CRAN.PACKAGE.COMPOSITIONS

Vázquez-Arias, A., Boquete, M. T., Fernández, J. Á., & Aboal, J. R. (2025). Assessing the effectiveness of seaweed transplants in reflecting seawater pollution levels. Environmental Pollution, 377, 126456. https://doi.org/10.1016/j.envpol.2025.126456

Vázquez-Arias, A., Boquete, M. T., Martín-Jouve, B., Tucoulou, R., Rodríguez-Prieto, C., Fernández, J. Á., & Aboal, J. R. (2024). Nanoscale distribution of potentially toxic elements in seaweeds revealed by synchrotron X-ray fluorescence. Journal of Hazardous Materials, 480, 136454. https://doi.org/10.1016/J.JHAZMAT.2024.136454

Vázquez-Arias, A., Pacín, C., Ares, Á., Fernández, J. Á., & Aboal, J. R. (2023). Do we know the cellular location of heavy metals in seaweed? An up-to-date review of the techniques. Science of the Total Environment, 856(September 2022). https://doi.org/10.1016/j.scitotenv.2022.159215

Vázquez-Arias, A., Rodríguez-Prieto, C., Yamada, Y., Ito, M., Fernández, J. Á., & Aboal, J. R. (n.d.). Deciphering uptake mechanisms of potentially toxic elements in seaweeds using high resolution imaging analysis. Under Review.

Vijayaraghavan, J., Zunaithur Rahman, D., & Thivya, J. (2021). Comparative assessment and optimization of Pb(II), Ni(II), and Zn(II) biosorption onto Gelidiella acerosa in single systems: equilibrium and kinetic modeling. Desalination and Water Treatment, 209, 254–266. https://doi.org/10.5004/DWT.2021.26487

Wang, W. X. (2002). Interactions of trace metals and different marine food chains. Marine Ecology Progress Series, 243, 295–309. https://doi.org/10.3354/MEPS243295

Xie, D., Wei, H., Huang, Y., Qian, J., Zhang, Y., & Wang, M. (2024). Elevated temperature as a dominant driver to aggravate cadmium toxicity: Investigations through toxicokinetics and omics. Journal of Hazardous Materials, 474, 134789. https://doi.org/10.1016/J.JHAZMAT.2024.134789

Xu, J., Bland, G. D., Gu, Y., Ziaei, H., Xiao, X., Deonarine, A., Reible, D., Bireta, P., Hoelen, T. P., & Lowry, G. V. (2021). Impacts of Sediment Particle Grain Size and Mercury Speciation on Mercury Bioavailability Potential. Environmental Science and Technology, 55(18), 12393–12402. https://doi.org/10.1021/ACS.EST.1C03572

Zhang, Y., Schluter, J., Zhang, L., Cao, X., Jenq, R. R., Feng, H., Haines, J., & Zhang, L. (2024). Review and revamp of compositional data transformation: A new framework combining proportion conversion and contrast transformation. Computational and Structural Biotechnology Journal, 23, 4088–4107. https://doi.org/10.1016/J.CSBJ.2024.11.003/

Zheng, J., Gu, X.-Q., Zhang, T.-J., Liu, H.-H., Ou, Q.-J., & Peng, C.-L. (2018). Phytotoxic effects of Cu, Cd and Zn on the seagrass Thalassia hemprichii and metal accumulation in plants growing in Xincun Bay, Hainan, China. Ecotoxicology, 27(5), 517–526. https://doi.org/10.1007/s10646-018-1924-6

Zhou, Q., Wang, S., Liu, J., Hu, X., Liu, Y., He, Y., He, X., & Wu, X. (2022). Geological evolution of offshore pollution and its long-term potential impacts on marine ecosystems. Geoscience Frontiers, 13(5), 101427. https://doi.org/10.1016/J.GSF.2022.101427

Declaration of generative AI and AI-assisted technologies in the writing process.

During the preparation of this work the authors used chat GPT in order to improve readability and language. After using this tool, the authors reviewed and edited the content as needed and take full responsibility for the content of the publication.

Acknowledgments

C. Pacín was supported by a predoctoral grant from Xunta de Galicia (ED481A 2022/374).

Author contributions

Carme Pacín: Formal analysis, Writing - Original Draft, Writing - Review & Editing; J. Ángel Fernández: Writing - Review & Editing; Jesús R. Aboal: Conceptualization, Writing - Review & Editing

Supporting information

Tracing Pollution in Brown Algae: A Compositional Analysis of Potentially Toxic Element Profiles

Carme Pacín[1*], J. Ángel Fernández[2], Jesús R. Aboal[2]

1. CIQUS Center, Department of Physical Chemistry, Universidade de Santiago de Compostela, Santiago de Compostela, 15782, Spain
2. CRETUS Center, Department of Functional Biology, Ecology Unit, Universidade de Santiago de Compostela, Santiago de Compostela, 15782, Spain

*corresponding author: mcarme.pacin@usc.es

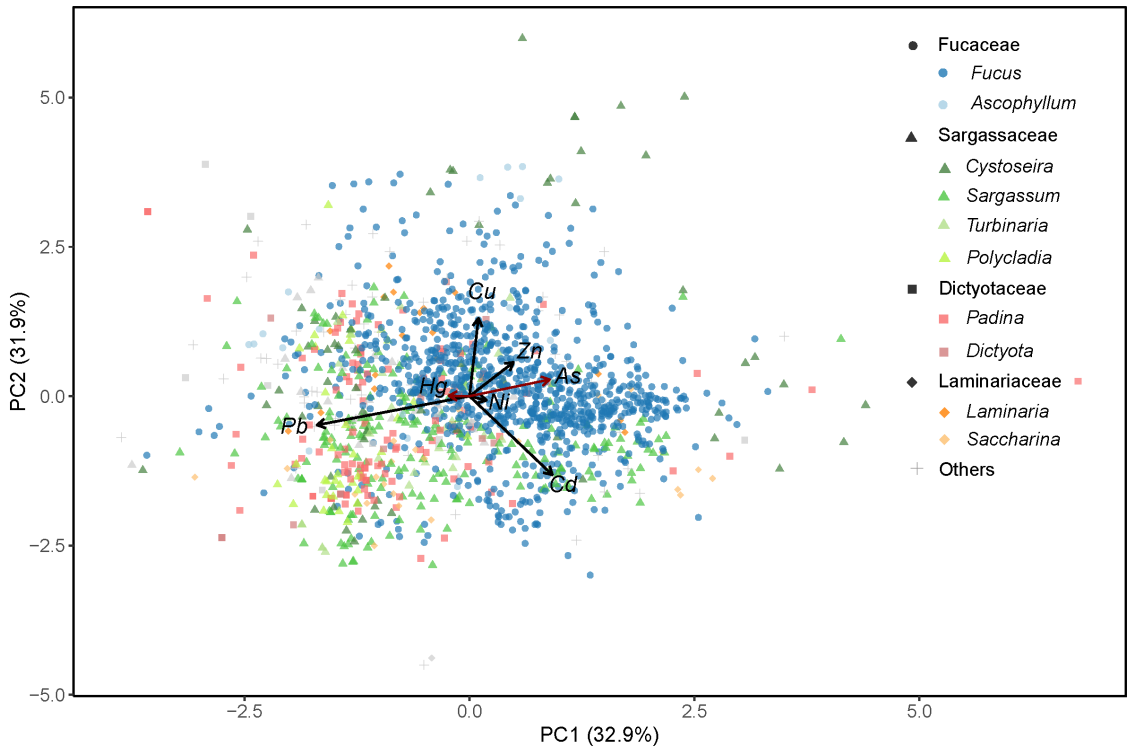

Figure S1. Principal Component Analysis of CLR-transformed Potentially Toxic Element composition in brown algae. Each point represents an individual sample, colored by genus and shaped by family. Grey symbols indicate genera not explicitly represented in the color legend but belonging to the same family. Arsenic (As) and mercury (Hg), included as supplementary variables, are represented as vectors based on their correlation with components 1 and 2.

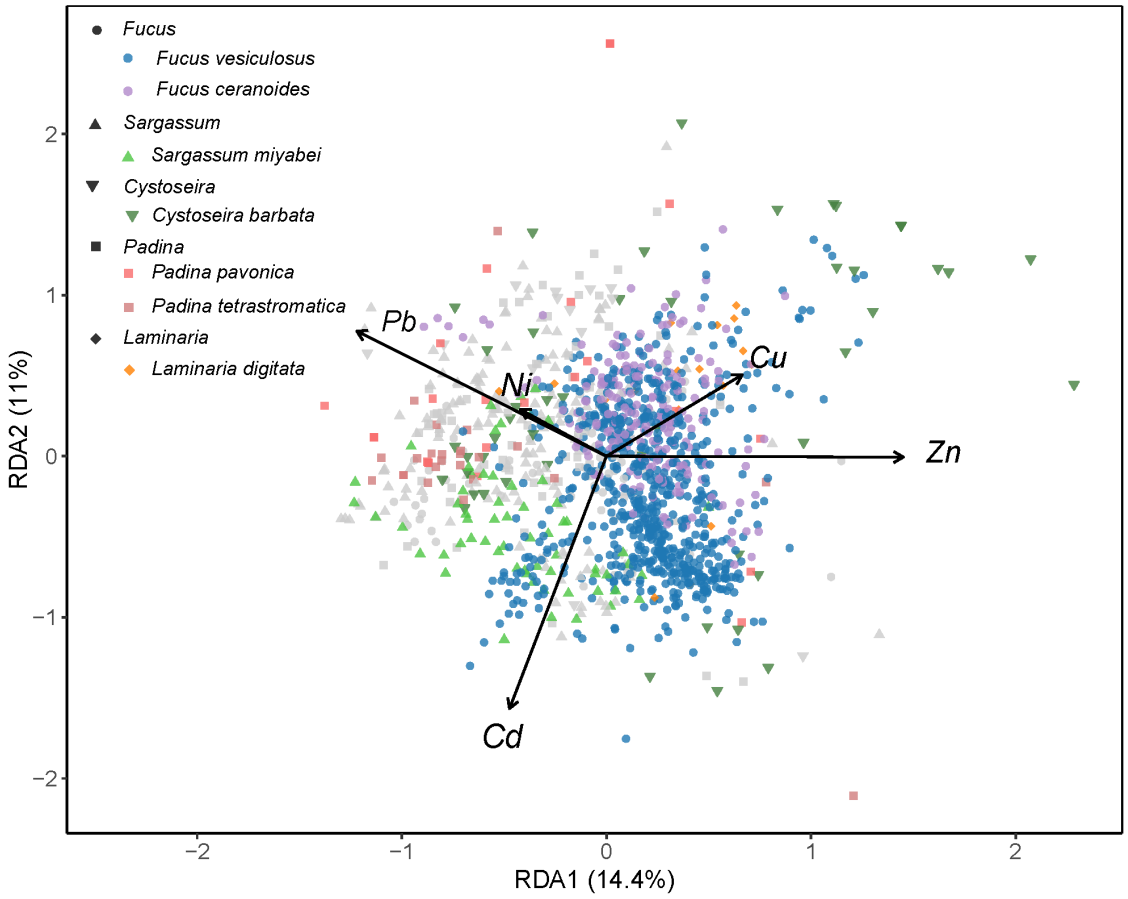

Figure S2. Redundancy Analysis of CLR-transformed trace Potentially Toxic ElEMENTS composition constrained by species identity. Each point represents an individual sample, colored by species and shaped by genus. Grey symbols indicate samples from species not highlighted in the legend but belonging to the same genera. Samples from other genera are not displayed but were included in the analysis. Arrows represent the loadings of individual elements, indicating their contribution to the constrained ordination space.

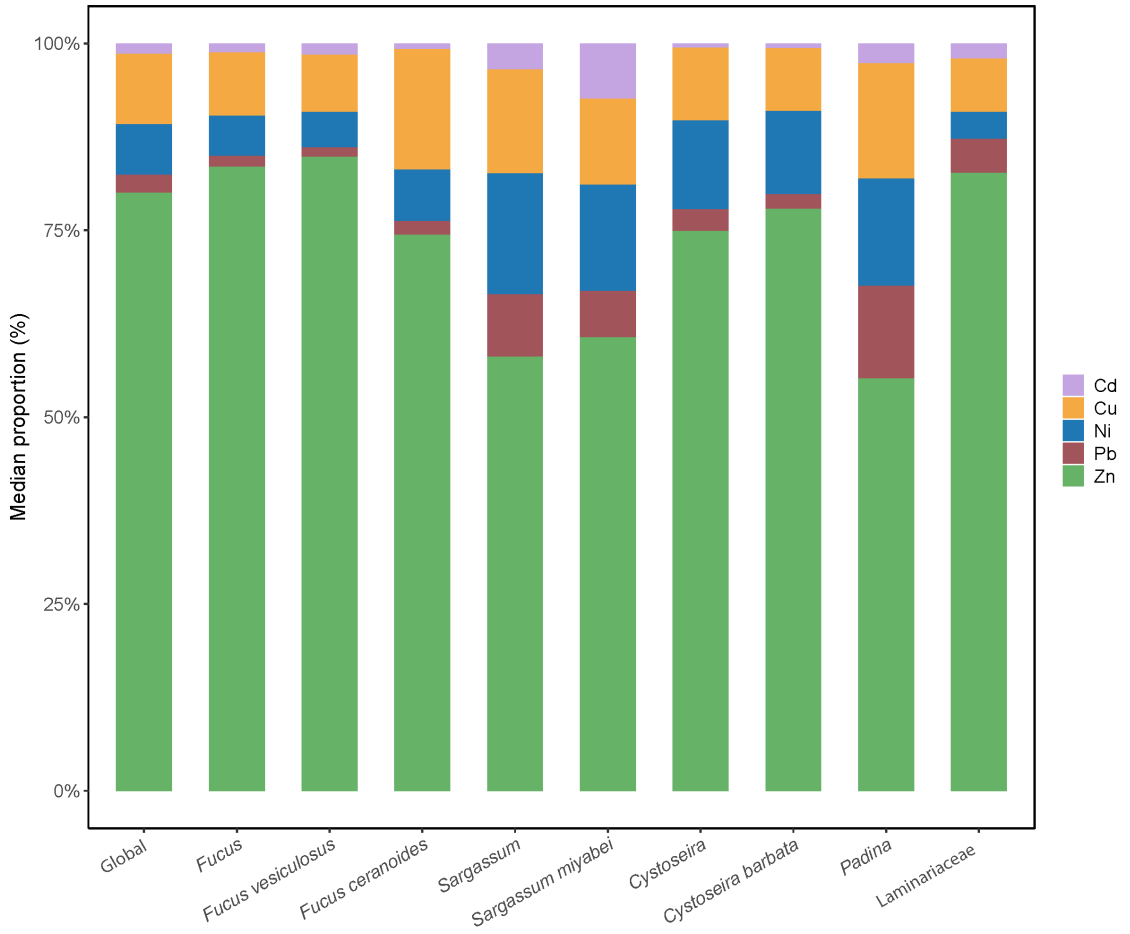

Figure S3. Median compositional profile of Potentially Toxic Elements (Ni, Cu, Zn, Cd, Pb) in brown algae for the overall dataset and top-ranking taxa. Stacked bars represent the median element proportions within each group, expressed as a percentage of the total content.

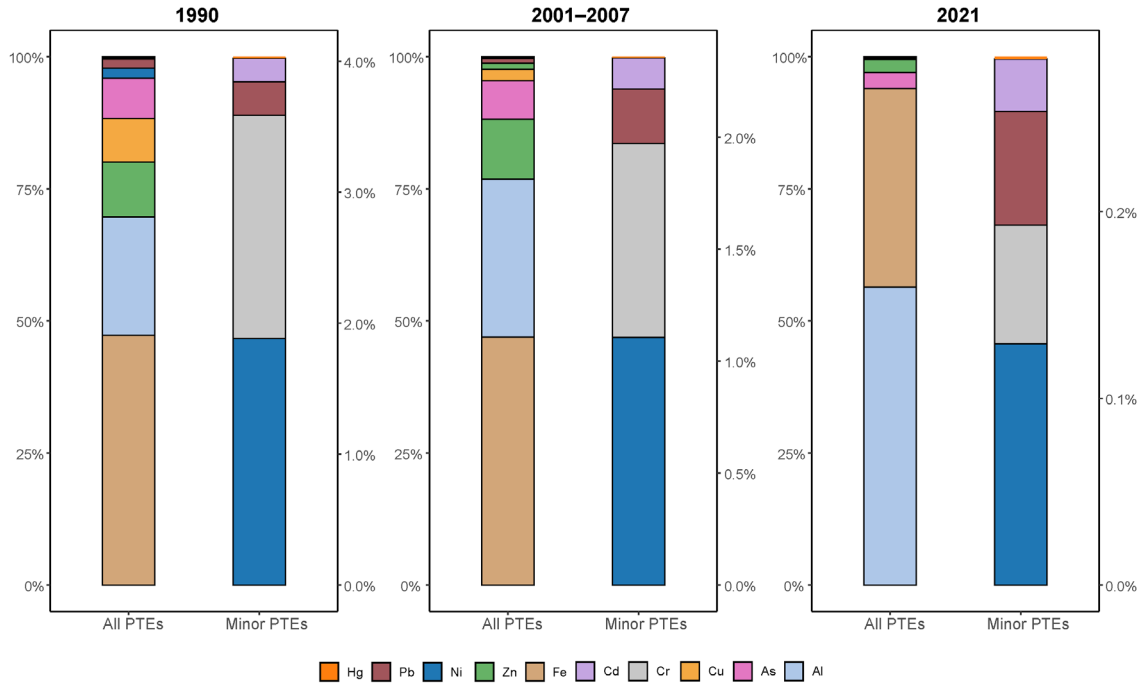

Figure S4. Compositional profiles of Potentially Toxic Elements in *Fucus* spp. across three time periods: 1990, 2001–2007, and 2021. Bars represent centered log-ratio (CLR)-transformed relative contributions of each element to the overall profile.

6. DISCUSIÓN XERAL

6.1. Contextualización

A biomonitorización con algas pardas converteuse nunha ferramenta útil para inferir a presenza e dispoñibilidade de contaminantes no medio mariño, así como para identificar vías de entrada á cadea trófica e avaliar o estado fisiolóxico e ecolóxico destes organismos clave nos ecosistemas costeiros. Con todo, esta aproximación **non evolucionou cara a unha disciplina cun corpo metodolóxico e conceptual claramente definido**. Pola contra, a maior parte dos estudos existentes son traballos illados, publicados por investigadoras e investigadores sen continuidade temática. De feito, segundo datos de *Scopus*, dos 4357 autores e autoras que publicaron sobre biomonitorización, acumulación ou contido de PTEs en algas pardas, só 177 asinan tres ou máis traballos nesta liña. Isto tradúcese nunha literatura **fundamentalmente descritiva**, cun **baixo grao de integración**, **escasa discusión crítica** e **limitado desenvolvemento metodolóxico**.

Para superar esta limitación, nesta tese, ademais de xerar novos datos, realizouse un esforzo sistemático por **recoller, integrar e reinterpretar a información xa dispoñible**, co obxectivo de responder á necesidade dunha visión global sobre a exposición das algas pardas aos contaminantes mariños. Este enfoque permitiu abordar cuestións clave como a caracterización das concentracións de PTEs en algas pardas, a identificación de asociacións entre elementos, a influencia da taxonomía na bioconcentración, a determinación das fontes e vías de entrada da contaminación, e, sobre todo, a **avaliación das tendencias temporais**.

A tese incorpora ademais avances metodolóxicos significativos, entre os que destaca a aplicación pioneira da **análise composicional de PTEs** en algas pardas (Capítulo 5), así como a primeira **caracterización *in vivo* da presenza e evolución temporal de AgNPs** en algas pardas baixo condicións ambientais reais (Capítulo 4).

Para abordar todas estas cuestións, deseñouse un enfoque multidimensional que permitiu analizar a exposición das algas pardas a PTEs e AgNPs desde distintas perspectivas complementarias, tanto a nivel espacial, temporal e taxonómico como a través de distintas escalas (rexional *vs.* global) e aproximacións analíticas (concentracións absolutas *vs.* perfís composicionais).

6.2. Caracterización xeral das concentracións

A calidade analítica foi avaliada sistematicamente mediante materiais de referencia certificados, brancos e réplicas, demostrando unha boa **precisión**, con recuperacións do 90–110 %, e diferenzas entre réplicas inferiores ao 9 %. A **sensibilidade** tamén foi adecuada ca superación do límite de cuantificación (LOQ) na práctica totalidade das mostras (agás Cr, co 4 % das mostras por debaixo deste limiar). A única excepción notable foi a cuantificación de AgNPs, cun coeficiente de variación do 36 %, reflexo da alta variabilidade intrínseca á detección de partículas a niveis traza en matrices biolóxicas. Este resultado subliña unha das maiores limitacións metodolóxicas actuais na nanotecnoloxía ambiental, onde a falta de protocolos estandarizados e a influencia da matriz poden xerar incertezas significativas[121].

Estatisticamente, os datos de PTEs amosaron **distribucións non normais** (test de Shapiro-Wilk, $p<0.05$), con asimetría e nesgo á dereita, consistente con fontes puntuais ou episodios de acumulación en ambientes mariños[122,123]. Para minimizar o impacto destes nesgos, empregáronse estatísticos robustos (medianas, rangos intercuartílicos, etc.).

As medianas de PTEs nas mostras rexionais de *Fucus* spp. (µg g^{-1} peso seco) seguiron a secuencia: Hg (0,023) < Ag (0,090) < Cd (0,66) < Pb (1,1) < Cr (3,16) < Ni (5,0) < Cu (10,1) < As (36,0) < Zn (43,3) < Al (180) < Fe (295) (Capítulos 2, 3 e 4). Estes valores son consistentes coa metanálise realizada a nivel global para algas pardas (Capítulo 1), con diferenzas menores ao 30%, agás para Cu (+66%), Ag (-47%) e Pb (−63 %) no conxunto rexional. Ademais, todos os valores están por debaixo dos límites legais para suplementos alimentarios (3 µg g^{-1} para Cd e Pb, e 0.1 µg g^{-1} Hg)[124].

En relación á **toxicidade potencial**, as concentración medianas de Fe, Ni, Zn e Cd obtidas foron comparables aos intervalos asociados á expresión diferencial en *Fucus* spp. de fitoquelatinas e metalotioneínas, que son moléculas implicadas na unión e detoxificación de PTEs. Pola contra, o Cu rexistrou medianas moi inferiores ao rango asociado a estas respostas (44,5-125 µg g^{-1})[125,126]. Outros estudos tamén detectaron correlacións significativamente positivas entre os niveis de Cu, Zn e As e a acumulación de especies reactivas de oxíxeno (ROS)[127]. Non obstante, esta resposta foi detectada para concentracións máis elevadas das observadas aquí (4-6 µg g^{-1} Cd e 3,4-6 µg g^{-1} Pb)[128]. Da mesma forma, a sobreprodución de polisacáridos da parede celular tamén foi observada para concentracións superiores de Zn e Cd[63].

Porén, a extrapolación dos efectos tóxicos é complexa. Así, a maior parte da evidencia dispoñible provén de estudos realizados en condicións de laboratorio, centrados en concentracións disoltas na auga e non nas efectivamente concentradas nos tecidos[129–132]. Ademais, a **toxicidade relativa** dos distintos PTEs nas algas pardas está pouco caracterizada, e os resultados dispoñibles mostran unha alta variabilidade entre estudos[133–135], dificultando a súa interpretación conxunta. Do mesmo xeito, as interaccións entre PTEs son pouco coñecidas, a pesar do potencial para modificar tanto a súa biodispoñibilidade como a súa toxicidade a través de mecanismos competitivos ou sinérxicos[136].

O **perfil multielemento de *Fucus* spp.** (n = 768, maioritariamente de Galicia) estivo dominado por *Fe* (42,4 %) e *Al* (40,2 %), o que suxire unha importante **contribución litoxénica**, asociada á presenza de partículas sedimentarias adheridas ao tecido[137]. A concentración activa de Fe como micronutriente esencial podería contribuír parcialmente, pero non explicaría os niveis tan elevados observados.

Os seguintes elementos máis abundantes foron Zn (8,6 %) e As (6,9 %), mentres que Cu, Ni, Pb, Cd e Hg representaron, no seu conxunto, tan só o 1,15% da composición relativa. O alto peso relativo do Zn é coherente co seu papel esencial no metabolismo e coa súa elevada fracción biodispoñible en auga mariña, que favorece tanto a adsorción nas paredes celulares como a súa concentración intracelular[94,138,139]. O As tamén aparece en proporcións relevantes, o que pode ser debido á súa similitude estrutural co fosfato, que permite a súa entrada mediante transportadores fosfato-dependentes[140].

Pola contra, elementos como o Cu e o Ni foron menos abundantes, posiblemente debido á súa menor dispoñibilidade[141] ou á existencia de mecanismos de regulación máis estritos. Cadmio, Pb e Hg, rexistráronse en niveis traza, o que reflicte a súa **escasa dispoñibilidade** disolta, ausencia de función biolóxica e incorporación pasiva a través de procesos inespecíficos[142]. No caso do Hg, a súa baixa abundancia tamén pode estar relacionada coa forte complexación con materia orgánica e a súa baixa afinidade polos sistemas de transporte celular das algas[37,141].

Ao considerar unicamente os cinco elementos dispoñibles para todas as mostras de algas pardas (Zn, Cu, Ni, Pb e Cd), observouse un perfil de *Fucus* spp. tamén dominado polo Zn (83 %), seguido polo Cu (8,4 %) e Ni (5,4 %), mentres que Pb (1,43 %) e Cd (1,22 %) foron

claramente minoritarios. Este perfil é moi semellante ao perfil composicional global obtido para todas as algas pardas, no que tamén predominan Zn (80 %), Cu (9,36 %) e Ni (6,78 %).

En calquera caso, a conservación da orde relativa dos elementos (Capítulo 5) e as diferenzas moderadas entre os valores medianos do conxunto global (Capítulos 1 e 4) e os rexionais de *Fucus* spp. (Capítulos 2, 3 e 4) suxiren a existencia de mecanismos que permiten ás algas manter unha composición multielemento relativamente estable, mesmo en condicións ambientais variables. Estes resultados apuntan, polo tanto, á existencia dun **control interno** que contribúe á estabilidade do perfil elemental.

En relación ás AgNPs, a concentración mediana obtida foi de 3,07 x 10^7 partículas g^{-1}. Porén, a contextualización destes valores é limitada, xa que só existe un estudo previo que avalíe o contido de AgNPs en organismos mariños baixo condicións naturais[143]. Aínda así, os valores obtidos son comparables aos observados en sedimentos mariños[144,145], e outras matrices biolóxicas mariñas[143], e exceden aos atopados en mostras de auga de mar[143,146].

6.3. Diferenzas taxonómicas

A análise composicional revelou patróns diferenciados na concentración de PTEs entre os distintos taxóns de algas pardas. O nivel específico explicou a maior varianza (33,1%), seguida polo xénero (20,2 %) e a familia (10,1 %). Estes resultados, consistentes entre análises restrinxidas (RDA) e non restrinxidas (PCA, PERMANOVA), indican que os patróns de captación de PTEs non responden a unha variabilidade aleatoria, senón a adaptacións estruturais e ecolóxicas propias de cada grupo.

A nivel de familia, Laminariaceae e Fucaceae amosaron unha maior proporción relativa de Zn, mentres que Dictyotaceae e Sargassaceae presentaron proporcións máis elevadas de Cd e Pb en comparación coas dúas primeiras. Estes patróns tamén se observaron na metaanálise das concentracións globais absolutas (análise nMDS do Capítulo 1), onde Fucaceae e Laminariaceae destacaron por cargar maiores niveis de PTEs en xeral, sobre todo para Zn. Porén, mentres que as diferenzas entre familias foron estatisticamente significativas na análise composicional, non o foron ao comparar as concentracións absolutas (ANOSIM R = 0,151, p > 0,05). Esta discrepancia reflicte a maior sensibilidade da primeira ao minimizar a variabilidade entre mostras, capturando os patróns relativos e as interaccións entre elementos[147]. Así, a **identidade taxonómica** estrutura principalmente a composición relativa de PTEs,

mentres que as concentracións absolutas integran factores ambientais locais, dificultando a detección de patróns taxonómicos consistentes.

Desde o punto de vista funcional, a maior capacidade de captación en Fucaceae e Laminariaceae podería estar relacionada co seu alto contido en polisacáridos da parede celular especialmente **fucoidanos** e **alxinatos**. Os **fucoidanos**, ricos en grupos sulfato ($–SO^{3-}$), presentan unha afinidade elevada polo Zn, mentres que os **alxinatos**, que conteñen grupos carboxilo ($–COO^{-}$), forman complexos estables con catións como Cd^{2+} e Pb^{2+}. A composición e proporción destes polisacáridos varía entre familias, sendo os fucoidanos máis abundantes en Fucaceae e Laminariaceae ca en Dictyotaceae e Sargassaceae, o podería contribuír ás diferenzas observadas[148,149].

A **posición na altura do mareal** tamén pode influír na exposición diferencial aos PTEs. Fucaceae e Laminariaceae habitan zonas intermareais ou submareais pouco profundas, máis susceptibles a fluctuacións de temperatura, radiación UV e contacto con partículas sedimentarias. Pola contra, moitas especies de Dictyotaceae e Sargassaceae predominan en hábitats submareais máis profundos, frecuentemente en rexións tropicais ou subtropicais. Nestes ambientes, a concentración de Zn disolto adoita ademais ser menor debido á limitada circulación e ao rápido consumo biolóxico deste elemento[150,151], o que podería contribuír ás menores proporcións relativas observadas.

A nivel de xénero, *Sargassum*, *Padina* e *Polycladia* presentaron as maiores proporcións de Cd e Pb, en concordancia con outros estudos que sinalan a elevada capacidade de concentración de *Sargassum* para estes elementos[152,153]. En contraste, *Fucus* presentou un perfil composicional claramente diferenciado, caracterizado por unha maior proporción de Zn e niveis comparativamente máis baixos de Cd e Pb.

As diferencias entre especies tamén foron significativas. *Fucus ceranoides*, típico de zonas estuarinas, presentou proporcións máis elevadas de Pb, Ni e Cu, e menores de Zn e Cd en comparación con *F. vesiculosus – F. spiralis* (PERMANOVA R^2 = 7 %). En relación ás concentracións absolutas, os estudos rexionais (Capítulos 2, 3 e 4) documentaron maiores niveis de Al, Cr, Fe, Ni, Cu, Zn, Pb e Hg en *F. ceranoides*, mentres que as diferenzas en Cd e Ag non foron significativas, e as concentracións de As foron superiores en *F. vesiculosus – F. spiralis*. Estes patróns reflicten principalmente diferenzas nos hábitats: *F. ceranoides* habita áreas con elevada carga sedimentaria e baixa salinidade, mentres que *F. vesiculosus* e *F. spiralis* ocupan

substratos rochosos máis expostos, cunha dispoñibilidade máis limitada de PTEs, especialmente daqueles asociados ás fraccións particuladas (e.g. Hg, Pb)[137,154].

A ausencia de diferenzas nos cocientes isotópicos de Pb ($^{206}Pb/^{207}Pb$ e $^{208}Pb/^{206}Pb$) entre estas especies indica que ambas estiveron expostas ás mesmas fontes de contaminación, e que o proceso de carga nos tecidos non altera a proporción natural dos isótopos. Esta falta de fraccionamento isotópico é ben coñecida e constitúe precisamente unha das razóns polas que os isótopos de chumbo son ferramentas tan valiosas para identificar fontes de contaminación[155,156].

En conxunto, os resultados evidencian que tanto a composición relativa como as concentracións absolutas de PTEs en algas pardas están condicionadas pola identidade taxonómica e polas características ambientais dos seus hábitats. As diferenzas entre taxa parecen derivar dunha **combinación de factores estruturais, ecolóxicos e bioxeoquímicos**, como a composición da parede celular, o tipo de substrato ou a dispoñibilidade local de PTEs. Estes patróns subliñan a importancia de considerar o contexto taxonómico e ecolóxico á hora de interpretar os niveis de PTEs, especialmente cando as algas se empregan como biomonitoras. Porén, a cobertura taxonómica non foi homoxénea, con xéneros como *Fucus* moito mellor representados, o que pode limitar a comparación entre grupos e o establecemento de conclusións en relación aos patróns de concentración observados.

6.4. Diferenzas espaciais

As diferenzas espaciais na carga de PTEs en algas pardas foron evidentes ao longo desta tese, froito da interacción complexa entre factores xeográficos, hidrodinámicos, xeolóxicos, ecolóxicos e bioquímicos. En Galicia, que foi a rexión de estudo dos Capítulos 2, 3 e 4, o sistema de rías proporciona un marco natural moi heteroxéneo, con marcados gradientes entre **zonas interiores, semiexpostas e expostas** ao océano aberto. Esta estrutura deriva en grandes variacións en salinidade, pH, oxixenación, condicións redox e acumulación de sedimentos, que condicionan fortemente a biodispoñibilidade dos PTEs dentro da propia ría[157,158].

As zonas interiores adoitan presentar unha maior deposición de partículas finas, elevada carga orgánica e unha renovación da auga máis limitada, o que favorece a acumulación de PTEs ligados á fracción particulada (eg. Pb, Cr, Fe). Ademais, estas áreas están estreitamente influencidas polos ríos, caracterizándose por unha salinidade reducida e pola entrada de contaminantes fluviais. Pola contra, as áreas máis abertas presentan unha maior circulación

mariña, menor sedimentación e maior dispersión dos contaminantes[159,160]. Este patrón xeral foi consistente cos resultados obtidos, que mostraron concentracións máis altas en zonas interiores para a maioría dos PTEs analizados, agás Cd, Ag e As, que non amosaron un patrón espacial definido. Estas excepcións apuntan a un comportamento bioxeoquímico distinto destes elementos, sendo menos dependente das achegas sedimentarias[161–163].

Porén, a **variabilidade dentro de cada ría foi moi elevada**, con puntos xeograficamente próximos que amosaron diferenzas considerables nas concentracións. Isto evidencia a influencia combinada de fontes locais puntuais, cambios na biodispoñibilidade, variacións fisicoquímicas a pequena escala e posibles diferenzas interpoboacionais na capacidade de captación dos PTEs[118,164]. Neste sentido, a ausencia de datos ambientais como a temperatura, o pH, a produtividade primaria, ou a carga sedimentaria a pequena escala impide identificar con precisión os factores responsables destas diferenzas. Con todo, a pesar da alta variabilidade, os modelos lineais mixtos (LMM) identificaron a ría como un factor significativo para todos os PTEs, indicando que o lugar de procedencia exerce un efecto estatisticamente robusto. Isto pon de manifesto que o ambiente local é un determinante importante da composición de PTEs nas algas, se ben non é o único.

A variabilidade entre rías tamén foi considerable, aínda que non se detectaron patróns latitudinais consistentes para a maioría dos elementos analizados. Só algúns casos illados, como o Ni (con concentracións máis elevadas no norte) ou as razóns isotópicas do Pb (con valores máis próximos ao fondo natural no sur), amosaron certa estrutura espacial. Galicia presenta unha elevada diversidade litolóxica, cun mosaico de granitos, esquistos, cuarcitas, serpentinitas, lousas e outras rochas que poden influír nas concentracións naturais de fondo dos PTEs. A coexistencia de zonas xeoloxicamente contrastadas, como a Mariña lucense co predominio de lousas, cuarcitas e serpentinitas fronte ao suoreste granítico, faría esperable a aparición de gradientes espaciais nos datos[165,166]. Porén, esta posible sinal pode verse enmascarada pola superposición con **factores antrópicos moi heteroxéneos** (zonas industriais, núcleos urbanos ou agricultura intensiva) e pola alta variabilidade local propia da dinámica de cada ría. Esta complexidade dificulta a detección de patróns rexionais claros.

Por outra banda, a análise espacial revelou unha elevada variabilidade entre elementos, sen que se detectase ningunha ría ou sitio de mostraxe que presentase de forma consistente os niveis máis altos para todos os PTEs. Con todo, algúns lugares como as **rías do Burgo e Vigo**

destacaron por acadar niveis elevados de determinados contaminantes, sen que isto se extendese ao conxunto dos PTEs estudados. Esta variabilidade pon de manifesto que cada elemento segue dinámicas propias en función da orixe, forma química e interacción co medio[141,142]. Así, conceptos xenéricos como "ría contaminada" resultan imprecisos cando non se especifica o contaminante de referencia. A clasificación binaria (contaminada/non contaminada), aínda que útil para casos extremos, non capta a complexidade real dos patróns de contaminación observados.

A nivel global (Capítulo 1), o patrón máis destacado foi a **marcada asimetría na distribución xeográfica** das mostras. O conxunto de datos estivo claramente dominado por rexistros de zonas temperadas do Atlántico Norte, especialmente de ambientes intermareais rochosos, mentres que outras rexións e hábitats foron claramente infrarrepresentadas, como o Ártico (n = 18), o Atlántico Sur (n = 88), ou as especies submareais da familia Laminariaceae (n = 154). Esta desigual cobertura compromete a capacidade para extrapolar patróns a escala global, xa que ecosistemas clave como arrecifes ou zonas tropicais submareais están insuficientemente representados. Ademais, estas áreas presentan condicións ambientais contrastadas con diferentes temperaturas, taxas de acidificación, réximes de afloramento, así como niveis de presión antrópica e medidas reguladoras moi diferentes.

En definitiva, os resultados destacan a **complexidade dos patróns espaciais de concentración de PTEs nas algas pardas**, tanto a escala rexional como global. A interacción entre factores naturais (como a litoloxía, a hidrodinámica ou a dispoñibilidade de sedimentos) e antrópicos (como o grao de urbanización ou actividade industrial) xera unha gran heteroxeneidade local que pode ocultar gradientes máis amplos. Así mesmo, a elevada variabilidade entre elementos, hábitats e grupos taxonómicos dificulta a aplicación de criterios uniformes de avaliación ambiental. Por iso, resulta fundamental ampliar e equilibrar a cobertura xeográfica, e taxonómica das redes de biomonitorización, garantindo unha caracterización máis robusta, representativa e interpretable da contaminación mariña por PTEs a distintas escalas.

6.5. Relación entre elementos

A análise conxunta das concentracións de PTEs a nivel global e rexional permitiu identificar patróns de covariación que apuntan a posibles fontes comúns, procesos de transporte compartidos ou mecanismos diferenciados de bioconcentración segundo o elemento. Porén,

estas relacións non foron sempre consistentes entre análises, algo esperable dada a distinta natureza estatística e conceptual das aproximacións empregadas.

Na metanálise global (Capítulo 1), a análise nMDS revelou dous agrupamentos principais: un entre Cu e Zn, e outro entre Pb e Cd, con Fe situado nunha posición intermedia. O agrupamento Cu-Zn foi consistente coa análise composicional (Capítulo 5), onde ambos elementos aparecen próximos en PC1 e PC2. Nos datos rexionais (PCA), Cu e Zn aparecen próximas, aínda que non no mesmo cadrante, posiblemente debido á influencia doutros elementos cunha maior covariación mutua, cunha correlación moderada-elevada ($\rho = 0.37$). A proximidade relativa destes PTEs nos distintos enfoques é coherente co feito de ser **PTEs esenciais**, fortemente regulados polas algas mediante transporte activo e almacenamento intracelular, o que dá lugar a patróns de captación máis coordinados[94,139].

En cambio, a asociación entre Pb e Cd observada no nMDS global non foi respaldada nin pola análise composicional nin polas análises rexionais. Esta discrepancia pode explicarse por diferenzas na mobilidade e nos mecanismos de carga de ambos elementos: mentres que o Pb tende a asociarse maioritariamente á fracción particulada e queda retido na parede celular[167,168], o Cd adoita atoparse en formas máis solubles e biodispoñibles, o que suxire que podería entrar ao interior celular, incluso utilizando transportadores do Zn[141,169]. Esta diferenza resulta coherente co patrón observado no Capítulo 2, onde *Fucus ceranoides*, a pesar de habitar zonas con elevada carga sedimentaria, presentou concentracións menores de Cd en comparación con *F. vesiculosus* - *F.spiralis*, o que suxire a ausencia de dependencia deste metal das achegas sedimentarias. Pola contra, a forte correlación entre Pb e Fe ($\rho = 0.58$) reforza a influencia dos aportes litoxénicos para este elemento.

O comportamento do Ni foi especialmente complexo. Na análise composicional situouse nunha posición máis illada, mentres que a nivel rexional amosou correlacións moi altas con Cr ($\rho = 0.77$) e Cu ($\rho = 0.66$). Estes elementos comparten propiedades na súa mobilidade e comportamento químico. En particular, Ni e Cr adoitan aparecer asociados tanto en fontes litoxénicas como antrópicas[170–172]. Ademais, no RDA da análise composicional, o Ni aliñouse co Pb, suxerindo certa covariación entre ambos elementos a nivel taxonómico, especialmente nas especies con menores concentracións de Zn.

No caso do As, a súa posición no análise composicional foi estimada mediante correlacións coas compoñentes principais do PCA, o que suxería certa asociación con Cu, Zn e Cd. Porén,

a nivel rexional observáronse correlacións negativas moderadas con Cu, Cr e Ni (~ −0.27), o que indica unha relación inversa coa distribución destes elementos. En liña con isto, no PCA rexional o As apareceu claramente separado do resto, reflectindo unha **dinámica diferenciada**. Esta discrepancia pode explicarse pola diferente metodoloxía analítica (estimación indirecta fronte a inclusión directa no modelo), pero tamén pola natureza particular do As, que pode responder a fontes, formas químicas e procesos de carga distintos aos doutros PTEs. Este comportamento máis autónomo podería explicar por que é o único elemento que mostrou incrementos temporais significativos no estudo (Capítulo 2) e concentracións máis elevadas para *F. vesiculosus – F. spiralis* que para *F. ceranoides*. Sen embargo, neste capítulo observáronse correlacións moderadas do As con Al ($\rho = 0.23$) e Fe ($\rho = 0.21$), suxerindo tamén algunha relación feble co fondo litolóxico.

En canto ao Hg, a súa posición no PCA da análise composicional (Capítulo 5), tamén estimada mediante correlacións cas compoñentes principais, mostrou unha lixeira proximidade ao Pb, suxerindo un certo paralelismo nos seus patróns de carga. A nivel rexional, o Hg amosou unha forte correlación con Cu ($\rho = 0.48$) e moderadas con Ni, Zn e Cr (ρ entre 0.38 e 0.47), así como asociacións máis febles con elementos litoxénicos como Fe ($\rho = 0.27$) e Al ($\rho = 0.14$). Estes patróns apuntan a unha posible asociación parcial con partículas sedimentarias[173], pero tamén a **fontes antrópicas compartidas** con elementos como o Cu, Ni, Zn e Cr, como a queima de combustibles fósiles, procesos industriais ou descargas urbanas e agrícolas[171,174].

Por último, Al e Fe mostraron unha correlación moi alta entre si ($\rho = 0.90$), o que confirma a súa orixe común vinculada ao sedimento[137]. En contraste, Ag mostrou unha correlación negativa significativa con Al ($\rho = –0.21$) e máis débil con Fe ($\rho = –0.11$), suxerindo mecanismos de carga distintos ou interaccións competitivas con fraccións particuladas.

En conxunto, os resultados apuntan á existencia de dous grupos principais: un formado por Cu, Zn, Cr e Ni, con patróns de carga similares e probablemente asociados a fontes antrópicas; e outro integrado por Al e Fe, que actúan como trazadores litoxénicos. Por outra banda, Cd, As, Ag, e, en parte, Pb, presentan comportamentos máis autónomos, o que reflicte dinámicas bioxeoquímicas propias. Neste contexto, factores como **a especiación química, a mobilidade no medio e a afinidade polos compoñentes da parede celular** poden desempeñar un papel clave na súa concentración diferencial.

6.6. Tendencias temporais

Os resultados desta tese revelan unha **tendencia temporal clara de descenso nas concentracións da gran maioría dos PTEs**, consistente a través dos distintos enfoques metodolóxicos e análises estatísticas aplicadas. Esta consistencia maniféstase entre enfoques de natureza moi distinta: por unha banda, un enfoque global cunha aproximación de ampla escala espazo-temporal, pero baixa resolución e metodoloxías non estandarizadas (Capítulos 1 e 4), e por outra, un enfoque rexional con alta resolución metodolóxica en espazos e períodos máis acoutados (Capítulos 2, 3 e 4). Ademais, estas tendencias tamén foron consistentes para o enfoque rexional (Capítulos 2, 3 e 4) a través das distintas análises estatísticas empregadas, tendo en conta tanto a estrutura de medidas repetidas (como o Wilcoxon signed-rank test, o Friedman test ou os LMM), como nas análises que non incluíron este control. A concordancia entre enfoques e análises estatísticos apunta, así, a un declive xeralizado, persistente e robusto da contaminación mariña por PTEs ao longo das últimas décadas.

A nivel global, observouse unha **redución significativa para todos os PTEs estudados**, cunhas reducións acumuladas que variaron entre un –84 % para o Pb e un –60 % para o Co, aínda que eses descensos se comezaron a producir en anos distintos (Capítulo 1). Así, mentres que o Pb amosou un descenso progresivo desde os anos 1970, o Co comezou a diminuír máis tarde, nos anos 1990, o que implica que, malia a maior redución acumulada do Pb, a súa taxa anual de cambio foi máis baixa (–1,6 %), fronte ao –2,1 % do Co. Da mesma forma, o Cu mostrou unha diminución global do –71,6 %, cunha taxa anual de cambio do –1,4 % ao tratarse dun longo período de descenso, mentres que o Cr, manifestou un descenso do 66 % pero presentou unha taxa anual de cambio máis elevada (–2,5 %), ao iniciar este descenso a partir de 2003. Algúns elementos, coma o Hg, amosaron ademais unha pequena estabilización ou efecto "damping" tras un pequeno período inicial de marcados descensos[175,176].

A prata tamén mostrou unha tendencia global descendente desde os anos 1980, aínda que cun patrón máis irregular e fortemente condicionado pola **escaseza de datos** dispoñibles (Capítulo 4). As reducións significativas só se observaron tras excluír tres outliers correspondentes a mostras recollidas en zonas próximas a efluentes industriais. Pola contra, a súa inclusión neutralizou a tendencia descendente significativa, o que subliña a fraxilidade do sinal observado. A incorporación dos datos rexionais desta tese (Capítulo 4) permite reforzar a

tendencia negativa, aínda que os patróns amosan unha **alta variabilidade interanual**, en contraste co comportamento máis consistente detectado para outros elementos.

A escala rexional (Capítulo 2 e 4) detectáronse fortes descensos en **Cr (–84,7 %), Cu (–84,7 %), Ni (–72,4 %), Hg (–49,6 %), Cd (–36,7 %) e Zn (–24,4 %)**, así como para **Ag (–58,1 %).** Estes valores tradúcense en taxas anuais de descenso que oscilan entre –0,81 % (Zn) e –2.82% (Cr e Cu). En contraste, algúns elementos como **Al (+367,9 %), Fe (+105,2 %) e As (+36,1 %) mostraron aumentos** rexionais. O Pb descendeu nun **–21.9%** pero este descenso non foi significativo (Capítulo 3).

Os descensos detectados foron consistentes cos detectados en algas pardas noutras rexións[104,105,177] e períodos[103], así como noutros compartimentos ambientais como sedimentos[178,179] e auga mariña[180], e en distintos organismos mariños[77]. Porén, estas tendencias non foron uniformes en todos os contextos, e tamén se teñen documentado **incrementos** noutros estudos[101,181,182], o que pon de manifesto a **complexidade e variabilidade** espacial e temporal da contaminación mariña por PTEs. Os incrementos rexionais detectados de Al e Fe están probablemente asociados a factores de orixe litoxénica, que se abordarán con máis detalle no apartado 6.8 da presente discusión. No caso do As, a tendencia ao incremento coincide coa detectada noutros estudos[57,183]. Por outra banda, o limitado descenso do Pb escala rexional (-21.9%) contrasta co pronunciado descenso a escala global (-84%) e con outras reducións documentadas[77,110,184].

Por último, a análise composicional (Capítulo 5) revelou cambios temporais significativos na composición relativa dos PTEs nas mostras rexionais de *Fucus* spp., explicando un 20,4% da variabilidade total. Estas diferenzas foron moderadas entre 1990 e 2001–2007, pero **moi pronunciadas en 2021**, con **incrementos de Al e Fe** que alteraron substancialmente o equilibrio relativo entre os demais elementos. Ao excluir o Al e o Fe, o **As adquiriu un maior peso composicional**, mentres que o Pb se incrementou lixeiramente e outros PTEs (Cu, Ni, Cd, Hg) experimentaron unha redución nas súas concentracións relativas. Estes patróns indican **mudanzas direccionais a longo prazo**, con maior intensidade nas últimas décadas. A comparación coas tendencias nas concentracións absolutas mostra algunhas diferenzas interpretativas, que non deben entenderse como contradicións, senón como o efecto relativo provocado pola caída e aumento doutros elementos. Por exemplo, o Zn e o Pb experimentaron un aumento 23.7% e do 19.2% en termos composicionais fronte unha diminución do -24,4% e

do -21.9% nas súas concentracións absolutas. De igual forma, o As incrementouse un 113% composicionalmente, fronte a un incremento do 36,1% en concentracións absolutas. Malia as transformacións rexistradas, a xerarquía composicional entre elementos mantívose amplamente estable, o que suxire a presenza de mecanismos reguladores internos que axudan a preservar os equilibrios relativos entre PTEs ao longo do tempo

6.7. Fontes de contaminación e a súa evolución

A identificación das fontes de PTEs e a súa evolución temporal abordouse mediante PMF e isótopos de Pb. Os modelos PMF (Capítulo 2) a través dos períodos 1990, 2001-2007 e 2021, resolveron catro factores ou fontes principais: (1) unha fonte de orixe natural dominada por Al e Fe[185,186]; (2) unha fonte antrópica relacionada con actividades **industriais, agrícolas e mineiras** composta por Zn, As, Cd e Hg[187–189]; (3) unha fonte mixta natural-antrópica dominada por Ni e Cr, aínda que en 2021 o Cr se agrupou con Al e Fe; e (4) un perfil específico de Cu asociado ao uso de **agroquímicos**[174,190]**,** especialmente para viñedos, **ou pinturas antifouling**[191] que en 2021 se agregou parcialmente ao Zn. En conxunto, as fontes identificadas mantivéronse relativamente estables ao longo do tempo. Non obstante, en 2021 os factores 1 e 3, asociados a fontes naturais, incorporaron nun maior grao elementos tradicionalmente vinculados a actividades antrópicas como Cu, Zn, Cd e Hg, o que suxire unha **diminución progresiva das emisións industriais e urbanas destes PTEs** e unha **maior contribución relativa das fontes naturais** no seu perfil de acumulación.

A análise de isótopos de Pb ($^{206}Pb/^{207}Pb$ e $^{208}Pb/^{206}Pb$) ao longo dos 30 anos revelou un cambio claro nas sinaturas isotópicas, pasando de valores característicos de **fontes antrópicas** (gasolinas con e sen chumbo, incineradoras, aerosois industriais) a valores máis próximos a **fontes naturais** (litolóxicas) (Capítulo 3). Estes cambios temporais foron altamente significativos e coinciden co observado en estudos isotópicos previos en sedimentos da mesma rexión e noutras rexións e compartimentos[77,192,193]. Os modelos MixSIAR reforzaron esta transición detectando una diminución drástica das aportacións asociadas ao carbón (do 48,4 % en 1990 ao 6,3 % en 2021), en consonancia co peche ou redución de actividade das principais centrais térmicas da zona (As Pontes e Meirama). As fontes asociadas ao tráfico tamén diminuíron, pasando do 46,9 % ao 32,2 %, demostrando que os combustibles fósiles seguen sendo un foco de contaminación, a pesar da prohibición da gasolina con Pb en todo o mundo[109]. En paralelo, as contribucións naturais aumentaron fortemente, pasando do 4,7 % ao 61,5 %.

Por outra banda, as estacións depuradoras de augas residuais (EDAR) están recoñecidas como unha fonte importante de determinados PTEs, como a Ag[194,195]. Non obstante, o tratamento adecuado destas augas contribúe de forma decisiva a **reducir a carga contaminante global que chega ao medio mariño**. Nas últimas décadas, Galicia experimentou unha mellora substancial tanto na **eficiencia como na cobertura das EDAR**, ca instalación de 21 novas plantas entre 1990 e 2000, 34 entre 2000 e 2010, e 11 entre 2010 e 2020, cun maior nivel de modernización[118]. Non obstante, a detección de **picos locais de concentración** en determinados elementos suxire que, malia os avances tecnolóxicos, as EDAR **seguen actuando como fontes puntuais relevantes**.

En conxunto, os resultados apuntan a unha transición clara cara a fontes máis naturais, favorecida pola diminución de presións industriais e enerxéticas tradicionais, pero tamén evidencian a persistencia de focos antrópicos locais, como o tráfico, a agricultura intensiva e os sistemas de saneamento, que condicionan a distribución espacial actual dos PTEs.

6.8. Causas das tendencias

A diminución temporal nas concentracións da maioría dos PTEs en *Fucus* spp. e noutras algas pardas pode explicarse pola combinación de factores ambientais, procesos biolóxicos e medidas de protección ambiental implementadas nas últimas décadas.

Por unha banda, estes descensos poden reflectir reducións reais na concentración de PTEs no medio mariño, resultado da aplicación de diversas políticas ambientais. Normativas como a Directiva de Tratamento de Augas Residuais Urbanas[106], a Directiva Marco da Auga[107],o Convenio de Minamata[196] ou a prohibición a nivel mundial da gasolina con Pb[109] contribuíron de maneira decisiva a limitar os vertidos de PTEs mediante a mellora do tratamento de augas e residuos e a redución das emisións. Xunto a estas medidas lexislativas, **cambios nos modelos produtivos**, como o peche de plantas de fundición non férrea e centrais térmicas de carbón, así como a valorización e reciclaxe de residuos, puideron desempeñar un papel relevante na diminución das emisións. Ademais, transformacións nos **hábitos de consumo**, como a desaparición do revelado fotográfico tradicional, no que se empregaban grandes cantidades de Ag tamén puideron contribuír á redución dos PTEs no medio.

Por outra banda, as diminucións observadas nas concentracións de PTEs nas algas poderían non reflectir exclusivamente unha redución real no ambiente, senón tamén **cambios na súa biodispoñibilidade**, influenciados polos efectos do **Cambio Global**. Procesos como a

acidificación oceánica, o **aumento da temperatura superficial** e as **variacións na salinidade** alteran a especiación e mobilidade dos PTEs, afectando a súa adsorción polas algas, a complexación con materia orgánica e os fluxos de intercambio sedimento-auga[141,142]. Neste contexto, os nosos resultados mostran correlacións significativas entre o pH, a temperatura superficial do mar e as concentracións de varios PTEs en algas pardas, o que suxire un efecto potencial destes factores ambientais sobre a carga de PTEs (Capítulo 1). Aínda que os mecanismos específicos seguen sen estar plenamente comprendidos, simulacións realizadas neste estudo revelaron un **incremento do 5,9 % na fracción libre de Pb^{2+} entre 1990 e 2021**, evidenciando unha maior biodispoñibilidade deste metal, mesmo nun contexto de posibles reducións nas emisións.

Adicionalmente, **cambios fisiolóxicos nas poboacións de algas** ao longo do tempo tamén poderían contribuír ás variacións observadas, incluíndo cambios na produción de **polisacáridos na parede celular**[63]. Ademais, adaptacións a ambientes contaminados que poderían incluír taxas de crecemento máis baixas, redución da superficie específica, ou a diminución de transportadores de catións na membrana, poderían tamén xogar un papel importante[164]. Por último, a variabilidade biolóxica natural e posibles mecanismos epixenéticos tamén poderían explicar a ausencia de tendencias claras para algúns PTEs ou períodos específicos[197]. Non obstante, resulta improbable que estes factores por si sós expliquen os descensos tan marcados e consistentes observados a nivel tanto global como rexional.

Porén, os capítulos 2 e 3 tamén detectaron **aumentos nas concentracións de Al, Fe e As**, así como **a estabilidade do Pb** ao longo do tempo. Os incrementos de **Al e Fe**, elementos de baixa toxicidade habitualmente empregados como trazadores de sedimento, apuntan a un **maior aporte sedimentario nas mostras máis recentes**, apoiado por unha maior contribución estimada do sedimento para distintos PTEs, así como polas **análises de correlación, PCA e PMF**. Así, a adhesión de partículas sedimentarias ás algas pode incrementar artificialmente as concentracións medidas de certos PTE. A pesar de que se aplicou o mesmo protocolo de lavado en todas as campañas, en 2021 detectáronse visualmente restos de partículas sedimentarias tras o lavado, evidenciando que este tipo de contaminación segue a ser unha limitación coñecida na biomonitorización e difícil de evitar sen comprometer a integridade do tecido[198]. As condicións ambientais, como aumento da escorrentía terrestre, choivas intensas, menor circulación mariña ou cambios na salinidade, poden favorecer a deposición e retención de sedimentos sobre as algas. Non obstante, sedimentación e bioconcentración son procesos diferentes: isto queda

patente no feito de que, aínda que as razóns isotópicas de Pb en algas e sedimentos recollidos simultaneamente en campo estaban correlacionadas, non eran iguais, o que indica que **as algas non reflicten directamente a composición do sedimento**, senón unha fracción específica influenciada pola súa fisioloxía e pola biodispoñibilidade do metal.

O **As**, pola súa banda, tamén se incrementou, pero amosou un **comportamento máis complexo**. A súa correlación positiva con Al e Fe suxire unha influencia sedimentaria, pero o feito de que outros PTEs con patróns similares (Cr, Zn, Hg) non se incrementaran indica que **deben existir fontes ou procesos adicionais** implicados. A súa separación clara no PCA e as maiores concentracións en *F. vesiculosus* e *F. spiralis* en comparación con *F. ceranoides* apuntan a **diferencias na ruta bioxeoquímica**. Ademais, factores ambientais como o pH, a temperatura, salinidade ou a presenza de materia orgánica poden **modular a mobilidade e biodispoñibilidade do As**[199]. Desta forma, maiores concentracións de As foron atopadas en algas pardas a menor pH[200]. Aínda que se reportaron diminuscións nas emisións antropoxénicas de As[201,202], os incrementos observados tanto neste como noutros estudos[57,183] suxiren posibles **fontes emerxentes pouco controladas**, como os vertidos de augas subterráneas. A complexidade e persistencia do As nos ecosistemas costeiros require, por tanto, máis investigación.

No caso do **Pb**, as concentracións nas algas mantivéronse relativamente estables ao longo do tempo en Galicia, a pesar das claras mudanzas nas súas razóns isotópicas cara a fontes máis naturais (Capítulo 3). Esta aparente contradición pode explicarse pola maior contribución sedimentaria detectada nas mostras máis recentes, como suxiren os elevados niveis de Al e Fe en 2021, as fortes correlacións Fe–Pb e a diminución das razóns Pb/Fe. A maiores, tal e como se comentou anteriormente, tamén se detectou un **aumento da fracción libre de Pb^{2+}** ao simular as condicións de pH e temperatura da rexiónde nos anos 1990 *vs.* estas condicións no 2021. Así os datos suxiren que a estabilidade do Pb en *Fucus* podería deberse a unha combinación de **aportes sedimentarios e aumento da fracción biodispoñible**, malia a redución das emisións.

En conxunto, a magnitude e robustez dos patróns detectados apuntan a que a principal causa da diminución das concentracións de PTEs en algas pardas en xeral e en *Fucus* spp. en particular, é unha **reducción real das emisións antropoxénicas**, particularmente nos países

con políticas ambientais máis estritas. Con todo, **os cambios na biodispoñibilidade e nas respostas biolóxicas das algas** tamén parecen estar a desempeñar un **papel relevante**.

6.9. Avaliación da biomonitorización como técnica

O uso de organismos como biomonitores xorde como unha alternativa máis directa, rápida e económica que a análise dos compoñentes abióticos[198]. Non obstante, para que estes organismos poidan empregarse con éxito neste contexto, é necesario que existan relacións claras e consistentes entre as concentracións que conteñen os organismos e as presentes nos compartimentos ambientais que se pretenden avaliar[203].

Con todo, estas relacións son frecuentemente complexas e non sempre evidentes. Por exemplo, en numerosas ocasións non se atoparon correlacións significativas entre os niveis de PTEs nas algas pardas e as concentracións medidas na auga de mar[95,96]. Este feito podería interpretarse como unha limitación da biomonitorización cando o obxectivo principal é **estimar de forma indirecta as concentracións ambientais.** Ademais, esta estratexia podería perder relevancia no futuro, a medida que as técnicas de análise directa no medio gañen precisión e accesibilidade.

Porén, a ausencia de correlación tamén ofrece unha lectura complementaria: se non é posible inferir de forma fiable as concentracións ambientais a partir dos organismos, tampouco é posible estimar o que conteñen os organismos a partir das concentracións ambientais. Neste sentido, a biomonitorización adquire un **valor engadido**, pois permite coñecer directamente os niveis de exposición biolóxica, é dicir, as concentracións efectivas que poden afectar negativamente os organismos e facilitar a transferencia dos contaminantes a través da cadea trófica.

Neste contexto, os resultados desta tese apoian o uso das algas pardas como ferramentas útiles de biomonitorización. A pesar das limitacións mencionadas, as tendencias observadas nas concentracións de PTEs ao longo do tempo suxiren que estes organismos si responden aos cambios ambientais e son capaces de reflectir, cando menos parcialmente, a evolución da contaminación no medio. A ausencia dunha correspondencia cuantitativa exacta coas concentracións ambientais non invalida a súa utilidade, senón que reforza o seu valor como biomonitoras da fracción biodispoñible, que é precisamente a que determina a exposición real dos organismos e os posibles efectos ecolóxicos. Así, a biomonitorización non só complementa

a análise dos compoñentes abióticos, senón que ofrece unha perspectiva insubstituíble sobre o risco ecolóxico efectivo e a evolución temporal da carga contaminante nos ecosistemas.

6.10. Limitacións

A pesar da amplitude do conxunto de datos analizado e do uso de múltiples enfoques complementarios, este traballo presenta certas limitacións metodolóxicas e interpretativas relevantes. A maioría dos estudos, incluídos os desta tese, céntranse na medición de concentración totais de PTEs, sen ter en conta a súa **especiación química**, a cal resulta fundamental para comprender a toxicidade e biodispoñibilidade reais, así como para avaliar de forma máis precisa a evolución da contaminación na costa.

Do mesmo xeito, a relación entre a presenza de certos PTEs e estruturas fisiolóxicas específicas das algas, como os fisodes (vesículas intracelulares ricas en compostos fenólicos) ou os polisacáridos da parede celular, segue sendo escasamente comprendida. Os **mecanismos de transporte** de PTEs nas algas pardas, as **funcións bioquímicas** específicas de cada elemento e as **formas de almacenamento** intracelular son tamén áreas pouco estudadas. Esta falta de coñecemento limita a interpretación dos patróns observados e dificulta o establecemento de conclusións. Ademais, a escaseza de datos fisicoquímicos como a temperatura ou o pH do medio a alta resolución espacial dificulta a análise de factores ambientais que poden estar afectando á carga de PTEs destes organismos.

Outro aspecto habitualmente ignorado, e que tampouco puido ser tratado nesta tese, é a exposición dual das algas intermareais como *Fucus* spp., que alternan períodos de exposición directa á atmosfera con períodos de inmersión na auga mariña durante os ciclos de marea. Esta condición dual implica que os contaminantes poden proceder tanto de **fontes atmosféricas como mariñas,** cunha contribución relativa de cada vía de exposición aínda descoñecida. Isto evidencia unha importante lagoa de coñecemento que merece ser explorada en traballos futuros.

En canto á representatividade espacial, a maior parte dos datos dispoñibles proceden do hemisferio norte, especialmente de Europa e América do Norte, mentres que outras rexións do planeta o Océano Atlántico Sur están escasamente representadas. Esta **distribución desigual** limita a comprensión global dos patróns de contaminación mariña e impide detectar gradientes e dinámicas específicas. Resulta, por tanto, necesario promover estudos en rexións subrepresentadas e establecer redes de mostraxe máis equilibradas a nivel global, que permitan obter unha visión máis completa e comparativa da contaminación mariña.

Neste contexto, os **bancos de mostras ambientais** xogan un papel crucial para a observación e avaliación dos cambios ambientais a longo prazo. Porén, estes bancos continúan a estar **infrarrepresentados e infrafinanciados**, e o seu potencial segue sen ser plenamente recoñecido. A súa implementación é desigual tanto en termos de financiamento como de cobertura xeográfica, e en moitos casos —como no banco utilizado nesta tese— están actualmente sen financiamento, o que compromete gravemente a continuidade das series temporais e o seguimento ambiental a longo prazo. Potenciar estas coleccións é fundamental para corrixir lagoas históricas de información e garantir un seguimento efectivo da saúde dos ecosistemas costeiros. Esta tese pretende por tanto poñer en valor a importancia destes bancos como ferramentas científicas esenciais nun contexto de cambio global.

En termos máis amplos, cómpre sinalar que, mentres os efectos do cambio climático e da acidificación oceánica reciben unha atención crecente, a contaminación mariña semella quedar nun segundo plano e aparece cada vez con menor frecuencia como eixo central dos programas de seguimento ambiental. A pesar diso, os contaminantes continúan exercendo presión sobre os ecosistemas e sobre os organismos mariños, polo que integralos de novo nas axendas de investigación e xestión ambiental resulta urxente.

7. CONCLUSIÓNS

- Significant and consistent declines in PTE concentrations were observed in brown algae worldwide over the past 40–50 years and in *Fucus* spp. along the NW Iberian Peninsula between 1990 and 2021.
- At the regional scale, increasing levels of Al, Fe and As and a stabilization of Pb in *Fucus* spp. suggest enhanced sediment input and broader changes in physicochemical conditions.
- Pb isotopic signatures ($^{206}Pb/^{207}Pb$ and $^{208}Pb/^{206}Pb$) revealed a clear shift from predominantly anthropogenic to more natural (lithogenic) sources between 1990 and 2021.
- Pb isotopes analysis proved essential for tracking pollution source, highlighting the limitations of relying solely on concentration data.
- The observed declines likely reflect the effectiveness of environmental regulations, although changes in PTE bioavailability linked to global change may partially offset these gains.
- Data coverage is geographically biased, with most records from the North Atlantic Ocean, and poor representation from regions such as the Arctic and South Atlantic Oceans.
- Multi-decadal datasets are crucial for capturing shifts in pollution sources and environmental processes that short-term studies might miss.
- PTE concentrations were consistently higher in inner estuarine areas and in *F. ceranoides* than in *F. vesiculous – F.* spiralis, except for As, Ag and Cd.
- No clear latitudinal gradients in PTE concentrations and evolution were identified across the region.
- The number of AgNPs declined over time and showed a positive correlation with total Ag levels, supporting the hypothesis of *in vivo* formation via algal-mediated reduction of ionic Ag.
- Zinc consistently dominated the elemental profiles, followed by Cu and Ni, while Pb and Cd showed greater variability and lower contributions.
- Taxonomy played a key role in shaping the composition and concentrations of PTEs, and distinct signatures were associated with different brown algal groups.

- Despite environmental variability, brown algae maintained relatively stable intracellular metal compositions, suggesting biological regulation of elemental uptake.

8. BIBLIOGRAFÍA

(1) Richter, D.; Grün, R.; Joannes-Boyau, R.; Steele, T. E.; Amani, F.; Rué, M.; Fernandes, P.; Raynal, J. P.; Geraads, D.; Ben-Ncer, A.; Hublin, J. J.; McPherron, S. P. The Age of the Hominin Fossils from Jebel Irhoud, Morocco, and the Origins of the Middle Stone Age. *Nature* **2017**, *546* (7657), 293–296. https://doi.org/10.1038/NATURE22335.

(2) Ruddiman, W. F.; Ellis, E. C. Effect of Per-Capita Land Use Changes on Holocene Forest Clearance and CO2 Emissions. *Quat Sci Rev* **2009**, *28* (27–28), 3011–3015. https://doi.org/10.1016/J.QUASCIREV.2009.05.022.

(3) Lyons, S. K.; Amatangelo, K. L.; Behrensmeyer, A. K.; Bercovici, A.; Blois, J. L.; Davis, M.; Dimichele, W. A.; Du, A.; Eronen, J. T.; Tyler Faith, J.; Graves, G. R.; Jud, N.; Labandeira, C.; Looy, C. V.; McGill, B.; Miller, J. H.; Patterson, D.; Pineda-Munoz, S.; Potts, R.; Riddle, B.; Terry, R.; Tóth, A.; Ulrich, W.; Villaseñor, A.; Wing, S.; Anderson, H.; Anderson, J.; Waller, D.; Gotelli, N. J. Holocene Shifts in the Assembly of Plant and Animal Communities Implicate Human Impacts. *Nature* **2016**, *529* (7584), 80–83. https://doi.org/10.1038/NATURE16447.

(4) Intergovernmental Panel on Climate Change (IPCC). *Sixth Assessment Report of the Intergovernmental Panel on Climate Change*; Cambridge University Press, 2021. https://doi.org/10.1017/9781009157896.021.

(5) Szymczyk, A.; Nita, M. Holocene Environmental Changes in a Prehistoric Mining and Metallurgical Region in the Light of Paleobotanical Studies of the Bogs of the Brynica River Drainage Basin (Southern Poland). *Science of The Total Environment* **2021**, *788*, 147755. https://doi.org/10.1016/J.SCITOTENV.2021.147755.

(6) Foley, R. A.; Lahr, M. M. Lithic Landscapes: Early Human Impact from Stone Tool Production on the Central Saharan Environment. *PLoS One* **2015**, *10* (3), e0116482. https://doi.org/10.1371/JOURNAL.PONE.0116482.

(7) Brooks, R. C. How Humans and Their Societies Respond When the World Changes. *Behavioural Responses to a Changing World: Challenges and Applications* **2024**, 313–328. https://doi.org/10.1093/OSO/9780192858979.003.0018.

(8) Larsen, C. S. The Agricultural Revolution as Environmental Catastrophe: Implications for Health and Lifestyle in the Holocene. *Quaternary International* **2006**, *150* (1), 12–20. https://doi.org/10.1016/J.QUAINT.2006.01.004.

(9) Pérez-Rodríguez, M.; Silva-Sánchez, N.; Kylander, M. E.; Bindler, R.; Mighall, T. M.; Schofield, J. E.; Edwards, K. J.; Martínez Cortizas, A. Industrial-Era Lead and Mercury Contamination in Southern Greenland Implicates North American Sources. *Science of*

The Total Environment **2018**, *613–614*, 919–930. https://doi.org/10.1016/J.SCITOTENV.2017.09.041.

(10) Longman, J.; Veres, D.; Finsinger, W.; Ersek, V. Exceptionally High Levels of Lead Pollution in the Balkans from the Early Bronze Age to the Industrial Revolution. *Proc Natl Acad Sci U S A* **2018**, *115* (25), E5661–E5668. https://doi.org/10.1073/PNAS.1721546115.

(11) Ritchie, H.; Roser, M. CO_2 Emissions. *Our World in Data* **2020**, *2* (2), 189–205. https://doi.org/10.4155/CMT.11.10.

(12) Pingali, P. L. Green Revolution: Impacts, Limits, Andthe Path Ahead. *Proc Natl Acad Sci U S A* **2012**, *109* (31), 12302–12308. https://doi.org/10.1073/PNAS.0912953109.

(13) Carson, R. *Silent Spring*; Fawcett Crest, 1962.

(14) Török, P.; Teleki, B.; Erdős, L.; McIntosh-Buday, A.; Ruprecht, E.; Tóthmérész, B. Scale Dependency of Taxonomic and Functional Diversity in Pristine and Recovered Loess Steppic Grasslands. *Science of The Total Environment* **2024**, *949*, 175110. https://doi.org/10.1016/J.SCITOTENV.2024.175110.

(15) Selkoe, K. A.; Halpern, B. S.; Ebert, C. M.; Franklin, E. C.; Selig, E. R.; Casey, K. S.; Bruno, J.; Toonen, R. J. A Map of Human Impacts to a "Pristine" Coral Reef Ecosystem, the Papahānaumokuākea Marine National Monument. *Coral Reefs* **2009**, *28* (3), 635–650. https://doi.org/10.1007/S00338-009-0490-Z/.

(16) Waters, C. N.; Zalasiewicz, J.; Summerhayes, C.; Barnosky, A. D.; Poirier, C.; Gałuszka, A.; Cearreta, A.; Edgeworth, M.; Ellis, E. C.; Ellis, M.; Jeandel, C.; Leinfelder, R.; McNeill, J. R.; Richter, D. D. B.; Steffen, W.; Syvitski, J.; Vidas, D.; Wagreich, M.; Williams, M.; Zhisheng, A.; Grinevald, J.; Odada, E.; Oreskes, N.; Wolfe, A. P. The Anthropocene Is Functionally and Stratigraphically Distinct from the Holocene. *Science (1979)* **2016**, *351* (6269). https://doi.org/10.1126/SCIENCE.AAD2622/.

(17) Steffen, W.; Broadgate, W.; Deutsch, L.; Gaffney, O.; Ludwig, C. The Trajectory of the Anthropocene: The Great Acceleration. *Anthropocene Review* **2015**, *2* (1), 81–98. https://doi.org/10.1177/2053019614564785.

(18) Steffen, W.; Richardson, K.; Rockström, J.; Cornell, S. E.; Fetzer, I.; Bennett, E. M.; Biggs, R.; Carpenter, S. R.; De Vries, W.; De Wit, C. A.; Folke, C.; Gerten, D.; Heinke, J.; Mace, G. M.; Persson, L. M.; Ramanathan, V.; Reyers, B.; Sörlin, S. Planetary Boundaries: Guiding Human Development on a Changing Planet. *Science (1979)* **2015**, *347* (6223). https://doi.org/10.1126/SCIENCE.1259855.

(19) (IPCC), I. P. on C. C. Oceans and Coastal Ecosystems and Their Services. *Climate Change 2022 – Impacts, Adaptation and Vulnerability* **2023**, 379–550. https://doi.org/10.1017/9781009325844.005.

(20) *The Ocean and Climate Change - NASA Science*. https://science.nasa.gov/earth/explore/the-ocean-and-climate-change/ (accessed 2025-06-21).

(21) Gruber, N.; Clement, D.; Carter, B. R.; Feely, R. A.; van Heuven, S.; Hoppema, M.; Ishii, M.; Key, R. M.; Kozyr, A.; Lauvset, S. K.; Monaco, C. Lo; Mathis, J. T.; Murata, A.; Olsen, A.; Perez, F. F.; Sabine, C. L.; Tanhua, T.; Wanninkhof, R. The Oceanic Sink for Anthropogenic CO 2 from 1994 to 2007. *Science (1979)* **2019**, *363* (6432), 1193–1199. https://doi.org/10.1126/SCIENCE.AAU5153.

(22) England, M. H.; Li, Z.; Huguenin, M. F.; Kiss, A. E.; Sen Gupta, A.; Holmes, R. M.; Rahmstorf, S. Drivers of the Extreme North Atlantic Marine Heatwave during 2023. *Nature* **2025**, *642* (8068), 636–643. https://doi.org/10.1038/S41586-025-08903-5.

(23) *Special Report on the Ocean and Cryosphere in a Changing Climate —*. https://www.ipcc.ch/srocc/ (accessed 2025-06-21).

(24) Yu, L.; Josey, S. A.; Bingham, F. M.; Lee, T. Intensification of the Global Water Cycle and Evidence from Ocean Salinity: A Synthesis Review. *Ann N Y Acad Sci* **2020**, *1472* (1), 76–94. https://doi.org/10.1111/NYAS.14354.

(25) Mostofa, K. M. G.; Liu, C. Q.; Zhai, W.; Minella, M.; Vione, D.; Gao, K.; Minakata, D.; Arakaki, T.; Yoshioka, T.; Hayakawa, K.; Konohira, E.; Tanoue, E.; Akhand, A.; Chanda, A.; Wang, B.; Sakugawa, H. Reviews and Syntheses: Ocean Acidification and Its Potential Impacts on Marine Ecosystems. *Biogeosciences* **2016**, *13* (6), 1767–1786. https://doi.org/10.5194/BG-13-1767-2016.

(26) Figuerola, B.; Hancock, A. M.; Bax, N.; Cummings, V. J.; Downey, R.; Griffiths, H. J.; Smith, J.; Stark, J. S. A Review and Meta-Analysis of Potential Impacts of Ocean Acidification on Marine Calcifiers From the Southern Ocean. *Front Mar Sci* **2021**, *8*, 584445. https://doi.org/10.3389/FMARS.2021.584445.

(27) Souter, D.; Planes, S.; Wicquart, J.; Logan, M.; Obura, D.; Staub, F. *Status of Coral Reefs of the World: 2020*; GCRMN, 2021. https://doi.org/10.59387/WOTJ9184.

(28) Brondizio, E. S.; Settele, J.; Díaz, S.; Ngo, H. T. *IPBES (2019): Global Assessment Report on Biodiversity and Ecosystem Services of the Intergovernmental Science-Policy Platform on Biodiversity and Ecosystem Services.*; Bonn, Germany, 2019. https://doi.org/https://doi.org/10.5281/zenodo.3831673.

(29) Beiras, R. *Marine Pollution*; Elsevier, 2018.

(30) Alava, J. J. Ocean Pollution and Warming Oceans: Toward Ocean Solutions and Natural Marine Bioremediation. *Predicting Future Oceans: Sustainability of Ocean and Human Systems Amidst Global Environmental Change* **2019**, 495–518. https://doi.org/10.1016/B978-0-12-817945-1.00046-0.

(31) UN Environment Management Group (EMG). *The United Nations System. Common Approach Towards a Pollution-Free Planet*; 2023.

(32) Campbell, P. G. C.; Hodson, P. V.; Welbourn, P. M.; Wright, D. A. *Ecotoxicology*; Cambridge University Press, 2022.

(33) Monteiro, R. C. P.; Ivar do Sul, J. A.; Costa, M. F. Plastic Pollution in Islands of the Atlantic Ocean. *Environmental Pollution* **2018**, *238*, 103–110. https://doi.org/10.1016/J.ENVPOL.2018.01.096.

(34) Seok, M. W.; Kim, D.; Park, G. H.; Lee, K.; Kim, T. H.; Jung, J.; Kim, K.; Park, K. T.; Kim, Y. H.; Mo, A.; Park, S.; Ko, Y. H.; Kang, J.; Kim, H.; Kim, T. W. Atmospheric Deposition of Inorganic Nutrients to the Western North Pacific Ocean. *Science of The Total Environment* **2021**, *793*, 148401. https://doi.org/10.1016/J.SCITOTENV.2021.148401.

(35) Guan, Y.; Wei, X.; Wang, S.; Lai, J.; Huang, C.; Wang, S.; Wang, L.; Li, G.; Liu, Z. Accumulation and Transport of 239+240Pu and 137Cs in Bays of the Northern South China Sea. *Mar Pollut Bull* **2025**, *219*, 118278. https://doi.org/10.1016/J.MARPOLBUL.2025.118278.

(36) Pourret, O.; Hursthouse, A. It's Time to Replace the Term "Heavy Metals" with "Potentially Toxic Elements" When Reporting Environmental Research. *International Journal of Environmental Research and Public Health 2019, Vol. 16, Page 4446* **2019**, *16* (22), 4446. https://doi.org/10.3390/IJERPH16224446.

(37) Nieboer, E.; Richardson, D. H. S. The Replacement of the Nondescript Term 'Heavy Metals' by a Biologically and Chemically Significant Classification of Metal Ions. *Environmental Pollution Series B, Chemical and Physical* **1980**, *1* (1), 3–26. https://doi.org/10.1016/0143-148X(80)90017-8.

(38) Hoch, M. Organotin Compounds in the Environment — an Overview. *Applied Geochemistry* **2001**, *16* (7–8), 719–743. https://doi.org/10.1016/S0883-2927(00)00067-6.

(39) Boening, D. W. Ecological Effects, Transport, and Fate of Mercury: A General Review. *Chemosphere* **2000**, *40* (12), 1335–1351. https://doi.org/10.1016/S0045-6535(99)00283-0.

(40) Shah, S. B. Heavy Metals in the Marine Environment—An Overview. **2021**, 1–26. https://doi.org/10.1007/978-3-030-73613-2_1.

(41) Saravanan, P.; Saravanan, V.; Rajeshkannan, R.; Arnica, G.; Rajasimman, M.; Baskar, G.; Pugazhendhi, A. Comprehensive Review on Toxic Heavy Metals in the Aquatic System: Sources, Identification, Treatment Strategies, and Health Risk Assessment. *Environ Res* **2024**, *258*, 119440. https://doi.org/10.1016/J.ENVRES.2024.119440.

(42) Szopińska, M.; Luczkiewicz, A.; Jankowska, K.; Fudala-Ksiazek, S.; Potapowicz, J.; Kalinowska, A.; Bialik, R. J.; Chmiel, S.; Polkowska, Ż. First Evaluation of Wastewater Discharge Influence on Marine Water Contamination in the Vicinity of Arctowski Station (Maritime Antarctica). *Science of The Total Environment* **2021**, *789*, 147912. https://doi.org/10.1016/J.SCITOTENV.2021.147912.

(43) Micella, I.; Kroeze, C.; Bak, M. P.; Strokal, M. Causes of Coastal Waters Pollution with Nutrients, Chemicals and Plastics Worldwide. *Mar Pollut Bull* **2024**, *198*, 115902. https://doi.org/10.1016/J.MARPOLBUL.2023.115902.

(44) Wang, Q.; Li, H.; Zhang, Y.; Wang, X.; Zhang, C.; Xiao, K.; Qu, W. Evaluations of Submarine Groundwater Discharge and Associated Heavy Metal Fluxes in Bohai Bay, China. *Science of The Total Environment* **2019**, *695*, 133873. https://doi.org/10.1016/J.SCITOTENV.2019.133873.

(45) Turner, A. Marine Pollution from Antifouling Paint Particles. *Mar Pollut Bull* **2010**, *60* (2), 159–171. https://doi.org/10.1016/J.MARPOLBUL.2009.12.004.

(46) Mayk, D.; Harper, E. M.; Fietzke, J.; Backeljau, T.; Peck, L. S. 130 Years of Heavy Metal Pollution Archived in the Shell of the Intertidal Dog Whelk, Nucella Lapillus (Gastropoda, Muricidae). *Mar Pollut Bull* **2022**, *185*, 114286. https://doi.org/10.1016/J.MARPOLBUL.2022.114286.

(47) *The Global Market for Nanomaterials 2010-2030 - Advanced and Emerging Technology Market Research*. https://www.futuremarketsinc.com/the-global-market-for-nanomaterials-2010-2030/ (accessed 2025-06-18).

(48) Mostafa, M.; Kandile, N. G.; Mahmoud, M. K.; Ibrahim, H. M. Synthesis and Characterization of Polystyrene with Embedded Silver Nanoparticle Nanofibers to Utilize as Antibacterial and Wound Healing Biomaterial. *Heliyon* **2022**, *8* (1), e08772. https://doi.org/10.1016/J.HELIYON.2022.E08772.

(49) Prabhu, S.; Poulose, E. K. Silver Nanoparticles: Mechanism of Antimicrobial Action, Synthesis, Medical Applications, and Toxicity Effects. *International Nano Letters 2012 2:1* **2012**, *2* (1), 1–10. https://doi.org/10.1186/2228-5326-2-32.

(50) Yang, Y.; Wang, K.; Liu, X.; Xu, C.; You, Q.; Zhang, Y.; Zhu, L. Environmental Behavior of Silver Nanomaterials in Aquatic Environments: An Updated Review. *Science of The Total Environment* **2024**, *907*, 167861. https://doi.org/10.1016/J.SCITOTENV.2023.167861.

(51) Fabrega, J.; Luoma, S. N.; Tyler, C. R.; Galloway, T. S.; Lead, J. R. Silver Nanoparticles: Behaviour and Effects in the Aquatic Environment. *Environ Int* **2011**, *37* (2), 517–531. https://doi.org/10.1016/J.ENVINT.2010.10.012.

(52) Lu, Y.; Yuan, J.; Lu, X.; Su, C.; Zhang, Y.; Wang, C.; Cao, X.; Li, Q.; Su, J.; Ittekkot, V.; Garbutt, R. A.; Bush, S.; Fletcher, S.; Wagey, T.; Kachur, A.; Sweijd, N. Major

Threats of Pollution and Climate Change to Global Coastal Ecosystems and Enhanced Management for Sustainability. *Environmental Pollution* **2018**, *239*, 670–680. https://doi.org/10.1016/J.ENVPOL.2018.04.016.

(53) Wei, H.; Zhu, Z.; Wang, W.; Tang, H.; Guan, Y.; Zheng, P.; Zhang, L.; Jia, R.; Liang, Q.; Li, S.; Lu, L.; Chen, Y.; Zhang, Z.; Chen, J.; Zhang, Q. Terrestrial Inputs and Physical Processes Control the Distributions of Potentially Toxic Elements (PTEs) in the Seawater of the Large-Range Beibu Gulf, the Northern South China Sea. *Mar Pollut Bull* **2023**, *196*, 115617. https://doi.org/10.1016/J.MARPOLBUL.2023.115617.

(54) Chiaia-Hernández, A. C.; Casado-Martinez, C.; Lara-Martin, P.; Bucheli, T. D. Sediments: Sink, Archive, and Source of Contaminants. *Environmental Science and Pollution Research* **2022**, *29* (57), 85761–85765. https://doi.org/10.1007/S11356-022-24041-1.

(55) Córdoba-Tovar, L.; Marrugo-Negrete, J.; Barón, P. R.; Díez, S. Drivers of Biomagnification of Hg, As and Se in Aquatic Food Webs: A Review. *Environ Res* **2022**, *204*, 112226. https://doi.org/10.1016/J.ENVRES.2021.112226.

(56) Levinton D, J. S.; Pochron, S. T. Temporal and Geographic Trends in Mercury Concentrations in Muscle Tissue in Five Species of Hudson River, USA, Fish. *Environ Toxicol Chem* **2008**, *27* (8), 1691–1697. https://doi.org/10.1897/07-438.1.

(57) Wang, L.; Wang, X.; Chen, H.; Wang, Z.; Jia, X. Oyster Arsenic, Cadmium, Copper, Mercury, Lead and Zinc Levels in the Northern South China Sea: Long-Term Spatiotemporal Distributions, Combined Effects, and Risk Assessment to Human Health. *Environmental Science and Pollution Research* **2022**, *29* (9), 12706–12719. https://doi.org/10.1007/S11356-021-18150-6.

(58) Gomes, T.; Pereira, C. G.; Cardoso, Ć.; Sousa, V. S.; Teixeira, M. R.; Pinheiro, J. P.; Bebianno, M. J. Effects of Silver Nanoparticles Exposure in the Mussel Mytilus Galloprovincialis. *Mar Environ Res* **2014**, *101* (1), 208–214. https://doi.org/10.1016/J.MARENVRES.2014.07.004.

(59) Zitoun, R.; Marcinek, S.; Hatje, V.; Sander, S. G.; Völker, C.; Sarin, M.; Omanović, D. Climate Change Driven Effects on Transport, Fate and Biogeochemistry of Trace Element Contaminants in Coastal Marine Ecosystems. *Communications Earth & Environment 2024 5:1* **2024**, *5* (1), 1–17. https://doi.org/10.1038/s43247-024-01679-y.

(60) Sfakianakis, D. G.; Renieri, E.; Kentouri, M.; Tsatsakis, A. M. Effect of Heavy Metals on Fish Larvae Deformities: A Review. *Environ Res* **2015**, *137*, 246–255. https://doi.org/10.1016/J.ENVRES.2014.12.014.

(61) Levard, C.; Hotze, E. M.; Lowry, G. V.; Brown, G. E. Environmental Transformations of Silver Nanoparticles: Impact on Stability and Toxicity. *Environ Sci Technol* **2012**, *46* (13), 6900–6914. https://doi.org/10.1021/ES2037405/.

(62) Gambardella, C.; Costa, E.; Piazza, V.; Fabbrocini, A.; Magi, E.; Faimali, M.; Garaventa, F. Effect of Silver Nanoparticles on Marine Organisms Belonging to Different Trophic Levels. *Mar Environ Res* **2015**, *111*, 41–49. https://doi.org/10.1016/J.MARENVRES.2015.06.001.

(63) Andrade, L. R.; Leal, R. N.; Noseda, M.; Duarte, M. E. R.; Pereira, M. S.; Mourão, P. A. S.; Farina, M.; Amado Filho, G. M. Brown Algae Overproduce Cell Wall Polysaccharides as a Protection Mechanism against the Heavy Metal Toxicity. *Mar Pollut Bull* **2010**, *60* (9), 1482–1488. https://doi.org/10.1016/j.marpolbul.2010.05.004.

(64) Hassan, I. A.; Sayegh, F. A.; El-Sheekh, M. M.; Walter, J. W.; El Maghraby, D. M. Interactive Effects of Salinity and Copper Toxicity on the Growth and Photosynthetic Efficiency of Germlings and Adult Brown Alga Fucus Ceranoides (Fucales, Phaeophyceae). *Rendiconti Lincei* **2021**, *32* (4), 737–745. https://doi.org/10.1007/S12210-021-01015-Y.

(65) Sáez, C. A.; González, A.; Contreras, R. A.; Moody, A. J.; Moenne, A.; Brown, M. T. A Novel Field Transplantation Technique Reveals Intra-Specific Metal-Induced Oxidative Responses in Strains of Ectocarpus Siliculosus with Different Pollution Histories. *Environmental Pollution* **2015**, *199*, 130–138. https://doi.org/10.1016/J.ENVPOL.2015.01.026.

(66) Thomsen, M.; South, P.; Staehr, P. Fabulous but Forgotten Fucoid Forests. *Ecol Evol* **2024**, *14*, e70491. https://doi.org/10.1002/ece3.70491.

(67) Castro, B. B.; Cotas, J.; Gomes, L.; Pacheco, D.; Pereira, L. Ecosystem Services Provided by Seaweeds. *Hydrobiology* **2023**, *2* (1), 75–96. https://doi.org/10.3390/HYDROBIOLOGY2010006.

(68) Mbandzi, N.; Vincent Nakin, M. D.; Oyedeji, A. O. Stable Isotopes Analysis and Heavy Metal Contamination in the Rocky Shore Intertidal Food Web on the East Coast of South Africa. *Mar Environ Res* **2022**, *177*, 105637. https://doi.org/10.1016/J.MARENVRES.2022.105637.

(69) Jormalainen, V.; Ramsay, T. Resistance of the Brown Alga Fucus Vesiculosus to Herbivory. *Oikos* **2009**, *118* (5), 713–722. https://doi.org/10.1111/J.1600-0706.2008.17178.X.

(70) Jormalainen, V.; Honkanen, T.; Mäkinen, A.; Hemmi, A.; Vesakoski, O. Why Does Herbivore Sex Matter? Sexual Differences in Utilization of Fucus Vesiculosus by the Isopod Idotea Baltica. *Oikos* **2001**, *93* (1), 77–86. https://doi.org/10.1034/J.1600-0706.2001.930108.X.

(71) Worms, I.; Simon, D. F.; Hassler, C. S.; Wilkinson, K. J. Bioavailability of Trace Metals to Aquatic Microorganisms: Importance of Chemical, Biological and Physical

Processes on Biouptake. *Biochimie* **2006**, *88* (11), 1721–1731. https://doi.org/10.1016/J.BIOCHI.2006.09.008.

(72) Freitas, R.; Leite, C.; Pinto, J.; Costa, M.; Monteiro, R.; Henriques, B.; Di Martino, F.; Coppola, F.; Soares, A. M. V. M.; Solé, M.; Pereira, E. The Influence of Temperature and Salinity on the Impacts of Lead in Mytilus Galloprovincialis. *Chemosphere* **2019**, *235*, 403–412. https://doi.org/10.1016/J.CHEMOSPHERE.2019.05.221.

(73) Xie, D.; Wei, H.; Huang, Y.; Qian, J.; Zhang, Y.; Wang, M. Elevated Temperature as a Dominant Driver to Aggravate Cadmium Toxicity: Investigations through Toxicokinetics and Omics. *J Hazard Mater* **2024**, *474*, 134789. https://doi.org/10.1016/J.JHAZMAT.2024.134789.

(74) Syaifudin, M.; Moussa, M. G.; Li, T.; Du, H. The Impact of Salinity on Heavy Metal Accumulation in Seaweed. *Mar Pollut Bull* **2025**, *214*, 117819. https://doi.org/10.1016/J.MARPOLBUL.2025.117819.

(75) Zhou, Q.; Zhang, J.; Fu, J.; Shi, J.; Jiang, G. Biomonitoring: An Appealing Tool for Assessment of Metal Pollution in the Aquatic Ecosystem. *Anal Chim Acta* **2008**, *606* (2), 135–150. https://doi.org/10.1016/J.ACA.2007.11.018.

(76) Phillips, D. J. H. The Use of Biological Indicator Organisms to Monitor Trace Metal Pollution in Marine and Estuarine Environments—a Review. *Environmental Pollution (1970)* **1977**, *13* (4), 281–317. https://doi.org/10.1016/0013-9327(77)90047-7.

(77) Barreira, J.; Araújo, D. F.; Knoery, J.; Briant, N.; Machado, W.; Grouhel-Pellouin, A. The French Mussel Watch Program Reveals the Attenuation of Coastal Lead Contamination over Four Decades. *Mar Pollut Bull* **2024**, *199*, 115975. https://doi.org/10.1016/J.MARPOLBUL.2023.115975.

(78) *German Environmental Specimen Bank*. https://umweltprobenbank.de/en/documents/investigations/results (accessed 2025-06-22).

(79) European Parliament and Council. *Directive 2000/60/EC Water Framework Directive*; 2000. https://eur-lex.europa.eu/eli/dir/2000/60/oj (accessed 2024-10-06).

(80) Ares, Á.; Fernández, J. Á.; Aboal, J. R.; Carballeira, A. Study of the Air Quality in Industrial Areas of Santa Cruz de Tenerife (Spain) by Active Biomonitoring with Pseudoscleropodium Purum. *Ecotoxicol Environ Saf* **2011**, *74* (3), 533–541. https://doi.org/10.1016/j.ecoenv.2010.08.019.

(81) Lu, G. Y.; Ke, C. H.; Zhu, A.; Wang, W. X. Oyster-Based National Mapping of Trace Metals Pollution in the Chinese Coastal Waters. *Environmental Pollution* **2017**, *224*, 658–669. https://doi.org/10.1016/J.ENVPOL.2017.02.049.

(82) Valsecchi, S.; Ademollo, N.; Patrolecco, L.; Rusconi, M.; Polesello, S. Contaminant Concentrations in Bivalve Tissues Are Not Necessarily Representative of the Chemical Status of a Site. *Integr Environ Assess Manag* **2017**, *13* (6), 1123–1124. https://doi.org/10.1002/IEAM.1941.

(83) Ferraro, A.; Parisi, A.; Barbone, E.; Race, M.; Mali, M.; Spasiano, D.; Fratino, U. Characterising Contaminants Distribution in Marine-Coastal Sediments through Multivariate and Nonparametric Statistical Analyses: A Complementary Strategy Supporting Environmental Monitoring and Control. *Environ Monit Assess* **2023**, *195* (1), 1–19. https://doi.org/10.1007/S10661-022-10617-4.

(84) Boquete, M. T.; Fernández, J. A.; Carballeira, A.; Aboal, J. R. Relationship between Trace Metal Concentrations in the Terrestrial Moss Pseudoscleropodium Purum and in Bulk Deposition. *Environmental Pollution* **2015**, *201*, 1–9. https://doi.org/10.1016/J.ENVPOL.2015.02.028.

(85) Fiévet, B.; Bailly du Bois, P.; Voiseux, C. Concentration Factors and Biological Half-Lives for the Dynamic Modelling of Radionuclide Transfers to Marine Biota in the English Channel. *Science of The Total Environment* **2021**, *791*, 148193. https://doi.org/10.1016/J.SCITOTENV.2021.148193.

(86) Vázquez-Arias, A.; Boquete, M. T.; Fernández, J. Á.; Aboal, J. R. Assessing the Effectiveness of Seaweed Transplants in Reflecting Seawater Pollution Levels. *Environmental Pollution* **2025**, *377*, 126456. https://doi.org/10.1016/j.envpol.2025.126456.

(87) Fourest, E.; Volesky, B. Alginate Properties and Heavy Metal Biosorption by Marine Algae. *Applied Biochemistry and Biotechnology - Part A Enzyme Engineering and Biotechnology* **1997**, *67* (3), 215–226. https://doi.org/10.1007/BF02788799.

(88) Zubia, M.; Payri, C.; Deslandes, E. Alginate, Mannitol, Phenolic Compounds and Biological Activities of Two Range-Extending Brown Algae, Sargassum Mangarevense and Turbinaria Ornata (Phaeophyta: Fucales), from Tahiti (French Polynesia). *J Appl Phycol* **2008**, *20* (6), 1033–1043. https://doi.org/10.1007/s10811-007-9303-3.

(89) Schiesari, L.; Leibold, M. A.; Burton, G. A. Metacommunities, Metaecosystems and the Environmental Fate of Chemical Contaminants. *Journal of Applied Ecology* **2018**, *55* (3), 1553–1563. https://doi.org/10.1111/1365-2664.13054.

(90) Kuo, D. T. F.; Rattner, B. A.; Marteinson, S. C.; Letcher, R.; Fernie, K. J.; Treu, G.; Deutsch, M.; Johnson, M. S.; Deglin, S.; Embry, M. A Critical Review of Bioaccumulation and Biotransformation of Organic Chemicals in Birds. *Reviews of Environmental Contamination and Toxicology 2022 260:1* **2022**, *260* (1), 1–55. https://doi.org/10.1007/S44169-021-00007-1.

(91) García-Seoane, R.; Fernández, J. A.; Villares, R.; Aboal, J. R. Use of Macroalgae to Biomonitor Pollutants in Coastal Waters: Optimization of the Methodology. *Ecol Indic* **2018**, *84*, 710–726. https://doi.org/10.1016/J.ECOLIND.2017.09.015.

(92) Deniaud-Bouët, E.; Hardouin, K.; Potin, P.; Kloareg, B.; Hervé, C. A Review about Brown Algal Cell Walls and Fucose-Containing Sulfated Polysaccharides: Cell Wall Context, Biomedical Properties and Key Research Challenges. *Carbohydr Polym* **2017**, *175*, 395–408. https://doi.org/10.1016/j.carbpol.2017.07.082.

(93) Fourest, E.; Volesky, B. Alginate Properties and Heavy Metal Biosorption by Marine Algae. *Applied Biochemistry and Biotechnology - Part A Enzyme Engineering and Biotechnology* **1997**, *67* (3), 215–226. https://doi.org/10.1007/bf02788799.

(94) Vázquez-Arias, A.; Boquete, M. T.; Martín-Jouve, B.; Tucoulou, R.; Rodríguez-Prieto, C.; Fernández, J. Á.; Aboal, J. R. Nanoscale Distribution of Potentially Toxic Elements in Seaweeds Revealed by Synchrotron X-Ray Fluorescence. *J Hazard Mater* **2024**, *480*, 136454. https://doi.org/10.1016/J.JHAZMAT.2024.136454.

(95) Chernova, E. N.; Shulkin, V. M. Concentrations of Metals in the Environment and in Algae: The Bioaccumulation Factor. *Russ J Mar Biol* **2019**, *45* (3), 191–201. https://doi.org/10.1134/S1063074019030027.

(96) Ryabushko, V. I.; Gureeva, E. V.; Kapranov, S. V.; Prazukin, A. V.; Toichkin, A. M.; Simokon, M. V.; Bobko, N. I. Element Composition of Several Marine Macrophytes (Crimea, Black Sea) and Correlations with the Element Abundances in Sediments and Seawater. *Environ Res* **2024**, *257*, 119380. https://doi.org/10.1016/J.ENVRES.2024.119380.

(97) Malea, P.; Kevrekidis, T. Trace Element Patterns in Marine Macroalgae. *Science of The Total Environment* **2014**, *494–495*, 144–157. https://doi.org/10.1016/J.SCITOTENV.2014.06.134.

(98) Morita, M.; Yoshinaga, J.; Mukai, H.; Ambe, Y.; Tanaka, A.; Shibata, Y. Specimen Banking at National Institute for Environmental Studies, Japan. *Chemosphere* **1997**, *34* (9–10), 1907–1919. https://doi.org/10.1016/S0045-6535(97)00052-0.

(99) Viana, I. G.; Aboal, J. R.; Fernández, J. A.; Real, C.; Villares, R.; Carballeira, A. Use of Macroalgae Stored in an Environmental Specimen Bank for Application of Some European Framework Directives. *Water Res* **2010**, *44* (6), 1713–1724. https://doi.org/10.1016/j.watres.2009.11.036.

(100) Mubiana, V. K.; Qadah, D.; Meys, J.; Blust, R. Temporal and Spatial Trends in Heavy Metal Concentrations in the Marine Mussel Mytilus Edulis from the Western Scheldt Estuary (The Netherlands). *Hydrobiologia* **2005**, *540*, 169–180. https://doi.org/10.1007/s10750-004-7134-7.

(101) Song, Y.; Yu, K.; Zhao, J.; Feng, Y.; Shi, Q.; Zhang, H.; Ayoko, G. A.; Frost, R. L. Past 140-Year Environmental Record in the Northern South China Sea: Evidence from Coral Skeletal Trace Metal Variations. *Environ Pollut* **2014**, *185*, 97–106. https://doi.org/10.1016/J.ENVPOL.2013.10.024.

(102) Lu, G.; Pan, K.; Zhu, A.; Dong, Y.; Wang, W. X. Spatial-Temporal Variations and Trends Predication of Trace Metals in Oysters from the Pearl River Estuary of China during 2011–2018. *Environmental Pollution* **2020**, *264*, 114812. https://doi.org/10.1016/J.ENVPOL.2020.114812.

(103) García-Seoane, R.; Fernández, J. A.; Boquete, M. T.; Aboal, J. R. Analysis of Intra-Thallus and Temporal Variability of Trace Elements and Nitrogen in Fucus Vesiculosus: Sampling Protocol Optimization for Biomonitoring. *J Hazard Mater* **2021**, *412*, 125268. https://doi.org/10.1016/J.JHAZMAT.2021.125268.

(104) Kozhenkova, S. I.; Khristoforova, N. K.; Chernova, E. N.; Kobzar, A. D. Long-Term Biomonitoring of Heavy Metal Pollution of Ussuri Bay, Sea of Japan. *Russ J Mar Biol* **2021**, *47* (4), 256–264. https://doi.org/10.1134/S106307402104009X.

(105) Chalkley, R.; Child, F.; Al-Thaqafi, K.; Dean, A. P.; White, K. N.; Pittman, J. K. Macroalgae as Spatial and Temporal Bioindicators of Coastal Metal Pollution Following Remediation and Diversion of Acid Mine Drainage. *Ecotoxicol Environ Saf* **2019**, *182*, 109458. https://doi.org/10.1016/J.ECOENV.2019.109458.

(106) Council Directive. *Urban Wastewater Treatment Directive (91/271/EEC)*; 1991.

(107) European Commission. *Water Framework Directive (2000/60/EC)*; 2000. https://environment.ec.europa.eu/topics/water/water-framework-directive_en.

(108) European Environment Agency. *Marine Strategy Framework Directive 2008/56/EC*; 2008. https://www.eea.europa.eu/policy-documents/2008-56-ec.

(109) Hanna Ritchie. How the World Eliminated Lead from Gasoline. *Our world in data*. 2022. https://ourworldindata.org/leaded-gasoline-phase-out (accessed 2024-11-29).

(110) Pinedo-González, P.; West, A. J.; Tovar-Sanchez, A.; Duarte, C. M.; Sañudo-Wilhelmy, S. A. Concentration and Isotopic Composition of Dissolved Pb in Surface Waters of the Modern Global Ocean. *Geochim Cosmochim Acta* **2018**, *235*, 41–54. https://doi.org/10.1016/J.GCA.2018.05.005.

(111) *Heavy metal emissions in Europe (Indicator) | European zero pollution dashboards*. https://www.eea.europa.eu/en/european-zero-pollution-dashboards/indicators/heavy-metal-emissions-in-europe-indicator (accessed 2025-05-21).

(112) Carballeira, A.; Aboal, J. *Bancos de Especímenes Ambientales: Una Propuesta Para Galicia*; Universidade de Santiago de Compostela. Servizo de Publicacións e Intercambio Científico: Santiago de Compostela, 2000.

(113) Vázquez-Arias, A.; Pacín, C.; Ares, Á.; Fernández, J. Á.; Aboal, J. R. Do We Know the Cellular Location of Heavy Metals in Seaweed? An up-to-Date Review of the Techniques. *Science of the Total Environment* **2023**, *856* (September 2022). https://doi.org/10.1016/j.scitotenv.2022.159215.

(114) Pacín, C.; Fernández, J. Á.; Conde-Amboage, M.; Lazzari, M.; García-Seoane, R.; Viana, I. G.; Varela, Z.; Real, C.; Villares, R.; Aboal, J. R. Three Decades of Change in Potentially Toxic Elements in Brown Algae in the Northeast Atlantic Ocean. *Environ Sci Technol* **2025**. https://doi.org/10.1021/ACS.EST.4C14013.

(115) García-Seoane, R.; Fernández, J. A.; Boquete, M. T.; Aboal, J. R. Application of Macroalgae Analysis to Assess the Natural Variability in Selected Pollution Concentrations (N and Hg), and to Detect Sources of It in Coastal Environments. *Science of The Total Environment* **2019**, *650*, 1403–1411. https://doi.org/10.1016/J.SCITOTENV.2018.09.156.

(116) García-García, A.; García-Gil, S.; Vilas, F. Quaternary Evolution of the Ría de Vigo, Spain. *Mar Geol* **2005**, *220* (1–4), 153–179. https://doi.org/10.1016/J.MARGEO.2005.06.015.

(117) Cartelle, V.; García-Gil, S. From a River Valley to a Ria: Evolution of an Incised Valley (Ría de Ferrol, North-West Spain) since the Last Glacial Maximum. *Sedimentology* **2019**, *66* (5), 1930–1966. https://doi.org/10.1111/SED.12565.

(118) *Censo Nacional de Vertidos (CNV)*. https://www.miteco.gob.es/es/cartografia-y-sig/ide/descargas/agua/censo-nacional-vertidos.html.

(119) *Natura 2000 - European Commission*. https://environment.ec.europa.eu/topics/nature-and-biodiversity/natura-2000_en (accessed 2025-06-23).

(120) Wallace, A. L.; Klein, A. S.; Mathieson, A. C. Determining the Affinities of Salt Marsh Fucoids Using Microsatellite Markers: Evidence of Hybridization and Introgression between Two Species of Fucus (Phaeophyta) in a Maine Estuary. *J Phycol* **2004**, *40* (6), 1013–1027. https://doi.org/10.1111/J.1529-8817.2004.04085.X.

(121) Langevin, D.; Raspaud, E.; Mariot, S.; Knyazev, A.; Stocco, A.; Salonen, A.; Luch, A.; Haase, A.; Trouiller, B.; Relier, C.; Lozano, O.; Thomas, S.; Salvati, A.; Dawson, K. Towards Reproducible Measurement of Nanoparticle Size Using Dynamic Light Scattering: Important Controls and Considerations. *NanoImpact* **2018**, *10*, 161–167. https://doi.org/10.1016/J.IMPACT.2018.04.002.

(122) Reimann, C.; Filzmoser, P. Normal and Lognormal Data Distribution in Geochemistry: Death of a Myth. Consequences for the Statistical Treatment of Geochemical and Environmental Data. *Environmental Geology* **2000**, *39* (9), 1001–1014. https://doi.org/10.1007/S002549900081.

(123) Helsel, D. R. Computing Summary Statistics and Totals. In *Statistics for Censored Environmental Data Using Minitab® and R* ; John Wiley & Sons, Ltd, 2011; pp 62–98. https://doi.org/10.1002/9781118162729.CH6.

(124) Council Directive. *Commission Regulation (EU) 2023/915 on Maximum Levels for Certain Contaminants in Food and Repealing Regulation (EC) No 1881/2006*; 2023. https://eur-lex.europa.eu/legal-content/es/TXT/?uri=CELEX%3A32023R0915.

(125) Pawlik-Skowrońska, B.; Pirszel, J.; Brown, M. T. Concentrations of Phytochelatins and Glutathione Found in Natural Assemblages of Seaweeds Depend on Species and Metal Concentrations of the Habitat. *Aquatic Toxicology* **2007**, *83* (3), 190–199. https://doi.org/10.1016/J.AQUATOX.2007.04.003.

(126) Oaten, J. F. P.; Gibson, M. C.; Hudson, M. D.; Jensen, A. C.; Williams, I. D. Metal Accumulation and Metallothionein Response in Fucus Spiralis. *International Journal of Environmental Pollution and Remediation* **2017**. https://doi.org/10.11159/IJEPR.2017.001.

(127) Gaete, H.; Moyano, N.; Jara, C.; Carrasco, R.; Lobos, G.; Hidalgo, M. E. Assessment Oxidative Stress Biomarkers and Metal Bioaccumulation in Macroalgae from Coastal Areas with Mining Activities in Chile. *Environ Monit Assess* **2016**, *188* (1), 1–11. https://doi.org/10.1007/S10661-015-5021-5.

(128) Maharana, D.; Jena, K.; Pise, N. M.; Jagtap, T. G. Assessment of Oxidative Stress Indices in a Marine Macro Brown Alga Padina Tetrastromatica (Hauck) from Comparable Polluted Coastal Regions of the Arabian Sea, West Coast of India. *Journal of Environmental Sciences* **2010**, *22* (9), 1413–1417. https://doi.org/10.1016/S1001-0742(09)60268-0.

(129) Wen, J.; Zou, D. Interactive Effects of Increasing Atmospheric CO2 and Copper Exposure on the Growth and Photosynthesis in the Young Sporophytes of Sargassum Fusiforme (Phaeophyta). *Chemosphere* **2021**, *269*, 129397. https://doi.org/10.1016/J.CHEMOSPHERE.2020.129397.

(130) Wang, L.; Yu, D. D.; Xu, D.; Li, Y. X. Physiological and Proteomic Alterations in Macrocystis Pyrifera under Chromium(VI) Stress. *Russ J Mar Biol* **2021**, *47* (3), 210–218. https://doi.org/10.1134/S1063074021030111.

(131) Ramesh, K.; Berry, S.; Brown, M. T. Accumulation of Silver by Fucus Spp. (Phaeophyceae) and Its Toxicity to Fucus Ceranoides under Different Salinity Regimes. *Ecotoxicology* **2015**, *24* (6), 1250–1258. https://doi.org/10.1007/S10646-015-1495-8.

(132) Lü, F.; Dind, G.; Liu, W.; Zhan, D.; Wu, H.; Guo, W. Comparative Study of Responses in the Brown Algae Sargassum Thunbergii to Zinc and Cadmium Stress. *J Oceanol Limnol* **2018**, *36* (3), 933–941. https://doi.org/10.1007/S00343-018-6334-3.

(133) Baumann, H. A.; Morrison, L.; Stengel, D. B. Metal Accumulation and Toxicity Measured by PAM—Chlorophyll Fluorescence in Seven Species of Marine Macroalgae. *Ecotoxicol Environ Saf* **2009**, *72* (4), 1063–1075. https://doi.org/10.1016/J.ECOENV.2008.10.010.

(134) Dong, Y.; Rosenbaum, R. K.; Hauschild, M. Z. Assessment of Metal Toxicity in Marine Ecosystems: Comparative Toxicity Potentials for Nine Cationic Metals in Coastal Seawater. *Environ Sci Technol* **2016**, *50* (1), 269–278. https://doi.org/10.1021/ACS.EST.5B01625.

(135) Mamboya, F. A. Heavy Metal Contamination and Toxicity : Studies of Macroalgae from the Tanzanian Coast, Stockholm University, 2007.

(136) Akhyar, O.; Wong, K. H.; Papry, R. I.; Kato, Y.; Mashio, A. S.; Zuka, M.; Hasegawa, H. Zn Ions and Fe Plaque Jointly Alleviate Cu Toxicity in Sargassum Patens C. Agardh. *Aquat Bot* **2023**, *189*, 103700. https://doi.org/10.1016/J.AQUABOT.2023.103700.

(137) Barreiro, R.; Picado, L.; Real, C. Biomonitoring Heavy Metals in Estuaries: A Field Comparison of Two Brown Algae Species Inhabiting Upper Estuarine Reaches. *Environmental Monitoring and Assessment 2002 75:2* **2002**, *75* (2), 121–134. https://doi.org/10.1023/A:1014479612811.

(138) Rainbow, P. S. Trace Metal Concentrations in Aquatic Invertebrates: Why and so What? *Environmental Pollution* **2002**, *120* (3), 497–507. https://doi.org/10.1016/S0269-7491(02)00238-5.

(139) Geddie, A. W.; Hall, S. G. An Introduction to Copper and Zinc Pollution in Macroalgae: For Use in Remediation and Nutritional Applications. *J Appl Phycol* **2019**, *31* (1), 691–708. https://doi.org/10.1007/S10811-018-1580-5.

(140) Ender, E.; Subirana, M. A.; Raab, A.; Krupp, E. M.; Schaumlöffel, D.; Feldmann, J. Why Is NanoSIMS Elemental Imaging of Arsenic in Seaweed (Laminaria Digitata) Important for Understanding of Arsenic Biochemistry in Addition to Speciation Information? *J Anal At Spectrom* **2019**, *34* (11), 2295–2302. https://doi.org/10.1039/C9JA00187E.

(141) Stockdale, A.; Tipping, E.; Lofts, S.; Mortimer, R. J. G. Effect of Ocean Acidification on Organic and Inorganic Speciation of Trace Metals. *Environ Sci Technol* **2016**, *50* (4), 1906–1913. https://doi.org/10.1021/ACS.EST.5B05624.

(142) Millero, F. J.; Woosley, R.; Ditrolio, B.; Waters, J. Effect of Ocean Acidification on the Speciation of Metals in Seawater. *Oceanography* **2009**, *22* (4), 72–85. https://doi.org/10.5670/OCEANOG.2009.98.

(143) Xu, L.; Wang, Z.; Zhao, J.; Lin, M.; Xing, B. Accumulation of Metal-Based Nanoparticles in Marine Bivalve Mollusks from Offshore Aquaculture as Detected by

Single Particle ICP-MS. *Environmental Pollution* **2020**, *260*, 114043. https://doi.org/10.1016/J.ENVPOL.2020.114043.

(144) Gottschalk, F.; Lassen, C.; Kjoelholt, J.; Christensen, F.; Nowack, B. Modeling Flows and Concentrations of Nine Engineered Nanomaterials in the Danish Environment. *International Journal of Environmental Research and Public Health 2015, Vol. 12, Pages 5581-5602* **2015**, *12* (5), 5581–5602. https://doi.org/10.3390/IJERPH120505581.

(145) Zhao, J.; Wang, X.; Hoang, S. A.; Bolan, N. S.; Kirkham, M. B.; Liu, J.; Xia, X.; Li, Y. Silver Nanoparticles in Aquatic Sediments: Occurrence, Chemical Transformations, Toxicity, and Analytical Methods. *J Hazard Mater* **2021**, *418*, 126368. https://doi.org/10.1016/J.JHAZMAT.2021.126368.

(146) Peters, R. J. B.; van Bemmel, G.; Milani, N. B. L.; den Hertog, G. C. T.; Undas, A. K.; van der Lee, M.; Bouwmeester, H. Detection of Nanoparticles in Dutch Surface Waters. *Science of The Total Environment* **2018**, *621*, 210–218. https://doi.org/10.1016/J.SCITOTENV.2017.11.238.

(147) Lewis, C.; Guitart, C.; Pook, C.; Scarlett, A.; Readman, J. W.; Galloway, T. S. Integrated Assessment of Oil Pollution Using Biological Monitoring and Chemical Fingerprinting. *Environ Toxicol Chem* **2010**, *29* (6), 1358–1366. https://doi.org/10.1002/ETC.156.

(148) Deniaud-Bouët, E.; Kervarec, N.; Michel, G.; Tonon, T.; Kloareg, B.; Hervé, C. Chemical and Enzymatic Fractionation of Cell Walls from Fucales: Insights into the Structure of the Extracellular Matrix of Brown Algae. *Ann Bot* **2014**, *114* (6), 1203–1216. https://doi.org/10.1093/AOB/MCU096.

(149) Anjana, K.; Arunkumar, K. Brown Algae Biomass for Fucoxanthin, Fucoidan and Alginate; Update Review on Structure, Biosynthesis, Biological Activities and Extraction Valorisation. *Int J Biol Macromol* **2024**, *280*, 135632. https://doi.org/10.1016/J.IJBIOMAC.2024.135632.

(150) *GBIF*. https://www.gbif.org/es/ (accessed 2025-06-27).

(151) Morel, F. M. M.; Price, N. M. The Biogeochemical Cycles of Trace Metals in the Oceans. *Science (1979)* **2003**, *300* (5621), 944–947. https://doi.org/10.1126/SCIENCE.1083545.

(152) Hashim, M. A.; Chu, K. H. Biosorption of Cadmium by Brown, Green, and Red Seaweeds. *Chemical Engineering Journal* **2004**, *97* (2–3), 249–255. https://doi.org/10.1016/S1385-8947(03)00216-X.

(153) Peng, Z.; Guo, Z.; Wang, Z.; Zhang, R.; Wu, Q.; Gao, H.; Wang, Y.; Shen, Z.; Lek, S.; Xiao, J. Species-Specific Bioaccumulation and Health Risk Assessment of Heavy

Metal in Seaweeds in Tropic Coasts of South China Sea. *Science of The Total Environment* **2022**, *832*, 155031. https://doi.org/10.1016/J.SCITOTENV.2022.155031.

(154) Carballeira, A.; Carral, E.; Puente, X.; Villares, R. Regional-Scale Monitoring of Coastal Contamination. Nutrients and Heavy Metals in Estuarine Sediments and Organisms on the Coast of Galicia (Northwest Spain). *Int J Environ Pollut* **2000**, *13* (1/2/3/4/5/6), 534. https://doi.org/10.1504/IJEP.2000.002333.

(155) Komárek, M.; Ettler, V.; Chrastný, V.; Mihaljevič, M. Lead Isotopes in Environmental Sciences: A Review. *Environ Int* **2008**, *34* (4), 562–577. https://doi.org/10.1016/J.ENVINT.2007.10.005.

(156) Bohdalkova, L.; Novak, M.; Stepanova, M.; Fottova, D.; Chrastny, V.; Mikova, J.; Kubena, A. A. The Fate of Atmospherically Derived Pb in Central European Catchments: Insights from Spatial and Temporal Pollution Gradients and Pb Isotope Ratios. *Environ Sci Technol* **2014**, *48* (8), 4336–4343. https://doi.org/10.1021/ES500393Z/SUPPL_FILE/ES500393Z_SI_007.PDF.

(157) Castaing, P.; Guilcher, A. Geomorphology and Sedimentology of Rias. In *Developments in Sedimentology*; Perillo, G. M. E., Ed.; Elsevier, 1995; Vol. 53, pp 69–111. https://doi.org/10.1016/S0070-4571(05)80024-X.

(158) Álvarez-Salgado, X. A.; Gago, J.; Míguez, B. M.; Gilcoto, M.; Pérez, F. F. Surface Waters of the NW Iberian Margin: Upwelling on the Shelf versus Outwelling of Upwelled Waters from the Rías Baixas. *Estuar Coast Shelf Sci* **2000**, *51* (6), 821–837. https://doi.org/10.1006/ECSS.2000.0714.

(159) Prego, R.; Cobelo-García, A. Twentieth Century Overview of Heavy Metals in the Galician Rias (NW Iberian Peninsula). *Environmental Pollution* **2003**, *121* (3), 425–452. https://doi.org/10.1016/S0269-7491(02)00231-2.

(160) Millward, G. E.; Liu, Y. P. Modelling Metal Desorption Kinetics in Estuaries. *Science of The Total Environment* **2003**, *314–316*, 613–623. https://doi.org/10.1016/S0048-9697(03)00077-9.

(161) Jiann, K. T.; Ho, P. Cadmium Mixing Behavior in Estuaries: Redox Controls on Removal and Mobilization. *Terrestrial, Atmospheric and Oceanic Sciences* **2014**, *25* (5), 655–664. https://doi.org/10.3319/TAO.2014.04.01.01(OC).

(162) Barriada, J. L.; Tappin, A. D.; Evans, E. H.; Achterberg, E. P. Dissolved Silver Measurements in Seawater. *TrAC Trends in Analytical Chemistry* **2007**, *26* (8), 809–817. https://doi.org/10.1016/J.TRAC.2007.06.004.

(163) Smedley, P. L.; Kinniburgh, D. G. A Review of the Source, Behaviour and Distribution of Arsenic in Natural Waters. *Applied Geochemistry* **2002**, *17* (5), 517–568. https://doi.org/10.1016/S0883-2927(02)00018-5.

(164) García-Seoane, R.; Aboal, J. R.; Boquete, M. T.; Fernández, J. A. Phenotypic Differences in Heavy Metal Accumulation in Populations of the Brown Macroalgae Fucus Vesiculosus: A Transplantation Experiment. *Ecol Indic* **2020**, *111*, 105978. https://doi.org/10.1016/J.ECOLIND.2019.105978.

(165) Taboada, T.; Martínez Cortizas, A.; García, C.; García-Rodeja, E. Uranium and Thorium in Weathering and Pedogenetic Profiles Developed on Granitic Rocks from NW Spain. *Science of The Total Environment* **2006**, *356* (1–3), 192–206. https://doi.org/10.1016/J.SCITOTENV.2005.03.030.

(166) Xunta de Galicia. *Atlas Geoquímico de Galicia*; 1992.

(167) Vázquez-Arias, A.; Rodríguez-Prieto, C.; Yamada, Y.; Ito, M.; Fernández, J. Á.; Aboal, J. R. Deciphering Uptake Mechanisms of Potentially Toxic Elements in Seaweeds Using High Resolution Imaging Analysis. *under review*.

(168) Chen, C. F.; Ju, Y. R.; Chen, C. W.; Dong, C. Di. Changes in the Total Content and Speciation Patterns of Metals in the Dredged Sediments after Ocean Dumping: Taiwan Continental Slope. *Ocean Coast Manag* **2019**, *181*, 104893. https://doi.org/10.1016/J.OCECOAMAN.2019.104893.

(169) Töpperwien, S.; Behra, R.; Sigg, L. Competition among Zinc, Manganese, and Cadmium Uptake in the Freshwater Alga Scenedesmus Vacuolatus. *Environ Toxicol Chem* **2007**, *26* (3), 483–490. https://doi.org/10.1897/06-181R.1.

(170) Cai, P.; Cai, G.; Yang, J.; Li, X.; Lin, J.; Li, S.; Zhao, L. Distribution, Risk Assessment, and Quantitative Source Apportionment of Heavy Metals in Surface Sediments from the Shelf of the Northern South China Sea. *Mar Pollut Bull* **2023**, *187*, 114589. https://doi.org/10.1016/j.marpolbul.2023.114589.

(171) Huang, P.; Li, T.; Li, A.; Yu, X.; Hu, N.-J. Distribution, Enrichment and Sources of Heavy Metals in Surface Sediments of the North Yellow Sea. *Cont Shelf Res* **2014**, *73*, 1–13. https://doi.org/10.1016/j.csr.2013.11.014.

(172) Song, Y.; Ji, J.; Yang, Z.; Yuan, X.; Mao, C.; Frost, R. L.; Ayoko, G. A. Geochemical Behavior Assessment and Apportionment of Heavy Metal Contaminants in the Bottom Sediments of Lower Reach of Changjiang River. *Catena (Amst)* **2011**, *85* (1), 73–81. https://doi.org/10.1016/j.catena.2010.12.009.

(173) Xu, J.; Bland, G. D.; Gu, Y.; Ziaei, H.; Xiao, X.; Deonarine, A.; Reible, D.; Bireta, P.; Hoelen, T. P.; Lowry, G. V. Impacts of Sediment Particle Grain Size and Mercury Speciation on Mercury Bioavailability Potential. *Environ Sci Technol* **2021**, *55* (18), 12393–12402. https://doi.org/10.1021/ACS.EST.1C03572.

(174) Brunetto, G.; Bastos de Melo, G. W.; Terzano, R.; Del Buono, D.; Astolfi, S.; Tomasi, N.; Pii, Y.; Mimmo, T.; Cesco, S. Copper Accumulation in Vineyard Soils: Rhizosphere

Processes and Agronomic Practices to Limit Its Toxicity. *Chemosphere* **2016**, *162*, 293–307. https://doi.org/10.1016/J.CHEMOSPHERE.2016.07.104.

(175) Jepson, P. D.; Law, R. J. Persistent Pollutants, Persistent Threats Perspectives: Polychlorinated Biphenyls Remain a Major Threat to Marine Apex Predators Such as Orcas. *Science (1979)* **2016**, *352* (6292), 1388–1389. https://doi.org/10.1126/SCIENCE.AAF9075.

(176) Jepson, P. D.; Deaville, R.; Barber, J. L.; Aguilar, À.; Borrell, A.; Murphy, S.; Barry, J.; Brownlow, A.; Barnett, J.; Berrow, S.; Cunningham, A. A.; Davison, N. J.; Ten Doeschate, M.; Esteban, R.; Ferreira, M.; Foote, A. D.; Genov, T.; Giménez, J.; Loveridge, J.; Llavona, Á.; Martin, V.; Maxwell, D. L.; Papachlimitzou, A.; Penrose, R.; Perkins, M. W.; Smith, B.; De Stephanis, R.; Tregenza, N.; Verborgh, P.; Fernandez, A.; Law, R. J. PCB Pollution Continues to Impact Populations of Orcas and Other Dolphins in European Waters. *Sci Rep* **2016**, *6* (1), 1–17. https://doi.org/10.1038/SREP18573.

(177) Søndergaard, J.; Mosbech, A. Mining Pollution in Greenland - the Lesson Learned: A Review of 50 Years of Environmental Studies and Monitoring. *Science of The Total Environment* **2022**, *812*, 152373. https://doi.org/10.1016/j.scitotenv.2021.152373.

(178) Garmendia, M.; Fdez-Ortiz de Vallejuelo, S.; Liñero, O.; Gredilla, A.; Arana, G.; Soto, M.; de Diego, A. Long Term Monitoring of Metal Pollution in Sediments as a Tool to Investigate the Effects of Engineering Works in Estuaries. A Case Study, the Nerbioi-Ibaizabal Estuary (Bilbao, Basque Country). *Mar Pollut Bull* **2019**, *145*, 555–563. https://doi.org/10.1016/J.MARPOLBUL.2019.06.051.

(179) Yang, L.; Ma, X.; Luan, Z.; Yan, J. The Spatial-Temporal Evolution of Heavy Metal Accumulation in the Offshore Sediments along the Shandong Peninsula over the Last 100 Years: Anthropogenic and Natural Impacts. *Environmental Pollution* **2021**, *289*, 117894. https://doi.org/10.1016/J.ENVPOL.2021.117894.

(180) Wepener, V.; Degger, N. Status of Marine Pollution Research in South Africa (1960–Present). *Mar Pollut Bull* **2012**, *64* (7), 1508–1512. https://doi.org/10.1016/J.MARPOLBUL.2012.05.037.

(181) Dong, M.; Chen, W.; Chen, X.; Xing, X.; Shao, M.; Xiong, X.; Luo, Z. Geochemical Markers of the Anthropocene: Perspectives from Temporal Trends in Pollutants. *Science of The Total Environment* **2021**, *763*, 142987. https://doi.org/10.1016/j.scitotenv.2020.142987.

(182) Jafarabadi, A. R.; Bakhtiyari, A. R.; Toosi, A. S.; Jadot, C. Spatial Distribution, Ecological and Health Risk Assessment of Heavy Metals in Marine Surface Sediments and Coastal Seawaters of Fringing Coral Reefs of the Persian Gulf, Iran. *Chemosphere* **2017**, *185*, 1090–1111. https://doi.org/10.1016/j.chemosphere.2017.07.110.

(183) Knopf, B.; Fliedner, A.; Radermacher, G.; Rüdel, H.; Paulus, M.; Pirntke, U.; Koschorreck, J. Seasonal Variability in Metal and Metalloid Burdens of Mussels: Using Data from the German Environmental Specimen Bank to Evaluate Implications for Long-Term Mussel Monitoring Programs. *Environ Sci Eur* **2020**, *32* (1), 1–13. https://doi.org/10.1186/S12302-020-0289-7.

(184) Logemann, A.; Reininghaus, M.; Schmidt, M.; Ebeling, A.; Zimmermann, T.; Wolschke, H.; Friedrich, J.; Brockmeyer, B.; Pröfrock, D.; Witt, G. Assessing the Chemical Anthropocene – Development of the Legacy Pollution Fingerprint in the North Sea during the Last Century. *Environmental Pollution* **2022**, *302*, 119040. https://doi.org/10.1016/J.ENVPOL.2022.119040.

(185) Liu, L.; Wang, Z.; Ju, F.; Zhang, T. Co-Occurrence Correlations of Heavy Metals in Sediments Revealed Using Network Analysis. *Chemosphere* **2015**, *119*, 1305–1313. https://doi.org/10.1016/J.CHEMOSPHERE.2014.01.068.

(186) Ranjbar Jafarabadi, A.; Raudonytė-Svirbutavičienė, E.; Shadmehri Toosi, A.; Riyahi Bakhtiari, A. Positive Matrix Factorization Receptor Model and Dynamics in Fingerprinting of Potentially Toxic Metals in Coastal Ecosystem Sediments at a Large Scale (Persian Gulf, Iran). *Water Res* **2021**, *188*, 116509. https://doi.org/10.1016/J.WATRES.2020.116509.

(187) Kuang, Z.; Wang, H.; Han, B.; Rao, Y.; Gong, H.; Zhang, W.; Gu, Y.; Fan, Z.; Wang, S.; Huang, H. Coastal Sediment Heavy Metal(Loid) Pollution under Multifaceted Anthropogenic Stress: Insights Based on Geochemical Baselines and Source-Related Risks. *Chemosphere* **2023**, *339*, 139653. https://doi.org/10.1016/j.chemosphere.2023.139653.

(188) Mao, L.; Kong, H.; Li, F.; Chen, Z.; Wang, L.; Lin, T.; Lu, Z. Improved Geochemical Baseline Establishment Based on Diffuse Sources Contribution of Potential Toxic Elements in Agricultural Alluvial Soils. *Geoderma* **2022**, *410*, 115669. https://doi.org/10.1016/j.geoderma.2021.115669.

(189) Huang, F.; Xu, Y.; Tan, Z.; Wu, Z.; Xu, H.; Shen, L.; Xu, X.; Han, Q.; Guo, H.; Hu, Z. Assessment of Pollutions and Identification of Sources of Heavy Metals in Sediments from West Coast of Shenzhen, China. *Environmental Science and Pollution Research* **2018**, *25* (4), 3647–3656. https://doi.org/10.1007/s11356-017-0362-y.

(190) Seiler, C.; Berendonk, T. U. Heavy Metal Driven Co-Selection of Antibiotic Resistance in Soil and Water Bodies Impacted by Agriculture and Aquaculture. *Front Microbiol* **2012**, *3*. https://doi.org/10.3389/fmicb.2012.00399.

(191) Soroldoni, S.; Abreu, F.; Castro, Í. B.; Duarte, F. A.; Pinho, G. L. L. Are Antifouling Paint Particles a Continuous Source of Toxic Chemicals to the Marine Environment? *J Hazard Mater* **2017**, *330*, 76–82. https://doi.org/10.1016/J.JHAZMAT.2017.02.001.

(192) Álvarez-Iglesias, P.; Rubio, B.; Millos, J. Isotopic Identification of Natural vs. Anthropogenic Lead Sources in Marine Sediments from the Inner Ría de Vigo (NW Spain). *Science of The Total Environment* **2012**, *437*, 22–35. https://doi.org/10.1016/J.SCITOTENV.2012.07.063.

(193) Zurbrick, C. M.; Boyle, E. A.; Kayser, R. J.; Reuer, M. K.; Wu, J.; Planquette, H.; Shelley, R.; Boutorh, J.; Cheize, M.; Contreira, L.; Barraqueta, J. L. M.; Lacan, F.; Sarthou, G. Dissolved Pb and Pb Isotopes in the North Atlantic from the GEOVIDE Transect (GEOTRACES GA-01) and Their Decadal Evolution. *Biogeosciences* **2018**, *15* (16), 4995–5014. https://doi.org/10.5194/BG-15-4995-2018.

(194) Deycard, V. N.; Schäfer, J.; Petit, J. C. J.; Coynel, A.; Lanceleur, L.; Dutruch, L.; Bossy, C.; Ventura, A.; Blanc, G. Inputs, Dynamics and Potential Impacts of Silver (Ag) from Urban Wastewater to a Highly Turbid Estuary (SW France). *Chemosphere* **2017**, *167*, 501–511. https://doi.org/10.1016/J.CHEMOSPHERE.2016.09.154.

(195) Liu, Y.; Li, F.; Li, H.; Tong, Y.; Li, W.; Xiong, J.; You, J. Bioassay-Based Identification and Removal of Target and Suspect Toxicants in Municipal Wastewater: Impacts of Chemical Properties and Transformation. *J Hazard Mater* **2022**, *437*, 129426. https://doi.org/10.1016/J.JHAZMAT.2022.129426.

(196) United Nations. *Minamata Convention on Mercury*; 2013.

(197) García-Seoane, R.; Richards, C. L.; Aboal, J. R.; Fernández, J. Á.; Schmid, M. W.; Boquete, M. T. A Field Study of the Molecular Response of Brown Macroalgae to Heavy Metal Exposure: An (Epi)Genetic Approach. *J Hazard Mater* **2024**, *480*, 136304. https://doi.org/10.1016/J.JHAZMAT.2024.136304.

(198) García-Seoane, R.; Fernández, J. A.; Villares, R.; Aboal, J. R. Use of Macroalgae to Biomonitor Pollutants in Coastal Waters: Optimization of the Methodology. *Ecol Indic* **2018**, *84*, 710–726. https://doi.org/10.1016/j.ecolind.2017.09.015.

(199) Ahmad, A.; Bhattacharya, P. Environmental Arsenic in a Changing World. *Groundw Sustain Dev* **2019**, *8*, 169–171. https://doi.org/10.1016/J.GSD.2018.11.001.

(200) Schultz, J.; Berry Gobler, D. L.; Young, C. S.; Perez, A.; Doall, M. H.; Gobler, C. J. Ocean Acidification Significantly Alters the Trace Element Content of the Kelp, Saccharina Latissima. *Mar Pollut Bull* **2024**, *202*, 116289. https://doi.org/10.1016/J.MARPOLBUL.2024.116289.

(201) European Environmental Agency. *Air quality in Europe 2022. Report 05/2022.* https://www.eea.europa.eu/publications/air-quality-in-europe-2022.

(202) Zhang, L.; Gao, Y.; Gao, Y.; Wu, S.; Zhang, S.; Smith, K. R.; Yao, X.; Yao, X.; Gao, H.; Gao, H. Global Impact of Atmospheric Arsenic on Health Risk: 2005 to 2015. *Proc Natl Acad Sci U S A* **2020**, *117* (25), 13975–13982. https://doi.org/10.1073/PNAS.2002580117.

(203) Markert, B.; Wappelhorst, O.; Weckert, V.; Herpin, U.; Siewers, U.; Friese, K.; Breulmann, G. The Use of Bioindicators for Monitoring the Heavy-Metal Status of the Environment. *J Radioanal Nucl Chem* **1999**, *240* (2), 425–429. https://doi.org/10.1007/BF02349387.

ANEXO 1: PERMISOS DAS REVISTAS

A revista "Journal of Hazardous Materials" nas que están publicados os capítulos 1 e 3 pertence á editorial Elsevier, que permite que as autoras e autores inclúan os seus artigos como parte das súas teses de doutoramento, tal e como se especifica na seguinte páxina:

https://www.elsevier.com/about/policies-and-standards/copyright

E na seguinte táboa:

Authors' rights in the article

	OA with CC BY	OA with CC BY-NC	OA with CC BY-NC-ND	Subscription
Receive proper attribution and credit for their published work	Yes	Yes	Yes	Yes
Re-use their article in their own new works, without permission from Elsevier or payment to Elsevier, including by: • making copies of the article (or part of the article) to promote companies or products they own, whether or not such promotion is commercial; • including the article in a thesis or dissertation; • extending the article to a book, including the article in a subsequent compilation of their own work, or re-using portions, excerpts, and their own figures, tables and images from the article in their own new works (which in each case may be published with Elsevier or with a third party commercial or non-commercial publisher, at the author's discretion)	Yes	Yes	Yes	Yes[1]

Táboa 1. Permiso de Elsevier para incluir os artigos en tesis. Obtida a través de https://www.elsevier.com/about/policies-and-standards/copyright

O Capítulo 3 está publicado na revista Environmental Science & Technology que pertence á editorial ACS e que permite que as autoras e autores inclúan os seus artigos como parte das súas teses de doutoramento, tal e como se especifica na seguinte páxina: https://pubs.acs.org/page/copyright/permissions_journals.html

American Chemical Society's Policy on Theses and Dissertations

This policy addresses permission to include **your article**(s) or portions of text from **your article**(s) in your thesis.

Reuse/Republication of the Entire Work in Theses or Collections: Authors may reuse all or part of the Submitted, Accepted or Published Work in a thesis or dissertation that the author writes and is required to submit to satisfy the criteria of degree-granting institutions. Such reuse is permitted subject to the ACS' "Ethical Guidelines to Publication of Chemical Research". Appropriate citation of the Published Work must be made as follows

"Reprinted with permission from [COMPLETE REFERENCE CITATION]. Copyright [YEAR] American Chemical Society." Insert the appropriate wording in place of the capitalized words. Citation information may be found after the "Cite this:" heading below the title of the online version and at the bottom of **the first page of the pdf or print version of your ACS journal article**.

If the thesis or dissertation to be published is in electronic format, a direct link to the Published Work must also be included using the ACS Articles on Request author-directed link.

If your university requires written permission and your manuscript has not yet received a DOI (published ASAP), send a request to copyright@acs.org that includes the manuscript number, the name of the ACS journal, and the date that you need to receive our reply.

If your university requires you to obtain permission for manuscripts in ASAP status or final published articles, you must use the RightsLink permission system. **See RightsLink instructions at http://pubs.acs.org/page/copyright/permissions.html and make requests at the "Rights & Permissions" link under the title of the online version of the article.**

Submission to a Dissertation Distributor: If you plan to submit your thesis to UMI or to another dissertation distributor, you should not include the unpublished ACS paper in your thesis if the thesis will be disseminated electronically, until ACS has published your paper. After publication of the paper by ACS, you may release the entire thesis (**not the individual ACS article by itself**) for electronic dissemination through the distributor; ACS's copyright credit line should be printed on the first page of the ACS paper.

Updated: 07/2021

As algas pardas, e en concreto Fucus spp., son amplamente utilizadas como biomonitoras pola súa capacidade para acumular Elementos Potencialmente Tóxicos (PTEs). Esta tese analiza a evolución dos PTEs e das nanopartículas de prata (AgNPs) en algas ao longo do último século. Os resultados mostran fortes descensos nas concentracións de PTEs a escala global e rexional (ata un –84 %), en paralelo á implementación de políticas ambientais, xunto cun aumento rexional do As e unha estabilización do Pb. Ademais, tamén se detectou unha transición de fontes antrópicas a naturais e unha diminución das AgNPs, posiblemente formadas in vivo. Os achados apuntan a unha redución real das emisións, influída pola biodispoñibilidade e factores ambientais asociados ao cambio global.